KINETICS AND MECHANISM OF OXIDATION OF METHYL GLYCOL AND ETHYL GLYCOL BY N-BROMOSUCCINIMIDE IN ALKALINE MEDIUM CATALYSED BY Os(VIII)

R. A. SINGH[a]*, KAMINI SINGH[a], ABHISHEK KUMAR[a], S. K. SINGH[b]

[a]*Chemical Kinetics Research Laboratory, Department of Chemistry, T. D. P. G. College, 222 002 Jaunpur (U.P.), India*
E-mail: *rasinghtdc@rediffmail.com*; *kamini_singhjNP@rediffmail.com*
[b]*Department of Chemistry, Sri J.N.P.G. College, Lucknow (U.P.), India*

ABSTRACT

The kinetics of Os(VIII)-catalysed oxidation of methyl and ethyl glycol by N-bromo-succinimide has been investigated in alkaline medium. The reaction shows first order kinetic with respect to methyl and ethyl glycols at their low concentration tended to zero order at their higher concentration. N-bromosuccinimide and osmium tetroxide also show first order kinetics. The dielectric constant of rate constant has positive effect. Negligible effect of variation of ionic strength of the medium on rate constant was observed. Increase in temperature markedly increase the rate constant of oxidation of methyl and ethyl glycols by N-bromosuccinimide under experimental condition. A plausible rate law can be proposed as

$$-\frac{d[NBS]}{dt} = \frac{k_d K_1 K_2 [NBS]\,[S]\,[Os(VIII)_T][OH^-]}{1 + K_1[OH^-] + K_1 K_2\,[OH^-]\,[S]},$$

where S = glycol, viz. methyl and ethyl glycol.

Keywords: oxidation, methyl glycol (MG), ethyl glycol (EG), osmium tetroxide, N-bromosuccinimide [NBS], kinetic and mechanistic approach.

AIMS AND BACKGROUND

Kinetic investigations involving aliphatic, cyclic, aromatic ketones and various oxidis-ing agents have been reported by many workers[1,2]. N-bromosuccinimide is a potent oxidising agent and has been used in the determination of several organic compounds[3]. Most of the investigations on NBS oxidation of organic substrates have assumed that the molecular NBS acts only through its positive polar end producing Br⁺, which is

---

* For correspondence.

subsequently solvated. Thus H_2O^+Br has been considered as the effective oxidising species of NBS in acidic medium. In the presence of mercuric acetate protonated form of NBS, i.e. N^+BSH, has been also considered[4] as reactive species of NBS in acidic medium. However, there are only few reports on the oxidation reaction of NBS in alkaline medium[5]. Some investigations involving NBS oxidation of ester[6], alcohol[7,8] and ketones[9,10] are reported.

Very little data are reported on Os(VIII) as an independent oxidant[11–13] although it has been widely used as a catalyst[14–16]. Recently some attempts have been made on kinetics studies of Os(VIII) oxidation of some substrate, but literature on kinetic investigation of oxidation of reducing substrate by Os(VIII) is scanty.

This paper reports the kinetics and mechanism of oxidation of methyl and ethyl glycols by osmium tetroxide in alkaline medium.

EXPERIMENTAL

All the reagents used were of highest purity available A. R. grade. The reagents employed were methyl and ethyl glycols (E. Merck), osmium tetroxide (Johnson & Matthey), N-bromosuccinimide (NBS) (E. Merck). All the solutions were prepared in doubly distilled water. Fresh solution of NBS was always prepared and its strength was checked iodometrically. The solution of methyl and ethyl glycols was prepared by weighing desired amount and dissolving the same in appropriate volume of doubly distilled water. Solutions of mercuric acetate (E. Merck) and sodium perchlorate were prepared in doubly distilled water. The solution of catalyst osmium tetroxide was prepared by dissolving the sample in NaOH of known strength.

Table 1. Effect of variation of concentration of reactants in the oxidation of methyl glycol at 35°C

$[Os(VIII)] \times 10^6$ (mol dm^{-3})	$[NBS] \times 10^4$ (mol dm^{-3})	[Methyl glycol] $\times$ 10^2 (mol dm^{-3})	$[NaOH] \times 10^2$ (mol dm^{-3})	$k_1 \times 10^4$ (s^{-1})
1	2	3	4	5
5.64	6.67	2.00	2.00	5.03
5.64	10.00	2.00	2.00	5.01
5.64	12.50	2.00	2.00	5.03
5.64	16.67	2.00	2.00	4.96
5.64	20.00	2.00	2.00	4.95
5.64	25.00	2.00	2.00	4.97
5.64	10.00	0.50	2.00	1.22
5.64	10.00	1.00	2.00	2.48
5.64	10.00	1.50	2.00	3.62
5.64	10.00	2.50	2.00	5.74
5.64	10.00	3.00	2.00	6.50
5.64	10.00	4.50	2.00	8.04

to be continued

Continuation of Table 1

1	2	3	4	5
1.41	12.50	2.00	2.00	1.30
2.82	12.50	2.00	2.00	2.57
4.23	12.50	2.00	2.00	3.78
7.05	12.50	2.00	2.00	6.40
8.46	12.50	2.00	2.00	7.67
5.64	10.00	2.00	2.00	1.89
5.64	10.00	2.00	2.00	3.01
5.64	10.00	2.00	2.00	3.73
5.64	10.00	2.00	2.00	5.55
5.64	10.00	2.00	2.00	6.26

Table 2. Effect of variation of concentration of reactant in the oxidation of ethyl glycol at 35°C

$[Os(VIII)] \times 10^6$ (mol dm^{-3})	$[NBS] \times 10^4$ (mol dm^{-3})	[Ethyl glycol] $\times$ 10^2 (mol dm^{-3})	$[NaOH] \times 10^2$ (mol dm^{-3})	$k_1 \times 10^4$ (s^{-1})
5.64	6.67	2.00	3.00	2.47
5.64	10.00	2.00	3.00	2.42
5.64	12.50	2.00	3.00	2.40
5.64	16.67	2.00	3.00	2.40
5.64	20.00	2.00	3.00	2.41
5.64	25.00	2.00	3.00	2.39
5.64	12.50	0.50	3.00	0.58
5.64	12.50	1.00	3.00	1.18
5.64	12.50	1.50	3.00	1.82
5.64	12.50	2.50	3.00	2.64
5.64	12.50	3.00	3.00	2.88
5.64	12.50	4.50	3.00	3.92
1.41	10.00	2.00	3.00	0.58
2.82	10.00	2.00	3.00	1.14
4.23	10.00	2.00	3.00	1.70
7.05	10.00	2.00	3.00	2.80
8.46	10.00	2.00	3.00	3.52
5.64	10.00	2.00	2.00	1.06
5.64	10.00	2.00	2.00	1.46
5.64	10.00	2.00	2.00	1.74
5.64	10.00	2.00	2.00	2.98
5.64	10.00	2.00	2.00	2.68

The rate increases with an increase in [glycol]$_0$ (Tables 1 and 2, Fig. 1). However, from the linear plots of $1/k_1$ versus 1/[glycols] with intercepts, it appears that the order in substrate falls from unity to zero at higher [glycol]. To study the effect of alkali on the reaction rate, kinetic studies were made on the sample in NaOH of known strength. The desired volumes of solution of NBS, osmium tetroxide, mercuric acetate, sodium

acetate and sodium hydroxide were taken in a black coated reaction vessel and ther-mostated water bath was used to maintain the desired temperature to within ±0.1°C. Requisite volumes of all reagents except NBS were introduced into a reaction vessel and equilibrated at 35°C, a measured volume of NBS solution equilibrated separately at the same temperature was rapidly poured into the examining aliquots of the reaction mixture and NBS was detrmined iodometrically using starch indicator.
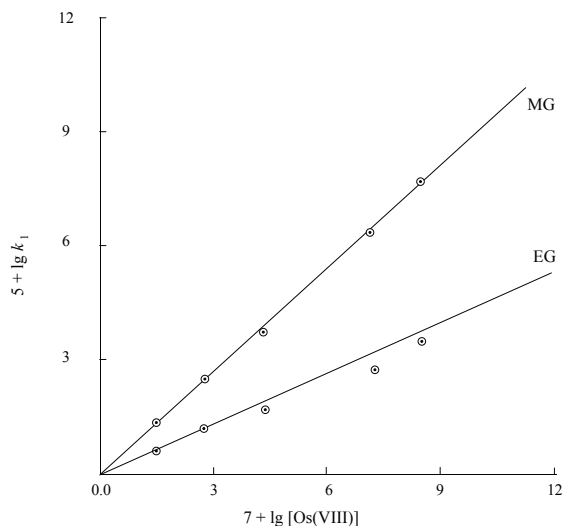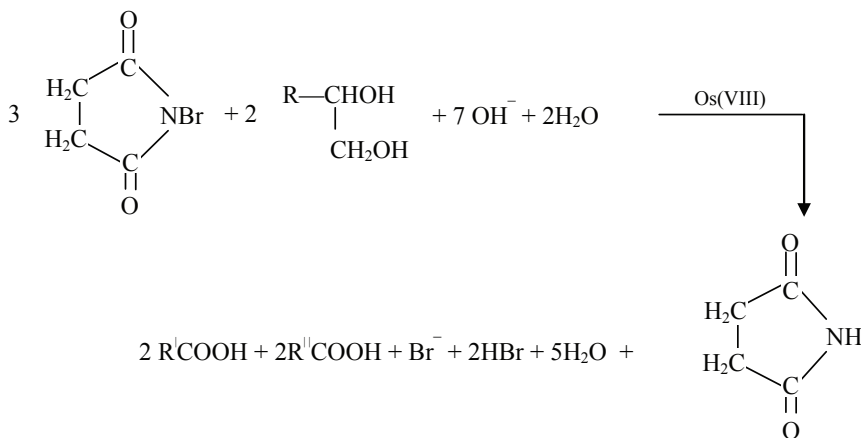

Fig. 1. Under the conditions of Tables 1 and 2

STOICHIOMETRY AND PRODUCT IDENTIFICATION

The reaction mixture containing a known excess of [N-bromosuccinimide] over [methyl glycol] and [ethyl glycol] were kept in the presence of alkaline medium and osmium tetroxide at 35°C.

The end products were the corresponding acids which were identified by spot test. Here R stands for CH_3 and C_2H_5 group. $R^{|}$ stands for H and $R^{||}$ stands for CH_3 and C_2H_5 group in methyl and ethyl glycol, respectively.

RESULTS AND DISCUSSION

The kinetics of oxidation of methyl and ethyl glycols by NBS was investigated at several initial concentrations of reactants. The linear plot of log [NBS] versus time indicates a first order dependence of rate on [NBS]. Effect of ionic strength was found to be negligible, which is maintained by sodium perchlorate both in methyl and ethyl glycols. On increasing the concentration of sodium hydroxide the value of first order rate constant increases non-linearly in oxidation both of methyl glycol and ethyl glycol by N-bromosuccinimide, showing positive effect of sodium hydroxide on the rate constant of reactions. The rate increases proportionally with increasing concentration of catalyst as confirmed by a plot of rate versus [Os(VIII)] that yields a straight line passing through origin. Thus, the oxidation of the both glycols, viz. methyl and ethyl glycols, respectively, exhibits the same results, which confirm first order dependence on [Os(VIII)]. All the results and data are collected in Tables 1 and 2.

The kinetic investigations of oxidation by N-bromosuccinimide have been carried out extensively in alkaline medium. In alkaline medium, N-bromosuccinimide gives hypobromite anion as:

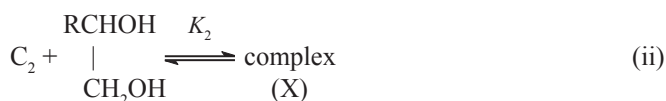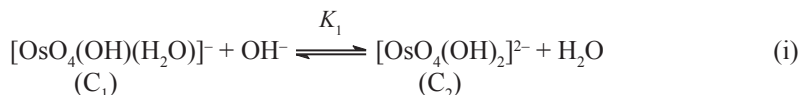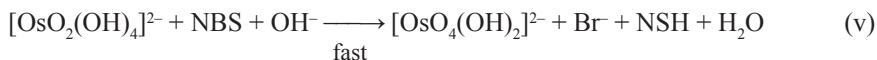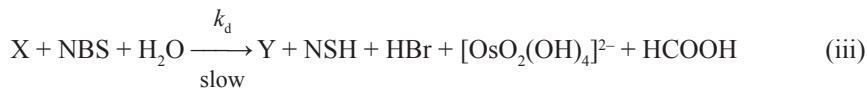$$RNBr + 2OH^- \rightleftharpoons RN^- + OBr^- + H_2O$$

The reactive species of the oxidant could be either hypobromite ion or NBS itself. The active species OBr^- is ruled out on the basis of our observation. Therefore, NBS has been taken as real oxidising species.

In alkaline medium osmium (VIII) gives octahedral complexes of the form $[OsO_4(OH)H_2O]^-$ and $trans$ $[OsO_4(OH)_2]^{2-}$. It has also been observed that $[OsO_4(OH)H_2O]^-$ species exists at lower $[OH^-]$, which at higher $[OH^-]$ takes the form $[OsO_4(OH)_2]^{2-}$ as follows:

$$[OsO_4(OH)H_2O]^- + OH^- \rightleftharpoons [OsO_4(OH)_2]^{2-} + H_2O$$
$$(C_1) \qquad\qquad\qquad (C_2)$$
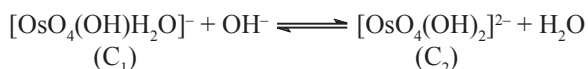
where C_2 is the active species of the catalyst OsO_4. Considering the reactive species of osmium tetroxide $[OsO_4(OH)_2]^{2-}$ and NBS in alkaline medium as well as taking into account the kinetic results, the following reaction steps are suggested:

$$\underset{(C_1)}{[OsO_4(OH)(H_2O)]^-} + OH^- \overset{K_1}{\rightleftharpoons} \underset{(C_2)}{[OsO_4(OH)_2]^{2-}} + H_2O \qquad (i)$$

$$C_2 + \begin{matrix} RCHOH \\ | \\ CH_2OH \end{matrix} \overset{K_2}{\rightleftharpoons} \underset{(X)}{complex} \qquad (ii)$$

$$X + NBS + H_2O \xrightarrow[\text{slow}]{k_d} Y + NSH + HBr + [OsO_2(OH)_4]^{2-} + HCOOH \qquad (iii)$$

$$Y + NBS + H_2O \xrightarrow[\text{fast}]{Os(VIII)/OH^-} RCOOH + NSH + HBr \qquad (iv)$$

$$[OsO_2(OH)_4]^{2-} + NBS + OH^- \xrightarrow[\text{fast}]{} [OsO_4(OH)_2]^{2-} + Br^- + NSH + H_2O \qquad (v)$$

where X stands for $\left[\begin{array}{c} RCHOH \\ | \\ H_2C-O-OsO_3(OH)_3 \end{array} \right]^{2-}$; R stands for $-CH_3$ and C_2H_5 in methyl

and ethyl glycols, respectively, and Y stands for RCHO and S stands for glycols.

Considering the above reaction steps, rate of the reaction in terms of loss of NBS can be written as follows:

$$-\frac{d[NBS]}{dt} = k_d\,[X]\,[NBS]. \qquad (1)$$

From step (1), we have

$$K_1 = \frac{[C_2]}{[C_1]\,[OH^-]}$$

Thus

$$[C_2] = K_1\,[C_1]\,[OH^-]. \qquad (2)$$

From step (2), we have

$$K_2 = \frac{[X]}{[C_2]\,[S]}.$$

Thus

$$[X] = K_2\,[C_2]\,[S]. \qquad (3)$$

Considering equations (1) and (3), we obtain the following:

$$-\frac{d[NBS]}{dt} = k_d\,K_2\,[C_2]\,[S]\,[NBS]. \qquad (4)$$

Total Os(VIII), i.e. $[Os(VIII)]_T$, can be written as

$$[Os(VIII)]_T = [C_1] + [C_2] + [X]. \qquad (5)$$

On substituting the value of C_1 from equation (2) and value of $[X]$ from equation (3) in equation (5), we have

$$[Os(VIII)]_T = \frac{[C_2]}{K_1\,[OH^-]} + [C_2] + K_2\,[C_2]\,[S]$$

$$[Os(VIII)]_T = [C_2]\,\frac{1 + K_1\,[OH^-] + K_1 K_2\,[OH^-]\,[S]}{K_1\,[OH^-]}$$

or

$$[C_2] = \frac{K_1\,[Os(VIII)]_T\,[OH^-]}{1 + K_1\,[OH^-] + K_1 K_2\,[OH^-]\,[S]} \tag{6}$$

By considering equations (4) and (6), we have

$$-\frac{d[NBS]}{dt} = \frac{k_d K_1 K_2 [NBS]\,[S]\,[Os(VIII)]_T\,[OH^-]}{1 + K_1[OH^-] + K_1 K_2\,[OH^-]\,[S]}. \tag{7}$$

The rate equation (7) explains all the observed kinetics. Hence the proposed mechanism is valid.

REFERENCES

1. R. SANEHI, M. C. AGARWAL, S. P. MUSHRAN: Mechanism of Oxidation of Some Aliphatic Ketones by N-bromosuccinimide in Acidic Media. J Phys Chem, **255**, 293 (1974).
2. J. N. TIWARI, A. KUMAR, S. P. MUSHRAN: Kinetics and Mechanism of Ru(III) Catalysed Oxidation of Some Polyhydric Alcohols by N-bromosuccinimide in Acidic Media. Annal de la Soc Sci de Brux, **66**, 847 (1969).
3. R. FILLER: Oxymercuration-demercuration of Limonene. Chem Rev, **63**, 21 (1963).
4. A. SHUKLA, S. K. UPADHYAY: Direct Ring Functionalisation of 1,4,7- trimethyl-1,4,7 triazacyclononane and Its Application in the Preparation of Functional($L_2Mn_2O_3$)- type Complexes. J Indian Chem Soc, **69**, 745 (1992).
5. S. K. MAVALANGI, S. M. DESAI, S. T. NANDIBEWOOR: Platinum(IV) Complexes of Reducing Sugar in an Alkaline Medium and Their Resistance to Reaction with N- bromosuccinmide. A Kinetic Study. Oxid Commun, **23**, 617 (2000).
6. P. S. RADHAKRISHNAMURTI, S. C. PATI: Kinetics and Mechanism of the Oxidation of Some Aliphatic Ketones by N-bromoacetamide in Acidic Media. J Indian Chem Soc, **66** (9), 847 (1969).
7. N. S. SRINIVASAN, N. VENKTASUBRAMANIAN: Kinetics and Mechanism of Oxidation of Cyclopentanone by N-bromsuccinimide. Indian J Chem, **9**, 726 (1971).
8. N. VENKTASUBRAMANIAN, V. THIAGARJAN: Mechanistic Investigation of Oxidation of Metronidazole and Tinidazole with N-bromosuccinimide in Acid Medium. A Kinetic Approach. Can J Chem, **47**, 694 (1969).
9. L. PANDEY, K. SINGH, S. P. MUSHRAN: Kinetic Study of Oxidation of Cycloheptanone by N-bromosuccinimide in Acidic Media. Curr Sci, **47** (17), 611 (1978).
10. K. SINGH, J. N. TIWARI, S. P. MUSHRAN: Kinetics and Mechanism of Oxidation of Diethyl Ketone by N-bromosuccinimide. Int J Chem, **10**, 995 (1978).
11. J. W. COOK, R. SCHOENTAL: The Reaction of Osmium Tetroxide–Pyridine Complexes with Nucleic Acid Components. Nature, **161**, 237 (1948).

12. B. L. CHANDWANI, G. D. MENGHANI: Kinetics and Mechanism of Oxidation of Some Alcohols by Osmium Tetroxide, **15A**, 560 (1977).

13. B. SINGH, B. B. SINGH, R. P. SINGH: Mechanism of Osmium Tetroxide Catalysed Oxidation of 2-bromopropionic Acid by Hexacyanoferrate(III) in Aqueous Alkaline Medium. J Inorg Nucl Chem, **43**, 1283 (1981).

14. V. N. SINGH, H. S. SINGH, B. B. L. SAXENA: Kinetics and Mechanism of the Osmium Tetroxide Catalyzed Oxidation of Acetone and Ethyl Methyl Ketone by Alkaline Hexacyanoferrate(III) Ion. J Am Chem Soc, **91**, 2645 (1968).

15. M. P. SINGH, H. S. SINGH, B. SINGH, A. K. SINGH: Mechanism of Osmium Tetroxide Catalysed Oxidation of 2-bromopropionic Acid by Hexacyanoferrate(III) in Aqueous Alkaline Medium. Proc Indian Nat Acad Sci, **41A**, 331 (1975).

16. B. H. ANAND, G. D. MENGHANI: Kinetics of Oxidation of Butane 2,3-diol by Osmium(VIII). J Indian Chem Soc, **57**, 374 (1981).

MECHANISM OF OXIDATION OF METHIONINE BY N-BROMONICOTINAMIDE. A KINETIC STUDY

L. PUSHPALATHA*, K. VIVEKANANDAN

Post-graduate and Research Department of Chemistry, National College, 620 001 Trichy, Tamilnadu, India
E-mail: lathaa_ramesh@yahoo.com

ABSTRACT

The kinetics of oxidation of methionine, an important sulphur-containing essential amino acid, by N-bromonicotinamide (NBN) in the presence of 0.8 mol dm^{-3} HCl in aqueous acetic acid medium at constant ionic strength has been studied. The reaction shows fractional order with respect to substrate, inverse first order about oxidant and hydrochloric acid. Addition of the reaction product, nicotinamide (NA), retarded the reaction. The rate increases with the increase in acetic acid proportion. Increase in temperature increases the rate. The activation parameters have been evaluated by studying the reaction at different temperatures. The stoichiometry of the reaction was found to be 1:1. HOBr has been postulated as the reactive oxidising species. Methionine sulphoxide was the product. The product obtained was isolated and identified.

Keywords: methionine, N-bromonicotinamide, kinetics, oxidation, mechanism.

AIMS AND BACKGROUND

The aim of the present work was to study the kinetics of oxidation of methionine by NBN in aqueous acetic acid medium in the presence of 0.8 mol dm^{-3} HCl and to propose a mechanistic pathway consistent with the observed kinetic data.

Our earlier work on the oxidation of amino acids had focused attention on the kinetic aspects of oxidation by N-chloronicotinamide (NCN) (Refs 1 and 2) and NBN (Refs 3–7) in aqueous acetic acid medium. In our continuing efforts to exploit NBN as oxidant, the kinetic features of oxidation of methionine are reported.

Methionine is a sulphur-containing essential amino acid which is not synthesised in the body and must be obtained from food. It contributes to supply mineral sulphur improving the tone and pliability of the skin, conditioning the hair and strengthens nails and protecting the cells from airborne pollutants. It contributes to other compounds

---

* For correspondence.

including S-adenosyl-methionine (SAM), which transfers labile methyl group and sulphur to over hundred biochemical reactions for normal brain function[8].

Methionine is a methyl donor and this process in the body is activated by adenosine triphosphate (ATP) and a liver enzyme such as phosphatase or dehydrogenase. Active methionine can transfer its methyl group to a variety of compounds and the high energy S-methyl bond is the prime reason for this behaviour. The oxidation of this biologically important amino acid is very important because it may reveal the mechanism of amino acid metabolism[9]. Methionine is used in pharmaceuticals, cosmetics, nutrition and biological studies and as a food and feed supplement. It is abundant in meat and other animal proteins. It is converted intracellularly to homocysteine through transmethylation with a methyl acceptor[10]. Homocysteine, i.e. the demethylated form of methionine, is not normally present in the aminoacid sequence of proteins, but it can accumulate in blood as well as in the intracellular fluids in a number of conditions, such as asteriosderosis, renal failure, the Alzheimer disease and neural tube defects[11].

N-halo reagents are widely used in fine organic synthesis. These include N-halo derivatives of amines, amides, imides, urea, saccharins, sulphonamides, sulphonimides, etc. N-halo reagents have the potential to promote important reactions such as halogenation, oxidation, and protection as well as formation of C–X, C–O, and C=O bonds. In addition to the numerous organic and inorganic halogenating agents, N-halo reagents play an especially important role in the chemistry of natural compounds[12]. NBN is chosen for the above reasons.

Vani and co-workers[13] investigated the effect of sodium dodecylsulphate micelles on the oxidation of L-methionine by chromium(VI) in perchloric acid medium. They have carried out oxidation of L-methionine with other oxidants[14–18] as manganese(III), iron(III)-2,2′-bipyridyl, iron(III)-1,10-henanthroline, bromate and thallium(III).

Elango[19] followed the kinetics and mechanism of oxidation of methionine by QCC in the presence of chloroacetic acid in water - acetic acid mixtures of varying mol fractions. Kinetics and mechanism of the oxidation of methionine was followed by scientists using various oxidants such as pyridinium chlorochromate[20], N-bromobenzenesulphonamide[21], periodate[22], N-bromosaccarin[23] and other amino acids with benzyltrimethylammonium dichloroiodate[24], chromium(VI):EDTA catalysis[9], osmium(VIII)-catalysed HCF[hexacyanoferrate(III)] (Ref. 8) leading to various products.

Elango[25] reported the kinetics and mechanism of oxidation of methionine by QFC in water–DMSO and water–acetic acid mixtures of varying mol fractions with a view to understand the utility of solvent variation studies in understanding the mechanism of this biologically important amino acid because it may reveal the mechanism of amino acid metabolism.

Kinetics of oxidation of methionine by sodium salts of 2-p-phenylsulphonic acid-2-phenyl-1-picrylhydrazyl and 2,2′-d-p-phenylsulphonic acid-2-phenyl-1-picrylhydrazyl at isoelectric point of amino acids has been studied by Ionita and co-

workers[26]. Kinetics of L-methionine oxidation by colloidal MnO_2 in perchloric acid (0.93 to 3.72×10^{-4} mol dm^{-3}) was studied spectrophotometrically by Ilyas[27]. Das[28] reported the kinetic and mechanistic studies on the reaction of DL-methionine with $[(H_2O)(tap)_2RuORu(tap)_2(H_2O)]^{2+}$ in aqueous medium at physiological pH. Kinetics of oxidation of methionine by manganese(III) in aqueous acetic acid (60%v/v) at 323 K was reported by Chidankumar[29].

The present study describes the kinetics of oxidation of methionine by NBN in aqueous acetic acid medium.

EXPERIMENTAL

Materials. N-bromonicotinamide (NBN) was prepared by the reported method[30]. Standard solution of NBN (m.p. 210°C) was prepared afresh in water and its purity was checked iodometrically. Methionine (A.R. Himedia) was used as such. Hydrochloric acid (AnalaR) was used as a source of hydrogen ions. Sodium perchlorate (Merck) was used to keep the ionic strength constant. Acetic acid (A.R.,Qualigen) was purified by refluxing with chromic oxide and acetic anhydride for 6 h followed by fractional distillation[31]. Mercuric acetate was added to suppress the formation of free bromine which otherwise would have vitiated the results. Mercuric acetate did not interfere with the results[32]. Ionic strength of the medium was kept at 0.1 mol dm^{-3} by employing concentrated aqueous solution of sodium perchlorate (Merck). Conductivity water was used throughout the study. Other chemicals used were of analytical grade.

Kinetic measurements. The reaction was carried out under pseudo-first order condition ([methionine] >> [NBN]). The reaction was followed potentiometrically by setting up a cell made up of the reactio mixture into which the platinum electrode and reference electrode(SCE) were dipped. The e.m.f. of the cell was measured periodically using an Equip-Tronics (EQ-DGD) potentiometer. The pseudo-first order rate constants computed from the linear ($r^2 > 0.9990$) plots of lg ($E_t - E_\infty$) against time. Duplicate kinetic runs showed that the rate constants were reproducible within ±3%. The course of the reaction was studied for more than two half-lives.

Stoichiometry and product analysis. A mixture of methionine (0.01 mol dm^{-3}), NBN(0.05 mol dm^{-3}) and HCl (0.8 mol dm^{-3}) was made up to 100 ml with water and acetic acid mixture (1:1). After the reaction was completed, the excess of NBN was determined iodometrically and indicated 1:1 stoichiometry. The overall stoichiometry of the oxidation reaction may be represented as follows:

$$NBN + MeSR + H_2O \rightarrow MeSOR + Br^- + NA \quad\quad (1)$$

where R = $-CH_2CH_2CH(NH_2)COOH$.

In a typical experiment, a mixture of methionine (7.46 g, 1 mol dm^{-3}) and NBN (1.5 g, 0.2 mol dm^{-3}) was made up to 50 ml with acetic acid–water mixture (1:1) in the presence of HCl (0.8 mol dm^{-3}). The mixture was allowed to stand for 12 h in the

dark to ensure completion of the reaction. The reaction mixture was allowed to stand for a few hours. Then, sodium bicarbonate was added and stirred vigorously, followed by a dropwise addition of benzoyl chloride solution. The precipitate N-benzoyl methionine sulfoxide was confirmed by its m.p. 183°C (Ref. 33). Acetone–ethanol mixture (1:1) added to the reaction mixture resulted in the precipitate of methionine sulphoxide, which was identified by its m.p. 238°C (Ref. 34).

RESULTS

The kinetic results for the oxidation of methionine by N-bromonicotinamide (NBN) can be summarised as follows. The kinetic studies were carried out under pseudo-first order conditions with [methionine] >> [NBN].

Effect of varying [*oxidant*]. The oxidation was carried out with different initial concentrations of NBN. The pseudo-first order rate constants decrease with increase in the initial concentration of the oxidant. But in each kinetic run, the reaction shows no deviation whatsoever from the first order plot (Table 1).

Table 1. Effect of variation of [NBN] on reaction rate
[Met]=0.04 mol dm^{-3}; [HCl]=0.8 mol dm^{-3}; [NaClO$_4$]=0.1 mol dm^{-3}; H$_2$O:CH$_3$COOH (1:1); Hg(CH$_3$COO)$_2$=0.005 mol dm^{-3}; temperature 308 K

[NBN] $\times$ 10^3 (mol dm^{-3})	k_{obs} $\times$10^5 (s^{-1})
4.0	4.45
5.0	4.29
6.0	4.19
7.0	4.11
8.0	4.05

Effect of varying [*methionine*]. At constant [H$^+$], with the [methionine] in excess, the plot of lg ($E_t - E_\infty$) (where E_t is the e.m.f. of the cell at time t and E_∞ – the corresponding value at the completion of the reaction) versus time is linear, indicating a first order dependence of rate on [NBN]. Increase in [methionine] has a slight positive effect on the rate, indicating fractional order dependence of rate on [methionine] (Ref. 35) (Table 2).

Table 2. Effect of variation of [Met] on reaction rate
[NBN]= 0.004 mol dm^{-3}; [HCl] = 0.8 mol dm^{-3}; [NaClO$_4$]=0.1 mol dm^{-3}; H$_2$O:CH$_3$COOH (1:1); Hg(CH$_3$COO)$_2$=0.005 mol dm^{-3}; temperature 308 K

[Met]$\times$ 10^2 (mol dm^{-3})	k_{obs} $\times$10^5 (s^{-1})
4.0	4.45
5.0	4.57
6.0	4.66
7.0	4.72
8.0	4.86

Effect of varying [*H*⁺]. The rates decreased with increase in [H⁺],at fixed [NBN] and [methionine], showing inverse order dependence in [H⁺] (Table 3).

Table 3. Effect of variation of [HCl]
[Met]=0.04 mol dm⁻³; [NBN]=0.004 mol dm⁻³; [NaClO₄]=0.1 mol dm⁻³; H₂O:CH₃COOH (1:1); Hg(CH₃COO)₂=0.005 mol dm⁻³; temperature 308 K

[HCl] (mol dm⁻³)	k_{obs} ×10⁵ (s⁻¹)
0.8	4.45
0.9	3.55
1.0	2.80
1.1	2.29

The effect of [H⁺] was investigated in the range 0.8–1.2 mol dm⁻³ of perchloric acid at constant [Cl⁻] (0.8 mol dm⁻³) and the rate decreases proportionally with increase in [H⁺]. The plot of lg k_{obs} versus lg [H⁺] is linear and with negative slope. The effect of [Cl⁻] on the rate of reaction was also studied by increasing the [NaCl] from 0.8–1.2 mol dm⁻³ at constant [HClO₄] and found to be constant (Table 4).

Table 4. Effect of variation of [H⁺] and [Cl⁻] on reaction rate
[Met] =0.04 mol dm⁻³; [NBN]=0.004 mol dm⁻³; H₂O:CH₃COOH (1:1); Hg(CH₃COO)₂= 0.005 mol dm⁻³; temperature 308 K

[HClO₄] (mol dm⁻³)	[NaCl] (mol dm⁻³)	k_{obs} ×10⁵ (s⁻¹)
0.8	0.8	4.45
0.9	0.8	3.89
1.0	0.8	3.05
1.1	0.8	2.35
1.2	0.8	1.90

Effect of variation of dielectric constant of the medium (*Table 5*). An increase in the rate constant is noticed on decreasing the dielectric constant of the medium. Plot of lg k_{obs} versus 1/D (r=0.9901), where D is the dielectric constant of the medium, gives straight line with positive slope[36]. An increase in the amount of acetic acid in the solvent results in an increase in the rate of oxidation. Thus according to Amis, an interaction between a dipole and a positive ion is indicated, though the behaviour is not ideal.

Table 5. Effect of variation of [CH₃COOH:H₂O] on reaction rate
[Met]=0.04 mol dm⁻³; [NBN]=0.004 mol dm⁻³; [HCl]=0.8 mol dm⁻³; Hg(CH₃COO)₂= 0.005 mol dm⁻³; [NaClO₄]= 0.1 mol dm⁻³; temperature 308 K

CH₃COOH (%)	H₂O (%)	D	k_{obs} ×10⁵ (s⁻¹)
50	50	37.50	4.45
55	55	34.75	5.25
60	40	31.50	6.23
65	35	28.50	7.35

Effect of addition of nicotinamide. The rate of reaction decreases on adding nicotinamide (NA). Thus added nicotinamide has a retarding effect on the rate of oxidation. Further the plot of $1/k_{obs}$ versus [NA] is linear indicating inverse dependence of rate on [NA] (Ref. 37).

Effect of added salts on reaction rate. The effect of added salts like Na_2SO_4, KCl, $BaCl_2$ and K_2SO_4 on the reaction rate was studied by adding various concentrations of these salts, keeping the concentrations of methionine, HCl and NBN constant. It was observed that the rates of oxidation did not altered by the addition of these neutral salts.

Test for free radicals. The possibility of free radical intervention in the reaction was tested as follows. The reaction mixture containing acrylonitrile scavenger was kept for 24 h in an inert atmosphere and then diluted. On dilution, formation of precipitate was not observed indicating the absence of free radical intervention in the reaction.

Table 6. Effect of temperature on reaction rate
[Met]=0.04 mol dm^{-3}; [NBN]=0.004 mol dm^{-3}; [HCl]=0.8 mol dm^{-3}; [$NaClO_4$]=0.1 mol dm^{-3}; H_2O:CH_3COOH (1:1); $Hg(CH_3COO)_2$=0.005 mol dm^{-3}

Temperature (K)	$k_{obs} \times 10^5$ (s^{-1})
308	4.45
313	5.45
318	6.63
323	8.02
328	9.63

Table 7. Activation parameters

Substrate	E_a (kJ mol^{-1})	ΔH^* (kJ mol^{-1})	ΔS^* (J K^{-1} mol^{-1})	ΔG^* (kJ mol^{-1})
Met	16.71	14.15	-176.20	68.40

Effect of temperature. Increase in temperature increases the rate of oxidation and plot of lg k_{obs} versus reciprocal of temperature is linear. The oxidation of methionine was studied at different temperatures (308 to 328 K) (Table 6). The activation parameters were evaluated (Table 7).

DISCUSSION

The possible oxidising species in acidified aqueous acetic acid solution are NBN, $NBNH^+$, NBNBr, Br_2, HOBr and H_2OBr^+ (Ref. 38). The observed first order dependence of the reaction rate on NBN rules out NBNBr and molecular bromine as the reactive oxidising species. $NBNH^+$ and H_2OBr may be discarded because of inverse dependence of reaction rate on [H^+] (Ref. 39). The same observation has been made in the oxidation of methionine by hypobromous acid (Table 3). Of the remaining two, HOBr and not NBN should be the oxidising species, since the rate is also inverse

function of nicotinamide concentration. A plot of inverse of the observed rate constant against the nicotinamide concentration is linear (r=0.9920).

Mechanism. Addition of nicotinamide decreases the rate of oxidation[37]. This retarding effect suggests that the pre-equilibrium step involves a process in which nicotinamide is one of the products.

$$NBN + H_2O \underset{k_{-1}}{\overset{k_1}{\rightleftharpoons}} NA + HOBr \qquad (2)$$
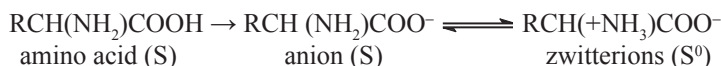
In acid medium, methionine exists in its protonated form (SH$^+$) which is resistant to attack by NBN. It is observed that the rate has inverse dependence on [H$^+$]. Thus the only species possibly controlling the rate of oxidation seems to be H$_3$CSCH$_2$CH$_2$CH(NH$_2$)COOH.

The electrophilic attack of HOBr on the nitrogen atom of methionine results in the formation of N-bromo derivative[21] which cleaves in fast steps to give the final product, methionine sulphoxide.

$$HOBr + S \xrightarrow{\text{fast}} products$$
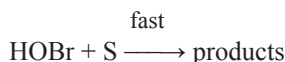
It may be pointed out that in the present study, oxidation by bromine was completely suppressed as the oxidative studies were carried out in the presence of mercuric acetate which combines with bromide ions formed in the reaction. Thus kinetics of only NBN oxidation was followed.

An α-amino acid is known to exist in the following equilibria in aqueous solution:

$$\underset{\text{amino acid (S)}}{RCH(NH_2)COOH} \rightarrow \underset{\text{anion (S)}}{RCH(NH_2)COO^-} \rightleftharpoons \underset{\text{zwitterions (S}^0)}{RCH(^+NH_3)COO^-}$$
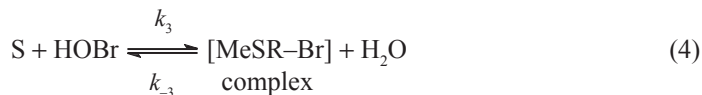
The dissociation of amino acid depends on the pH of solution. In fact, under the experimental conditions the concentration of anion-form will be very low and the possibility of its participation in the reaction will be least. The only possible reactive reducing species may be either the cation-form of amino acid or its zwitterion[40].

The first order dependence on [methionine] and [NBN] reveals that overall rate may involve the interaction of HOBr and methionine in the rate-determining step. But first order in the [methionine] and a definite intercept in the $1/k_{obs}$ versus 1/[sub] plot suggest that the decomposition of the complex formed from the substrate and HOBr (Ref. 21) is the rate-determining step as shown in Scheme.

<div align="center">S c h e m e</div>

$$SH^+ \underset{k_{-2}}{\overset{k_2}{\rightleftharpoons}} S + H^+ \qquad (3)$$

$$S + HOBr \underset{k_{-3}}{\overset{k_3}{\rightleftharpoons}} \underset{\text{complex}}{[MeSR\text{--}Br]} + H_2O \tag{4}$$

$$[MeSR\text{--}Br] \rightarrow MeSOR + Br^- \tag{5}$$

where $R = -CH_2CH_2CH(NH_2)COOH$.

The rate law for the above mechanism may be divided as follows:

$$\text{rate} = -\frac{d[NBN]}{dt} = k_d[\text{complex}]. \tag{6}$$

Substituting [NBN] in equation (6) and on rearranging the equation:

$$\left(\frac{k_{-1}k_{-2}k_{-3}[NA]\,[H^+]}{k_d k_1 k_2 k_3} + \frac{k_{-2}k_{-3}[H^+]}{k_d k_2 k_3} \right) \frac{1}{[SH^+]} + \frac{1}{k_d} = \frac{1}{k_{obs}}. \tag{7}$$

The rate-determining step proposed in the above mechanism predicts negligible salt effect which has been experimentally observed.

The formation of the complex involves the charge separation which leads to a negative solvent effect. This has been confirmed by the increase in rate with decreasing dielectric constant of the medium. The involvement of amino acid molecule in the rate-determining step leads to different values of k_{obs} for different initial concentrations of amino acids under study, namely, non-essential amino acids.

The proposed mechanism is well supported by the moderate values of energy of activation and thermodynamic parameters. The negative entropy of activation indicates the complex formation as suggested in the above reaction mechanism, and also indicates that the complex is more ordered than reactants[41]. High positive values of the free energy of activation and the enthalpy of activation show that the transition state is highly solvated.

CONCLUSIONS

The rate of the reaction depends on the first power of concentration of H^+ and NBN. Increase in acetic acid percentage increases the rate. Added nicotinamide retards the reaction. Addition of salts to the reaction medium has no effect on the rate. Increase in temperature increases the rate of reaction. The activation parameters are evaluated from the study of oxidation at different temperatures. The product obtained, methionine sulphoxide, was isolated and identified.

ACKNOWLEDGEMENTS

REFERENCES

1. K. VIVEKANANDAN: Oxidative Decarboxylation and Deamination of Proline, Histidine, Arginine, Lysine and Tyrosine by N-chloronicotinamide in Aqueous Acetic Acid Medium. A Kinetic Study. Oxid Commun, **27**(1), 195 (2004).
2. K. VIVEKANANDAN, K. NAMBI: N-chloronicotinamide – A New, Mild, Stable, Efficient and Inexpensive Oxidant for Organic Substrates. J Indian Chem Soc, **76**, 198 (1999).
3. L. PUSHPALATHA, K. VIVEKANANDAN: Oxidative Decarboxylation and Deamination of Essential Amino Acids by N-bromonicotinamide – A Kinetic Study. J Indian Chem Soc, **86**, 475 (2009).
4. L. PUSHPALATHA, K. VIVEKANANDAN: N-bromonicotinamide Oxidation of Essential Amino Acids. A Kinetic Study. Oxid Commun, **32** (1), 85 (2009).
5. L. PUSHPALATHA, K. VIVEKANANDAN: Oxidation of Acidic Amino Acids by N-bromonico-tinamide. A Kinetic Study. Oxid. Commun., **31** (3), 598 (2008).
6. L. PUSHPALATHA, K. VIVEKANANDAN: Oxidative Kinetics of Serine and Threonine by N-bromonicotinamide. J Indian Chem. Soc., **85,** 1027 (2008).
7. L. PUSHPALATHA, K. VIVEKANANDAN: Kinetics of Oxidation of Cysteine by NBN and NCN in Aqueous Acetic Acid Medium. A Comparative Study. Oxid Commun (in press).
8. T. P. JOSE, S. T. NANDIBEWOOR, S. M. TUWAR: Osmium(VIII) Catalysed Oxidation of a Sulphur Containing Amino Acid- a Kinetic and Mechanistic Approach. J Sulphur Chem, **27** (1), 25 (2006).
9. S. MEENAKSHISUNDARAM, R. VINOTHINI: Kinetics and Mechanism of Oxidation of Methionine by Chromium(VI): EDTA Catalysis. Croat Chem Acta, **76** (1), 75 (2003).
10. P. TESSARI, E. KIWANUKA, A. CORACINA, M. ZARAMELLA, M. VETTORE, A. VALERIO, G. GARIBOTTO: Effects of Insulin on Methionine and Homocysteine Kinetics in Type-2 Diabetes. Am J Physiol Endocrinol Metab, **288**, E1270 (2005).
11. M. J. WOODA, J. H. PRIETOB, E. A. KOMIVESB: Structural and Functional Consequences of Methionine Oxidation in Thrombomodulin. Biochim Biophys Acta, **1703**, 141 (2005).
12. E. KOLVARI, A. GHORBANI-CHOGHAMARANI, P. SALEHI, F. SHIRINI, M. A. ZOLFIGOL: Application of N-halo Reagents in Organic Synthesis. J Iran Chem Soc, **4** (2), 126 (2007).
13. K. KRISHNA KISHORE, A. KALYAN KUMAR, N. ANNAPURNA, P. VANI: Effect of Sodium Dodecylsulphate Micelles on the Oxidation of L-methionine by Chromium(VI) in Perchloric Acid Medium. J Indian Chem Soc, **84**, 373 (2007).
14. P. VANI, T. RAJARAJESWARI, L. S. A. DIKSHITULU: Mechanism of Oxidation of L-methionine with Manganese(III). React Kinet Catal Lett, **52**, 175 (1994).
15. P. VANI, T. RAJARAJESWARI, L. S. A. DIKSHITULU: Mechanism of Oxidation of L-methionine with Iron(III)-2,2′-bipyridyl. Transit Metal Chem, **20**, 170 (1995).
16. P. VANI, K. KRISHNA KISHORE, R. RAMBABU, L. S. A. DIKSHITULU: Mechanism of Oxidation of L-methionine with Iron(III)-1,10-phenanthroline. Proc Indian Acad Sci (Chem Sci), **113**, 351 (2001).
17. P. VANI, T. RAJARAJESWARI, L. S. A. DIKSHITULU: Mechanism of Oxidation of L-methionine with Bromate in Sulphuric Acid Medium. J Indian Chem Soc, **72**, 867 (1995).
18. P. VANI, T. RAJARAJESWARI, L. S. A. DIKSHITULU: Mechanism of Oxidation of L-methionine with Thallium(III). J Indian Chem Soc, **78**, 44 (2001).
19. D. S. BHUVANESWARI, B. JOHN, M. PANDEESWARAN, K. P. ELANGO: Kinetics and Mechanism of Oxidation of Methionine by QCC in Presence of Chloroacetic Acid. J Indian Chem Soc, **82**, 616 (2005).
20. V. SHARMA, P. K SHARMA, K. K. BANERJI: Kinetics and Mechanism of Oxidation of DL-methionine by Pyridinium Fluoro Chromate. J Indian Chem Soc, **74**, 607 (1997).
21. S. ANANDA, K. S. RANGAPPA, D. S. MAHADEVAPPA: Oxidation of Methionine by Sodium N-bromobenzenesulphonamide: A Kinetic Study. J Indian Chem Soc, **63**, 581 (1986).
22. J. R. CLAMP, L. HOUGH: The Periodate Oxidation of Amino Acids with Reference to Studies on Glycoproteins. Biochem J, **94**, 17 (1965).

23. C. MOHANADAS, P. INDRASENAN: Kinetics and Mechanism of Oxidation of Methionine by N-bromosaccharin. Indian J Chem, **26A**, 55 (1987).
24. DIMPLE GARG, SEEMA KOTHARI: Kinetics and Mechanism of Oxidation of Amino Acids by Benzyltrimethylammonium Dichloroiodate. J Indian Chem Soc, **83**, 172 (2006).
25. D. S. BHUVANESWARI, B. JOHN, M. PANDEESWARAN, K. P. ELANGO: Kinetics and Mechanism of Oxidation of Methionine by QFC. J Serb Chem Soc, **70** (2), 145 (2005).
26. G. IONITA, V. E. SAHINI, G. SEMENESCA, P. IONITA: Kinetics of Oxidation of Methionine by Sodium Salts of 2-*p*-phenylsulphonic Acid-2-phenyl-1-picrylhydrazyl and 2,2'-di-*p*-phenylsulphonic Acid-2-phenyl-1-picrylhydrazyl at Isoelectric Point of Amino Acids. Acta Chim Slov, **47**, 111 (2000).
27. M. ILYAS, M. A. MALIK, Z. KHAN: A Kinetic Study of Oxidation of L-methionine by Water Soluble Colloidal MnO_2. Colloid Polym Sci, **285**, 1169 (2007).
28. T. DAS, A. K. DATTA, A. K. GHOSH: Kinetic and Mechanistic Studies on the Reaction of DL-methionine with $[(H_2O)(tap)_2RuORu(tap)_2(H_2O)]^{2+}$ in Aqueous Medium at Physiological pH. Research Letters in Inorganic Chemistry, 2009.
29. C. S. CHIDANKUMAR, S. CHANDRAJU, N. M. MADE GOWDA: Kinetics of Oxidation of Methionine by Manganese(III) in Aqueous Acetic Acid. Synth React Inorg Me, **39**, 645 (2009).
30. C. R. HAUSER, W. B. RENFROW, Jr.: The Removal of HX from Organic Compounds by Means of Bases.III. The Rates of Removal of Hydrogen Bromide from Substituted N-bromobenzamides and Their Relative Ease of Rearrangement in the Presence of Alkali. The Hofmann Rearrangement. J Am Chem Soc, **59**, 121 (1923).
31. D. D. PERRIN, W. L. AMAREGO, D. R. PERRIN: Purification of Organic Compounds. Pergamon, Oxford, 1966.
32. A. AGARWAL, S. MITTAL, K. K. BANERJI: Kinetics and Mechanism of Oxidation of Amino Acids by N-bromoacetamide in Acid Medium. Indian J Chem, **26A**, 339 (1987**)**.
33. K. B. GOSWAMI, G. CHANDRA, S. N. SRIVASTAVA: Kinetics and Mechanism of Oxidation of Methionine. J Indian Chem Soc, **58**, 252 (1981).
34. G. NATILE, E. BORDIGNON, L. CATTALINI: Mechanism of Oxidation of L-methionine. Inorg Chem, **15**, 246 (1976).
35. S. YATHIRAJAN, C. R. RAJU, K. N. MOHANA, S. SHASHIKANTH, P. NAGARAJA: Kinetics and Mechanism of Oxidation of L-isoleucine and L-ornithine Hydrochloride by Sodium N-bromobenzenesulpnonamide in Perchloric Acid Medium. Turk J Chem, **27**, 571 (2003).
36. E. S. AMIS: Solvent Effects on Reaction Rates and Mechanisms. Academic Press, New York, 1976.
37. S. C. NEGI, K. K. BANERJI: Kinetics and Mechanism of Oxidation of Secondary Alcohols by N-bromoacetamide in Acid Medium. Indian J Chem, **21B**, 846 (1982); S. C. NEGI, K. K. BANERJI: Kinetics and Mechanism of Oxidation of the Alcohols by N-bromoacetamide in Alkaline Solution. J Org Chem, **48**, 3329 (1983).
38. K. K. BANERJI: Kinetics and Mechanism of Oxidation of Amino Acids by N-bromoacetamide in Acid Medium. J Org Chem, **51**, 4764 (1986).
39. M. K. REDDY, Ch. S. REDDY, E. V. SUNDARAM: Oxidative Kinetics of Amino Acids by N-bromoacetamide. A Study of Solvent Effect and General Base Catalysis. Tetrahedron, **41** (15), 3071 (1985).
40. S. P. MUSHRAN, J. N. TIWARI, A. K. BOSE, K. SINGH: Kinetics of Oxidation of Alanine and Valine by N-bromosuccinimide. Indian J Chem, **16A**, 35 (1978).
41. A. WEISSBERGER: Techniques of Chemistry. Investigations of Rate and Mechanism of Reaction. Wiley Interscience Publication, New York, 1974.

PHYSICAL CHEMISTRY KINETICS OF OXIDATION OF CYSTEINE BY N-BROMONICOTINAMIDE AND N-CHLORONICOTINAMIDE IN AQUEOUS ACETIC ACID MEDIUM. A COMPARITIVE STUDY

K. VIVEKANANDAN*, L. PUSHPALATHA

*Postgraduate and Research Department of Chemistry, National College,
620 001 Trichy Tamil nadu, India
E-mail*: *viveksabathi@gmai.com*

ABSTRACT

The kinetics of oxidation of L-cysteine was studied using N-bromonicotinamide (NBN) in the presence of 0.8 mol dm^{-3} HCl in aqueous acetic acid medium. The reaction exhibits fractional order in cysteine concentration indicating that the zwitter ionic form of cysteine is more reactive. Cystine, the disulphide of cysteine, is identified as the product of oxidation. A suitable mechanism involving the formation of sulphur-bonded intermediate is proposed. The activation parameters of the reaction are computed using the linear least square method. It is of interest to compare the kinetics of oxidation of cysteine by NCN, the chlorine analog of the present oxidant, NBN. Mercaptoacetaldehyde is the product in the latter reaction.

Keywords: cysteine, N-bromonicotinamide, N-chloronicotinamide, kinetics, oxidation, mechanism.

AIMS AND BACKGROUND

The aims of the paper were to follow the kinetics of oxidation of cysteine, a dispensable amino acid by N-bromonicotinamide, a N-halo reagent, in acetic acid - water medium in the presence of hydrochloric acid at constant ionic strength and to suggest a mechanism consistent with the observed results. It is also of significance to compare the results of the present study with that of its chlorine analog, namely, N-chloronicotinamide.

The development of N-halo reagents for the versatile applications in synthetic organic chemistry continues to be a subject of interest. The reagent employed in this

---

* For correspondence.

investigation, N-bromonicotinamide (NBN), $C_6H_5N_2OBr$, has emerged as a useful and versatile oxidant which has been used for the oxidation of amino acids[1–5] and aromatic aldehydes[6].

Cysteine is a tribasic acid $HSCH_2CH(NH_2)COOH$. It is a dispensable amino acid. The wish to generate designer proteins that rival the properties of their natural counterparts has been a long sought goal after. The complexities involved in the *de novo* design of proteins are overwhelming and current computational methods do not permit any great degree of freehand protein design. Bioconjugation is the simplest and longest standing method for the introduction of non-natural amino acids into proteins. The most widely used bioconjugation strategy exploits the latent nucleophilicity of the thiol side chain of cysteine[7].

Thiols have been oxidised by a variety of oxidants. The oxidants include bromate[8], potassium hexacyanoferrate(III) (Ref. 9) in the presence of sodium dioctylsulpho-succinate, quinolinium dichromate (QDC) (Ref. 10), alkaline hexacyanoferrate(III) (Ref. 11), N-bromosaccharin (NBSa) (Ref. 12), chromium(VI) (Ref. 13) at neutral pH, 12-tungstocobaltate(III) (Ref. 14), tris-oxalocobaltate(III) (Ref. 14), μ-oxobisaquo(2,2′-bipyridine)ruthenium(III) (Ref. 14), chloramine-T (Ref. 15) and bromamine-B (Ref. 16). In most of its oxidations, cysteine is reported to be the main product of oxidation. Jacob et al.[17] studied the aspects of the biological redox chemistry of cysteine. Cysteine[18] kinetics and oxidation at different intakes of methionine and cystine in young adults were carried out by Raguso and co-workers[18].

Vani et al. reported the mechanism of oxidation of cysteine by hexachloroiridate(IV) (Ref. 14). Oxidation of cysteine by ferrozineiron(III) complex in aqueous acidic medium was carried out by Warad et al.[19]. Khalid[20] investigated the oxidative kinetics of cysteine by peroxydisulphate. Quyoom and Khan[21] reported the potentiometric and UV spectral studies of binary and ternary complexes of some metal ions with N-acetylcysteine and some biologically important amino acids.

EXPERIMENTAL

Materials. N-bromonicotinamide (NBN) was prepared by the reported method[22]. Standard solution of NBN (m.p. 210°C; yield 70%) was prepared afresh in water and its purity was checked iodometrically. The amino acids (A. R. Loba) were used as such. Hydrochloric acid(AnalaR) was used as a source of hydrogen ions. Sodium perchlorate (Merck) was used to keep the ionic strength constant. Acetic acid (A. R., Qualigen) was purified by refluxing with chromic oxide and acetic anhydride for 6 h followed by fractional distillation[23]. Mercuric acetate was added to suppress the formation of free bromine which otherwise would have vitiated the results. Mercuric acetate did not interfere with the results[24]. Ionic strength of the medium was kept at 0.1 mol dm^{-3} by employing concentrated aqueous solution of sodium perchlorate (Merck). Conductivity water was used throughout the study. Other chemicals used were of analytical grade.

N-chloronicotinamide (NCN) (Ref. 25) was prepared by passing a slow stream of chlorine into a solution of nicotinamide (15 g in 30 ml 3N HCl) at 30°C for 30 min. The NCN formed as a white precipitate was filtered and the process of passing chlorine into the filtrate and filtering off the precipitate was repeated till no precipitate was obtained. It was filtered, washed with ether and recrystallised from ethanol (m.p. 223°C; yield 75%).

Kinetic measurements. The reaction was carried out under pseudo-first order condition ([cysteine] >> [NBN]). The reaction was followed potentiometrically by setting up a cell made up of the platinum electrode and reference electrode (SCE) dipped into the reaction mixture. The e.m.f. of the cell was measured periodically using an Equip-Tronics (EQ-DGD) potentiometer. The pseudo-first order rate constants were computed from the linear ($r^2 > 0.9990$) plots of lg ($E_t - E_\infty$) against time. Duplicate kinetic runs showed that the rate constants were reproducible within ±3%. The course of the reaction was studied for more than two half-lives.

STOICHIOMETRY

A mixture of cysteine (0.01 mol dm^{-3}), NBN (0.005 mol dm^{-3}) and HCl (0.8 mol dm^{-3}) was made up to 100 ml with water and acetic acid mixture (1:1). After the reaction was complete, the excess of NBN was determined iodometrically and indicated 2:1 stoichiometry. The overall stoichiometry of the oxidation reaction may be represented as follows:

$$NBN + 2HSCH_2CH(NH_2)COOH \rightarrow cystine + CO_2 + NH_3 + Br^- + NA$$

100 ml of 0.01 mol dm^{-3} of cysteine in 50% of acetic acid and 100 ml of 0.005 mol dm^{-3} of NCN in water were taken in 2 different bottles and thermostated at 300 K. Different volumes of each of these solutions were mixed with 0.8 mol dm^{-3} HCl in the reaction vessels, so that the ratio of concentrations of NCN and cysteine was different.

$$NCN + cysteine \rightarrow HSCH_2CHO + CO_2 + {}^+NH_4 + Cl^-$$

PRODUCT ANALYSIS

In a typical experiment, a mixture of cysteine (1 mol dm^{-3}) and NBN (1.5 g, 0.2 mol dm^{-3}) was made up to 50 ml with acetic acid - water mixture (1:1) in the presence of HCl (0.8 mol dm^{-3}). The mixture was allowed to stand for 12 h in the dark to ensure completion of the reaction. It was taken in ether, washed with water, the ether evaporated, and the residue refluxed with toluene for 1 h. The solution was concentrated and allowed to cool overnight. Crystals of the disulphide were precipitated, which were recrystallised from ether (m.p. 260°C; yield ~ 75%).

L-cysteine (1.2116 g, 0.2 M) and NCN (1.556 g, 0.02 M) were dissolved in 50 ml of 1:1 acetic acid, water and allowed to stand in the dark for 24 h to ensure the completion of the reaction. The mixture was then treated with an excess (125 ml) of

a saturated solution of 2,4-dinitrophenylhydrazine in HCl (2 mol dm^{-3}) and set aside for 10 h. The precipitated 2,4-dinitrophenylhydrazone(DNP) was filtered off, dried, weighed and recrystallised from ethanol (m.p. 127°C; yield ~ 80%). The product is mercaptoacetaldehyde. The presence of sulphur in the product was qualitatively ascertained by standard methods[26].

RESULTS

The kinetic results for the oxidation of cysteine by N-bromonicotinamide(NBN) and N-chloronicotinamide (NCN) can be summarised as follows. As the results are similar, only representative data are given. The kinetic studies were carried out under pseudo-first order conditions with [cysteine]>>[oxidant].

Effect of varying [oxidant]. The oxidation was carried out with different initial concentrations of NBN and NCN. The pseudo-first order rate constants decrease with increase in the initial concentration of the oxidant. But in each kinetic run, the reaction shows no deviation whatsoever from the first order plot (Table 1 A and B).

Table 1. A. Effect of variation of [NBN] on reaction rate
[Cys]=0.04 mol dm^{-3}; [HCl]=0.8 mol dm^{-3}; [NaClO$_4$]=0.1mol dm^{-3}; H$_2$O:CH$_3$COOH (1:1); Hg(CH$_3$COO)$_2$=0.005 mol dm^{-3}; temperature 308 K

B. Effect of variation of [NCN] on reaction rate
[Cys]=0.025 mol dm^{-3}; [HCl]=0.6 mol dm^{-3}; [NaClO$_4$]=0.4mol dm^{-3}; H$_2$O:CH$_3$COOH (1:1); temperature 300 K

[NBN] × 10^3 (mol dm^{-3})	k_{obs}× 10^5 (s^{-1})	[NCN] × 10^3 (mol dm^{-3})	k_{obs} ×10^3 (s^{-1})
4.0	7.60	3.5	3.80
5.0	7.32	4.0	3.43
6.0	7.05	4.5	3.20
7.0	6.88		
8.0	6.76		

Effect of varying [amino acid]. At constant [H$^+$], with the [cysteine] in excess, the plot of lg ($E_t - E_\infty$) (where E_t is the e.m.f. of the cell at time t and E_∞ – the corresponding value at the completion of the reaction) verus time is linear, indicating a first order dependence of rate on [NBN] and [NCN]. Increase in [cysteine] has a slight positive effect on the rate, indicating fractional order dependence of rate on [cysteine] (Ref. 27) (Table 2 A and B).

Table 2. Effect of variation of [Cys] on reaction rate

A. [NBN]= 0.004 mol dm^{-3}; [HCl] = 0.8 mol dm^{-3}; [NaClO$_4$]=0.1 mol dm^{-3}; H$_2$O:CH$_3$COOH (1:1); Hg(CH$_3$COO)$_2$=0.005 mol dm^{-3}; temperature 308 K

B. [NCN]=0.0035 mol dm^{-3}; [HCl]=0.6 mol dm^{-3}; [NaClO$_4$]=0.4 mol dm^{-3}; H$_2$O:CH$_3$COOH (1:1); temperature 300 K

[Cys] × 10^2 (mol dm^{-3})	k_{obs} × 10^5 (s^{-1})	[Cys] × 10^2 (mol dm^{-3})	k_{obs} × 10^3 (s^{-1})
4.0	7.60	2.0	3.80
5.0	7.88	3.0	4.16
6.0	8.06	4.0	4.53
7.0	8.24	5.0	4.83
8.0	8.49		

Effect of varying [*H*$^+$]. The rates decreased with increase in [H$^+$], at fixed [NBN] and [cysteine], showing inverse order dependence in [H$^+$]. The rate of the reaction was found to increase with increase of hydrochloric acid concentration in NCN oxidation (Table 3 A and B). The plot of lg k_{obs} versus lg [HCl] was linear with a unit slope indicating first order dependence of hydrochloric acid concentration. Therefore, the reaction is acid-catalysed.

Table 3. Effect of variation of [HCl] on reaction rate

A. [Cys]=0.04 mol dm^{-3}; [NBN]=0.004 mol dm^{-3}; [NaClO$_4$]=0.1 mol dm^{-3}; H$_2$O:CH$_3$COOH (1:1); Hg(CH$_3$COO)$_2$=0.005 mol dm^{-3}; temperature 308 K

B. [NCN]=0.0035 mol dm^{-3}; [Cys]=0.025 mol dm^{-3}; [NaClO$_4$]=0.4 mol dm^{-3}; H$_2$O:CH$_3$COOH (1:1); temperature 300 K

[HCl] (moldm^{-3})	k_{obs} ×10^5 (s^{-1})	[HCl] (mol dm^{-3})	k_{obs} ×10^3 (s^{-1})
0.8	7.60	0.6	3.80
0.9	6.40	0.7	4.39
1.0	5.70	0.8	4.80
1.1	5.20	0.9	5.52

The effect of [H$^+$] was investigated in the range 0.8–1.2 mol dm^{-3} of perchloric acid at constant [Cl$^-$] (0.8 mol dm^{-3}) and the rate decreases proportionally with increase in [H$^+$] in oxidation by NBN. The plot of lg k_{obs} versus lg [H$^+$] is linear and with negative slope. The effect of [Cl$^-$] on the rate of reaction was also studied by increasing the [NaCl] from 0.8–1.2 mol dm^{-3} at constant [HClO$_4$] and found to be constant. Similarly the influence of variation of NaCl concentration on the rate of NCN oxidation was studied by varying the concentration of added NaCl at constant [HCl] (Table 4). The rate of the reaction is found to increase with increase in [NaCl]. The plot of lg k_{obs} versus lg [NaCl] is linear with unit slope indicating first order dependence of NaCl. Therefore the reaction is also catalysed by Cl$^-$.

Table 4. Effect of variation of [NaCl] on reaction rate
[NCN]=0.0035 mol dm^{-3}; [Cys]=0.025 mol dm^{-3}; [NaClO$_4$]=0.4 mol dm^{-3}; H$_2$O:CH$_3$COOH (1:1); [HClO$_4$]=0.4 mol dm^{-3}; temperature 300 K

[NaCl] (mol dm^{-3})	k_{obs} ×10^3 (s^{-1})
0.6	3.80
0.7	4.43
0.8	4.98
0.9	5.62

Effect of variation of dielectric constant of the medium. An increase in the rate constant is noticed on decreasing the dielectric constant of the medium in both oxidations. Plot of lg k_{obs} versus 1/D (r=0.9901), where D is the dielectric constant of the medium, gives a straight line with positive slope[28]. An increase in the amount of acetic acid in the solvent results in an increase in the rate of oxidation. Thus according to Amis, an interaction between a dipole and a positive ion is indicated, though the behaviour is not ideal. Both oxidations show the same trend (Table 5 A and B).

Table 5. Effect of variation of [CH$_3$COOH:H$_2$O] on reaction rate
A. [Cys]=0.04 mol dm^{-3}; [NBN]=0.004 mol dm^{-3}; [HCl]=0.8 mol dm^{-3}; [NaClO$_4$]= 0.1 mol dm^{-3}; Hg(CH$_3$COO)$_2$=0.005 mol dm^{-3}; temperature 308 K   B. [NCN]=0.0035 mol dm^{-3}; [Cys]=0.025 mol dm^{-3}; [NaClO$_4$]=0.4 mol dm^{-3}; [HCl]= 0.6 mol dm^{-3}; temperature 300 K

CH$_3$COOH (%)	H$_2$O (%)	D	k_{obs} ×10^5 (s^{-1})	CH$_3$COOH (%)	H$_2$O (%)	D	k_{obs} ×10^3 (s^{-1})
50	50	37.50	7.60	50	50	37.50	3.80
55	45	34.75	8.90	55	45	34.75	5.90
60	40	31.50	11.48	60	40	31.50	9.54
65	35	28.50	15.80	65	35	28.50	13.86

Effect of addition of nicotinamide. The effect of one of the product of the reaction has been studied by adding various concentration of nicotinamide, keeping concentration of cysteine, NBN and NCN constant. The rate of reaction decreases on adding nicotinamide (NA). Thus added nicotinamide has a retarding effect on the rate of oxidation. Further the plot of 1/k_{obs} versus [NA] is linear indicating inverse dependence of rate on [NA] (Ref. 29). It is found to be true in the case of cysteine oxidation by NCN as well.

Effect of added salts on reaction rate. The effect of added salts like Na$_2$SO$_4$, KCl, BaCl$_2$ and K$_2$SO$_4$ on the reaction rate was studied by adding various concentrations of these salts, keeping the concentrations of cysteine, HCl, NBN and NCN constant. It was observed that the rates of oxidation were not altered by the addition of these neutral salts.

Effect of chlorine scavenger. The possibility of free radical intervention in the NBN oxidation reaction was tested by the following procedure. The reaction mixture containing acrylonitrile scavenger was kept for 24 h in an inert atmosphere and then diluted. On dilution, formation of precipitate was not observed indicating the absence of free radical intervention in the reaction. It was observed that the rate of oxidation of cysteine by NCN had a distinct retarding effect on initially added cobalt(II) chloride, the typical chlorine scavenger.

Effect of temperature. Increase in temperature increases the rate of oxidation and plot of lg k_{obs} versus reciprocal of temperature is linear. The oxidation of cysteine by NBN was studied at different temperatures (308 to 328 K) and the activation parameters were evaluated (Table 6 A and B). Similarly the oxidation of cysteine by NCN was studied at temperatures from 300 to 320 K and the activation parameters were evaluated (Table 7).

Table 6. Effect of temperature on reaction rate

A. [Cys]=0.04 mol dm^{-3}; [NBN]=0.004 mol dm^{-3}; [HCl]=0.8 mol dm^{-3}; [NaClO$_4$]=0.1 mol dm^{-3}; H$_2$O:CH$_3$COOH (1:1); Hg(CH$_3$COO)$_2$=0.005 mol dm^{-3}

B. [NCN]=0.0035 mol dm^{-3}; [Cys]=0.025 mol dm^{-3}; [NaClO$_4$]=0.4 mol dm^{-3}; [HCl]=0.6 mol dm^{-3}

Temperature (K)	$k_{obs} \times 10^5$ (s^{-1})	Temperature (K)	$k_{obs} \times 10^5$ (s^{-1})
308	7.60	300	3.80
313	9.62	305	5.47
318	11.96	310	7.39
323	14.63	315	11.48
328	17.90	320	14.51

Table 7. Activation parameters of cysteine oxidation

Oxidant	E_a (kJ mol^{-1})	ΔH^* (kJ mol^{-1})	ΔS^* (J K^{-1} mol^{-1})	ΔG^* (kJ mol^{-1})
NBN	18.11	15.55	− 169.64	67.79
NCN	55.64	53.12	− 114.30	34.34

DISCUSSION – NBN OXIDATION

The possible oxidising species in acidified aqueous acetic acid solution are NBN, NBNH$^+$, NBNBr, Br$_2$, HOBr and H$_2$OBr$^+$ (Ref. 30). The observed first order dependence of the reaction rate on NBN rules out NBNBr and molecular bromine as the reactive oxidising species. NBNH$^+$ and H$_2$OBr may be discarded because of inverse dependence of reaction rate on [H$^+$] (Ref. 31). The same observation has been made in the oxidation of cysteine by hypobromous acid (Table 3). Of the remaining two, HOBr and not NBN should be the oxidising species, since the rate is also inverse function of nicotinamide concentration. A plot of inverse of the observed rate constant against the nicotinamide concentration is linear (*r*=0.9920).

Mechanism - NBN oxidation. Addition of nicotinamide decreases the rate of oxidation[32]. This retarding effect suggests that the pre-equilibrium step involves a process in which nicotinamide is one of the products.

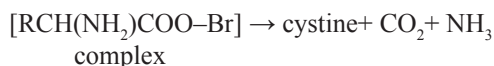$$NBN + H_2O \underset{k_{-1}}{\overset{k_1}{\rightleftharpoons}} NA + HOBr \tag{1}$$

In acid medium, amino acid exists in its protonated form (SH^+) which is resistant to attack by NBN. It is observed that the rate has inverse dependence on $[H^+]$. Thus the only species possibly controlling the rate of oxidation seems to be RCH (NH_2) COOH.

The electrophilic attack of HOBr on the nitrogen atom of the amino acid results in the formation of N-bromo derivative which in turn cleaves to give the disulphide and ammonia as the final products. Fractional order in $[H^+]$ may be explained by assuming the steps shown in Scheme, as in the $[H^+]$ range ($0.8 - 1.1$ ml dm^{-3}), it is likely that [RNHBr] increases with increase in $[H^+]$.

It may be pointed out that in the present study the oxidation by bromine was completely suppressed as the oxidative studies were carried out in the presence of mercuric acetate which combines with bromide ions formed in the reaction. Thus kinetics of only NBN oxidation were followed.

<div align="center">S c h e m e</div>

$$SH^+ \underset{k_{-2}}{\overset{k_2}{\rightleftharpoons}} S + H^+ \tag{2}$$

$$S + HOBr \underset{k_{-3}}{\overset{k_3}{\rightleftharpoons}} [RCH\ (NH_2)COO{-}Br] + H_2O \tag{3}$$
<div align="center">complex</div>

$$[RCH(NH_2)COO{-}Br] \rightarrow cystine + CO_2 + NH_3$$
<div align="center">complex</div>

$R = SHCH_2^-$.

The rate law for the above mechanism may be divided as follows:

$$rate = -\ \frac{d[NBN]}{dt} = k_d\,[complex] \tag{4}$$

$$= \frac{k_d k_1 k_2 k_3\,[NBN]\,[SH^+]}{k_{-1} k_{-2} k_{-3}\,[NA][H^+]} \tag{5}$$

$$-\ \frac{d[NBN]_T}{dt} = \frac{k_d k_1 k_2 k_3 [NBN]_T\,[SH^+]}{k_{-1} k_{-2} k_{-3}[NA]\,[H^+] + k_{-1} k_{-2} k_{-3}[H^+] + k_1 k_2 k_3[SH^+]}\ . \tag{6}$$

590

On re-arranging the equation

$$\left(\frac{k_{-1}k_{-2}k_{-3}[\text{NA}]\,[\text{H}^+]}{k_d k_1 k_2 k_3} + \frac{k_{-2}k_{-3}[\text{H}^+]}{k_d k_2 k_3} \right) \frac{1}{[\text{SH}^+]} + \frac{1}{k_d} = \frac{1}{k_{obs}},\qquad(7)$$

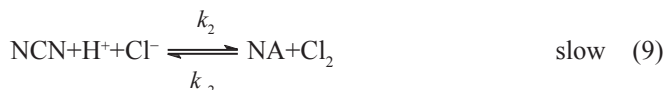where $[\text{NBN}]_T$ is the total NBN concentration, and $[\text{NBN}]$ – NBN concentration in the equilibrium.

The rate-determining step proposed in the above mechanism predicts negligible salt effect which has been experimentally observed. The formation of the complex involves the charge separation which leads to a negative solvent effect. This has been confirmed by the increase in rate with decreasing dielectric constant of the medium. The involvement of cysteine molecule in the rate-determining step leads to different values of k_{obs} for its different initial concentrations. The proposed mechanism is well supported by the moderate values of energy of activation and thermodynamic parameters. The negative entropy of activation indicates the complex formation as suggested in the above reaction mechanism, and also indicates that the complex is more ordered than reactants[29]. High positive values of the free energy of activation and the enthalpy of activation show that the transition state is highly solvated.
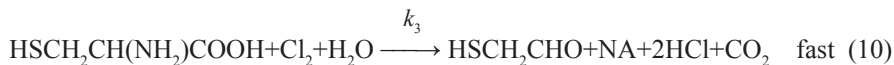
DISCUSSION – NCN OXIDATION

The above experimental results clearly reveal that cysteine is involved in the fast step while NCN participates in a slow reaction. The oxidant reacts with hydrochloric acid in a slow step to give the reaction species, namely molecular chlorine. The molecular chlorine oxidises the substrate, cysteine, in a fast step to give mercaptoacetaldehyde and other products. The formation of molecular chlorine in the course of the reaction can also be inferred from the observation that the addition of chlorine scavenger like cobalt(II) chloride has appreciable retarding effect on the rate of oxidation[33].

The oxidation of amino acids by N-chlorobenzamide[34] and chlorobenzotriazole[35] has been reported to take place through the intermediate forms of protonated species of the oxidant or molecular chlorine. The similar formulation can also be extended to the oxidation of amino acids with NCN, since it also belongs to same class of N-haloamides. More recently a simultaneous attack by H^+ and Cl^- ions on the N-haloamide leading to the release of elemental chlorine has been recommended[36].

Mechanism – NCN oxidation. Addition of nicotinamide decreases the rate of oxidation[32]. This retarding effect suggests that the pre-equilibrium step involves a process in which nicotinamide is one of the products.

$$\text{NCN}+\text{H}_2\text{O} \underset{k_{-1}}{\overset{k_1}{\rightleftharpoons}} \text{NA}+\text{HOCl}\qquad(8)$$

$$\text{NCN}+\text{H}^++\text{Cl}^- \underset{k_{-2}}{\overset{k_2}{\rightleftharpoons}} \text{NA}+\text{Cl}_2 \qquad \text{slow}\quad(9)$$

$$HSCH_2CH(NH_2)COOH + Cl_2 + H_2O \xrightarrow{k_3} HSCH_2CHO + NA + 2HCl + CO_2 \quad \text{fast} \quad (10)$$

The corresponding rate law is given by

$$-\frac{d[NCN]}{dt} = \frac{k_2 k_3 [NCN]\,[H^+][\,Cl^-][cysteine]}{k_{-2}[NA] + k_3[cysteine]} \; . \tag{11}$$

Since step (10) is fast and [cysteine] is fairly large, k_3[cysteine] $\gg k_{-2}$[NA] may be taken as suitable approximation. This leads to the following rate law:

$$-\frac{d[NBN]}{dt} = k_2\,[NCN]\,[H^+][Cl^-]. \tag{12}$$

The increase of rate with increase in percentage of acetic acid content of the medium is indication of an interaction between a positive ion and a neutral species in the rate-determining step. This is in a good agreement with equation (9) in the above mechanism.

The observed trend of rate constant variation on addition of nicotinamide and increase in [NCN] shows the retarding effect on oxidative reaction. This trend is the same in NBN oxidation as well.

CONCLUSIONS

The rate of oxidation of cysteine by the N-haloreagents, N-bromonicotinamide and N-chloronicotinamide is studied and compared. Added nicotinamide retards the reaction. The NCN oxidation is faster than NBN oxidation. HOBr is the oxidising species in NBN oxidation whereas molecular chlorine is the oxidising species in NCN oxidation. Cystine is the product of oxidation by NBN. NCN oxidation leads to mercaptoacetaldehyde. The products are isolated and identified. Suitable mechanisms in accordance with experimental observations were proposed and the rate laws were derived for both oxidations. NBN can be used as a better oxidant for the facile oxidation in the grounds of its easy method of synthesis, handling, rate of oxidation, shelf life and versatility.

REFERENCES

1. L. PUSHPALATHA, K. VIVEKANANDAN: Oxidation of Acidic Amino Acids by N-bromonicotinamide. A Kinetic Study. Oxid Commun, **31** (3), 598 (2008).
2. L. PUSHPALATHA, K. VIVEKANANDAN: Oxidative Kinetics of Serine and Threonine by N-bromonicotinamide. J Indian Chem Soc, **85**, 1027 (2008).

3. L. PUSHPALATHA, K. VIVEKANANDAN: N-bromonicotinamide Oxidation of Essential Amino Acids. A Kinetic Study. Oxid Commun, **32** (1), 85 (2009).

4. L. PUSHPALATHA, K. VIVEKANANDAN: Oxidative Decarboxylation and Deamination of Essential Amino Acids by N-bromonicotinamide. A Kinetic Study. J Indian Chem Soc, **86**, 475 (2009).

5. L. PUSHPALATHA, K. VIVEKANANDAN: Kinetics of Oxidative Cleavage of Non-essential Amino Acids by N-bromonicotinamide in Aqueous Acetic Acid Medium. Oxid Commun, (in press); M. N. ABUBACKER, L. PUSHPALATHA, K. VIVEKANANDAN: Synthesis and Antifungal Activity of N-bromonicotinamide (NBN). Int J Plant Sci, **4** (2), 399 (2009).

6. N. MATHIYALAGAN: Kinetics of Oxidation of Ethers by N-chloronicotinamide. J Indian Chem Soc, **82**, 1 (2005).

7. D. R. W. HODGSON, J. M. SANDERSON: The Synthesis of Peptides and Proteins Containing Non-natural Amino Acids. Chem Soc Rev, **33**, 422 (2004).

8. C. C. TSEN: Oxidation of Sulfhydryl Groups of Flour by Bromate under Various Conditions and during the Breadmaking Process. Cereal Chem, **45** (6), 531 (1968).

9. H. J. Y. El AILA: Kinetic Study of Cysteine Oxidation by Potassium Hexacyanoferrate(III) in the Presence of Sodium Dioctylsulfosuccinate. J Disper Sci Technol, **25** (2), 157 (2004).

10. E. KARIM, M. K. MAHANTI: Kinetics of Oxidation of Sulphur Containing Amino Acids by Quinolinium Dichromate. Oxid Commun, **14** (3), 157 (1991).

11. D. LALOO, M. K. MAHANTI: Kinetics of Oxidation of Cysteine by Alkaline Hexacyanoferrate(III). Oxid Commun, **11** (3,4), 231 (1988).

12. C. MOHANADAS, P. INDRASENAN: N-bromosaccharin as an Oxidimetric Titrant: Direct Potentiometric and Visual Titrations of Some Typical Reductants in Aqueous Acetic Acid Medium. Indian J Chem, **26A**, 55 (1987).

13. D. W. J. KWONG, D. E. PENNINGTON: Stoichiometry, Kinetics and Mechanism of the Chromium(VI) Oxidation of L-cysteine at Neutral pH. Inorg Chem, **23**, 2528 (1984).

14. K. K. KISHORE, A. K. KUMAR, P. VANI: Mechanism of Oxidation of L-cysteine by Hexachloroiridate(IV). A Kinetic Study. Transit Metal Chem, **30**, 773 (2005) and references therein.

15. J. D. SALDANHA RAVI, S. ANANDA, B. M. VENKATESHA, M. P. JAGADEESHA: Oxidation of L-cysteine by Sodium N-chlorotoluene Sulphonamide (Chloramine-T) in $HClO_4$ and H_2SO_4 Media: A Kinetic and Mechanistic Study. Oxid Commun, **22** (2), 464 (1999).

16. M. RANGASWAMY, S. ANANDA: Oxidation of L-cysteine by Bromamine-B in H_2SO_4 and $HClO_4$ Media: A Kinetic and Mechanistic Study. J Indian Council Chem, **18**, 12 (2001).

17. C. JACOB, I. KNIGHT, P. G. WINYARD: Aspects of the Biological Redox Chemistry of Cysteine: From Simple Redox Responses to Sophisticated Signaling Pathways. Biol Chem, **387** (10/11), 1385 (2006).

18. C. A. RAGUSO, M. M. REGAN, V. R. YOUNG: Cysteine Kinetics and Oxidation at Different Intakes of Methionine and Cystine in Young Adults. Am J Clin Nutr, **71**, 491 (2000).

19. I. WARAD, M. ABU EID, B. SHARYDEH: Kinetics and Mechanism of Oxidation of L-cysteine by Ferrozineiron(III) Complex in Aqueous Acidic Medium. J Saudi Chem Soc, **10** (2), 271 (2006).

20. M. A. A. KHALID: Oxidative Kinetics of Amino Acids by Peroxydisulphate. Arab J Sci Eng, **33** (24), 199 (2007).

21. S. QUYOOM, BADR-UD-DIN KHAN: Potentiometric and UV Spectral Studies of Binary and Ternary Complexes of Some Metal Ions with N-acetylcysteine and Amino Acids. E-J Chem, **6** (S1), S117 (2009).

22. C. R. HAUSER, W. B. RENFROW, Jr.: The Removal of HX from Organic Compounds by Means of Bases. III. The Rates of Removal of Hydrogen Bromide from Substituted N-bromobenzamides and Their Relative Ease of Rearrangement in the Presence of Alkali. The Hofmann Rearrangement. J Am Chem Soc, **59**, 121 (1923).

23. D. D. PERRIN, W. L. AMAREGO, D. R. PERRIN: Purification of Organic Compounds. Pergamon, Oxford, 1966.

24. A. AGARWAL, S. MITTAL, K. K. BANERJI: Kinetics and Mechanism of Oxidation of Amino Acids by N-bromoacetamide in Acid Medium. Indian J Chem A, **26**, 339 (1987).
25. K. VIVEKANANDAN, K. NAMBI: N-chloronicotinamide: A New, Mild, Stable, Efficient and Inexpensive Oxidant for Organic Substrates. Indian J Chem B, **35**, 1117 (1996).
26. A. I. VOGEL: Quanlitative Inorganic Analysis. Textbook of Practical Organic Chemistry. 4th ed. (Eds B. S. Furniss, A. Hannaford, V. Roges, P. W. G.Smith, A. R. Tatchell). Longman, London, 1978.
27. S. YATHIRAJAN, C. R. RAJU, K. N. MOHANA, S. SHASHIKANTH, P. NAGARAJA: Kinetics and Mechanism of Oxidation of L-isoleucine and L-ornithine Hydrochloride by Sodium N-bromobenzenesulpnonamide in Perchloric Acid Medium. Turk J Chem, **27**, 571 (2003).
28. E. S. AMIS: Solvent Effects on Reaction Rates and Mechanisms. Academic Press, New York, 1976.
29. A. WEISSBERGER: Techniques of Chemistry. Investigations of Rate and Mechanism of Reaction. Wiley Interscience Publication, New York, 1974.
30. K. K. BANERJI: Kinetics and Mechanism of Oxidation of Substituted Benzaldehydes by N-bromobenzamide. J Org Chem, **51**, 4764 (1986).
31. M. K. REDDY, Ch. S. REDDY, E. V. SUNDARAM: Oxidative Kinetics of Aminoacids by N-bromoacetamide. A Study of Solvent Effect and General Base Catalysis. Tetrahedron, **41** (15), 3071 (1985).
32. S. C. NEGI, K. K. BANERJI: Kinetics and Mechanism of Oxidation of Secondary Alcohols by N-bromoacetamide in Acid Medium. Indian J Chem B, **21**, 846 (1982); S. C. NEGI, K. K. BANERJI: Kinetics and Mechanism of Oxidation of the Alcohols by N-bromoacetamide in Alkaline Solution. J Org Chem, **48**, 3329 (1983).
33. I. GRANOTH: Deoxygenation of Aromatic Sulphoxides by Thionyl Chloride in the Presence of Cyclohexene. Synthesis of Substituted Phenoxanthiins. J Chem Soc Perkin T 1, 2166 (1974).
34. M. C. AGRAWAL, A. LAL: Kinetics of Oxidation of Histidine by N-chlorobenzamide in Aqueous Methanol. Indian J Chem A, 2**6**, 696 (1987); M. C. AGRAWAL, A. LAL: Kinetics of Oxidation of Some Amino Acids by N-chlorobenzamide in Water - Methanol Mixtures. Indian J Chem A, **23**, 411 (1984).
35. S. C. HIREMATH, S. M. MAYANNA, N. VENKATASUBRAMANIAN: Chloride Ion-catalysed Oxidation of Arginine, Threonine and Glutamic acid by Chlorobenzotriazole: A Kinetic and Mechanistic Study. J Chem Soc Perkin T 1, 1569 (1987).
36. M. C. AGRAWAL, A. LAL: Kinetics of Oxidation of Some Amino Acids by N-chlorobenzamide in Perchloric Acid. J Indian Chem Soc, **67**, 164 (1990).

KINETICS AND MECHANISM OF Ru(III) CATALYSIS IN OXIDATION OF METHYL DIETHYLENE GLYCOL BY KBrO₃ IN ACIDIC MEDIUM

R. A. SINGH[a]*, KAMINI SINGH[a], ABHISHEK KUMAR[a], S. K. SINGH[b]

[a]*Chemical Kinetics Research Laboratory, Department of Chemistry, T. D. P. G. College, 222 002 Jaunpur (U.P.), India*
E-mail: *rasinghtdc@rediffmail.com*
[b]*Department of Chemistry, Sri J.N.P.G. College, Lucknow (U.P.), India*

ABSTRACT

Kinetics of Ru(III)-catalysed oxidation of methyl diethylene glycol by potassium bromate in perchloric acid has been studied using mercuric acetate as bromide ion scavenger. The reaction is found to be zero order with respect to potassium bromate and hydrogen ion. First order kinetics with respect to methyl diethylene glycol (MDG) and Ru(III) chloride has been observed. Successive addition either of mercuric acetate and potassium chloride did not bring about significant change in the rate of reaction. Negligible effect of ionic strength on the rate of the reaction was observed. On the basis of experimental findings a suitable mechanism has been proposed. The reaction product was identified and the results were also confirmed by statistical regression analysis data.

Keywords: kinetics, mechanism, oxidation, methyl diethylene glycol, Ru(III).

AIMS AND BACKGROUND

Several papers have been devoted to the kinetics and mechanism of oxidation of a few alcohols, ketones, acids, diols and some labile substrates by potassium bromate[1–5]. Scant data on catalyzed potassium bromate oxidation are available. A number of catalysts like osmium tetroxide[6], ruthenium trichloride[7], iridium trichloride are used by several workers to investigate the effect of catalysts on oxidation of glycols, but the Ru(III) chloride-catalyzed oxidation of diethylene glycol by potassium bromate has not been studied till now. This prompted us to undertake the present work, which constitutes the kinetics of Ru(III)-catalysed oxidation of methyl diethylene glycol by potassium bromate in the presence of mercuric acetate as scavenger.
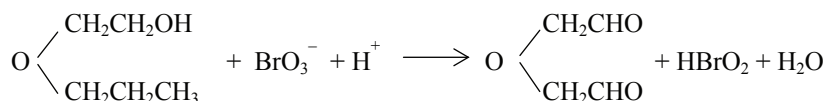
---

* For correspondence.

EXPERIMENTAL

Solution of diethylene glycol (E. Merck), potassium bromate (BDH, AR), mercuric acetate and sodium perchlorate (E. Merck), perchloric acid (60%) of E. Merck (F.R.G.) grade (used as a source of hydrogen ions) were prepared in doubly distilled water. Aqueous solution of ruthenium trichloride was prepared by dissolving $RuCl_3.3H_2O$ (Johnson and Matthey) in 0.2 M HCl solution.

A thermostated water bath was used to maintain the desired temperature to within $\pm 0.1^{\circ}C$. The reaction was initiated by addition of potassium bromate solution to other reagents equilibrated separately at $35^{\circ}C$ at which potassium bromate was maintained. The kinetics was followed by periodically examining aliquots of the reaction mixture for unconsumed potassium bromate iodometrically using starch indicator.

Stoichiometry and product identification. Solutions with varying $KBrO_3$-methyl diethylene glycol ratio were equilibrated at $35^{\circ}C$ for 48 h under kinetic conditions. Estimation of unreacted $[KBrO_3]$ shows that 1 mol of $KBrO_3$ was required for oxidation of each mol of methyl diethylene glycol.

The stoichiometric equation is as follows:

$$O \underset{CH_2CH_2CH_3}{\overset{CH_2CH_2OH}{\diagup}} \; + \; BrO_3^- \; + \; H^+ \; \longrightarrow \; O \underset{CH_2CHO}{\overset{CH_2CHO}{\diagup}} \; + \; HBrO_2 + H_2O$$

The product, i. e. the corresponding aldehyde, was detected and identified according to Ref. 8 and thin layer chromatography[9] and also through dinitrophenyl hydrazine (DNP) derivatives[10].

RESULTS AND DISCUSSION

The oxidation of methyl diethylene glycol by $KBrO_3$ studied over a wide range of concentration of the reactants showed that the reaction follows first order with respect to methyl diethylene glycol (Fig. 1, Tables 1 and 2). It gives a straight line with unit slope which confirms the first order kinetics. A linear increase in first order rate constant with an increase in the initial concentration of Ru(III) was observed which shows the first order reaction with respect to Ru(III). The reaction shows zero order kinetics with respect to $KBrO_3$ and perchloric acid (medium) (Table 1). Addition of potassium chloride and mercuric acetate has no significant effect on the reaction rate. Variation of ionic strength of the medium shows negligible effect (Table 2). The reaction was studied at 4 different temperatures, i.e. 30, 35, 40 and $45^{\circ}C$, which provides calculation of several thermodynamic parameters by usual method collected in Table 3.

Table 1. Effect of variation of [H$^+$], [KBrO$_3$], methyl diethylene glycol [MDG] and Ru(III) on reaction rate at 35°C
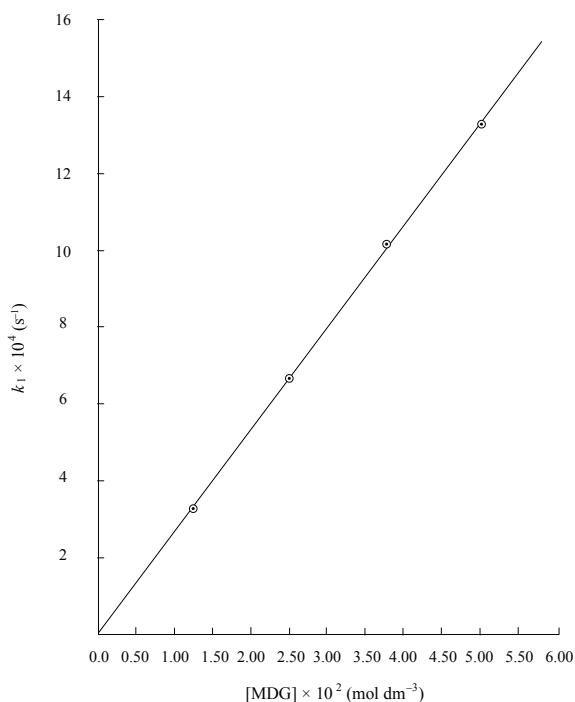
[MDG] × 10^2 (mol dm^{-3})	[KBrO$_3$] × 10^4 (mol dm^{-3})	[HCLO$_4$] × 10^2 (mol dm^{-3})	[Ru(III)] × 10^5 (mol dm^{-3})	[−dc/dt] × 10^7 (mol dm^{-3}s^{-1})	k_1 × 10^4 (s^{-1})
5.00	1.67	1.00	4.80	1.34	13.40
5.00	2.67	1.00	4.80	2.80	13.20
5.00	4.16	1.00	4.80	4.86	13.21
5.00	6.67	1.00	4.80	8.14	13.56
5.00	8.34	1.00	4.80	10.64	13.30
1.25	3.34	1.00	4.80	1.22	3.32
2.50	3.34	1.00	4.80	2.48	6.74
3.75	3.34	1.00	4.80	3.78	10.27
6.25	3.34	1.00	4.80	6.16	16.74
7.50	3.34	1.00	4.80	7.64	20.76
5.00	3.34	0.50	4.80	3.48	13.00
5.00	3.34	1.50	4.80	3.44	12.80
5.00	3.34	2.00	4.80	3.50	13.00
5.00	3.34	2.50	4.80	3.56	13.20
5.00	3.34	3.00	4.80	3.52	13.10
5.00	3.34	1.00	0.80	0.82	2.23
5.00	3.34	1.00	1.60	1.58	4.29
5.00	3.34	1.00	2.40	2.50	6.79
5.00	3.34	1.00	3.20	3.28	8.91
5.00	3.34	1.00	4.00	4.18	11.36

Table 2. Effect of ionic strength, mercuric acetate and temperature on the rate constant
[KBrO$_3$] = 3.34 × 10^{-4} mol dm^{-3}; [MDG] = 5.00 × 10^{-2} mol dm^{-3}; [HClO$_4$] = 1.00 × 10^{-3} mol dm^{-3}; [Ru(III)] = 4.80 × 10^{-5} mol dm^{-3}

Temperature (°C)	[NaClO$_4$] × 10^3 (mol dm^{-3})	μ × 10^3 (mol dm^{-3})	[Hg(OAc)$_2$] × 10^3 (mol dm^{-3})	k_1 × 10^4 (s^{-1})
35	0.00	11.96	3.50	13.21
35	2.00	13.92	3.50	13.91
35	4.00	15.92	3.50	13.22
35	6.00	17.92	3.50	13.17
35	8.00	19.92	3.50	13.12
35	10.00	21.92	3.50	13.26
35	−	11.90	1.25	−
35	−	12.52	1.25	−
35	−	13.15	1.25	−
35	−	14.40	1.25	−
35	−	7.34	0.50	13.08
35	−	8.54	0.70	13.00
35	−	9.34	1.00	13.04
35	−	12.84	1.50	12.96
35	−	16.34	2.00	12.98
30	−	14.5	0.00	28.60
40	−	14.5	0.00	62.20
45	−	14.5	0.00	90.19

Table 3. Thermodynamic parameters

ΔE (kJ mol^{-1})	lg A	ΔS^* (J K^{-1}mol^{-1})	ΔG^* (kJ mol^{-1})
63.84	10.45	-48.84	78.88

Fig. 1. Plot of k_1 versus [MDG]

Potassium bromate being strong electrolyte gives bromate ions as given below:

$$KBrO_3 \rightarrow BrO_3^- + K^+ \tag{a}$$

$$BrO_3^- + H^+ \underset{}{\overset{k}{\rightleftharpoons}} HBrO_3 \tag{b}$$

$$C_1 + S \underset{k_{-1}}{\overset{k_1}{\rightleftharpoons}} C_2 + H_2O \tag{c}$$
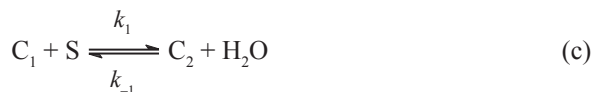
where S is substrate; $C_1 - [RuCl_2(H_2O)_4]^+$, and $C_2 - [RuCl_2(H_2O)_3OHCH_2CH_2R]$;

$$C_2 \overset{k_2}{\rightarrow} X + C_1 + HBrO_2 \tag{d}$$

where X is product.

On the basis of these steps, the rate of the reaction in terms of consumption of potassium bromate may be written as follows:

598

$$-\frac{d[BrO_3^-]}{dt} = k_2 [C_2]. \tag{1}$$

On applying steady state treatment to C_2 as given below:

$$-\frac{d[C_2]}{dt} = k_1 [C_1] [S] - k_{-1} [C_2] - k_2 [C_2]$$

or

$$[C_2] (k_{-1} + k_2) = k_1 [C_1] [S]$$

or

$$[C_2] = \frac{k_1 [C_1] [S]}{k_{-1} + k_2} . \tag{2}$$

From equations (1) and (2) we have

$$-\frac{d[BrO_3^-]}{dt} = \frac{k_2 k_1 [C_1] [S]}{k_{-1} + k_2} . \tag{3}$$

The total concentration of Ru(III) may be written as:

$$[Ru(III)]_T = [C_1] + [C_2] \tag{4}$$

From step (3) we have

$$K_1 = \frac{[C_2] [H_2O]}{[C_1] + [S]} ,$$

where $K_1 = k_1/k_{-1}$
or

$$[C_2] = \frac{K_1 [C_1] [S]}{[H_2O]} . \tag{5}$$

From equations (4) and (5), we have the following:

$$[Ru(III)]_T = C_1 + \frac{K_1 [C_1] [S]}{[H_2O]}$$

or

$$[Ru(III)]_T = [C_1] \left(1 + \frac{K_1 [S]}{[H_2O]} \right)$$

or

$$[Ru(III)]_T = [C_1] \frac{[H_2O] + K_1 [S]}{[H_2O]}$$

or

$$[C_1] = \frac{[Ru(III)]_T \, [H_2O]}{[H_2O] + K_1 \, [S]} \, .$$

(6)

From equations (3) and (6), we have

$$-\frac{d[BrO_3^-]}{dt} = \frac{k_2 k_1 \, [Ru(III)]_T \, [S] \, [H_2O]}{(k_{-1} + k_2) \, ([H_2O] + K_1 \, [S])} \, .$$

(7)

On assuming $k_{-1} \gg k_2$ and $[H_2O] \gg K_1 \, [S]$, from equation (7):

$$-\frac{d[BrO_3^-]}{dt} = \frac{k_1}{k_{-1}} k_2 [Ru(III)]_T \, [S]$$

$$-\frac{d[BrO_3^-]}{dt} = K_1 \, k_2 [Ru(III)]_T \, [S],$$

(8)

since $K_1 = k_1/k_{-1}$,

where S is substrate, i.e. methyl diethylene glycol. The rate law is in agreement with all observed kinetics. Hence the proposed mechanism is valid.

REFERENCES

1. R. NATARAJAN, N. VENKTASUBRAMANIAN: Oxidative Behaviours and Relative Reactivities of Some α-hydroxy Acids towards Bromate Ion in Hydrochloric Acid Medium. Tetrahedron Lett, **57**, 5021 (1969).
2. VIJAYLAKSHMI, E. V. SUNDARAM: Inhibitory Effect of Ruthenium(III) on the Oxidation of Dimethyl Sulphoxide by N-bromosuccinimide and N-bromothalamide. A Novel Observation. J Indian Chem Soc, **55**, 567 (1978).
3. V. AWASTHI, A. C. CHATTERJI: Kinetics and Mechanism of Rhodium(III) Catalysed Oxidation of Polyhydric Alcohols by Acidified Potassium Bromate. Z Phys Chem (Leipzig), **245**, 154 (1970).
4. S. ANANDAN, R.GOPALAN: Oxidative Kinetics of Aminoacids by N-bromoacetamide. A Study of Solvent Effect and General Base Catalysis. J Indian Chem Soc, **62**, 216 (1985).
5. C. S. REDDY, E. V. SUNDARAM: Mechanism of Ru(III) Catalysis in N-bromoacetamide Oxidation of Some Glycols in Perchloric Acid Media. J Indian Chem Soc, **62**, 209 (1985).
6. H. S. SINGH, A. K. SISODIA, S. M. SINGH, R. K. SINGH, R. N. SINGH: A Kinetic Study of Osmium Tetroxide Catalysed Oxidation of Methyl Digol and Ethyl Digol by Hexacyanferrate(III) in Aqueous Alkaline Medium. Extrait du Journal de Chimie, **3**, 289 (1976).
7. B. SINGH, A. K. SINGH, D. SINGH: Mechanism of Ru(III) Catalysis in N-bromacetamide Oxidation of Some Glycols in Perchloric Acid Media. J Mol Catal, **48**, 207 (1998).
8. R. D. HARTLY, G. J. LAWSON: Kinetics and Mechanism of Osmium Tetroxide Catalyzed Oxidation of Cyclohexanal and Methyl Cyclohexanal by Alkaline Hexacyanoferrate(III) Ions. J Chromatogr, **4**, 410 (1960).
9. F. FEIGL: Spot Test in Organic Chemistry. Elsevier, New York, 1960. 369 p.
10. A. I. VOGEL: Quantitative Organic Analysis. Part III. ELBS, Longmann, London, 1958. 739 p.

OXIDATION OF CHROMIUM(III) COMPLEX OF DL-TRYPTOPHAN BY PERIODATE. KINETIC AND MECHANISTIC STUDY

H. A. EWAIS[a,b]*, A. H. QUSTI[a], I. M. I. ISMAIL[a], A. A. ADEL-KHALEK[b]

[a]*Chemistry Department, Faculty of Science, King Abdulaziz University, P. O. Box 80 203, 21 413 Jeddah, Saudi Arabia*
E-mail: *hshalby2002@yahoo.com*
[b]*Chemistry Department, Faculty of Science, Beni-Suef University, Beni-Suef City, Egypt*

ABSTRACT

The oxidation of $[Cr(III)(Try)_2(H_2O)_2]^+$ (Try = DL-tryptophan) by periodate in aqueous solution to Cr(VI) has been studied kinetically under pseudo-first order conditions at different pH, ionic strength and temperatures. The kinetics of oxidation obeyed the following rate law:

$$\text{rate} = k_1 K_2 [Cr(III)]_T [I(VII)]_T / 1 + [H^+]/K_1 + K_2[I(VII)]_T$$

where k_1 is the rate constant for the electron transfer process; K_1 – the equilibrium constant for dissociation of $[Cr(III)(Try)_2(H_2O)_2]^+$ to $[Cr(III)(Try)_2(H_2O)_2]^+ + H^+$; K_2 – the pre-equilibrium formation constant. Values of $k_1 = 4.67 \times 10^{-3}$ s^{-1}, $K_1 = 7.99 \times 10^{-4}$ mol dm^{-3} and $K_2 = 122$ dm^3 mol^{-1} have been obtained at 30°C and $I = 0.2$ mol dm^{-3}. The rate oxidation increases with increasing of pH, temperatures and independent on ionic strength. Thermodynamic activation parameters have been calculated. It is proposed that electron transfer proceeds through an inner-sphere mechanism via coordination of IO_4^- to chromium(III).

Keywords: DL-tryptophan, periodate, oxidation kinetics, inner-sphere mechanism, thermodynamic activation parameters.

AIMS AND BACKGROUND

The oxidation reactions by periodate has been reported to play an important role in biochemical studies[1,2]. They are used in the spectrophotometric determination of glucose and fructose in invert sugar syrups[1]. Alpha-amino acids in proteins can be determined by measuring the ammonia produced through oxidation with periodate in carbonate medium[2].

---

* For correspondence.

Periodate oxidation exerts a number of biological effects including the enhancement of lymphocyte activation and increased frequency to target cell binding[3]. Also, periodate has been used in the modification of human serum transferrin by conjugation to an oligosaccharide[4].

The oxidation of chromium from the trivalent to hexavalent states is an important environmental process because of the high mobility and toxicity of chromium(VI) (Ref. 5). Recently, Cr(III) oxidation to Cr(V) and/or Cr(VI) in biological systems came into consideration as a possible reason of anti-diabetic activities of some Cr(III) complexes, as well as of long-term toxicities of such complexes[6]. The specific interactions of Cr(III) ions with cellular insulin receptors[7] are caused by intra- or extracellular oxidations of Cr(III) to Cr(V) and/or Cr(VI) compounds, which act as protein tyrosine phosphatase (PTP) inhibitors. Oxidations of inorganic substrates[8] and transition metal complexes[9–11] by periodate are reported to proceed through an inner-sphere mechanism either by formation of labile or inert complexes possessing at least one bridging ligand.

The kinetics of oxidation of the chromium(III) complex of DL-aspartic acid[12], guanosine[13], 2-aminopyridine[14] and uridine[15] by periodate were carried out. In all cases the electron transfer proceeds through an inner-sphere mechanism via coordination of IO_4^- to chromium(III). Binary and ternary chromium(III) complexes of nitrilotriacetate involving histidine and aspartate as secondary ligands[16,17] by periodate in acid medium were investigated in order to study the effect of secondary ligands on the stability of $[Cr(III)(NTA)(H_2O)_2]$ (Ref. 16) (NTA = nitrilotriacetate) towards oxidation.

The kinetics of oxidation of cobalt(II) complexes of propylenediaminetetraacetate (PDTA) (Ref. 18), 1,3-diamino2-hydroxypropanetetraacetate (HPDTA) (Ref. 18), diethylenetriaminepentaacetate (DPTA) (Ref. 19), trimethylenediaminetetraacetate (TMDTA) (Ref. 20) and ethyleneglycol,bis(2-aminoethyl)ether,N,N,N′,N′-tetraacetate (EGTA) (Ref. 20) by periodate gave only the final cobalt(III) product.

Inner-sphere oxidation of the binary and ternary N-(2-acetamido)iminodiacetatocobaltate(II) complexes[21–23] involving malonate[22] succinate and maleate[23] as secondary ligands by periodate has been investigated. In all cases, initial cobalt(III) products were formed, and these changed slowly to the final cobalt(III) products. It is proposed that the reaction follows an inner-sphere mechanism, which suggested relatively faster rates of ring closure compared to the oxidation step.

In this paper, the kinetics of oxidation of $[Cr(III)(Try)_2(H_2O)_2]^+$ (Try = DL-tryptophan) are reported in order to assume the effect of complex formation on the resistance of chromium(III) towards oxidation.

EXPERIMENTAL

Materials and solutions. Chromium(III)–DL-tryptophan complex was prepared by the reported method[24]. All chemicals used in this study were of reagent grade (Analar, BDH, Sigma). Buffer solution were prepared from NaCl and HCl of known concentration. $NaNO_3$ was used to adjust ionic strength in the different buffered so-

lution. Doubly distilled H_2O was used in all kinetic runs. A stock solution of $NaIO_4$ (Aldrich) was prepared by accurate weighing and wrapped in aluminum foil to avoid photochemical decomposition[25].

Kinetic procedures. The UV-vis. absorption spectra of the products of oxidation of $[Cr(III)(Try)_2(H_2O)_2]^+$ by IO_4^- were followed spectrophotometrically for a definite period of time using a JASCO UV-530 spectrophotometer. The oxidation rates were measured by monitoring the absorbance of Cr(VI) at 355 nm, on a Milton-Roy 601 spectropho-tometer, where the absorption of the oxidation products is maximum at the reaction pH. The pH of the reaction mixture was measured using a Chertsey 7065 pH-meter.

Pseudo-first order conditions were maintained in all runs by the presence of a large excess (>10-fold) of IO_4^-. The ionic strength was kept constant by the addition of $NaNO_3$ solution. The pH of the reaction mixture was found to be always constant during the reaction run.

Oxidation products. The UV-vis. absorption spectrum of the oxidation products (Fig. 1) indicates that the chromium(III) peak at 573 nm has disappeared and has been replaced by another peaks at 355 nm which corresponds to chromium(VI). The presence of one isosbestic point at 512 nm in the absorption spectra was taken as the criterion for the presence of 2 absorbing species in equilibrium.
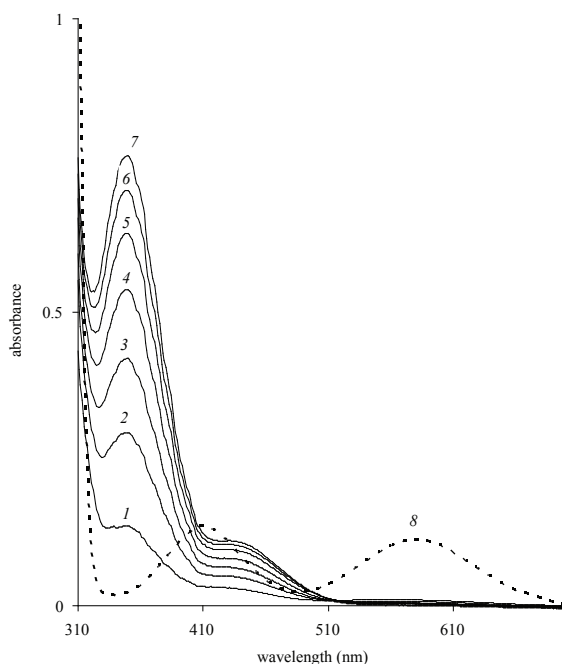

Fig. 1. Change in absorbance as a function of time. Curves *1–7* were recorded at 5, 10, 15, 20, 25, 30 and 40 min, respectively, from the time of initiation; [complex] = 5.0×10^{-4} mol dm^{-3}; [IO_4^-] = 0.02 mol dm^{-3}; $I = 0.2$ mol dm^{-3} ($NaNO_3$); pH = 3.12; $T = 30$°C. Curve *8* – spectrim of Cr(III) complex (5.0×10^{-2} mol dm^{-3}) at the same pH

RESULTS

The oxidation kinetics of $[Cr(III)(Try)_2(H_2O)_2]^+$ by periodate was studied over the 2.32–3.48 pH range, 0.2–0.6 mol dm^{-3} ionic strength and 20–40°C over a range of complex and periodate concentrations. The concentration ratio of IO_4^- initially present to chromium(VI) produced was found to be 3:2 (Table 1). Therefore, the stoichiometry of the reaction can be represented as follows:

$$2Cr(III) + 3I(VII) \rightarrow 2Cr(VI) + 3I(V) \tag{1}$$
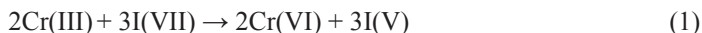
where Cr(III) and I(VII) represented the total chromium(III) and periodate, respectively. The stoichiometry is also consistent with the observation that IO_3^- does not oxidise the chromium(III) complex over the pH range studied.

Table 1. Stoichiometric results of oxidation of $[Cr(III)(Try)_2(H_2O)_2]^+$ by $[IO_4^-]$

$[Cr(III)(Try)_2(H_2O)_2^+]_0 \times 10^3$ (mol dm^{-3})	$[IO_4^-]_0 \times 10^4$ (mol dm^{-3})	$[Cr(VI)] \times 10^4$ (mol dm^{-3})	$[IO_4^-]/[Cr(VI)]$
2.5	2.5	1.65	1.51
5.0	5.0	3.23	1.54
7.5	7.5	4.91	1.53

Plots of ln ($A_\infty - A_t$) versus time were linear up to 85% of reaction where A_t and A_∞ are absorbance at time t and infinity, respectively. Pseudo-first order rate constants, k_{obs}, obtained from the slopes of these plots, are collected in Table 2.

Table 2. Variation of k_{obs} with different concentrations of periodate and different temperatures $[Cr(III)(Try)_2(H_2O)_2^+] = 2.5 \times 10^{-4}$ mol dm^{-3}; pH = 3.12, $I = 0.2$ mol dm^{-3}

$[IO_4^-] \times 10^2$ (mol dm^{-3})	$k_{obs} \times 10^3$ (s^{-1})				
	20°C	25°C	30°C	35°C	40°C
0.5	0.69	0.91	1.11	1.30	1.74
1.0	1.08	1.42	1.82	2.33	2.64
1.5	1.46	1.87	2.18	2.57	3.33
2.0	1.74	2.30	2.66	3.25	3.75
3.0	1.85	2.64	3.03	3.61	4.33
4.0	2.24	2.86	3.49	4.16	4.79
5.0	2.32	3.16	3.77	4.44	5.40

$k_{obs} \times 10^3 = 2.62, 2.71, 2.82$ and 2.77 s^{-1}; $[Cr(III)(Try)_2(H_2O)_2^+] \times 10^4 = 1.25, 3.75, 5.0$ and 6.25 mol dm^{-3}, respectively at 30°C and $[IO_4^-] = 0.02$ mol dm^{-3}.
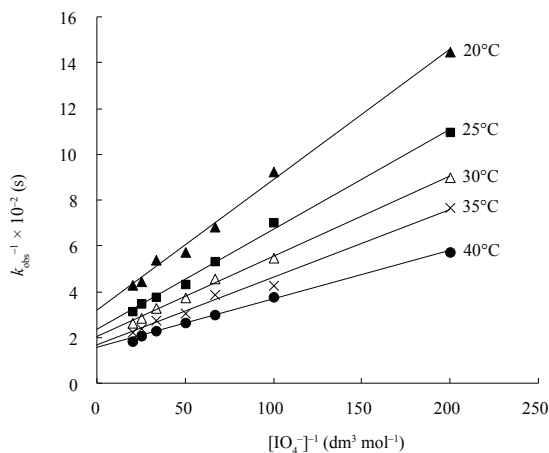
Fig. 2. Plots of $1/k_{obs}$ versus $1/[IO_4^-]$ at different temperatures

The results (Table 2) show that k_{obs} was unaffected when the concentration of the chromium(III)-complex was varied at constant periodate concentration, indicating first order dependence on complex concentration

$$d[Cr(VI)]/dt = k_{obs} [Cr(III)]_T, \qquad (2)$$

where $[Cr(III)]_T$ represents the total chromium(III) concentration present. At constant $[H^+]$ and ionic strength, $1/k_{obs}$ varies linearly with $1/[IO_4^-]$ at different temperatures (Fig. 2), and the kinetics of the reaction is described by the following equation:

$$k_{obs} = a [IO_4^-]/(1 + b [IO_4^-]) \qquad (3)$$

or

$$1/k_{obs} = 1/a [IO_4^-] + b/a \qquad (4)$$

Values of constants (a) and (b) were obtained from the slope and intercept as 28.1×10^{-2} dm³ mol⁻¹ s⁻¹ and 55.34 dm³ mol⁻¹, respectively, at 30ºC, $I = 0.2$ mol dm⁻³ and pH = 3.12. Plots of $1/k_{obs}$ versus $1/[IO_4^-]$ at different pH values (2.32–3.48) (Fig. 3), show that the reaction rate increased as the pH increased over the range studied (Table 3). The reaction rate is independent on the ionic strength when varied between 0.2–0.5 mol dm⁻³.
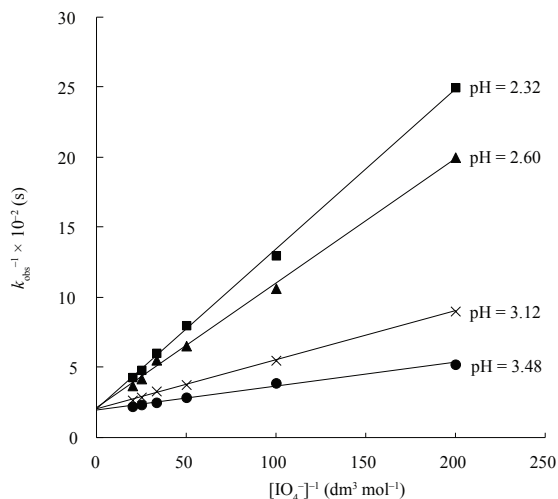
Fig. 3. Plots of $1/k_{obs}$ versus $1/[IO_4^-]$ at different pH

Table 3. Effect of pH on k_{obs}
$[Cr(III)(Try)_2(H_2O)_2^+] = 2.5 \times 10^{-4}$ mol dm^{-3}, $I = 0.2$ mol dm^{-3} and temperature 30°C

$[IO_4^-] \times 10^2$	$k_{obs} \times 10^4$ (s^{-1}) at pH			
(mol dm^{-3})	3.48	3.12	2.60	2.32
0.5	1.92	1.11	0.50	0.40
1.0	2.58	1.82	0.94	0.77
2.0	3.51	2.66	1.53	1.25
3.0	4.02	3.03	1.81	1.66
4.0	4.29	3.49	2.39	2.08
5.0	4.54	3.77	2.71	2.33

DISCUSSION

In acid medium the chromium(III)-complex is in equilibrium:

$$[Cr(III)(Try)_2(H_2O)_2]^+ \rightleftharpoons [Cr(III)(Try)_2(H_2O)(OH)] + H^+ \quad (K_1) \qquad (5)$$
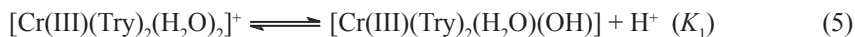
K_1 was measured potentiometrically and has the value 8.80×10^{-4} at 30°C, $I = 0.2$ mol dm^{-3}. From the values of pH (2.32 – 3.48) and K_1, it is clear that $[Cr(III)(Try)_2(H_2O)(OH)]$ may be the reactive species. Also, the rate of reaction is independent on ionic strength. This behaviour is expected since the reaction takes place between charged and uncharged species. Therefore, $[Cr(III)(Try)_2(H_2O)(OH)]$ may be the reactive species. An inner-sphere process may still be accommodated through replacement of coordinated H$_2$O in $[Cr(III)(Try)_2(H_2O)_2]^+$ by IO$_4^-$ (Refs 15 and 16).

Of the possible hydrates of I(VII) oxide, only paraperiodic acid, H$_5$IO$_6^-$, exists as a solid in equilibrium with its aqueous solution, so the acidic periodate solutions

contain 2 species, IO_4^- and H_5IO_6. The proportion of H_5IO_6 increases with decrease in pH. This acid undergoes the following equilibria[26]:

$$H_5IO_6 \rightleftharpoons H_4IO_6^{2-} + H^+ (K' = 1.98 \times 10^{-3} \text{ dm}^3 \text{ mol}^{-1}) \tag{6}$$

$$H_4IO_6^- \rightleftharpoons 2H_2O + IO_4^- (K'' = 0.025) \tag{7}$$

$$H_4IO_6^- \rightleftharpoons H_3IO_6^{2-} + H^+ (K''' = 5.0 \times 10^6 \text{ dm}^3 \text{ mol}^{-1}) \tag{8}$$
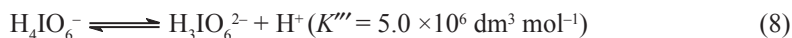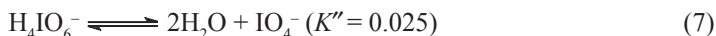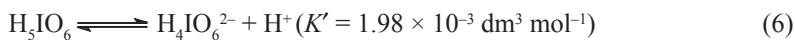
It was reported that at pH = 4.2, 99.8% of periodate are present as $H_4IO_6^-$ and IO_4^- and 0.2% as H_5IO_6 (Ref. 27).

A possible mechanism is described by equations (9)–(11):

$$[Cr(III)(Try)_2(H_2O)_2]^+ \rightleftharpoons [Cr(III)(Try)_2(H_2O)(OH)] + H^+ \quad K_1 \tag{9}$$

$$[Cr(III)(Try)_2(H_2O)(OH)] + I(VII) \rightleftharpoons [Cr(III)(Try)_2(OH)(I(VII))]^- + H_2O \quad K_2 \tag{10}$$

$$[Cr(III)(Try)_2(OH)(I(VII))]^- \rightarrow \text{products} \quad k_1 \tag{11}$$

From the above mechanism, the rate of the reaction is given by:

$$\begin{aligned}
d[Cr(VI)]/dt &= k_1[Cr(III)(Try)_2(OH)(I(VII))]^- \\
&= k_1K_2[Cr(III)(Try)_2(H_2O)(OH)][I(VII)]
\end{aligned} \tag{12}$$

If $[Cr(III)]_T$ represents the total concentration of Cr(III) species, then:

$$\begin{aligned}
[Cr(III)]_T &= [Cr(III)(Try)_2(H_2O)(OH)][H^+]/K_1 + [Cr(III)(Try)_2(H_2O)(OH)] \\
&+ K_2[Cr(III)(Try)_2(H_2O)(OH)][I(VII)]_T
\end{aligned} \tag{13}$$

Substitution for $[Cr(III)(Try)_2(H_2O)(OH)]$ from equation (13) into equation (12) gives:

$$d[Cr(VI)]/dt = k_1K_2[Cr(III)]_T [I(VII)]_T/(1 + [H^+]/K_1 + K_2[I(VII)]_T) \tag{14}$$

and

$$k_{obs} = k_1K_2[I(VII)]_T/(1 + [H^+]/K_1 + K_2[I(VII)]_T) \tag{15}$$

which on rearrangment, gives

$$1/k_{obs} = (K_1 + [H^+])/k_1K_1K_2 [I(VII)]_T + 1/k_1 \tag{16}$$

At constant $[H^+]$, equation (17) follows, in which A is a constant:

$$1/k_{obs} = A/k_1K_1K_2 [I(VII)]_T + 1/k_1 \tag{17}$$

which is identical to the experimental results shown in equation (4) where $a = k_1K_1K_2/A$ and $b = K_1K_2/A$. Values of k_1 at the temperature used, calculated from equation (16), are listed in Table 4. The activation parameters associated with k_1 obtained from a least square fit to the transition state theory equation are $\Delta H^* = 26.9$ kJ mol^{-1} and $\Delta S^* = -152.9$ J K^{-1} mol^{-1}. The intra-molecular electron transfer step is endothermic as indicated by the positive ΔH^* value. The negative ΔS^* value was claimed to be largely the result of substantial mutual ordering of the solvated water molecules[28] of the equilibria and the intra-molecular electron-transfer step.

Table 4. Values of k_1 at different temperatures

Temperature (°C)	$k_1 \times 10^3 \, (s^{-1})$
20	3.03
25	4.08
30	4.67
35	5.76
40	6.22

From equation (16), it follows that the slope of the plots can be represented by the following equation:

$$\text{slope} = [H^+]/k_1 K_1 K_2 + 1/k_1 K_2 \qquad (18)$$
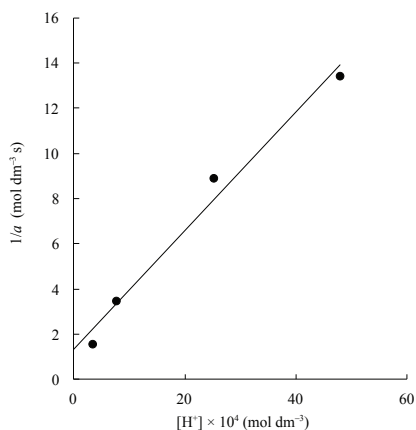
Fig. 4. Plot of $1/a$ versus $[H^+]$ at 30°C

It is obvious from equation (18) that the slope is dependent on $[H^+]$. This is shown in Fig. 4, which indicates the validity of our proposed mechanism. The values of K_1 and K_2 were calculated from equation (18) and Fig. 4 as 7.99×10^{-4} mol dm^{-3} and 122 dm^3 mol^{-1}, at 30°C and $I = 0.2$ mol dm^{-3}, respectively. Value of K_1 is in a good agreement with that obtained potentiometrically ($K_1 = 8.08 \times 10^{-4}$) at 30°C. This indicates the validity of our proposed mechanism.

From the above discussion, the following mechanism is proposed for the oxidation of $[Cr(III)(Try)_2(H_2O)_2]^+$ by periodate which supported by the observation that the ion is capable of acting as a ligand, as is apparent from its coordination to copper(III) (Ref. 29) and nickel(IV) (Ref. 30). The oxidation of $[Cr(III)(Try)_2(H_2O)_2]^+$ by periodate may proceed via 1- or 2-electron transfer giving chromium(IV) or chromium(V), respectively, in the rate-determining step leading to chromium(VI). The fact that acrylonitrile was not polymerised seems to support 2-electron transfer process.

Values of enthalpies and entropies for the oxidation of some Cr(III)-complexes with periodate are collected in Table 5 and represented in Fig. 5. There is a similar

change in ΔH^* and ΔS^* values. This indicates a common mechanism for the oxidation of these Cr(III)-complexes by periodate in the step preceding the rate-determining intra-molecular electron transfer with the precursor complex. Similar behavior has been observed for a large number of redox reaction[17] .

Table 5. Enthalpies and entropies of activation for the oxidation of some chromium(III) complexes by periodate

Complex	$k^{et} \times 10^3$ (s^{-1})	ΔH^* (kJ/mol)	$-\Delta S^*$ (J K^{-1} mol^{-1})	Ref.	Fig. 5 key
[Cr(III)(HIDA)$_2$(H$_2$O)]	10.9	12.3	240	31	(1)
[Cr(III)(HIDA)(Arg)(H$_2$O)$_2$]$^+$	1.82	15.9	227	32	(2)
[Cr(III)(Try)$_2$(H$_2$O)$_2$]$^+$	4.67	26.9	152	this work	(3)
[Cr(III)(Ud)(Asp)(H$_2$O)$_3$]$^{2+}$	0.70	59.5	107	17	(4)
[Cr(III)(NTA)(Asp)(H$_2$O)]$^-$	3.93	64.6	76	17	(5)
[Cr(III)(TOH)(H$_2$O)]	2.95	76	38.7	10	(6)
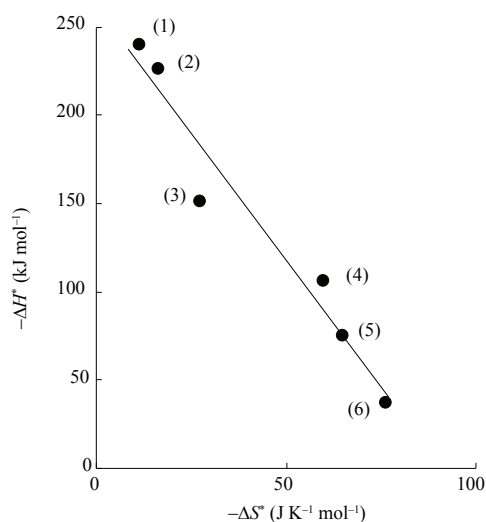
Fig. 5. Isokinetic relationship for the Cr(III)-complexes by periodate

CONCLUSIONS

The oxidation of [Cr(III)(Try)$_2$(H$_2$O)$_2$]$^+$ by periodate may proceed through an inner-sphere mechanism via 2-electron transfer giving chromium(VI). The reaction rate increases with increasing of pH. A common mechanism for the oxidation of chromium(III) complexes by periodate is proposed, and this is supported by an excellent isokinetic relationship between ΔH^* and ΔS^* values for these reactions.

REFERENCES

1. M. JOSIANE, C. TOLOTI, D. B. CRISITI, Z. A. ELIAS, M. L. SANTOSE: Determination of Glucose and Fructose in Syrup. Analyt Chim Acta, **531**, 279 (2005).

2. D. D. V. SLYKE, A. HILLER, D. A. MACFADYEN, A. B. HASTINGS, F. W. KEMPERER: Oxidation of Alpha-amino Acid by Periodate in Carbonate Medium. J Biol Chem, **133**, 287 (1994).

3. I. NODA, S. FUJIEDA, H. SAITO, T. SAITO, T. OTSUBOO, M. YAGITA: Enhancement of Cytolytic Activity of Human Peripheral Blood Lymphocytes by Sodium Periodate Possible Involvement of Protein Kinase C. Inter J Immunopharm, **20**, 15 (1998).

4. D. M. ANNA, D. GABRIELE, O. ARDUINO: Peroxidase-labelling of Human Serum Transferrin by Conjugation to Oligosaccharide Moieties. Clinica Chimica Acta, **274**, 189 (1998).

5. A. LEVINA, R. CODD, C. T. DILLON, P. A. LAY: Chromium in Biology Toxicology and Nutritional Aspects. Prog Inorg Chem, **51**, 145 (2003).

6. A. LEVINA, P. A. LAY: Mechanistic Studies of Relevance to the Biological Activities of Chromium. Coord Chem Rev, **249**, 281 (2005).

7. J. B. VINCENT, J. M. LATOUR: Characterization of Chromodulin by X-ray Absorption and Electron Paramagnetic Resonance Spectroscopies and Magnetic Susceptibility Measurements. J Am Chem Soc, **125**, 774 (2003).

8. F. R. El-ZIRI, Y. SULFAB: Oxidation of Hexaaquoiron(II) by Periodate in Aqueous Acidic Solution. Inorg Chim Acta, **25**, 15 (1977).

9. A.Y. KASSIM, Y. SULFAB: Kinetics and Mechanism of Oxidation of Hexacyanoferrate(II) by Periodate in Acidic Solutions. Evidence for Copper Catalysis. Inorg Chim Acta, **22**, 169 (1977).

10. A. A. ABDEL-KHALEK, Y. SULFAB: Kinetics and Mechanism of the Oxidation of Cobalt(II) Aminopolycarboxylate Complexes by Periodate. J Inorg Nucl Chem, **43**, 3257 (1981).

11. D. J. B. GALLIFORD, J. M. OTTAWAY: An Analytical and Kinetic Study of the Periodate Oxidation of Vanadium(IV) in Acidic Medium. Analyst, **91**, 415 (1972).

12. A. A. ABDEL-KHALEK, A. A. MOHAMED, H. A. EWAIS: Kinetics and Mechanism of Oxidation of the Chromium(III)-DL-aspartic Acid Complex – Periodate Reaction. Evidence for Iron(II) Catalysis. Trans Met Chem, **24**, 233 (1999).

13. H. A. EWAIS, S. A. AHMED, A. A. ABDEL-KHALEK: Kinetics and Mechanism of Oxidation of Chromium(III) Complex of Gaunosine by Periodate. Inorg Reac Mech, **5**, 125 (2004).

14. A. M. ABDEL-HADY: Kinetics and Mechanism of Oxidation of the Chromium(III) Complex of Aqua 2-amino Pyridine by Periodate. Trans. Met Chem, **25**, 437 (2000).

15. E. S. H. KHALEDK: Inner-sphere Oxidation of Chromium(III) Complex of Uridine by Periodate. Inorg Reac Mech, **6**, 247 (2007).

16. A. A. ABDEL-KHALEK, M. M. ELSEMONGY: Kinetics of the Oxidation of Diaqua(nitrilotriacetato) chromium(III) by Periodate in Aqueous Solutions. Trans Met Chem, **14**, 206 (1989).

17. H. A. EWAIS, M. A. HABIB, S. A. K. ELROBY: Kinetics and Mechanism of Periodate Oxidation of Two Ternary Nitrilotriacetato – Chromium(III) Complexs Involving Histidine and Aspartate Co-ligands. Trans Met Chem, **35**, 73 (2010).

18. R. M. NAIK, J. SARKER, D. D. CHATURVEDI, A. VERMA, S. K. SINGH: Kinetics of Oxidation of Cobalt(II) Complexes of Propylenediaminetetraacetate and 1,3-diamino2-hydroxypropanetetraacetate by Periodate. Ind J Chem Sect A, **42**, 1639 (2003).

19. M. H. ABU-ELENIEN, N. I. Al-SHATTI, M. A. HUSSEIN, Y. SULFAB: Kinetics and Mechanism of the Oxidation of Diethylenetriaminepentaacetatocobaltate(II) by Periodate. Polyhed, **9**, 99 (1990).

20. R. M. NAIK, A. SRIVASTAVA, A. K. TIWARI, S. B. S. YADAV, A. K. VERMA: Kinetic and Mechanistic Studies of Oxidation of Amine-N-polycarboxylates Complexes of Cobalt(II) by Periodate Ions in Aqueous Medium. Iran Chem Soc, **4**, 63 (2007).

21. A. A. ABDEL-KHALEK, I. M. I. ISMAIL M. A. NAGDY, H. A. EWAIS: Kinetics and Mechanism of Oxidation of N-(2-acetamido)-iminodiacetatocobaltate(II) by Periodate in Presence of Manganese(II) Catalyst in Acetate and Aqueous Micellar Media. Oxid Commun, **35**, 327 (2012).

22. H. A. EWAIS, M. A. NAGDY, A. A. ABDEL-KHALEK: Electron Transfer Mechanism for the Oxidation of Ternary N-(2-acetamido)-iminodiacetatocobaltate(II) Complexes Involving Succinate and Maleate as a Secondary Ligands by Periodate. Trans Met Chem, **37**, 525 (2012).

23. H. A. EWAIS, M. R. SHEHATA, M. A. NA GDY, A. A. ABDEL-KHALEK: Kinetics and Mechanism of Oxidation of the Ternary Complex of Cobalt(II) Involving N-(2-acetamido)-iminodiacetic Acid and Malonate by Periodate in Acetate Medium. Inorg Chem Indian J, **5**, 84 (2010).

24. H. OKIAND, Y. TAKAHASHI: Chromium(III) Complexes of Some Amino Acids. Bull Chem Soc Jpn, **50**, 2288 (1977).

25. M. C. R. SYMONS: Photodecomposition of Periodate. J Chem Soc, 2794 (1955).

26. S. H. LAUIRE, J. M. WILLAMS, C. J. NYMAN: Solubility of Tetraphenylarsonium Periodate and the Equilibria between Periodate Species in Aqueous Solutions. J Phys Chem, **68**, 13111 (1964).

27. K. KUSTIN, E. C. LIEBERMAN: Kinetics of Periodate Hydration Dehydration in Aqueous Solution. J Phys Chem, **68**, 3869 (1964).

28. M. J. WEAVER, E. L. YEE: Activation Parameters for Homogeneous Outer-sphere Electron-transfer Reactions. Comparisons between Self-exchange and Cross Reactions Using Marcus' Theory. Inorg Chem, **19**, 1936 (1980).

29. I. HADINCE, L. JENOVSKY, A. LINEK, V. SYNECEK: The Structure of Complex of Percuprates. Naturwiss, **47**, 377 (1960)

30. P. RAY: Sodium and Potassium Nickel (IV) Paraperiodates. Inorg Synth, **5**, 201 (1957).

31. H. A. EWAIS, F. D. DAHMAN, A. A. ABDEL-KHALEK: Kinetics and Mechanism of Oxidation of Iminodiacetatochromium(III) by Periodate. Inorg React Mech, 6, 39 (2007).

32. H. A. EWAIS, F. D. DAHMAN, A. A. ABDEL-KHALEK: Inner-sphere Oxidation of Ternary Iminodiacetatochromium(III) Complexes Involving DL-valine and L-arginine as Secondary Ligands. Isokinetic Relationship for the Oxidation of Ternary Iminodiacetato-chromium(III) Complexes by Periodate. Cent J Chem, **3**, 3 (2009).

PYRIDINIUM FLUOROCHROMATE OXIDATION OF BENZALDEHYDE IN N,N-DIMETHYL FORMAMIDE MEDIUM. KINETICS AND MECHANISM

B. L. HIRAN*, J. KHUNTWAL, R. K. MALKANI

Chemical Kinetics and Polymer Research Laboratory, Department of Chemistry, University College of Science, Mohan Lal Sukhadia University, 313 001 Udaipur, India
E-mail: *hiranbl@rediffmail.com*; *jyoti_khuantwal@rediffmail.com*

ABSTRACT

The kinetics of oxidation of benzaldehyde (BA) by pyridinium fluorochromate (PFC) in N,N-dimethyl formamide (DMF) medium in the presence of toluene *para*-sulphonic acid (TsOH) was studied in the temperature range of 298–328 K. The reaction exhibits first order dependence each on [PFC] and [BA]. The oxidation rate is positively influenced by acidity and the order with respect to H^+ is unity. The rate of oxidation remains unaltered by the variation of $NaClO_4$, but addition of $MnSO_4$ decreases the rate. The effects of the dielectric constant of the medium and the ionic strength indicate the reaction to be of ion–dipole type. The stoichiometry of the reaction is 1:1 and the products of oxidation are benzoic acid and Cr(III). There is no effect of free radical scavenger acrylonitrile on the rate of reaction. Activation energy and various thermodynamic parameters have been evaluated. A plausible mechanism and rate law have been proposed.

Keywords: kinetics and mechanism, oxidation, benzaldehyde, pyridinium fluorochromate, N,N-dimethyl formamide.

AIMS AND BACKGROUND

Aldehydes are the major participants of the naturally occurring biological processes necessary for growth and maintenance of life and organo-synthetic pathways. They are the derivatives of proteins, peptides and amino acids and are also the key intermediates for the production of a variety of fine or special chemicals such as pharmaceuticals, drugs, dyestuffs, pesticides and perfume composition. Benzaldehyde as an aromatic aldehyde has many applications such as it acts as a potato tuber sprout inhibitor.

---

* For correspondence.

A variety of compounds containing chromium(VI) have been proved to be versatile reagents capable of oxidising almost every oxidisable functional group[1]. A number of new chromium(VI)-containing compounds, like butyltriphenylphosphonium dichromate[2], morpholinium chlorochromate[3], isoquinolinium bromochromate[4], pyridinium chlorochromate[5], pyridinium bromochromate[6–8], quinolinium bromochromate[9], imidazolium fluorochromate[10], benzimidazolium dichromate[11], tripropyl ammonium fluorochromate[12] and benzyltriphenylphosphonium chlorochromate[13] have been developed to improve the selectivity of oxidation of organic compounds.

In this study we have taken PFC as an oxidant for the oxidation of benzaldehyde. A number of reports on the kinetics and mechanism of oxidation of several substrates by PFC are available in literature. PFC oxidises benzyl alcohol, ethanol and cyclohexanol[14], substituted aliphatic and aromatic alcohols[15,16], naphthalene and phenanthrene[17], hydroxy acids[18], diols[19], thioacids[20], benzaldoxime[21], substituted mandelic acids[22], secondary alcohols[23], aromatic aldehydes[24], methionine[25], aromatic acetals[26], β-benzoyl propionic acid and *para*-substituted β-benzoyl propionic acids[27], substituted phenols[28] and α-naphthol and β-naphthol[28] and their reactions were also studied kinetically. PFC supported on trisyl silicas was also prepared by co-adsorption used to oxidise organic compounds[29].

The transformation of benzaldehyde to benzoic acid is an important reaction in organic synthesis. The oxidants used for this transformation are 2,2-bipyridinium chlorochromate[30], 4-methyl pyridinium dichromate[31], imidazolium dichromate[32], quinolinium dichromate[33], benzyltrimethylammonium chlorobromate[36], 4-(dimethylamino) pyridinium chlorochromate[35], benzyltrimethylammonium dichloroiodate[34], quinolinium bromochromate[9,37,38], oxone[39] and tetrabutyl ammonium fluoride[40].

Literature survey has unveiled the fact that the use of PFC for the oxidation of aromatic aldehyde like benzaldehyde in non-aqueous medium is lacking. Hence the present investigation is initiated in an effort to probe into the kinetic and mechanistic aspects of PFC oxidation of benzaldehyde in DMF.

EXPERIMENTAL

Materials and method. All chemicals used were of high purity analytical grade. Doubly distilled AnalaR grade DMF (Thomas Baker Ltd.) was used as a source of solvent. Benzaldehyde (S.d. Fine-chem. Ltd.) was a commercial product used after fractional distillation in N_2 atmosphere and the middle fraction was collected. Its purity was checked by b.p. which comes out to be in the range of 176–178°C. Stock solution of BA prepared by direct dissolving a known volume in DMF medium was stored in refrigerator and used up to one week.

Due to the non-aqueous nature of the solvent DMF, TsOH (S.d. Fine-chem. Ltd.) of A.R. grade was used as a source of hydrogen ion. Its purity was checked by m.p. which comes out to be 106°C (Ref. 41). The stock solution of TsOH was made by direct weighing a known amount and dissolving it in DMF.

Acetic acid (S.d. Fine-chem. Ltd., A.R. grade) used for solvent variation was purified by refluxing with chromium trioxide followed by distillation over KMnO$_4$. Middle fraction boiling at 117–118°C (literature value 118.5°C) was used. Sodium perchlorate (B.D.H., AnalaR grade) was used for determining the ionic strength and its purity was checked by m.p. determination.

Preparation of the oxidant (*pyridinium fluorochromate*)

fluorochromic acid   pyridinium fluorochromate
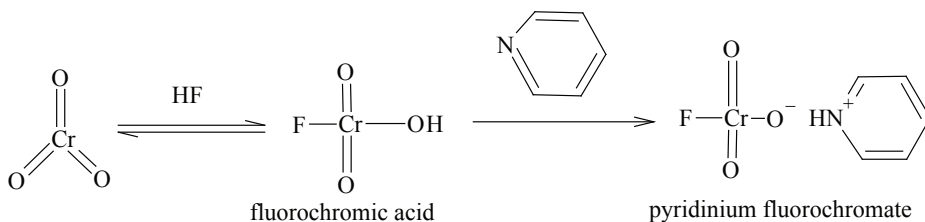
PFC was prepared in the lab by the method described by Bhattacharjee et al.[42], and its purity was checked by iodometric method, m.p. determination and IR spectral analysis (ν_{max}(KBr) = 3033, 2366, 1616, 1466, 1299, 949, 733 cm^{-1}). The m.p. of PFC was obtained in the range of 140–142°C which is in agreement with the literature value. The stock solution of PFC was prepared in DMF.

Standardisation of benzaldehyde. The solution of benzaldehyde was standardised by the following method. In a 250-ml conical flask, 2 ml of benzaldehyde solution were taken and dissolved in DMF medium. To this, 50 ml of 0.1 N sodium bisulphate solutions in DMF were added and the mixture was shaken vigorously. It was allowed to stand for half an hour. The excess bisulphate was titrated against 0.1 N iodine solution using starch as an indicator. A blank titration taking 50 ml of sodium bisulphate solution was also performed by similar method and the quantity of benzaldehyde was estimated by the difference in the volumes of I$_2$ used.

50 ml of NaHSO$_3$ = V ml of I$_2$

Excess of NaHSO$_3$ = V_1 ml of I$_2$

$V - V_1$ ml of I$_2$ = [aldehyde].

Kinetic measurements. Reactions were carried out in glass-stopper flask under pseudo-first order conditions by maintaining a large excess (×10) of the [BA] over [PFC] in the temperature range of 298–328 K. The reaction mixture prepared by mixing the requisite volume of benzaldehyde, toluene *para*-sulphonic acid solution and DMF, was allowed to stand in a thermostatic bath. The reaction was then started by adding a solution of the oxidant (PFC) which has been equilibrated in the thermostat previously by means of a pipette. The reactions were carried out at constant temperature (±0.1 K). The progress of the reaction was followed by measuring the absorbance of PFC at λ_{max} 354 nm in 1-cm thick cell placed in the thermostated compartment of Jasco model 7800 UV-vis. spectrophotometer (Shimadzu). No other reactant or product has any significant absorption at this wavelength.

The kinetic runs were followed for more than 60–70% completion of the reaction and good first order kinetics was observed. Rate constants (k_{obs}) were evaluated from the linear ($r > 0.996$) plots of lg [PFC] against time. The values reported were the mean of two or more runs (reproducibility $\pm 3\%$). The reactions were also carried out in DMF–acetic acid mixtures for studying the effect of dielectric constant on the rates of the reactions. All reactions were performed under N_2 atmosphere.

Stoichiometry. To determine the stoichiometry, PFC (0.001 mol) and BA (0.0001 mol) were made up to 100 ml in DMF in the presence of 0.6 mol dm^{-3} TsOH at 303 K, in different experiments. The reaction was allowed to stand for 24 h to ensure the completion of the reaction. The residual PFC was determined spectrophotometrically. Several determinations with different concentrations of PFC and benzaldehyde showed that the reaction exhibited 1:1 stoichiometry, i.e. 1 mol of PFC was consumed by 1 mol of benzaldehyde. In this oxidation PFC undergoes a 2-electron change. It has already been shown earlier that it acts as a 2-electron oxidant and is reduced to Cr(IV) species by determining the oxidation state of chromium by magnetic susceptibility, ESR and IR studies[43].

Product analysis. The oxidation of benzaldehyde leads to the formation of benzoic acid. The qualitative and quantitative product analysis was carried out under kinetic conditions, i.e. with an excess of the reductant. In a typical experiment, BA (0.1 mol) and PFC (0.01 mol) were made up to 50 ml with DMF and the mixture was kept in the dark for 24 h to ensure completion of the reaction in the presence of 0.6 mol dm^{-3} TsOH. After completion of the reaction under kinetic conditions, the reaction mixture was treated with solid $NaHCO_3$ and filtered. After complete neutralisation, the reaction mixture was extracted with ether to remove unreacted benzaldehyde. Non-aqueous layer was treated with conc. HCl drop by drop till bicarbonate was neutralised. Again ether was added, the product was washed with cold water, dried and weighed and identified as benzoic acid by melting point analysis, TLC, chemical test, sublimation test and also by IR spectral analysis (> C=O str, 1686 cm^{-1}; O–H str, 3006 cm^{-1}; C–H str 2834 cm^{-1}). Melting point observed for the compound was 120°C and this agreed with literature value.

RESULTS AND DISCUSSION

Oxidation of benzaldehyde by PFC has been conducted in DMF medium in the presence of TsOH at 303 K maintaining pseudo-first order conditions and the kinetic results along with conditions are given in Tables 1–4. Oxidation resulted in the formation of benzoic acid. The product analysis and stoichiometric determination suggested the following overall reaction:

$$\text{ArCHO} + \text{PFC [Cr(VI)]} \xrightarrow{\text{H}^+} \text{ArCOOH} + \text{[Cr (III)]}$$
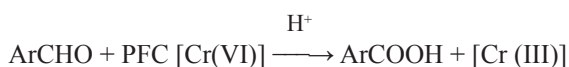
Stability of the oxidant pyridinium fluorochromate. The solution of PFC in DMF medium obeys the Beer–Lambert law at $\lambda = 354$ nm. There was no change in optical density and spectra of PFC solution, without substrate in DMF on long standing or heating up to 60–70°C.

Effect of varying oxidant concentration. The concentration of PFC was varied in the range 0.25–2.50×10^{-3} mol dm^{-3} at constant [BA], [TsOH] at 303 K and the rates were measured (Table 1). The near constancy in the value of k_{obs} (pseudo-first order rate constant) irrespective of the concentration confirms the first order dependence on PFC.

Table 1. Effect of variation of [PFC], [benzaldehyde], [PTSA] and temperature on oxidation of benzaldehyde by PFC at 303 K

[PFC] $\times 10^3$ (mol dm^{-3})	[Benzaldehyde] $\times 10^2$ (mol dm^{-3})	[PTSA] $\times 10$ (mol dm^{-3})	Temperature (K)	$k_{obs} \times 10^4$ (s^{-1})
1	2	3	4	5
0.25	1.00	0.6	303	11.7069
0.50	1.00	0.6	303	11.7837
0.75	1.00	0.6	303	11.7453
1.00	1.00	0.6	303	11.7453
1.25	1.00	0.6	303	11.7837
1.50	1.00	0.6	303	11.7069
1.75	1.00	0.6	303	11.7453
2.00	1.00	0.6	303	11.7453
2.25	1.00	0.6	303	11.7069
2.50	1.00	0.6	303	11.7453
1.00	**0.5**	0.6	303	5.6039
1.00	**0.75**	0.6	303	8.4827
1.00	**1.00**	0.6	303	11.7453
1.00	**1.25**	0.6	303	13.7412
1.00	**1.50**	0.6	303	16.6583
1.00	**1.75**	0.6	303	20.2664
1.00	**2.00**	0.6	303	28.1734
1.00	**2.27**	0.6	303	30.5531
1.00	**2.50**	0.6	303	33.4318
1.00	**2.85**	0.6	303	35.6965
1.00	**3.00**	0.6	303	39.9186
1.00	1.00	**0.0**	303	1.5353
1.00	1.00	**2.0**	303	3.8383
1.00	1.00	**4.0**	303	7.7150
1.00	1.00	**6.0**	303	11.7841
1.00	1.00	**8.0**	303	15.5836
1.00	1.00	**10.0**	303	19.3836

Continuation of Table 1

1	2	3	4	5
1.00	1.00	**12.0**	303	23.6057
1.00	1.00	**14.0**	303	27.2521
1.00	1.00	**16.0**	303	31.4743
1.00	1.00	0.6	**298**	8.5979
1.00	1.00	0.6	**303**	11.7069
1.00	1.00	0.6	**308**	16.9654
1.00	1.00	0.6	**313**	23.1835
1.00	1.00	0.6	**318**	34.4682
1.00	1.00	0.6	**323**	44.7933
1.00	1.00	0.6	**328**	77.4576
1.00	1.00	0.6	303	11.7453*

* Contained 0.001 mol dm^{-3} acrylonitrile.

Effect of pyridine concentration. There is no effect on addition of pyridine on the rate of reaction, indicating that PFC is not hydrolysed in the reaction. Further, this indicates stability of PFC during the reaction.

Effect of varying substrate concentration. The concentration of the substrate benzaldehyde (BA) was varied in the range of $0.50–3.00 \times 10^{-2}$ mol dm^{-3} at 303 K and keeping all other reactant concentration as constant and the rates were measured (Table 1). The rate of oxidation increased progressively on increasing the concentration of BA. The plot of lg k_{obs} versus lg [BA] gave the slope of 1.1 ($r = 0.9902$) indicating first order dependence on BA. Under pseudo-first order conditions, the plot of $1/k_1$ versus $1/[S]$ (where S is the reactant taken in excess) was linear with a negligible intercept indicating that the intermediate formed in slow step got consumed in a subsequent fast step.

Effect of toluene para-sulphonic acid. TsOH has been used as a source of H^+ in reaction medium. The concentration of TsOH was varied in the range 0.20–1.60 mol dm^{-3} keeping all other reactant concentration constant at 303 K and the rates were measured (Table 1). The acid-catalysed nature of this oxidation is confirmed by the increase in the rate on the addition of TsOH. The plot of k_1 versus lg $[H^+]$ is a straight line (R^2 = 0.9974) with a slope of 1.06. Therefore, order with respect to H^+ is one. PFC may become protonated in the presence of acid. The protonated PFC may function as an effective oxidant[14] similar to that of chromium trioxide oxidation[1].

Protonated PFC is likely to be a better electrophile and a better oxidant compared to a neutral one. The effects of the dielectric constant of the medium and the ionic strength indicate the reaction to be of ion–dipole type. Thus in the reaction mechanism the protonated PFC species behaves as a dipole.

Effect of temperature. The reactions were studied in the temperature range from 298 to 328 K to calculate the rate constants and various thermodynamic parameters

(Tables 1 and 2). A plot of lg k_{obs} versus $1/T$ (inverse of absolute temperature) is a straight line with negative slope. This shows that the Arrhenius equation is valid for this oxidation. According to Glasston[44], the large negative value of entropy of activation ΔS^* suggests slow bimolecular reaction in rate-determining step (rds) and that the rate-determining transition state is less disorderly than the reactants, i.e. a rigid transition state by an associative process. This transition state complex is unstable and the chromate ester bond breaks to form the product. According to Pearson[45], the large negative entropy value obtained in the present study suggests that the solvent molecules are strongly oriented or 'frozen' around the ions, thereby resulting in the loss of entropy and accounts for the lowering of rate coefficient values with increasing in the polarity of the medium.

Table 2. Thermodynamic activation parameters

Activation parameters	Values
Energy of activation ΔE_a^*	57.9028 kJ mol^{-1}
Enthalpy of activation ΔH^*	55.3837 kJ mol^{-1}
Entropy of activation ΔS^*	-53.8172 J K^{-1} mol^{-1}
Frequency factor pZ	1.5463×10^{10}
Free energy change ΔF^*	71.6903 kJ mol^{-1}

Effect of ionic strength. The effect of ionic strength was studied to observe the effect of salt on the rate of oxidation in the Debye–Hückel limit by varying concentration of NaClO$_4$ from 0.001–0.01 mol dm^{-3} provided other conditions being constant (Table 3). The rate of reaction remains almost unchanged while increasing the NaClO$_4$ concentration. It proves that the interaction in the rate-determining step is not of ion–ion type[46].

Table 3. Effect of ionic strength on oxidation of benzaldehyde by PFC at 303 K

[NaClO$_4$] $\times 10^3$ (mol dm^{-3})	$k_{obs} \times 10^4$ (s^{-1})
0.0	11.7069
1.0	11.7069
3.0	11.7453
5.0	11.7837
7.0	11.7453
8.0	11.7837
9.0	11.7453
10.0	11.7069

Effect of solvent composition. The influence of solvent polarity has been studied in acetic acid–DMF mixture. The acetic acid % (v/v) has been varied from 0 to 90% at fixed ionic strength, [BA], [PFC], [H$^+$] and temperature (Table 4). The rate of oxidation

increases with decrease in polarity of solvent. In other words, a decrease in rate with increase in dielectric constant is observed, suggesting that a medium of low dielectric constant favours the oxidation process. This is due to polar character of the transition state as compared to that of reactants. The plot of lg k_{obs} versus $1/D$ (dielectric constant) is linear with positive slope of 20.025 suggesting the presence either of dipole–dipole or ion–dipole type of interaction between the oxidant and the substrate[47]. Plot of lg k_{obs} versus $(D-1)/(2D+1)$ is a curvature indicating absence of dipole-dipole interaction in the rds (Fig. 1). The positive slope of lg k_{obs} versus $1/D$ plot indicates that the reaction involves a cation-dipole type of interaction in rds. Amis[48] holds the view that in an ion–dipole reaction involving a positive ionic reactant, the rate would decrease with increasing dielectric constant of the medium and if the reactant was to be a negatively charged ion, the rate would increase with increasing dielectric constant. In this case there is a possibility of a positive ionic reactant, as the rate decreases with increasing dielectric constant of the medium. Due to the polar nature of the solvent, transition state is stabilised, i.e. the polar solvent molecules surrounds the transition state and results in less disproportion.

Table 4. Effect of varying solvent composition on oxidation of benzaldehyde by PFC

Acetic acid : DMF	Dielectric constant $(D)^*$	$k_{obs} \times 10^4 \, (s^{-1})$
0 : 100	38.30	11.7836
10 : 90	34.10	12.0523
20 : 80	30.19	12.4746
30 : 70	26.52	13.0503
40 : 60	23.08	16.2361
50 : 50	19.85	20.8037
60 : 40	16.80	32.3571
70 : 30	13.92	58.4194
80 : 20	11.21	237.5928

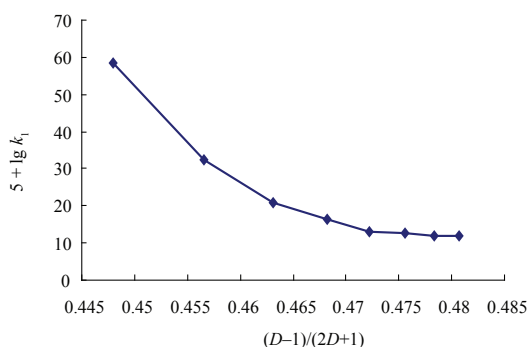* Dielectric constant calculated by law of mixtures.

Fig. 1. Plot of lg k_{obs} versus $(D-1)/(2D+1)$

Effect of added MnSO$_4$ concentration. To find out effect and involvement of various oxidation states such as [Cr(V)] and [Cr(IV)], we have studied the effect of [MnSO$_4$] on rate of oxidation by varying its concentration in the range of 001–0.005 M (Table 5).

Table 5. Effect of [MnSO$_4$] on oxidation of benzaldehyde by PFC at 303 K

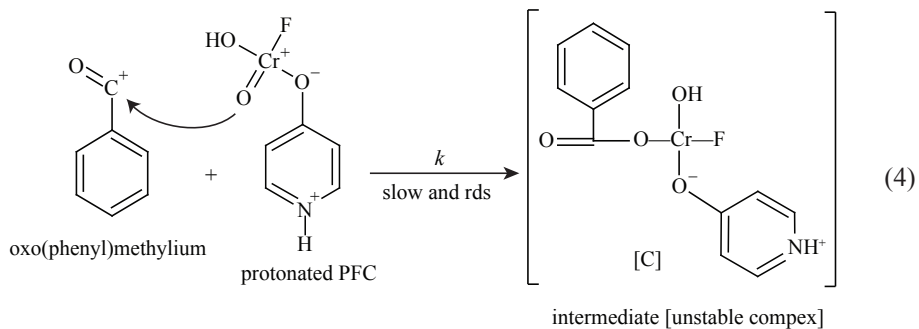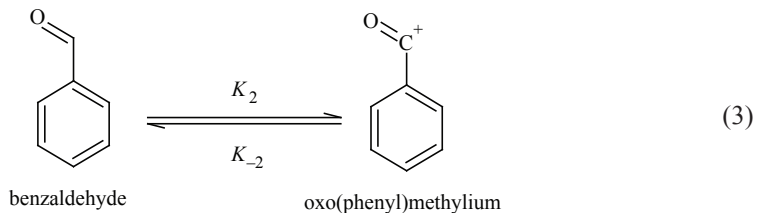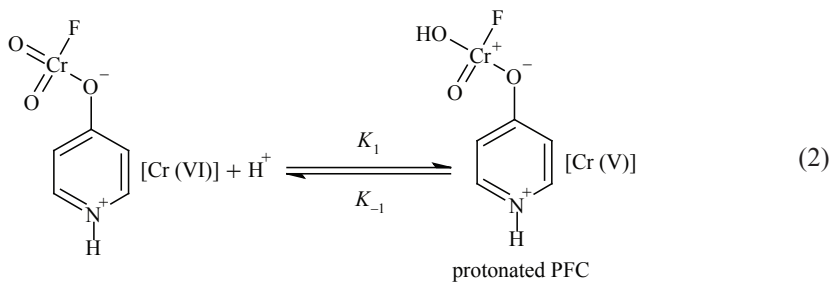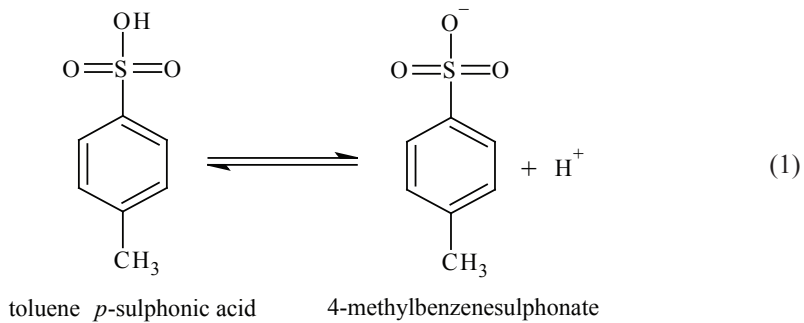| [MnSO$_4$] × 10^3 (mol dm^{-3})	k_{obs} × 10^4 (s^{-1})
0.0	11.7069
1.0	10.7089
2.0	10.2867
3.0	9.2888
4.0	8.9049
5.0	7.8686

It has been observed that addition of low concentration of Mn(II) ion can be explained by the disproportion of intermediate valence states of Cr(VI) and Cr(V). The addition of Mn(II) fixes the Cr(IV) species as Cr(III) and thus the total concentration of Cr(IV) available in a given time is lowered by the addition of Mn(II) and hence observed deceleration with increasing addition of Mn(II) ion. This may be taken as evidence for the formation of Cr(IV) species and hence PFC acts as a 2-electron transfer oxidant.
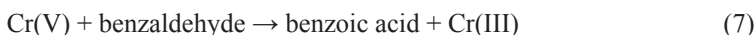
Induced polymerisation of acrylonitrile. The reaction mixture to which a known amount of acrylonitrile scavenger had been added initially was kept for 24 h in an inert atmosphere of N$_2$ and fails to induce the polymerisation of acrylonitrile. Then on dilution of the reaction mixture with methanol, no turbidity occurred, indicating the absence of free radical intervention.

MECHANISM AND RATE LAW

At fixed [H$^+$] the order with respect both to [PFC] and [BA] is unity. The oxidant undergoes protonation. The observed salt and solvent effects showed that the reaction is between an ion and a dipole in the slow rds and the ionic species is carbonium ion. The protonated PFC reacts with this oxo (phenyl) methylium ion (carbonium ion) to form a chromate ester which is an unstable species in rds. This unstable complex breaks fast to form benzoic acid. The following scheme and rate law is proposed to explain the kinetic observations.

S c h e m e

toluene *p*-sulphonic acid   4-methylbenzenesulphonate   (1)

$[Cr (VI)] + H^+$ ⇌ [Cr (V)]   (2)

protonated PFC

benzaldehyde   oxo(phenyl)methylium   (3)

oxo(phenyl)methylium   protonated PFC   intermediate [unstable compex]   (4)

621

$$\text{intermediate [unstable compex]}$$

$$Cr(IV) + Cr(VI) \rightarrow 2Cr(V) \tag{6}$$

$$Cr(V) + \text{benzaldehyde} \rightarrow \text{benzoic acid} + Cr(III) \tag{7}$$
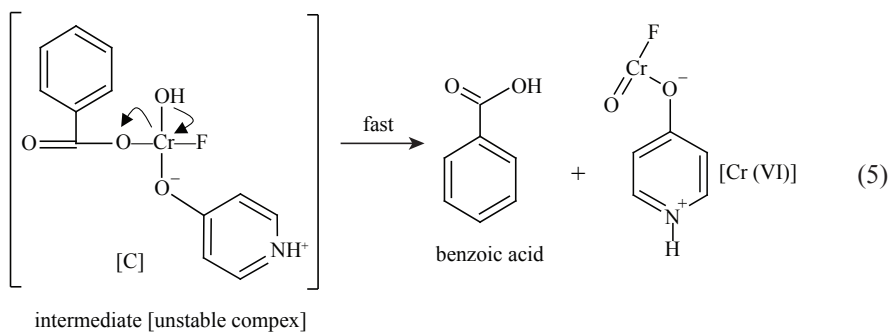
RATE LAW

$$\text{rate} = -d[PFC]/dt = k[C]$$

$$R = k\,[Ald^+]\,[H^+PFC]$$

$$d[H^+PFC]/dt = K_1\,[PFC]\,[H^+] - K_{-1}\,[H^+PFC] = 0$$

$$K_1\,[PFC]\,[H^+] = K_{-1}\,[H^+PFC]$$

$$[H^+PFC] = K_1\,[PFC]\,[H^+]/K_{-1}$$

$$d[Ald^+]/dt = K_2\,[Ald] - K_{-2}\,[Ald^+] = 0$$

$$K_2\,[Ald] = K_{-2}\,[Ald^+]$$

$$[Ald^+] = K_2\,[Ald]/K_{-2}.$$

Putting values

$$R = k\,K_2/K_{-2}\,[Ald]\,K_1/K_{-1}\,[PFC]\,[H^+]$$

$$R = k_{obs}\,[PFC] = k_1\,[PFC]$$

where $k_{obs} = k\,K_2/K_{-2}\,[Ald]\,K_1/K_{-1}\,[H^+] = k_1$

$$k_1 = k_s\,[Ald]\,[H^+]$$

where $k_s = k\,K_2/K_{-2}\,K_1/K_{-1}$, i.e. specific rate constant

$$k_s = k_1/[Ald]\,[H^+].$$

CONCLUSIONS

The oxidation of aromatic aldehyde like benzaldehyde in non-aqueous medium by PFC proceeds via the formation of an unstable chromate ester which is formed in rds. This chromate ester breaks to form the product benzoic acid and Cr(III).

REFERENCES

1. K. B. WIBERG: Oxidation in Organic Chemistry. Part A. Academic Press, Wiley, New York, 1965, p. 69.
2. K. M. DILSHA, S. KOTHARI: Kinetics and Correlation Analysis of Reactivity in the Oxidation of Organic Sulfides by Butyltriphenylphosphonium Dichromate. J Chem Sci, **121** (2), 189 (2009).
3. N. SONI, V. TIWARI, V. SHARMA: Correlation Analysis of Reactivity in the Oxidation of Substituted Benzyl Alcohols by Morpholinium Chlorochromate. Indian J Chem, **47** (A), 669 (2008).
4. S. V. KHANSOLEA, S. B. PATWARIA, A. Y. VIBHUTE, Y. B. VIBHUTE: Isoquinolinium Bromochromate: An Efficient and Stable Reagent for Bromination of Hydroxylated Aromatic Compounds and Oxidation of Alcohols. Chinese Chem Lett, **20** (3), 256 (2009).
5. B. L. HIRAN, S. JAIN, C. V. BHATT: Kinetics and Mechanism of the Oxidation of Lactic Acid and Mandelic Acid by Pyridinium Chlorochromate in Aqueous Acidic Medium. E-J Chem, **6** (1), (2009).
6. B. L. HIRAN, V. JOSHI, J. CHAUDHARY, N. SHORGAR, P. VERMA: Studies on Oxidation of Tyrosine by Pyridinium Bromochromate in Acetic Acid–Water Medium. Int J Chem Sci, **2** (2), 164 (2004).
7. B. L. HIRAN, N. NALWAYA, A. JAIN: Kinetics of Oxidation of Glycine by Pyridinium Bromochromate in Acetic Acid Medium. J Indian Chem Soc, **79** (1), 587 (2002).
8. G. VANANGAMUDI, S. SRINIVASAN: Kinetic Studies on the Oxidation of Some *para*- and *meta*-substituted Cinnamic Acids by Pyridinium Bromochromate in the Presence of Oxalic Acid (A Co-oxidation Study). E-J Chem, **6** (3), 920 (2009).
9. B. L. HIRAN, R. K. MALKANI, P. CHOUDHARY, P. VERMA, N. SHORGAR: Kinetics and Mechanism of Oxidation of *para*-substituted Benzaldehydes by Quinolinium Bromochromate in Aquo–Acetic Acid Medium. Asian J Chem, **18** (4), 3081 (2007).
10. A. THIRUMOORTHY, D. S. BHUVANESHWARI, K. P. ELANGO: Preferential Solvation Effects on the Cr(VI) Oxidation of Benzylamines in Benzene/2-methylpropan-2-ol mixtures. Int J Chem Kinet, **42** (3), 159 (2010).
11. P. KUMAR, D. PANDAY, S. KOTHARI: Kinetics and Mechanism of the Oxidation of Aliphatic Aldehydes by Benzimidazolium Dichromate. Croat Chem Acta, **84** (1), 53 (2011).
12. S. HUSSAIN, T. SURENDRA, M. FAROOQUI: Kinetics and Mechanism of Oxidation of 2-methyl-1-butanol by Tripropyl Ammonium Florochromate. The Experiment, **7** (2), 395 (2013).
13. S. GHAMMAMY, M. R. BAGHY, M. MIRRAHIMI, M. D. VAIRA, Z. JAVANSHIR, K. MEHRANI, S. MALEKI: Synthesis, Characterization, X-ray Structural Analysis and Study of Oxidative Properties of a Chlorochromate(VI) Complex with Benzyltriphenylphosphonium Cation. Transit Metal Chem, **34**, 565 (2009).
14. M. N. BHATTACHARJEE, M. K. CHAUDHURI, H. S. DASGUPTA: Kinetics and Mechanism of Oxidation of Alcohols by Pyridinium Fluorochromate. Bull Chem Soc Jpn, **57** (1), 258 (1984).
15. K. K. BANERJI: Oxidation of Aliphatic Alcohols by Pyridinium Fluorochromate: A Kinetic Study. J Chem Soc Perk T, **2**, 547 (1988).
16. K. K. BANERJI: Oxidation of Aromatic Alcohols by Pyridinium Fluorochromate: A Kinetic Study. J Chem Soc Perk T, **2**, 2062 (1988).
17. B. BHATTACHARJEE, M. N. BHATTACHARJEE, M. BHATTACHARJEE, A. K. BHATTACHARJEE: Oxidation of Naphthalene and Phenanthrene by Pyridinium Fluorochromate (PFC) – A Kinetic and Mechanistic Study. Int J Chem Kinet, **17** (6), 629 (2004).

18. R. ASOPA, S. AGARWAL, K. K. BANERJI: Kinetics and Mechanism of the Oxidation of Some Hydroxyacids by Pyridinium Fluorochromate. Proc Indian Acad Sci (Chem Sci), **103** (4), 563 (1991).

19. R. KHANCHANDANI, P. K. SHARMA, K. K. BANERJI: Kinetics and Mechanism of the Oxidation of Diols by Pyridinium Fluorochromate. J Chem Res-S, **432**, (M), 2622 (1995).

20. S. AGARWAL, K. CHAUDHARY, K. K. BANERJI: Kinetic Study of the Oxidation of Thioacids by Pyridinium Fluorochromate. Trans Metal Chem, **16** (6), 641 (1991).

21. V. M. KAMBLE, S. B. JOSHI: Pyridinium Fluorochromate Oxidation of Benzaldoxime in Acid Medium. Orient J Chem, **22** (1), 145 (2006).

22. R. ASOPA, P. BHATT, K. K. BANERJI: Correlation Analysis of Reactivity in the Oxidation of Substituted Mandelic Acids by Pyridinium Fluorochromate. Indian J Chem A, **31**, 706 (1992).

23. R. KHANCHANDANI, K. K. BANERJI, P. K. SHARMA: Kinetics and Mechanism of the Oxidation of Secondary Alcohols by Pyridinium Fluorochromate. J Indian Chem Soc, **42**, 75 (1998).

24. S. AGARWAL, K. CHOWDHURY, K. K. BANERJI: Kinetics and Mechanism of the Oxidation of Aromatic Aldehydes by Pyridinium Fluorochromate. J Org Chem, **56** (17), 5111 (1991).

25. V. SHARMA, P. K. SHARMA, K. K. BANERJI: Kinetics and Mechanism of the Oxidation of DL-methionine by Pyridinium Fluorochromate. J Chem Res-S, 290 (1996).

26. P. S. RAMAKRISHNAN, K. NAMBI: Linear Free Energy Relationship and Conformational Effects on Oxidation of Aromatic Acetals by Pyridinium Fluorochromate. J Indian Chem Soc, **77**, 232 (2000).

27. S. KAVITHA, A. PANDURANGAN, I. ALPHONSE: Kinetics and Mechanism of Oxidation of Beta Benzoylpropionic Acids by Pyridinium Fluorochromate in Aqueous Acetic Acid Medium. Indian J Chem, **44** (4), 715 (2005).

28. (a) S. G. PATIL, S. B. JOSHI: Kinetics and Mechanism of Oxidation of Substituted Phenols by Pyridinium Fluorochromate in Glacial Acetic Acid. Orient J Chem, **22** (3), (2006); (b) S. G. PATIL, S. B. JOSHI: Kinetics and Mechanism of Oxidation of Naphthols by Pyridinium Fluorochromate in Glacial Acetic Acid. Orient J Chem, **22** (3) (2006).

29. F. AYDIN, E. TURUNC: The Use of Pyridinium Fluorochromate (PFC) Supported on TriSyl Silica Gel for Oxidation Reactions. J Serb Chem Soc, **72** (2), 129 (2007).

30. P. K. SHARMA: Structure–peactivity Correlation in the Oxidation of Substituted Benzaldehydes by 2,2-bipyridinium Chlorochromate. J Indian Chem Soc, **85**, 1281 (2008).

31. J. CHAUDHARY: Studies in Kinetics and Mechanism of Electron Transfer Reaction between Organic Compounds and Cr(VI) Complexes. Ph. D. Thesis, Mohan Lal Sukhadia University, Udaipur, India, 2002.

32. S. SHEIK MANSOOR, S. SYED SHAFI: Kinetics and Mechanism of Oxidation of Aromatic Aldehydes by Imidazolium Dichromate in Aqueous Acetic Acid Medium. E-J Chem, **6** (S1), S522 (2009).

33. H. A. A. MEDIEN: Kinetics of Oxidation of Benzaldehydes by Quinolinium Dichromate. Z Naturforsch, **58b**, 1201 (2003).

34. V. S. R. RAJU, P. K. SHARMA, K. K. BANERJI: Kinetics and Mechanism of the Oxidation of Substituted Benzaldehydes by Benzyltrimethylammonium Chlorobromate. J Org Chem, **65**, 3322 (2000).

35. K. KRISHNASAMY, D. DEVANATHAN, J. DHARMARAJA: Kinetics and Mechanism of Oxidation of Substituted Benzaldehydes by 4-(dimethylamino) Pyridinium Chlorochromate. Transit Metal Chem, **32**, 922 (2007).

36. P. GUPTA, S. KOTHARI, K. K. BANERJI: Kinetics and Correlation Analysis of Reactivity in the Oxidation of Substituted Benzaldehydes by Benzyltrimethylammonium Dichloroiodate. Oxid Commun, **24**, 565 (2000).

37. N. NALWAYA: Kinetics and Mechanism of Oxidation of Some Aromatic Hydroxy and Carbonyl Compounds by Quinolinium Halo Chromates. Ph.D. Thesis, Mohan Lal Sukhadia University, Udaipur, India, 2002.

38. B. L. HIRAN, N. NALWAYA, P. VERMA, N. SHORGAR: Kinetics and Mechanism of Oxidation of Some Substituted Benzaldehyde by Quinolinium Bromochromate in Acetic Acid–Perchloric Acid–Water Medium. Oxid Commun, **28**, 695 (2005).
39. R. GANDHARI, P. P. MADDUKURI, K. V. THOTTUMKARA: Oxidation of Aromatic Aldehydes Using Oxone. J Chem Educ, **84** (5), 852 (2007).
40. K. H. CHUNG, B. C. MOON, C. H. LIM, J. P. KIM, J. H. LEE, D. Y. CHI: Oxidation of Aromatic Aldehydes with Tetrabutylammonium Fluoride: Competition with the Cannizzaro Reaction. Bull Korean Chem Soc, **27** (8), (2006).
41. Merck Index. 11th ed., 1989, p. 9459.
42. M. N. BHATTACHARJEE, M. K. CHOUDHARY, H. S. DASGUPTA, N. ROY, D. T. KHATHING: Pyridinium Fluorochromate Synthesis, 1982, 588–590.
43. M. N. BHATTACHARJEE, M. K. CHAUDHARY, S. PURKESYATHA: Easy Synthesis of Pyridinium Fluorochromate, $[C_5H_5NH[CrO_3F]$, and Its Crystal Structure. J Fluorine Chem (Elsevier Sequoia, Lausanne), **81** (2), 211 (1997).
44. S. GLASSTONE, K. J. LAIDLER, H. ERYING: The Theory of Rate Process. Mc Graw-Hill, New York, Chapters III and IV, 1941.
45. F. BASOLO, R. G. PEARSON: Mechanism of Inorganic Reactions. A Study of Metal Complexes in Solution. 2nd ed. Wiley-Eastern, New Delhi, 1973, p. 129.
46. K. J. LAIDLER: Chemical Kinetics. 3rd ed. Pearson Education, New Delhi, 2005, p. 198.
47. (a) G. J. SCATCHARD: Chem Phys, **10**, 229 (1932); (b) G. J. SCATCHARD: Chem Phys, **7**, 657 (1939); S. Z. AHMED, S. S. SHAFI, S. Sh. MANSOOR: Oxidation of Lactic Acid by Pyridinium Fluorochromate: A Kinetic and Mechanistic Study. Pelagia Research Library Advances in Applied Science Research, **3** (1), 123 (2012).
48. E. S. AMIS: Solvent Effects on Reaction Rates and Mechanisms. Academic Press, New York, 1967, p. 42.

KINETICS OF OXIDATION OF SOME SUBSTITUTED N,α-DIPHENYLNITRONES BY NICOTINIUM DICHROMATE IN AQUEOUS DIMETHYL FORMAMIDE IN THE PRESENCE OF OXALIC ACID

G. RAJARAJAN[a], S. MAHALAKSHMI[b], N. JAYACHANDRAMANI[b], J. JAYABHARATHI[a], V. THANIKACHALAM[a]*

[a]*Department of Chemistry, Annamalai University, 608 002 Annamalai Nagar Chidambarm, Tamil Nadu, India*
[b]*Department of Chemistry, Pachaiyappa's College, 600 030 Chennai, India*
E-mail: *pvta1998@yahoo.co.in*

ABSTRACT

The kinetics of oxidation of *para*- and *meta*-substituted aldonitrones by nicotinium dichromate (NDC) has been studied in aqueous dimethyl formamide (DMF) in the presence of oxalic acid. It is worthwhile investigating whether oxalic acid undergoes co-oxidation or just functions as a catalyst in the reaction. The reaction was followed iodometrically. The reaction is first order with respect to [nitrone], [NDC] and [oxalic acid]. There was no discernible effect on rate with an increase in ionic strength and the rate of oxidation decreased with decreasing dielectric constant of the medium. A mechanism involving the protonated nitrone and NDC as the reactive oxidant has been proposed. The activation parameters were calculated and presented.

Keywords: aldonitrones, nicotinium dichromate, isokinetic plot, entropy, enthalpy, free energy, oxalic acid.

AIMS AND BACKGROUND

Nicotinium dichromate (NDC) has been reported as a mild and selective oxidising agent in synthetic organic chemistry. We are interested in the kinetics of reactions of complexed Cr(VI) species and have reported the kinetics and mechanism of oxidation of alcohols to carbonyl compounds[1], mercaptans, polynuclear aromatic hydrocarbons[1], diphenylsulphide[2], *para*-toluenesulphonic acid, various 4-substituted-1,4-dihydropyridines[3], primary aliphatic alcohols[4], methionine[5], anilines[6], benzaldehydes[7], benzylalcohols[8], phenols[9] 2-naphthol[10], amines to carbonyl compounds[11], cleavage of cyclic ketones[12] by nicotinium dichromate. A survey of literature shows that there

---

* For correspondence.

are only a few reports on the kinetic studies with nitrones[13–21]. Oxalic acid is found to catalyse the oxidation of organic substrate by Cr(VI) (Refs 19, 22 and 23). We report in this paper the kinetics of oxidation of some substituted aldonitrones by NDC in aqueous DMF in the presence of oxalic acid.

EXPERIMENTAL

Reagents. All the chemicals used were of high purity mostly either of AR or GR grade. Aldonitrones[24] and NDC (Ref. 1) were prepared by known methods and their purity checked by TLC and iodometric method was used for NDC. Solutions were prepared by dissolving appropriate amounts of recrystallised samples in DMF. Experiments were conducted in a thermostat which could maintain the temperature with an accuracy of $\pm 0.1°C$.

Product analysis and stoichiometry. The product analysis was carried out under kinetic conditions. In a typical experiment the nitrone and other reagents were mixed together. After 24 h the reaction mixture was extracted with chloroform. The solvent was removed at reduced pressure after drying over anhydrous sodium sulphate. The products obtained were analysed by Co-TLC and IR. Spectral data coincided with reported values in literature[25]. The analysis showed that benzaldehyde and nitrosobenzene were the products formed in the reaction.

Nitrone in solution was mixed with an excess of NDC in DMF - water in the presence of perchloric acid and oxalic acid. The concentration of NDC in the reaction mixture after 24 h was determined by titrating against standard sodium thiosulphate solution. From the decrease in the concentration of NDC, the stoichiometry of the reaction was determined as 1:1:

$$PhCH\overset{+}{=}N-Ph \; + \; HCrO_4^- \; \xrightarrow[\text{OxH}_2]{\text{H}^+} \; PhCHO \; + \; PhNO \; + \; CrO_2 \; + \; H_2O \quad (1)$$
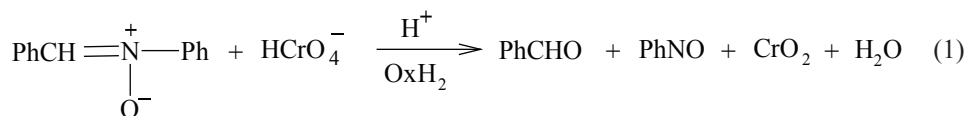
Kinetic measurements. The reactions were carried out under pseudo-first order conditions by maintaining a large excess of [nitrone] over [NDC] in the presence of oxalic acid. The solvent was DMF - water (50% v/v). The reactions were followed at a constant temperature ($\pm 0.1°C$). The pseudo-first order rate constant, k_{obs}, was evaluated from the linear (r = 0.990–0.999) plots of lg [NDC] against time. Duplicate kinetic runs showed that the rate constants were reproducible to within $\pm 3\%$. The rate constant, k_2, was calculated using the relation $k_2 = k_{obs}/[\text{nitrone}]$.

RESULTS AND DISCUSSION

The kinetics of oxidation of nitrones by NDC was carried out in 50% DMF–water (v/v) in the presence of oxalic acid in order to study the behaviour of oxalic acid. It is

imperative to find out whether it undergoes co-oxidation or just functions as a catalyst in the reaction. In the presence of oxalic acid, the reaction is first order with respect to [NDC]. Further, the pseudo-first order rate constant, k_{obs}, is found to be independent of the initial concentration of NDC.

The substrate (aldonitrone) concentration was varied in the range 5 to 15×10^{-3} M at 308 K in the presence of oxalic acid keeping all the other constituents and conditions constant (Table 1). The k_{obs} values increased with increasing concentration of nitrone. The plot of lg k_{obs} versus lg [nitrone] is a straight line with a slope of unity. The plot of k^{-1}_{obs} versus [nitrone]$^{-1}$ is also linear ($r = 0.997$). The effect of the acid on reaction rate was studied at constant [NDC] and [nitrone] at 308 K. With increasing [H$^+$], the rate of NDC oxidation of nitrone also increases. The plot of lg k_{obs} versus lg [H$^+$] is linear with slope less than unity (Table 1) (Ref. 26 and 27).

Table 1. Effect of variation of [NDC], [nitrone], [HClO$_4$], [OxH$_2$] and % of DMF on the rate of oxidation of nitrone by NDC at 308 K

[NaClO$_4$] = 0.1 M

[NDC] × 10³ (M)	[Nitrone] × 10² (M)	[HClO$_4$] × 10³ (M)	[OxH$_2$] × 10² (M)	% DMF (v/v)	k_{obs} × 10³ (s^{-1})
0.50	1.00	6.00	1.00	50	1.603
0.75	1.00	6.00	1.00	50	1.630
1.00	1.00	6.00	1.00	50	1.603
1.25	1.00	6.00	1.00	50	1.615
1.50	1.00	6.00	1.00	50	1.620
1.00	0.50	6.00	1.00	50	0.857
1.00	0.75	6.00	1.00	50	1.220
1.00	1.00	6.00	1.00	50	1.603
1.00	1.25	6.00	1.00	50	2.170
1.00	1.50	6.00	1.00	50	2.467
1.00	1.00	3.00	1.00	50	1.488
1.00	1.00	6.00	1.00	50	1.603
1.00	1.00	9.00	1.00	50	1.687
1.00	1.00	15.00	1.00	50	1.862
1.00	1.00	17.50	1.00	50	1.961
1.00	1.00	6.00	0.50	50	0.798
1.00	1.00	6.00	0.75	50	1.212
1.00	1.00	6.00	1.00	50	1.603
1.00	1.00	6.00	1.50	50	2.405
1.00	1.00	6.00	2.00	50	3.120
1.00	1.00	6.00	1.00	40	1.646
1.00	1.00	6.00	1.00	50	1.603
1.00	1.00	6.00	1.00	60	1.274
1.00	1.00	6.00	1.00	70	1.150
1.00	1.00	6.00	1.00	80	0.953

The effect of oxalic acid on the reaction was studied by varying its concentration from 5 to 20×10^{-3} M at constant [NDC], [nitrone] and [H^+] ion at 308 K. The rate of oxidation increased with increasing concentration of oxalic acid. The results are collected in Table 1. The slope of the plot of lg k_{obs} versus lg [oxalic acid] is found to be unity ($ca = 0.9854$, $r = 0.999$). When the experiment was repeated with oxalic acid in the absence of nitrone, there was no oxidation of oxalic acid. But, the addition of oxalic acid enhances the rate of oxidation of nitrone. This observation clearly establishes that oxalic acid does not undergo co-oxidation under the experimental conditions employed in this investigation and it acts only as a catalyst[19,22,23]. The addition of MnSO$_4$ (Table 2) caused a very little change in the rate of oxidation[28]. It shows that 3-electron changes in the slow step do not take place. The influence of ionic strength on the rate of oxidation of nitrones was studied by the addition of sodium perchlorate. There was no discernible effect with an increase in concentration of sodium perchlorate (Table 3), indicating the involvement of molecules in the rate-determining step.

Table 2. Effect of [MnSO$_4$] on the rate of oxidation of nitrone by NDC at 308 K in the presence of oxalic acid
[NDC] $= 1.0 \times 10^{-3}$ M; [nitrone] $= 1.0 \times 10^{-2}$ M; DMF–water $= 50\%$ (v/v); [H^+] $= 6.0 \times 10^{-3}$ M; [OxH$_2$] $= 1.0 \times 10^{-2}$ M

[MnSO$_4$] $\times 10^3$ (M)	$k_{obs} \times 10^3$ (s^{-1})
0.00	1.603
1.00	1.482
2.00	1.342
3.00	1.195
4.00	1.085

Table 3. Effect of ionic strength on the rate of oxidation of nitrone by NDC at 308 K in the presence of oxalic acid
[NDC] $= 1.0 \times 10^{-3}$ M; [nitrone] $= 1.0 \times 10^{-2}$ M; DMF–water $= 50\%$ (v/v); [H^+] $= 6.0 \times 10^{-3}$ M; [OxH$_2$] $= 1.0 \times 10^{-2}$ M

[NaClO$_4$] $\times 10^2$ (M)	$k_{obs} \times 10^3$ (s^{-1})
5.00	1.605
7.00	1.607
10.00	1.603
12.00	1.550
15.00	1.456

It was found that the rate of oxidation decreased on decreasing the dielectric constant of the medium by increasing the percentage of DMF in the solvent mixture (Table 1). This result also supports the involvement of ion–dipole species in the slow step[29]. Addition of acrylonitrile to the reaction mixture did not show any polymerisation thereby ruling out the possibility of a free radical mechanism[30].

The reactions were carried out at 4 different temperatures (298, 303, 308 and 313 K) in the presence of oxalic acid and the thermodynamic parameters, viz. entropy of activation, enthalpy of activation and free energy of activation were calculated from the linear plot of ln (k_2/T) versus $1/T$. The calculated values are summarised in Table 4.

Table 4. Rate constants and activation parameters for the oxidation of nitrones by NDC
[Nitrone] = 1.0×10^{-2} M; [NDC] = 1.0×10^{-3} M; [OxH$_2$] = 1.0×10^{-2} M; [NaClO$_4$] = 0.1 M; DMF–water = 50 % (v/v)

S No	R=	$k_2 \times 10^2$ (dm^3 mol^{-1} s^{-1})				ΔH^* (kJ mol^{-1})	ΔS^* (J K^{-1} mol^{-1})	ΔG^* (kJ mol^{-1})	r
		298 K	303 K	308 K	313 K				
1	H	5.90	10.40	16.03	18.92	58.58	71.17	80.50	0.975
2	*p*-Me	6.00	11.10	18.02	20.86	63.18	50.50	80.27	0.971
3	*p*-OMe	7.67	12.80	19.82	22.88	55.27	80.20	79.97	0.976
4	*p*-F	5.62	9.67	15.73	18.52	60.68	64.56	80.56	0.978
5	*p*-Cl	5.18	9.35	13.44	17.61	60.22	66.81	80.80	0.986
6	*p*-Br	5.00	9.16	12.80	16.84	59.31	70.11	80.90	0.983
7	*p*-NO$_2$	3.82	7.09	9.51	13.28	60.13	69.54	81.58	0.985
8	*m*-F	5.30	8.57	11.43	14.19	47.88	108.16	81.19	0.984
9	*m*-Cl	5.80	8.80	11.29	14.00	42.42	125.83	81.78	0.988
10	*m*-Br	5.47	8.52	11.38	13.73	44.89	117.95	81.22	0.984
11	*m*-NO$_2$	4.04	7.28	10.14	13.30	58.19	75.67	81.50	0.984

Mechanism and rate law. The kinetics of oxidation of nitrones by NDC was carried out in 50% DMF–water in the presence of oxalic acid. The oxidation by Cr(VI) depends on the nature of Cr(VI) species used and the rate and type of the reaction may vary with the solvent employed. It is found that in dilute aqueous solutions (< 0.05 M), most of the Cr(VI) is only in the monomeric form (Fig. 1) (Refs 31–33). The reaction is found to be first order each with respect to [NDC], [nitrone] and [oxalic acid]. The reaction is catalysed by acid. The increase in oxidation rate with acidity suggests the participation of protonated nitrone prior to the rate-limiting step.
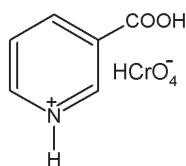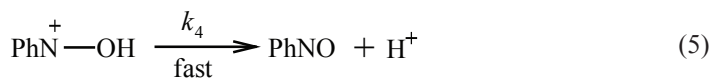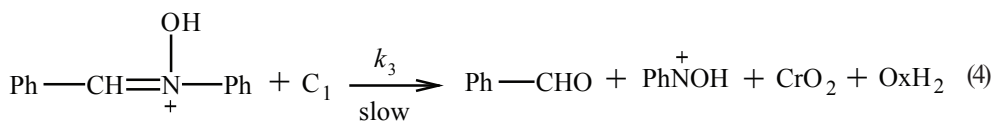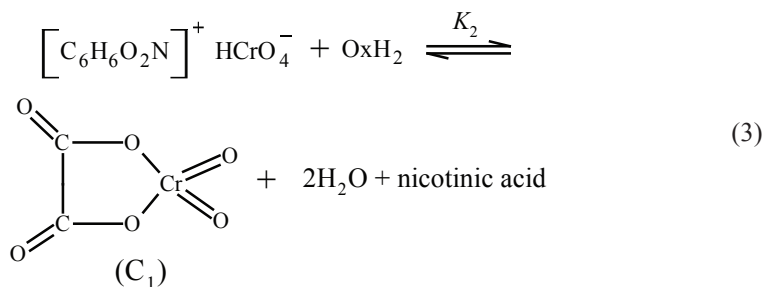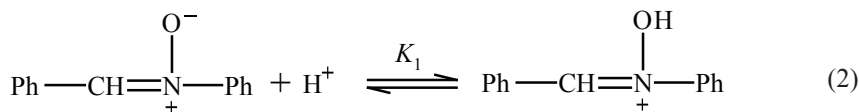

Fig. 1. Structure of nicotinium chromate ion

Based on the above observations a mechanism involving the protonated nitrone and Cr-oxalic acid complex is proposed for the reaction.

$$Ph-CH=\overset{+}{N}-Ph \;+\; H^+ \;\underset{}{\overset{K_1}{\rightleftharpoons}}\; Ph-CH=\overset{OH}{\underset{+}{N}}-Ph \qquad (2)$$

where the left structure bears O^- on nitrogen.

$$\left[C_6H_6O_2N\right]^+ HCrO_4^- \;+\; OxH_2 \;\overset{K_2}{\rightleftharpoons}\;$$

$$(C_1) \;+\; 2H_2O \;+\; nicotinic\ acid \qquad (3)$$

$$Ph-CH=\overset{OH}{\underset{+}{N}}-Ph \;+\; C_1 \;\xrightarrow[slow]{k_3}\; Ph-CHO \;+\; Ph\overset{+}{N}OH \;+\; CrO_2 \;+\; OxH_2 \qquad (4)$$

$$Ph\overset{+}{N}-OH \;\xrightarrow[fast]{k_4}\; PhNO \;+\; H^+ \qquad (5)$$

The rate law for the suggested mechanism is:

$$-\frac{d[NDC]}{dt} = \frac{K_1 K_2 k_3 [NDC][S][H^+][OxH_2]}{1 + K_1[H^+]} \qquad (6)$$

$$k_{obs} = \frac{K_1 K_2 k_3 [S][H^+][OxH_2]}{1 + K_1[H^+]}, \qquad (7)$$

where S is nitrone.

Effect of substituents. The effect of substituents on the rate of oxidation was studied by selecting a number of *meta-* and *para*-substituted-N,α-diphenylnitrones at 4 different temperatures in the presence of oxalic acid, the activation parameters were calculated and summarised in Table 4. The electron-releasing groups enhanced and the electron-withdrawing groups retarded the oxidation rate. The order of reactivity of the different substituents is as follows: *p*-OMe > *p*-Me > –H > *p*-F > *p*-Cl > *p*-Br > *m*-F > *m*-Cl > *m*-Br > *m*-NO$_2$ > *p*-NO$_2$. The lg (k_x/k_H) values were plotted against the σ values in a Hammett plot (Fig. 1) (Ref. 34). The values of reaction constant (ρ) were calculated as –0.226, –0.224, –0.313, –0.242 at 298, 303, 308 and 313 K, respectively. The small negative ρ values obtained indicate only a small structural influence on the rate. The negative ρ value is attributed to the development of a positively charged transition state.

631

The enthalpy, entropy and free energy of activation were calculated using the Erying plot (Table 4). A linear relationship between enthalpy of activation (ΔH^*) and entropy of activation (ΔS^*) has been observed for the oxidation of nitrones by NDC (Ref. 35). A plot of ΔH^* versus ΔS^* gave a straight line with a good correlation coefficient ($r = 0.998$; $\beta = 299$ K) in the presence of oxalic acid (Fig. 2). A negative value of entropy of activation (ΔS^*) suggests the formation of an ordered activated complex with a reduction in the degrees of freedom of reacting molecules[36]. The Exner plots[37] (Fig. 3) also support the operation of a common mechanism in this reaction. Constancy of ΔG^* values for all the nitrones indicates the operation of the same mechanism in all the cases.
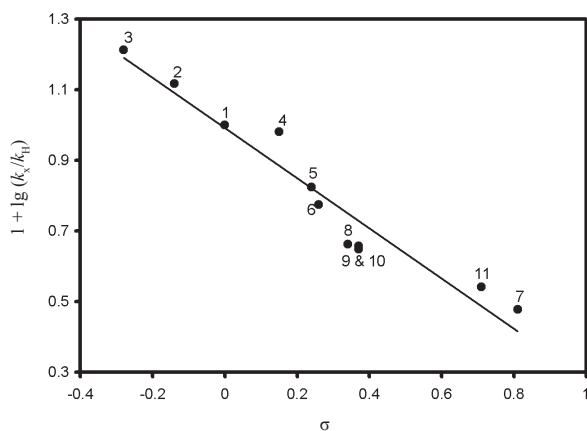

Fig. 2. The Hammett plot of $1 + \lg (k_x/k_H)$ versus σ for the oxidation of nitrones with NDC in the presence of oxalic acid (numbered as in Table 4)
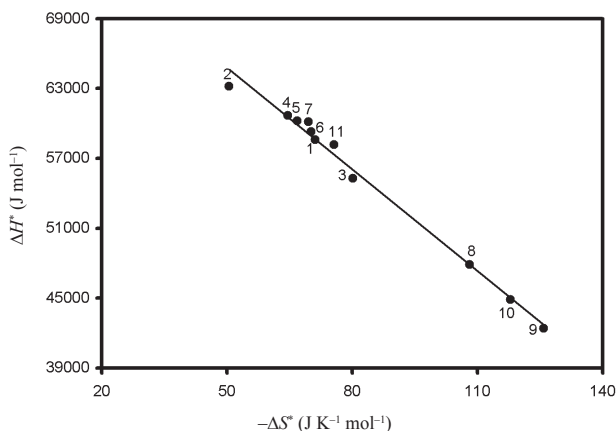

Fig. 3. Isokinetic plot of ΔH^* versus $-\Delta S^*$ for the oxidation of nitrones with NDC in the presence of oxalic acid (numbered as in Table 4)
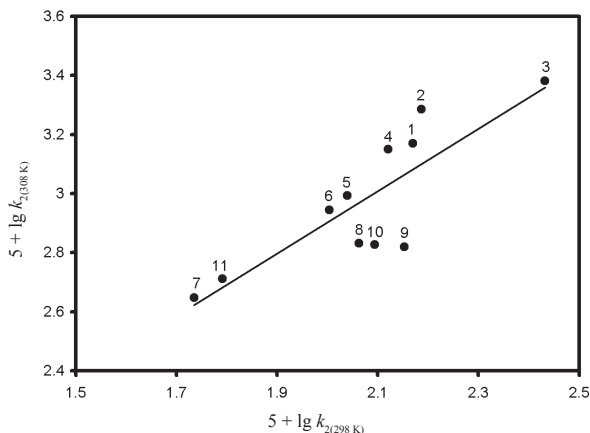
Fig. 4. The Exner plot of $5 + \lg k_{2(308 \text{ K})}$ versus $5 + \lg k_{2(298 \text{ K})}$ for the oxidation of nitrones by NDC in the presence of oxalic acid (numbered as in Table 4)

CONCLUSIONS

The kinetics and oxidation of nitrones by NDC in the presence of oxalic acid have been studied. The reaction is of first order with respect to concentration of substrate, oxidant and oxalic acid and fractional order with respect to concentration of acid. The rate of oxidation is influenced by the dielectric constant of the medium. The Gibbs free energy values show that all the nitrones followed a common mechanism of oxidation.

REFERENCES

1. C. LOPEZ, A. GONZALEZ, F. P. COSSIO, C. PALOMO: 3-Carboxypyridinium Dichromate (NDC) and 4-carboxypyridinium Dichromate (INDC) Two New Mild, Stable Efficient and Inexpensive Chromium(VI) Oxidation Reagents. Synth Commun, **15**, 1197 (1985).
2. C. KARUNAKARAN, V. CHIDAMBARANATHAN: Kinetic Study on Nicotinium and Isonicotinium Dichromates Oxidation: Oxidation of Diphenyl Sulphides. Rev. Ronum Chim, **44**, 491 (1985); C. KARUNAKARAN, V. CHIDAMBARANATHAN: Linear Free Energy Relationships Near Isokinetic Temperature Oxidation of Organic Sulphides with Nicotinium Dichromate. Croat Chem Acta, **74**, 51 (2001).
3. M. M. SADEGHI, I. MOHAMMADPOOR-BALTORK, H. R. MEMARIAN, S. SOBHANI: Efficient Oxidation of Hantzsch 1,4-dihydropyridines with Nicotinium Dichromate. Synth Commun, **30**, 1661 (2000).
4. C. KARUNAKARAN, S. SURESH: Similar Substituent Effects in the Oxidations of Primary Aliphatic Alcohols with Dichromate and Halochromates of Heterocyclic Bases. Int J Chem Kinet, **37**, 5 (2005).
5. D. MALARVIZHI, M. PANDESWARAN, D. S. BHUVANESWARI, K. P. ELANGO: Solvent Effects on the Kinetics of Oxidation of Methionine by Nicotinium Dichromate. J Indian Chem Soc, **83**, 895 (2006).
6. D. S. BHUVANESWARI, K. P. ELANGO: Effect of Preferential Solvation on the Kinetics and Thermodynamics of Oxidation of Anilines by Nicotinium Dichromate. Z Naturforsch, **60**, 1105 (2005):

D. S. BHUVANESWARI, K. P. ELANGO: Correlation Analysis of Reactivity in the Oxidation of Anilines by Nicotinium Dichromate in Non-aqueous Media. Int J Chem Kinet, **38**, 657 (2006).

7. K. G. SEKAR: Kinetic Studies on the Oxidation of Some *para-* and *meta*-substituted Benzaldehydes by Nicotinium Dichromate. J Chem Res, 626 (2002).

8: S. PATEL, B. K. MISHRA: A Novel Lipopathic Cr(VI) Oxidant for Organic Substrates: Kinetic Study of Oxidation of Benzyl Alcohol. Int J Chem Kinet, **38**, 651 (2006).

9. K. GUNASEKAR, K. ANBARASU: Linear Free Energy Relationships in the Chromium(VI) Oxidation of Phenol. Croat Chem Acta, **82**, 819 (2009).

10. M.VELLAISAMY, K. SURYAKALA, M. RAVISHANKAR: Kinetics and Mechanism of Oxidation of 2-naphthol by Nicotinium Dichromate. J Chem Pharm Res, **3**, 678 (2011).

11. S. SOBHANI, S. ARYANEJAD, M. F. MALEKI: Nicotinium Dichromate (=3-carboxy-pyridinium Dichromate; NDC) as an Efficient Reagent for the Oxidative Deamination of Amines and Aminophosphonates. Helv Chim Acta, **95**, 613 (2012).

12. S. K. NIGAM, P. PATEL, A. K. S. TIWARI, A. TIWARI: Kinetic Study of Oxidation of Acettyl Acetone by Nicotinium Dichromate. Nano Vision, **3**, 70 (2013).

13. M. UMA, M. GOPALAKRISHNAN, J. JAYABHARATHI, V. THANIKACHALAM: Kinetics of Oxidation of Some Substituted N,α-diphenylnitrones by Bromamine-B in the Presence of Acid Medium. Indian J Chem B, **34**, 612 (1995).

14. M. UMA, M. GOPALAKRISHNAN, J. JAYABHARATHI, V. THANIKACHALAM: Kinetics of Oxidation of Some Substituted N,α-diphenylnitrones by Chloramine-B in the Presence of Acid Medium. J Indian Chem Soc, **73**, 92 (1996).

15. M. GOPALAKRISHNAN, J. JAYABHARATHI, V. THANIKACHALAM: Separation of Electronic and Steric Effects: Oxidation of *ortho*-substituted N,α-diphenylnitrones by Pyridinium Fluorochromate in Aqueous DMF Medium. Asian J Chem, **11**, 1459 (1999).

16. M. GOPALAKRISHNAN, M. UMA, J. JAYABHARATHI, V. THANIKACHALAM: Kinetics and Oxidation of N,α-diphenylnitrones by Pyridinium Fluorochromate in Aqueous DMF Medium. Afinidad, **59**, 688 (2002).

17. M. GOPALAKRISHNAN, J. JAYABHARATHI, M. UMA, V. THANIKACHALAM: Oxidation of N,α-diphenylnitrones by Pyridinium Chlorochromate in Aqueous DMF Medium – A Kinetic Study. Oxid Commun, **30**, 625 (2007); S. MANIVARMAN, G. MANIKANDAN, J. JAYABHARATHI, V. THANIKACHALAM, M. SEKAR: Kinetics and Mechanism of Oxidation of Some Substituted Nitrones by N-bromosuccinimide in Aqueous Alkaline Medium – A Kinetic Study. Oxid Commun, **30**, 823 (2007).

18. G. RAJARAJAN, N. JAYACHANDRAMANI, S. MANIVARMAN, J. JAYABHARATHI, V. THANIKACHALAM: Kinetics and Mechanism of Oxidation of N,α-diphenylnitrones by 4-(dimethylamino) pyridinium Chlorochromate (DMAPCC) in Aqueous DMF Medium. Transt Metal Chem, **33**, 393 (2008).

19. G. RAJARAJAN, J. JAYACHANDRAMANI, S. MANIVARMAN, J. JAYABHARATHI, V. THANIKACHALAM: Kinetics and Mechanism of Oxidation of Some Substituted Aldonitrones by Quinolinium Chlorochromate (QCC) in Aqueous DMF Medium in the Absence and Presence of Oxalic Acid. J Serb Chem Soc, **74**, 171 (2009).

20. S. MANIVARMAN, G. RAJARAJAN, G. MANIKANDAN, M. SEKAR, J. JAYABHARATHI, V. THANIKACHALAM: A Mechanistic Investigation of the Oxidation of N,α-diphenylnitrones by Dichloramine-T in Aqueous Acetonitrile Medium – A Non-linear Hammett Plot. J Serb Chem Soc, **74**, 493 (2009).

21. G. RAJARAJAN, N. JAYACHANDRAMANI, S. MANIVARMAN, G. MANIKANDAN, J. JAYABHARATHI, V. TAHNIKACHALAM: Nicotinium Dichromate Oxidation of Nitrones in Aqueous DMF Medium. A Kinetic Study. Oxid Commun, **32**, 383 (2009).

22. G. F. VANDERGRIFT, J. ROCEK: Catalysis in Oxidation Reactions. II. The Oxalic Acid Catalyzed Oxidation of Iodide. J Am Chem Soc, **98**, 1371 (1976).

23. R. E. HINTZ, E. J. ROCEK: Catalysis in Oxidation Reactions. 3. The Oxalic Acid Catalyzed Chromic Acid Oxidation of *tris*(1,10-phenanthroline) Iron(II). J Am Chem Soc, **99**, 132 (1977).

24. A. I. VOGEL: A Text Book of Practical Organic Chemistry. Longmann, London, ELBS, 1978, p. 722.

25. G. M. BRADLEY, H. L. STRAUSS: Infrared Studies of Nitrosobenzene. J Phys Chem, **79**, 1953 (1975).

26. G. MANGALAM, R. GURUMURTHI, R. ARUL, R. KARTHIKEYAN: Conformational Effects upon the Oxidation of Some Substituted Oxan-4-ols. Indian J Chem B, **35**, 413 (1996).

27. K. NAGARAJAN, S. SUNDARAM, N. VENKATASUBRAMANIAN: Oxidation of Secondary Alcohols by Cr(VI) in Presence of Oxalic Acid. Indian J Chem A, **18**, 335 (1979).

28. M. A. OLATUNJI, G. A. AYOKO: Kinetics and Mechanism of the Oxidation of L-methionine by Aqueous Solution of Chromium(VI). Polyhedron, **7**, 11 (1988); D. C. GASWICK, J. H. KRUEGER: Kinetics and Mechanism of the Chromium(VI)-iodide Reaction. J Am Chem Soc, **91**, 2240 (1969).

29. J. E. QUINLAN, E. A. AMIS: The Alkaline Hydrolysis of Methyl Propionate in Acetone–Water Mixtures and Solutions of Different Ionic Strength. J Am Chem Soc, **77**, 4187 (1955); P. D. SHARMA, Y. K. GUPTA: Kinetics and Mechanism of the Reduction of Thallium(III) by Arsenic(III) in Perchloric Acid Solution. J Chem Soc Dalton, 52 (1972).

30. J. S. LITTLER, W. A. WATERS: Oxidations of Organic Compounds with Quinquevalent Vanadium. Part I. General Survey; The Oxidation of Pinacol. J Chem Soc, 1299 (1959).

31. D. G. LEE, R. STEWART: The Nature of Chromium(VI) in Acid Solution and Its Relation to Alcohol Oxidation. J Am Chem Soc, **86**, 3051 (1964).

32. M. L. FREEDAM: Polymerisation of Anions: The Hydrolysis of Sodium Tungstate and of Sodium Chromate. J Am Chem Soc, **80**, 2072 (1958).

33. K. B. WIBERG: Oxidation in Inorganic Chemistry. Part A (Ed. K. B. Wiberg). Academic Press, New York, 1965.

34. J. MARCH: Advanced Organic Chemistry: Reactions, Mechanisms and Structure. McGraw Hill Book Company, New York, 1968, p. 241.

35. J. E. LEFFLER: Entropy Requirements of the Hammett Relationship. J Chem Phys, **23**, 2199 (1955).

36. A. K. SINGH, D. CHOPRA, S. RAHMANI, B. SINGH: Kinetics and Mechanism of Pd(II) Catalysed Oxidation of D-arabinose, D-xylose and D-galactose by N-bromosuccinimide in Acidic Solution. Carbohyd Res, **314**, 157 (1998).

37. O. EXNER: On the Enthalpy–Entropy Relationship. Collect Czech Chem Com, **29**, 1094 (1964).

HEALTH REASONS FOR IMPROVING THE OXIDATIVE STABILITY OF SUNFLOWER OIL. REVIEW

M. STOIA[a], S. OANCEA[b]*

[a] *'Victor Papilian' Faculty of Medicine, 'Lucian Blaga' University of Sibiu, 2A Lucian Blaga Street, 550 012 Sibiu, Romania*
E-mail: *medmuncii@dspsibiu.ro*
[b] *Faculty of Agricultural Sciences, Food Industry and Environmental Protection, 'Lucian Blaga' University of Sibiu, 7–9 I. Ratiu Street, 550 012 Sibiu, Romania*
E-mail: *simona.oancea@ulbsibiu.ro*

ABSTRACT

As key agents for improving the oxidative stability of vegetable oils, antioxidants are of practical interest concerning the health promoting effects in functional foods. This paper reviews the nutraceutical and phytopharmaceutical properties of sunflower oil, explores reported efficient indigenous antioxidant plant-based extracts, summarises current research on antioxidant plasma ability, favourable outcomes on blood lipids and other health benefits of sunflower oil, and puts forward the proposal of gradual replacing the lipid lowering drugs with a healthy dietary practice. In order to protect consumers health, more human intervention studies are expected to fulfill health claims related especially to antioxidant defense and prevention of premature cell-ageing and lately cognitive decline.

Keywords: natural antioxidants, fatty acids, sunflower oil, health.

AIMS AND BACKGROUND

Concerns about the safety of synthetic antioxidants as oils and fats stabilisers have given rise to a large body of research on natural sources of antioxidants, because they bring less rigorous burden-of-safety proof than required for synthetic products. Public health stands for the main argument in experimenting natural antioxidants and food is the most controllable factor in favour of a healthy life-style through reducing the incidence of chronic and degenerative diseases.

World production of major oilseeds ranks sunflower seed oil on the 5th place, with 33 million t in 2010, 38.8 million t estimated by 2011/12, and 35.2 million t

---

* For correspondence.

forecasted by 2012/13, because sunflower seed production has primarily suffered from adverse weather in the EU, the Ukraine and Russian Federation[1]. The 2012/13 crop forecasts translate into a 3% increase in global oils/fats production, through expansion in soy and palm oil production, whereas sunflower, rapeseed and cottonseed oil are expected to fall short of last season record. Global olive oil production could suffer a sharp decline, with total output estimated to fall by 0.7 million t (Ref. 1). In Europe, sunflower cultivated area ranks Romania on the first place among the EU Member States while production ranks France on the first place with 1884.6 thousand t in 2011 (Ref. 2).

In natural form, sunflower oil is susceptible to autoxidation and thermal oxidation under light exposure, storage and frying condition, resulting rancid odours, unpleasant flavour, discolouration, alteration of nutritional quality and safety problems. These consequences are corrected by antioxidants (additives) allowed for use in food processing as long as they are nontoxic, effective at low concentrations, capable of surviving processing, stable in the finished products, and adherent to regulatory guidelines. The role of antioxidants in humans was mentioned since 1927, when Henry Mattill used the term 'antioxidiser' to describe the action of dietary factors that prevented oxidation[3]. When food additives started to become common around the middle of the 20th century, butylated hydroxyl amine (BHA), butylated hydroxyl toluene (BHT), and *t*-butyl hydroquinone (TBHQ) were among the first oil stabilisers, followed by propyl gallate (PG), ascorbyl palmitate (AP), and tocopherol concentrate. Recent scientific results indicate the effectiveness of 0.02% antioxidants in the order as TBHQ > BHT > BHA > BHA + BHT, during 21 weeks of sunflower oil storage and frying at 180°C (Ref. 4).

Design of potent antioxidant phytochemicals for oil industry will be a great challenge on essentially inter-disciplinary research topic, expected to protect consumers health and to develop green processes/green chemistry in small and medium enterprises. Dilemma 'natural versus synthetic' should advocate food producers for a responsible choice considering the fact that natural antioxidants provide multiple health benefits, preventing cardio-vascular and neurodegenerative diseases[5], while synthetics may cause adverse effects in humans, i.e. liver enlargement, mutagenesis, or increased microsomal activity[6].

HEALTH CLAIMS

Health claims are statements that describe the relationship between a substance (specific food or food component) and a disease, directed to the general population or designated subgroups (e.g. the elderly) and are intended to assist the consumer in maintaining healthful dietary practices[7]. In evaluating a petition for an authorised health claim, Food and Drug Administration (FDA) issues regulations and considers whether the evidence supporting the relationship that is the subject of the claim meets the significant scientific agreement standard. In this respect, the design of new sun-

flower oil stabilised with natural antioxidants has to be armed with scientifically-based information about the likely health benefits (physiological effects). Regarding multiple beneficial effects of natural antioxidants in chronic and degenerative diseases, there is a bulk of scientific evidence as publicly available data[3,8,9], sustained by information regarding antioxidant capacity of food[10], as important database for further dose/response relationship studies. According to FDA, an evidence-based review system for the scientific evaluation of health claims should comprise primarily in human studies (randomised, controlled intervention studies, and prospective or retrospective observational studies), and secondary in animal and *in vitro* studies. The significant scientific agreement standard is intended to provide a high level of confidence in the validity of the substance/disease relationship.

We consider healthy edible oils should meet the scientific requirements for health claims related to antioxidants, oxidative damage, cardiovascular health, and health claims related to functions of the nervous system[11,12]. According to European Food Safety Authority (EFSA), there is no pre-established formula as to how many or what types of studies are needed to substantiate a claim, but we selected the following recommendations:

1. Claims on antioxidant properties of foods, based on their capability of scavenging free radicals *in vitro*;

2. Claims on antioxidant status and antioxidant defense: *in vivo* human studies;

3. Claims on the protection of cells from premature ageing: a variety of *in vitro* and *in vivo* animal and human studies assessing the effects on a variety of outcomes, including the antioxidant capacity of foods; changes in antioxidant status; oxidative damage to proteins, lipids and deoxyribonucleic acid (DNA); non-oxidative DNA damage; neoplastic degeneration of cells;

4. Cardiovascular disease risk reduction claims: reduction in blood low density lipoprotein (LDL)-cholesterol concentration, and reduction in systolic blood pressure (endpoint risk biomarkers) are considered beneficial for coronary heart disease and stroke risk;

5. Claims on cognitive function: human intervention studies on improving cognitive decline (considered on a case-by-case basis) or development of cognitive function in infants and small children.

As the World Health Organisation predicts 29 million individuals living with dementia by the year 2020 (Ref. 13), it is of major interest to prevent late-life cognitive dysfunction with healthy dietary practices. In this respect, systematic reviews show that dietary polyunsaturated fatty acids (PUFAs) and antioxidants such as vitamins E, C and flavonoids are among most studied factors which substantiate health claims on cognitive function[14]. Naturally occurring polyphenols are the best promising new findings for reducing major risk factors associated with ageing, as more and more scientific literature produces evidence in favour of the preventive and therapeutic benefits[15]. For example resveratrol, a polyphenol from grape skin and red wine, extends the lifespan of diverse species by inducing telomere maintenance factors to protect

chromosome ends from fusion and degradation[16]. It is well known that the ageing process could be affected by alteration of variety of gene expression and accumulation of oxidative DNA damage induced by epigenetic and environmental changes, several human diseases resulting from impaired DNA repair[17].

When designing sunflower oil as a nutraceutical by adding natural antioxidants versus synthetic, ones should consider all dietary components/nutrients of the new resulted product, in a holistic approach. While observational studies have demonstrated protective effects of natural antioxidants and PUFA, randomised controlled trials have yielded weak or negative findings, suggesting that further studies should consider careful control of other dietary components or confounding variables[14].

In vitro STUDIES

The use of and search for antioxidants derived from plants have accelerated in recent years, since industrialised societies are developing new nutraceuticals. Experiments in designing 'healthy' sunflower oil by improving oxidative and thermal stability have followed, mainly, 3 directions:

I. Use of individual natural antioxidants;

II. Blend with oils rich in natural antioxidants;

III. Use of antioxidant mixtures (synthetic and natural).

I. Antioxidant herbal extracts are soluble fractions that can be removed from plant materials by solubilising the component(s) of interest in an aqueous, lipid, alcohol, solvent, or supercritical CO_2 phase[18]. A systematical review of all successful studies on experimenting individual natural antioxidants as novel stabilisers of sunflower oil reveals significant results (Table 1) (Refs 19–73 are cited in the table).

Methodological quality of these *in vitro* studies consists in using various standardized methods regarding both plant extracts and oil peroxidation tests. The majority of cited experiments used solvents for extraction, such as methanol, ethanol, *n*-butanol, acetone, petroleum ether, ethyl acetate, but also other methods, such as supercritical CO_2, in the case of Lamiaceae[40] (see Table 1).

It is well known that extracts of many members of the Labiatae (Lamiaceae) family like oregano, savory, sage, rosemary, thyme, and basil have high total phenolics content[74], so these herbs were most experimented in stabilising sunflower oil. The antioxidant components of rosemary, sage, basil, black pepper, and garlic appear to be relatively stable[18].

II. In order to improve oxidative stability with natural compounds, some researchers had the initiative to blend sunflower oil with oils rich in natural antioxidants (essential oils). Conclusions of these experiments are shown in Table 2 (Refs 75–85 are cited in the table). Chemically, essential oils are complex mixtures containing compounds of every major functional group class, and are isolated by steam distillation, extraction (solvent or CO_2), or mechanical expression from the plant material[18].

Table 1. Natural antioxidants extracts experimented as stabilisers of sunflower oil

Name and origin of plant	Active extract	Oxidative stability performances on sunflower oil	Ref.
1	2	3	4
Artemisia persica, Pakistan	methanol extract	its activity was quite comparable with the synthetic antioxidant BHA, during storage	19
Barley (*Hordeum vulgare*), Pakistan	methanol seeds extracts	suppress the primary and secondary oxidation products in the accelerated storage at 60°C for 30 days	20
Bamboo (*Phyllostachys nigra*), China	ethanol leaves extract	the fortification level of antioxidant in sunflower seed oil was about 0.05%	21
Basil (*Ocimum basilicum*), Slovakia	ethanol leaves extract	the highest protection effect during storage was exhibited by 2 mg kg^{-1} basil	22
Broccoli (*Brassica oleracea*), China	natural plants extracts (NPE)	broccoli sprout, rosemary and citrus can effectively inhibit the lipid oxidation of microencapsulated high oleic sunflower oil after 30 days storage at 60°C, better as a mixture than single	23, 24
Chamomile (*Matricaria chamomilla*), Iran	water/ethanol extract	antioxidant activity in crude sunflower oil by measuring of peroxide and thiobarbituric acid	25
Citrus (*Citrus medica*), China	natural plants extracts (NPE)	1% citrus extract in natural plant mixture prevent various microencapsulated seed oils from lipid oxidation	23, 24
Coffee (*Coffea arabica*), Poland	coffee beans water extracts	reduce the extent of thermal negative changes; the effectiveness decreased in the order: green Robusta >green Arabica > roasted Robusta > roasted Arabica	26
Combretum hartmannianum Sudan	methanol leaves extract	concentration of 0.5% was effective during storage at 70°C, having an antioxidant activity relative to BHA	27
Coriander (*Coriandrum sativum*), Brazil	ethanol extract	delayed lipid oxidation and promoted the retention of α-tocopherol at 180°C	28
Cowpea seed (*Vigna unguiculata*), South Africa	dried aqueous acetone extract	the Bechuana white cowpea was effective in reducing the formation of hydroperoxides at 65°C during 16 days, but lower than TBHQ	29

to be continued

640

Continuation of Table 1

1	2	3	4
Crude olive leaf juice/extract (*Kronakii cultivar*)	concentrated crude olive leaf juice; methanol extract	addition of olive leaf juice to oil heated at 180 °C induced remarkable antioxidant activity and at 800 ppm level was superior to that of BHT; methanolic extract was comparable with BHA and BHT, at 70 °C	30, 31
Cumin seed (*Cuminum cyminum*), Iran	methanol extract (CEx)	the addition of CEx significantly improved oxidative stability at the levels of 800 ppm and higher, whereas the essential oil indicated no antioxidant activity at the levels experimented	32
Drumstick tree (*Moringa oleifera*), Pakistan	methanol and acetone leaves extract	the best antioxidant efficacy was for 80% methanolic extract during accelerated ageing (65 °C), 18 days	33
Evening primrose (*Oenothera biennis*), Slovakia	ethyl acetate extract; ethanol-ethyl acetate extract	exhibited a stronger antioxidant activity than BHT, at 110°C; addition of ethyl acetate and ethanol-ethyl acetate extracts could extend the sunflower and rapeseed oils shelf-life	34
Finger millet (*Eleusine coracana*), India	methanol extract	the stability period by the Rancimat test was found to increase from 0.89 to 1.04 h at 140°C	35
Garlic (*Allium sativum*), Pakistan	methanol extract	appreciably high thermal stability of garlic extract shows an added advantage at high processing temperatures (185°C), contrary to synthetic antioxidants	36
Ginkgo biloba, Slovakia	ethanol and commercial extract	both extracts showed higher antioxidant activity in the more polyunsaturated sunflower oil at 110°C	37
Grape (*Vitis vinifera*), Romania	solvent seed extract	significantly inhibitory effect on lipid oxidation during convective and microwave heating, similar to BHT	38
Green tea (*Camellia sinensis*), Denmark	solvent extract	strong synergistic effect was found in combination with α-tocopherol in a methyl linoleate o/w-emulsion and in the pure bulk oil	39
Guiera senegalensis, Sudan	methanol leaves and root extract	root extract has the highest amount of total phenolic compounds, suppressing fat rancidity at 70°C in the dark, but has less inhibition of oxidation than BHA	27

to be continued

641

Continuation of Table 1

1	2	3	4
Hyssop (*Hyssop officinalis*), Serbia	fractional extraction with CO_2	less effective than other Lamiaceae herbs, at 98°C; prooxidative action at 60°C	40, 41
Lemon balm (*Melissa officinalis*), Netherlands	solvent extract	thyme and lemon balm extracts inhibited hexanal generation more than formation of conjugated dienes	42
Marigold (*Calendula officinalis*), Slovakia	ethanol petals extract	the optimum dose was found to be 10 mg kg^{-1}, lower than the necessary doses of the synthetic BHT, in storage	22
Mint (*Mentha piperita*), Iran	methanol acetone extracts	methanol extract was higher efficiency as compared to acetone and hexane extracts; antioxidant properties higher than basil	43
Mountain tea (*Sideritis euboea*), Greece	solvent extract of aerial parts	the extracted kaempherol showed the highest antioxidant activity among all antioxidants tested at 50°C and UV light	44
Mushroom (*Schizophyllum commune*), Malaysia	crude extract, formic acid fraction	retarded secondary oxidation and extended the shelf life 1 1/2 years and 2 years, respectively	45
Nettle (*Urtica dioica*), Iran	water and ether extracts	protection comparable to BHT; post-flowering extracts more potent, at 60°C	46
Nigella (*Nigella sativa*), Tunisia	natural seed extract	antioxidant effects similar to synthetic BHT during accelerated oxidation (140°C)	47, 48
Oat (*Avenis sativa*), Pakistan	methanol extract	the order of efficiency of the plant extracts (ambient and accelerated storage): oat groats and hull > coffee beans > *M. oleifera* leaves > *Lawsonia alba* > *Iris germanica* > rice bran > wheat bran	49
Olive (*Olea europaea*), Egypt	ethanol cake extract	good oxidative stability parameters in 180°C heated oil, during 5 days	50
Oregano (*Origanum vulgare*), Netherlands	ethanol extract	more active in oil than in emulsion, at 60°C; as for the cold pressed sunflower oil, a prooxidative effect was found	41, 51
Osage orange (*Maclura aurantiaca*), Serbia	ethanol extracts and fruit powder	citric acid exhibited a strong synergistic effect on raw sunflower oil in the combination both with extract and powder	52

to be continued

Continuation of Table 1

1	2	3	4
Paprika powder (*Capsicum annuum*)	solvent extraction of flavonoids, carotenoids	flavonoids were effective in retarding oil oxidation both under photooxidation and thermal autoxidation tests	53
Persian walnut (*Juglans regia*), Iran	methanol extract	the results revealed that 320 ppm of the Persian walnut leaves extract was comparable with 200 ppm BHA	54, 55
Phaffia rhodozyma, Poland	carotenoid yeast cells extraction	potential antioxidant effect of emulsified linoleic acid (at 37°C) and bulk sunflower oil system (at 110°C)	56
Phlomis bruguieri, Iran	methanol extract	antioxidant effectiveness (peroxide value) in sunflower oil stored 28 days at 70°C	57
Pomegranate (*Punica granatum*), Pakistan	methanol extract	thermal stability was evaluated by heating the extract at 185°C up to 80 min, suggesting higher efficiency over BHT	58
Pomposia fruits (*Syzygium cumini*), Egypt	concentrated juice extract	800 and 1200 ppm exhibited antioxidant effect similar to that of 200 ppm synthetic BHT, at 180°C	59
Propolis, Egypt	water extract	better antioxidant than BHT, but lower than TBHQ during 4 days at 63°C	60
Rice bran (*Oryza sativa*), Pakistan	methanol and acetone extract	the antioxidant activity of methanolic extract was significantly higher than acetone extracts at 65°C during 24 days	61
Roselle (*Hibiscus sabdariffa*), Malaysia	roselle seed extract (RSE)	RSE was more effective in stabilisation of sunflower oil compared to tocopherol, after 5 days of accelerated storage	62
Rosemary (*Rosmarinus officinalis*), Serbia, China	fractional extraction with CO_2; ethanol extract; carnosic acid extract (CA)	the antioxidant activity of the investigated plant extracts (Lamiaceae family) after 12 h of storage at 98°C; rosemary extract >BHA>sage extract>flavour' plus>thyme extract >hyssop extract; CA exhibited stronger antioxidant activity than BHT and BHA	23, 24, 40, 48, 63

to be continued

Continuation of Table 1

1	2	3	4
Sage (*Salvia officinalis*), (*Salvia fruticosa*), (*Salvia leriinfolia*), Iran	ethanol and acetone extracts. methanol root extract (SLR)	the presence of carnosic acid significantly contributed to antioxidant activities of rosemary and sage extracts; SLR: more effective than BHT and α-tocopherol in oil heated at 80°C	40, 41, 64, 65
Savory (*Satureja hortensis*), Greece	ethanol and acetone extracts	summer savory extracts retarded the thermal oxidation reactions during oil heating at 180°C, showing a more pronounced effect than the Greek sage	64
Self-heal (*Prunella vulgaris*), Slovakia	ethanol leaves/flowers extract	the optimum dose was 15 mg kg^{-1}; exhibit stabilisation effect after 10 weeks of oil storage, comparable to basil	22
Sesame (*Sesamum indicum*), Egypt, India	methanol cake extract; sesamol (ethanol extract)	exhibited stronger antioxidant activity than BHT and BHA during accelerated storage, but less than TBHQ; sesamol 500 ppm improve storage stability very close to TBHQ	66, 67
Sorghum (*Sorghum phatafuli*), Malawi	acetone phenolic extract	exert an antioxidant effect by acting both as radical scavengers and metal chelators, at 65°C	68
Stachys laxa, Iran	methanol extract	antioxidant effectiveness in oil stored at 70°C; peroxide value less than BHA	57
Sunflower (*Helianthus annuus*)	phenolic seeds extract	stabilisation effect on cold-pressed oil oxidation at 110 and 30°C	69
Sweet pepper (*Capsicum*)	water/ethanol/ oil solutions	confirm stabilisation effect on thermal oxidation (160 °C)	70
Tennocalyx obovatus, Zimbabwe	acetone dried leaf extract	protection against oxidation more efficiently as compared to rosemary, ethanol/methanol extracts and TBHQ	71
Thyme (*Thymus vulgaris*)	ethanol extract	prolonged stability of sunflower oil stored in darkness at 4, 18 and 38°C	40, 41, 72
Verbascum macrurum, Greece	methanol extract of aerial parts	acteoside showed the highest protection factor against oxidative rancidity; activity is comparable to the synthetic antioxidant BHT and superior to α-tocopherol	73
Wool mullein (*Verbascum densiflorum*), Slovakia	ethanol flowers extract	towards the end of the storage period, wool mullein concentrate was more effective than self-heal concentrate	22

Table 2. Essential oils experimented as stabilisers of sunflower oil

Sources of essential oil	Oxidative stability performances on sunflower oil	Ref.
1	2	3
Anise, caraway, cumin fruits, Egypt	the irradiated and microwaved essential oils exhibited an antioxidant activity superior to that of sunflower oil catalysed by a mixture of BHT + BHA, during storage	75
Boswellia serrata, Commiphora myrrh, Pistacia lentiscus	satisfactory antioxidant activity in sunflower oil, significant especially for *P. lentiscus* essential oil and resin	76
Carum copticum B e n t h & H o o k essential oil	all concentrations had antioxidant effect in comparison to BHA and BHT, during storage at 37°C	77
Centella asiatica	essential oil delivered a strong antioxidant activity by prohibiting the increase in oxidative parameters	78
Fennel (*Foeniculum vulgare*), Jordan	inhibited the formation of primary and secondary oxidation products during heating and storage of sunflower oil under light exposure	79
Ginger (*Zingiber officinale*), Jordan	same effect as fennel (aromatic plants)	79
Lemon balm (*Melissa officinalis*), Iran	conjugated dienes changes in oil sample containing essential oil and BHA are same approximately	42
Melon bug (*Aspongopus viduatus*), Sudan	storage at 70°C showed that the increase of the peroxide value as a measure of oxidation was remarkably lower for the blend than for pure sunflower oil; addition of 40% of this oil in the blend results in a comparable improvement of the oxidative stability as 0.02% BHA	80
Mint (*Mentha piperita*), Iran	essential oil did not show considerable antioxidative effect, compared to water and methanol extracts, at 60°C, for 7 days	81
Roselle (*Hibiscus sabdariffa*), Malaysia	roselle seed oil (RSO) is less rich in phenolic content than RSE; antioxidant activity follows the order: RSE>RSO>tocopherol	62

to be continued

Continuation of Table 2

1	2	3
Rosemary (*Rosmarinus officinalis*)	the decreases in *trans* C 18:1, t–9 production with the addition of rosemary oil and lutein were statistically significant in comparison with the control, during heat treatment	82
Satureja khuzestanica, Iran	concentration of 0.08% was the most stable during storage at 60°C; essential oil also was able to reduce the stable free radical 2,2-diphenyl-1-picrylhydrazyl	83
Sclerocarya birrea, Sudan	more pronounced effect than melon bug oil; 10% addition of this oil resulted in a remarkable improvement of the oxidative stability	80
Thymbra capitata, Portugal	peroxide content of sunflower oil with added essential oil at 60°C and kept in the dark for a total period of 78 days is comparable to BHT and BHA additives	84
Thymus camphoratus, Portugal	peroxide content of sunflower oil with added essential oil was lower than BHT and BHA	84
Thymus mastichina, Portugal	peroxide content of sunflower oil with added essential oil was lower than BHT and BHA; significantly lower acid value than the control during the last days of the experiment; antioxidant activity higher than capacity for scavenging of free radicals	84
Zataria multiflora B o i s s.	concentration of 0.075% essential oil was the most stable during storage at 37 and 47°C, but lower antioxidant than BHA and BHT	85

Recently, the use of vegetable oil blends for obtaining a desirable fatty acids ratio (7:16:7 of saturated, monounsaturated and polyunsaturated fatty acids) gives reason for getting natural antioxidants enriched oil blends which may be termed as health oils, especially for frying process[86]. Table 3 summarises these experiments. Subsequently, the oil blends would have longer shelf-life stability, more nutritional value, and are relatively economic.

Table 3. Selected vegetable oil blends for use as health oils

Vegetable oils used in mixtures	Ratio, characteristics	Ref.
1	2	3
Palm, rice bran and sesame oils were blended with sunflower, ground-nut and mustard oil to exploit the nutritional potential and associated benefits of natural antioxidants	20:80; 20:20:20:40, w/w the oil blends did not show much changes in their physical/chemical characteristics, fatty acid composition and natural antioxidants compared to the originals	87
Tiger nut (*Cyperus esculentus* L.): blending sunflower oil with tiger nut oil rich in phenols and MUFA	from 20:80 to 50:50 w/w improved the quality and the stability of sunflower oil during frying process	88
Mixing sunflower oil with palm or canola oils rich in MUFA	60: 40, 40:60 and 20:80 (v/v) blend lowered the formation of *trans*-C18 fatty acids during frying	89
Sunflower oil and soybean oil, admixed with cold pressed olive oil	10, 20 and 40 % v/v 20% virgin olive oil blend is superior to other blends stability at 60°C, for 32 days	90
Roasted sesame seed oil (RSSO) extracted by cold pressing blended with soybean and/or sunflower oils	the addition of 20 and 40% RSSO either to soybean or sunflower oils improved the antioxidant property of the oil blends at 60°C for 32 days	91
Moringa oleifera oil mixed with sunflower oil and soybean oil	significantly increased the oxidative stability of both oils	92
Sunflower oil, corn oil and refined, bleached and deodourised palm olein under deep frying of potato chips at 180°C	50:50 sunflower with each other oil showed that the iodine value decreased significantly with increased replication time of frying, whereas peroxide value and free fatty acid increased up	93
Sunflower oil and grape seed oil (rich in protianidines and PUFA)	80:20 v/v of mixture provides a relatively high stability or a lower rate of accumulation of primary and secondary products of oxidation in 2 month of storage	94
Sunflower oil and dried distillers grain oil	0.5–1% w/w significantly increased the oxidative stability index for stripped sunflower, and high-oleic sunflower oil during accelerated storage	95

1	2	3
Sunflower oil and Bene (pistachio) hull oil 2%	antioxidant activity during frying process of sunflower oil better than sesame and rice bran oils	96
Sunflower oil and tea seed oil 5%	enhance the shelf life of sunflower oil at 63°C	97

III. In order to develop new, effective antioxidant mixture for enhancing the stability of sunflower oil during storage and high-processing temperatures, there are trends in using a minor portion of synthetic antioxidants for protection of natural antioxidants. In this respect, the effects of the recommended synthetic (BHA, BHT, PG and TBHQ) and natural/semi-natural antioxidants (mixed tocopherols, AP and monoacylglycerol citrate) were studied, and the optimum antioxidant mixture was achieved by the combination of 0.13% AP, 0.05% TBHQ and 0.02% monoacylglycerol citrate[98]. Another mixture (coriander extract and AP) showed a higher antioxidant effect of sunflower oil at 180°C, thereby demonstrating their synergy under these conditions[28]. Sitostanyl ferulate and α-tocopherol (alone or as a mixture) were found to prevent polymerisation of high oleic sunflower oil at 100 and 180°C (Ref. 99). Another interesting combination of α-tocopherol with ascorbic acid and ethylenediamine-tetraacetic acid (EDTA) in salad dressings containing linoleic/α-tocopherol sunflower oil revealed antioxidant effects of ascorbic acid and EDTA after 12 months of storage at 4°C, compared to 3 month stability of storage in case of α-tocopherol alone[100]. The mixture between α-tocopherol and myricetin was also found to be synergistic in antioxidant effect on triacylglycerols of sunflower oil, at 100°C (Ref. 101).

Recently, Rege[102] underlines the antioxidant activity of a mixture of curcuminoids, for example demethoxycurcumin and *bis*-demethoxycurcumin, in refined sunflower oil and also the profound effect on the activity of curcumin. While researching biological properties of certain natural resins, Assimopoulou[76] discovered that the combination of *Pistacia lentiscus* resin with citric acid presented a synergistic antioxidant effect both in sunflower and corn oils.

It is well known that important parts of the tocopherols are wasted during sunflower oil processing stages, almost 38% (Ref. 103). Therefore, adding a mixture of tocopherols (α, γ, and δ) to stripped mid-oleic sunflower oil seems to offer a good fry life for oil and stability for fried tortilla chips[104].

In vivo STUDIES

Development of new functional food should always consider the measurable impact on public health through *in vivo* studies, especially in humans, but this scientific research requires time-consuming randomised controlled trials which are difficult to fund, comparable to *in vitro* studies. Systemic and topic health effects of sunflower

Table 4. Studied effects of sunflower oil in humans

Clinical trials, meta-analyses	Conclusions	Ref.
1	2	3
Vegetable oils in relation to individual cardiovascular risk factors: coronary heart disease (CHD); cardiovascular disease (CVD)	13614 participants provide evidence that consuming PUFA in place of SFA reduces CHD events (10 % risk reduction, $p = 0.017$)	105
	486 Iranian adult women higher intakes of partially hydrogenated vegetable oil were associated with a greater risk of individual cardiovascular risk factors, while those of non-hydrogenated vegetable oils (sunflower oil, maize oil, rapeseed oil, soybean oil, olive oil) were associated with a reduced risk	106
	27 studies met the inclusion criteria, and no significant effect on total mortality ($RR = 0.98$) or cardiovascular mortality ($RR = 0.91$) was found between the intervention and control groups	107
	in the 9 studies included, increasing n–6 polyunsaturated fats in the diet provides no benefit, and may be harmful. For mixed n–3/n–6 PUFA was a CHD death decreased risk of 22% ($RR = 0.78$)	108
	40757 Spanish adults aged 29–69 the results did not vary between those who used olive oil for frying and those who used sunflower oil; no association was observed between fried food consumption and all cause mortality or CHD	109
	18 subjects substitution of foods rich in saturated fat with foods rich in high-oleic-acid sunflower oil and margarine has favourable outcomes on blood lipids and factor VIIc	110
	21 healthy young men, sunflower oil intake the results indicated that serum cholesterol decreases and partial thromboplastin time increases significantly ($p < 0.05$), but triglycerides and other coagulating factors were not different ($p > 0.05$)	111
	serum peroxides, plasma α-tocopherol and thromboxane B_2 levels were higher after the high oleic sunflower oil diet compared with the extra virgin olive oil diet, in postmenopausal women; there was no significant difference between dietary treatments on LDL peroxides	112
	22 healthy volunteers hydroxytyrosol-enriched sunflower oil group displayed a significantly higher level of arylesterase activity and significantly lower levels of oxidised LDL and soluble vascular cell adhesion molecule than the control group, that may help prevent CVD	113

to be continued

1	2	3
Risk of nonfatal acute myocardial infarction (MI) influenced by vegetable oils	28 subjects the significant increase in LDL oxidation and the significantly higher HDL cholesterol on the MUFA-enriched sunflower oil diet would be expected to be associated with a decrease in CHD risk	114
	the cases ($n = 2111$) were survivors of a first acute MI palm oil users were more likely to have an MI than users of soybean oil or other cooking oils (sunflower oil)	115
	cases ($n=1819$) with a first non-fatal acute MI consumption of vegetable oils rich in α-linolenic acid could confer important cardiovascular protection; the apparent protective effect of α-linolenic acid is most evident among subjects with low intakes	116
Sunflower oil and peripheral vascular disease	20 Spanish male subjects with peripheral vascular disease provide further evidence that sunflower oil enriched diets do not protect LDL against oxidation as virgin olive oil does in patients with peripheral vascular disease	117
Effect of combination of edible oils on blood pressure	38 hypertensive patients nifedipine and oil-mix (sesame + sunflower oil) provided good protection over blood pressure and lipid peroxidation, and brought enzymatic and non-enzymatic antioxidants, lipid profile, and electrolytes towards normalcy in hypertensive patients	118
Breast cancer-related effects of eating sunflower oil	72571 cancer-free participants in the Shanghai Women Health Study: no association of breast cancer risk to dietary intake of linoleic acid, arachidonic acid, α-linolenic acid or marine-derived n–3 PUFA; statistically significant interaction between n–6 PUFA intake, marine-derived n–3 PUFA intake and breast cancer risk	119
	8393 German post-menopausal women results provide evidence for a reduced post-menopausal breast cancer risk associated with increased consumption of sunflower and pumpkin seeds and soybeans	120
Vegetable oils and maternal vitamin A status	90 rural, pregnant Tanzanian women sunflower oil consumption seems to conserve breast-milk retinol similarly to consumption of red palm oil	121
Sunflower oleodistillate (SOD) and atopic dermatitis	an initial clinical evaluation of the care effect of a 2% SOD emulsion in 20 adult volunteers with atopic skin revealed the moisturising properties of SOD; finally, a strong steroid-sparing effect and a positive effect on quality-of-life parameters were demonstrated for the 2% SOD cream in infants and babies with AD	122

Continuation of Table 4

1	2	3
Vitamin E and F-containing tooth-paste for healthy and strong gums	231 subjects the delivery of zinc and triclosan from a new oral health toothpaste containing zinc citrate trihydrate and triclosan was unaffected by the addition of α-tocopherol acetate (vitamin E) and sunflower oil (vitamin F); the new toothpaste was effective in reducing plaque levels and improving gingival conditions to the same degree as a clinically proven control	123
Tocopherols and antioxidant capacity in LDL and human plasma	28 healthy nonsmoking male volunteers, 19–31 year old the antioxidant potential of corn oil *in vivo* (total antioxidative capacity in plasma and LDL) was as efficient as the mixture olive/sunflower oil; this positive finding might be explained by a synergism between α- and γ-tocopherol in the corn oil diet significant correlation between the total tocopherol content in human plasma and the lipophilic antioxidant capacity measured by α-tocopherol equivalent antioxidant capacity and 2,2-diphenyl-1-picrylhydrazyl	124 125
Essential fatty acid intake biomarker	Costa Rican men (*n* = 99) and women (*n* = 101) high correlations were observed between whole-blood alpha-linolenic and linoleic acid and adipose tissue and plasma	126

651

Table 5. Effects of sunflower oil in lab animal studies

Animal studies	Conclusions	Ref.
1	2	3
Oxidative DNA damages; oxidative stress in liver microsomes or blood	female F344 rats results indicate that a high linoleic acid diet (sunflower oil) may contribute to oxidative stress in the liver of female rats leading to a marginal increase in oxidative DNA-damage. neither the diet based on olive oil nor the diet based on rapeseed oil exerted any significant protective effect against oxidative DNA damage	127
	in rats, the intake of fried oil led to higher levels of lipid peroxidation and a lower concentration of plasma antioxidants; microsomal fatty acid and antioxidant profiles were also altered; the highly unsaturated sunflower oil was less resistant to the oxidative stress produced by frying and led to a higher degree of lipid peroxidation in liver microsomes than virgin olive oil	128
	40 hypertensive rats the two MUFA oils studied (olive oil and high oleic sunflower oil), with the same high content of oleic acid, but different content of natural antioxidants, had similar effects on the antioxidant enzyme activities studied and may yield a benefit in the hypertension status	129
	the highest level of oxidised glutathione, the lowest reduced glutathione ratio in erythrocytes, and the highest plasma activity to reduce ferric ions were observed in rats fed both diets containing linoleic acid-rich sunflower oil	130
Inflammatory and insulin-resistance effect	C57BL/6 male mice high fat diet induced whole and muscle-specific insulin resistance associated with increased inflammatory markers in insulin-sensitive tissues and macrophage cells; in conclusion, sunflower oil supplementation improves lipid profile, but it does not prevent or attenuate insulin resistance and inflammation	131
	soybean and sunflower oil treatments (subcutaneous injections) might generate insulin resistance by targeting GLUT4 expression and translocation specifically in white adipose tissue	132
Exocrine pancreatic secretion	dietary intake of oils evoked different effects on *in vivo* pancreatic secretor activity; resting flow rate and amylase output were significantly enhanced by sunflower oil feeding	133

to be continued

652

Continuation of Table 5

1	2	3
Treatment of high cholesterol blood levels	the study suggests that mid-oleic sunflower oil reduces risk factors such as lipoprotein cholesterol and oxidative stress associated with early atherosclerosis greater than the typical high-linoleic sunflower oil in hypercholesterolemic hamsters; the high-oleic olive oil not only significantly reduced oxidative stress but also reduced aortic cholesterol ester, a hallmark of early aortic atherosclerosis	134
Atherosclerosis preventing diets	30 high-cholesterol diet fed albino rats generally, rats fed blended oils (soy oil, sunflower oil, and flaxseed oil) showed significantly lower levels of total cholesterol, triacylglycerol, and LDL cholesterol as well as higher levels of HDL cholesterol, in comparison with animals fed high-cholesterol diet and cholesterol-free diet	135
	60 male Wistar rats adapted to cholesterol-free or 1% cholesterol diets; rapeseed and to less degree sunflower oils possess hypolipidemic and plasma antioxidant properties	136
	the Sprague-Dawley rats fed 20% optimised sunflower oil (high oleic); the reduction in plasma triglyceride and total cholesterol levels was 43 and 20%, respectively; the serum ferric antioxidant capacity, superoxide dismutase, glutathione peroxidase and reduced glutathione significantly increased and lipid peroxidation decreased	137
	40 rabbits encouraging and favourable results in blood lipid levels were observed in the group on mixed oil supplementation (mustard + sunflower); it significantly decreased total cholesterol by 14%, TG by 27%, LDL by 18% and VLDL by 27.20%	138
Ageing-related changes in liver	in comparison with sunflower, dietary olive oil decreased oxidative stress in liver of aged rats, resulting in lower levels of membrane hydroperoxides and higher coenzyme Q levels in plasma membrane; plasma membrane Mg^{2+}-dependent neutral sphingomyelinase was strongly activated in aged rats fed on the sunflower oil diet	139
Protective effects in ethanol-induced gastric ulcer	rats treated with absolute ethanol (1ml 200 mg^{-1} weight) gastric ulcer index was significantly reduced in rats pretreated with ozonised sunflower oil, these protective effects being mediated partially by stimulation of some important antioxidant enzymes	140

Continuation of Table 5

1	2	3
The anti-cancer potentials of sesame and sunflower oil	sesame oil and sunflower oil offered 20 and 40% protection, respectively, in the mouse skin tumor model; the antioxidant capabilities of these compounds could not solely explain the observed anti-cancer characteristics	141
Topic antifungal ring-worm treatment	60 CF1 mice with experimental dermatophytosis treated with 1, 2 and 3% AMO3 cream (ozonised sunflower oil) showed 100% clinical cure and 94% average mycological cure	142
Luminal intestinal fat compounds and their digestibility	24 Wistar rats: 12 fasted (FT) and 12 non-fasted (NFT) gastric emptying in FT was significantly slower than in NFT; the luminal gastric fat profile differed from that of the oils administered (fried or not), suggesting that nonoxidised triacylglycerols passed quickly into the intestines	143

Table 6. Benefits of sunflower oil studied in cell cultures

Microorganisms / cells	Conclusions	Ref.
Staphylococcus aureus, Escherichia coli, Bacillus subtilis, Pseudomonas aeruginosa, Candida albicans Agar isolates	the oil from sunflower seed was effective on these microorganisms, measured by antimicrobial activity index (zone of culture inhibition)	144
Giardia duodenalis cultivated trophozites	a direct chemical-oxidation attack by the active substances from Oleozon® (ozonised sunflower oil)	145
Caco2 cells for digestion and absorption tests	supplementation of the rosemary extract with sunflower oil and lecithin 37 mg g^{-1} enhanced abietanes micellation (almost 2-fold); *in vitro* digestion of this mixture reduced 50% the bioaccesibility in terms of antioxidant activity	146

oil have been well outlined through all kinds of *in vivo* studies (humans, animals and cell cultures), most of them referring to blood/tissues lipid profile changes. We found significant evidence in humans shown in Table 4, followed by lab animal experiments shown in Table 5, and few studies on microorganisms/cell cultures mentioned in Table 6. Researchers refer to antioxidant plasma ability, favourable outcomes on blood lipids and factor VIIc, conserving breast-milk retinol, good protection over blood pressure under Nifedipine and oil-mix. Since sunflower oil is known and used as vegetable cosmetic product for anti-wrinkling and anti-ageing properties[147], we found data on other local effect in humans (atopic dermatitis treatment, reducing plaque levels and improving gingival conditions), and in animals, respectively (topic antifungal ring-worm treatment, protective effects in ethanol-induced gastric ulcer, intestinal digest-ibility of fat compounds). Sunflower oil has also an antimicrobial effect on common bacteria involved in urinary tract infection and diarrhea diseases, and parasitocidal effect on *Giardia duodenalis*.

DISCUSSION

As a result of unsaturated fatty acids oxidation, dietary advanced lipid oxidation end-products act as injurious chemicals (cytotoxic compounds) that activate an inflamma-tory response, possible one mechanism through which unhealthy diets are linked to metabolic and cardiovascular diseases[148–150]. In this respect, modern approach of public health emphasises the role of behavioural and social change in diet, from Western dietary pattern to traditional Mediterranean dietary pattern, scientific knowledge being translated into nutritional guidelines[151–154]. A well-deserved first place among healthy oils is attributed to olive oil, studied since 1960, but this is an expensive commodity, compared to sunflower oil[155–157].

During last decade, a bulk of *in vitro* studies have successfully tested natural antioxidants for stabilising sunflower oil, individual or in mixtures, worldwide re-searchers tending to capitalise indigenous potent plants. The most active extracts were from Labiatae family, in particular rosemary, which possesses also anti-inflammatory properties and is the most important commercially available natural antioxidant, beside tocopherols and ascorbic acid[158]. Reviewing these experiments, we can notice the fact that most of tested plant extracts developed antioxidant activity comparable to synthetic antioxidants (BHA and BHT), but some of them were better than BHT, as follows: crude olive leaf juice, evening primrose, garlic, pomegranate, propolis, rosemary, sage, and sesame. *Temnocalyx obovatus* showed better activity than rosemary and TBHQ. Preserving or acting synergistic to α-tocopherol is a remarkable property of coriander and green tea that can be exploited in further studies, as mixtures of antioxidants. Experiments with individual natural plant extracts seem to have better results on stabilising sunflower oil than essential oils, although the antioxidant and anti-inflammatory activities of the essential oils are well documented, especially when speaking about spice plants used in the Mediterranean diet[159]. A relevant aspect should

be mentioned in the case of rosemary essential oil, which decreases production of *trans*-C 18:1, t–9 in heated sunflower oil. *Trans*-fatty acids should be limited by less than 7% daily calories consumption, as American Heart Association recommends[160], and sunflower, canola and soybean oils were the most commonly used oil ingredients for all of the products introduced in 2005 and 2006 that have claimed to contain no *trans*-fats[161]. Although this review refers to plant extracts *per sé* when speaking about natural compounds, we should mention here that substances like mixed tocopherols, citric acid, ascorbic acid and AP are also considered natural antioxidants in literature, but maybe 'naturally-derived' or 'semi-natural' will be a more appropriate term, because they are industrially processed. Among this class, ascorbic acid and δ-tocopherol seem to be the best antioxidant performers[162].

Another solution to improve oxidative stability of sunflower oil by natural antioxidants and optimum balanced content of fatty acids was blending with other vegetable oils, more advantageous from the economical point of view. Taking into account that red palm oil is rich in vitamin A and tocotrienols with proved health benefits[121,163], mixture of this oil with sunflower oil brings advantages to both components which also include the degree of unsaturated fatty acids and lower the formation of *trans*-C 18 fatty acids during frying. Researchers propose a few unconventional blends with good results, like sunflower oil with tiger nut oil, *Moringa oleifera* oil, tea seed oil or bene hull oil. As virgin olive oil is the best of healthy oils, a 20% blend with sunflower oil is superior to other blends stability at 60°C according to Abdel-Razek, and seems to be a feasible solution.

In order to reduce the weight of synthetic antioxidants, there were experimented *in vitro* mixtures of natural, semi-natural and synthetic compounds. In this respect, particular attention should be given to experiments which preserve α-tocopherol with ascorbic acid, EDTA, myricetin or sitostanyl ferulate. Reblova[164] experimented the ability of phenolic acids and found that gallic, caffeic, and gentisic acids are able to protect tocopherols (α-tocopherol) during frying but are not able to protect fatty acids. Beddows[165] found that rosemary, thyme, turmeric, sage, oregano and cumin extracts (2000 mg kg^{-1}) delayed rancidity and preserved α-tocopherol in sunflower oil as a model system. The increased delay in the onset of rancidity was due directly to the improved preservation of α-tocopherol. Increasing the content of tocopherols in fried foods may have a practical impact, because α-tocopherol was the focus of early research and is the most common form of vitamin E, with a recommended intake of 300 mg/day for adults[166]. But the great achievement of the 21st century was tocotrienol with 40–60% higher antioxidant potential than tocopherol and possessing anti-inflammatory, antidiabetic, antiadipogenic, antitumor, and antiatherogenic effect[167,168]. Tocotrienol does not occur in sunflower oil, but mainly in palm oil, rice bran oil, mustard oil and sesame oil[169]. At this time, health benefits of vitamin E are still controversial and, furthermore, vitamin E supplements were found to increase mortality, according to a meta-analysis of 78 randomised trials[170].

In the present review we have noticed a wide range of plants experimented as individual antioxidants, from medicinal plants[171], to fruits, included berries in recent times[172–174], and spices[175]. Based on *in vitro* experimental values, the new interest in the bioactivity of natural antioxidants (especially phenolic compounds) focuses on the relationship between their antioxidant activity and their chemical structures, mathematical expressed in predictive models for new chemicals[176–180]. In this respect, the quantitative structure–activity relationship (QSAR) method is a proposal to be considered for the design of functional foods and nutraceuticals.

Since development of new functional food is of significant proportion, we used a holistic approach by comparison of *in vitro* to *in vivo* studies regarding health benefits of sunflower oil that have already been proved. There is a numeric disproportion in favour of *in vitro* experiments, which were not generally followed by human or animal studies subjected to antioxidant ability, excepting the role of tocopherols in humans and the benefits of mixed oils (sunflower + mustard, sesame or olive oil) in several human and animal studies. We found one single study regarding the effects of sunflower oil supplemented with rosemary extract as natural antioxidant and lecithin, mixture that enhanced abietanes micellation in Caco2 cells during digestion and absorption tests due to the rosemary derivatives and digestion products[146]. The antioxidant capacities of sesame and sunflower oil in the mouse skin tumor model are probably not solely involved in the Kapadia anti-cancer study.

The benefits of sunflower oil diet supplementation were studied not only in humans, but also in chickens regarding meat oxidative status, and herbivorous animals in relationship to rumen *Butyrivibrio*, improving lactation or airway obstruction[181–184].

Actually, both antioxidant-additives and unsaturation degree of fatty acids are contributing to oxidative stability of sunflower oil. Recently, a considerable work was done on the development of genetically modified sunflower seeds for new sunflower oil with high content of oleic, palmitic and stearic acid and containing γ- and δ-tocopherol as the most abundant natural antioxidant[185–189]. But this will be another challenge for further *in vivo* studies, including genetically modified organisms related risks.

Fatty acid composition of vegetable oils, especially *n*–3/*n*–6 PUFA, was subjected to the main part of the *in vivo* studies, most representatives related to CHD/CVD risk and, recently, to breast cancer risk. Finally, epidemiological studies suggest that a high omega-3 to omega-6 ratio may be the optimum strategy to decrease both CVD and breast cancer risk[190]. Most of the lab animal studies concluded that sunflower oil supplementation improves lipid profile and is a good reason for atherosclerosis preventing diets and treatment of high cholesterol blood levels, but it does not prevent or attenuate insulin resistance and inflammation. According to Walczewska[130], linoleic acid may have dual effect, prooxidant in blood cells but maintaining total antioxidant plasma ability. Summarising *in vivo* human studies related to sunflower oil health effects, we can remark that sunflower oil has been often used by comparison with other vegetable oils in order to emphasise the benefits of virgin olive oil, corn or sesame oil. On the other side, comparison to palm oil commonly used in Costa Rica

recommends sunflower oil in risk reduction of nonfatal acute myocardial infarction, as shown by the above cited authors. Therefore, more human studies are required to clarify certain health benefits of the discussed sunflower oil because studies in which dietary intake was strictly controlled confirm that fatty acid biomarkers can complement dietary assessment methodologies and have the potential to be used more quantitatively, at this time[191].

Finally, we advocate in favour of sunflower oil diet benefits and put forward the proposal of a prospective study aimed at promoting the gradual decrease of high blood cholesterol levels by a PUFA n–3/n–6 balanced diet supplied with natural antioxidants instead of the administration of lipid lowering drugs, because a rapid decrease of this biomarker may be responsible in increasing the risk for depression and suicidal behaviour[192].

ABBREVIATIONS

BHA – butylated hydroxyl amine; BHT – butylated hydroxyl toluene; TBHQ – tertiary butyl hydroquinone; PG – propyl gallate; AP – ascorbyl palmitate; DNA – deoxyribonucleic acid; PUFA – polyunsaturated fatty acid; MUFA – monounsaturated fatty acid; CO_2 – carbon dioxide; CHD – coronary heart disease; CVD – cardiovascular disease; LDL – low density lipoprotein; VLDL – very low density lipoprotein; HDL – high density lipoprotein.

CONCLUSIONS

Nutraceutical, cosmectic and phytopharmaceutical quality of edible sunflower oil is underlined, showing that *in vitro* and *in vivo* experiments should further sustain more health reasons for improving oxidative stability of this product. Plant extracts from Labiatae family were the most active in scavenging free radicals, preserving α-tocopherol or acting as anti-inflammatory antioxidants (rosemary), but a lot of indigenous plants were successfully experimented in the last years. Human evidences on antioxidant property of tocopherols, blended oils or rosemary added extract are still insufficient to support health claims. In our opinion, the *in vitro* cited studies accomplish claims on antioxidant properties of foods, but researchers should collaborate with health professionals in order to fulfill the other health claims (antioxidant defense, protection against premature ageing, and disease risk reduction).

ACKNOWLEDGEMENTS

REFERENCES

1. Food and Agriculture Organization of the United Nations (FAO): Food Outlook: Global Market Analysis, November 2012, Rome (Italy), 41–43.

2. Romanian National Institute of Statistics (INS): Main Crops Capacities in 2011. Available from: http://www.insse.ro/.

3. S. SAMMAN: Antioxidants and Public Health. Antioxid Redox Sign, **13** (10), 1513 (2010).

4. H. AKHTAR, I. TARIQ, S. MAHMOOD, S. HAMID, R. KHANUM: Effect of Antioxidants on Stability, Nutritional Values of Refined Sunflower Oil during Accelerated Storage and Thermal Oxidation in Frying. Bangladesh J Sci Ind Res, **47** (2), 223 (2012).

5. M. STOIA, S. OANCEA: Workplace Health Promotion Program on Using Dietary Antioxidants (Anthocyanins) in Chemical Exposed Workers. Procedia Eng, **42**, 2176 (2012).

6. E. O. ALUYOR, M. ORI-JESU: The Use of Antioxidants in Vegetable Oils – A Review. Afr J Biotechnol, **7** (25), 4836 (2008).

7. Food and Drug Administration (FDA): Guidance for Industry: Evidence-based Review System for the Scientific Evaluation of Health Claims – Final. College Park, January 2009. Available from: http://www.cfsan.fda.gov/guidance.html.

8. A. K. MUKHOPADHYAY: Antioxidants: Natural and Synthetic. Amani Int'l Publishers, Kiel, 2006, 1–10.

9. D. BEARDSELL, J. FRANCIS, D. RIDLEY, K. ROBARDS: Health Promoting Constituents in Plant Derived Edible Oils. J Food Lipids, **9**, 1 (2002).

10. N. PELLEGRINI, M. SERAFINI, B. COLOMBI, D. DEL RIO, S. SALVATORE, M. BIANCHI, F. BRIGHENTI: Total Antioxidant Capacity of Plant Foods, Beverages and Oils Consumed in Italy Assessed by Three Different *in vitro* Assays. J Nutr, **133**, 2812 (2003).

11. European Food Safety Authority (EFSA), Parma, Italy: Guidance on the Scientific Requirements for Health Claims Related to Antioxidants, Oxidative Damage and Cardiovascular Health. EFSA Panel on Dietetic Products, Nutrition and Allergies (NDA)**.** EFSA J, **9** (12), 2474 (2011).

12. European Food Safety Authority (EFSA), Parma, Italy: Guidance on the Scientific Requirements for Health Claims Related to Functions of the Nervous System, Including Psychological Functions. EFSA Panel on Dietetic Products, Nutrition and Allergies (NDA). EFSA J, **10** (7), 2816 (2012).

13. D. P. RICE, H. M. FILLIT, W. MAX, D. S. KNOPMAN, J. R. LLOYD, S. DUTTAGUPTA: Prevalence, Costs, and Treatment of Alzheimer's Disease and Related Dementia: A Managed Care Perspective. Am J Manag Care, **7**, 809 (2001).

14. P. J. SMITH, J. A. BLUMENTHAL: Diet and Neurocognition: Review of Evidence and Methodological Considerations. Curr Ageing Sci, **3**, 57 (2010).

15. B. L. QUEEN, T. O. TOLLEFSBOL: Polyphenols and Ageing. Curr Ageing Sci, **3**, 34 (2010).

16. F. UCHIUMI, T. WATANABE, S. HASEGAWA, T. HOSHI, Y. HIGAMI, S. TANUMA: The Effect of Resveratrol on the Werner Syndrome RecQ Helicase Gene and Telomerase Activity. Curr Ageing Sci, **4**, 1 (2011).

17. F. COPPEDÈ, L. MIGLIORE: DNA Repair in Premature Ageing Disorders and Neurodegeneration. Curr Ageing Sci, **3**, 3 (2010).

18. M. S. BREWER: Natural Antioxidants: Sources, Compounds, Mechanisms of Action, and Potential Applications. Compr Rev Food Sci Food Saf, **10**, 221 (2011).

19. A. RASHID, M. Z. QURESHI, S. A. RAZA, J. WILLIAM, M. ARSHAD: Quantitative Determination of Antioxidant Potential of *Artemisia persica*. Annals of the University of Bucharest. Chemistry (New Series), **19** (1), 23 (2010).

20. F. ANWAR, H. M. A. QAYYUM, A. I. HUSSAIN, S. IQBAL: Antioxidant activity of 100% and 80% Methanol Extracts from Barley seeds (*Hordeum vulgare* L.): Stabilization of Sunflower Oil. Int J Fats Oils, **61** (3), 237 (2010).

21. Y. ZHANG, B. BAO, B. LU, Y. REN, X. TIE, Y. ZHANG: Determination of Flavone *C*-glucosides in Antioxidant of Bamboo Leaves (AOB) Fortified Foods by Reversed-phase High-performance Liquid Chromatography with Ultraviolet Diode Array Detection. J Chromatogr A, **1065**, 177 (2005).

22. M. MARIASSYOVA: Antioxidant Activity of Some Herbal Extracts in Rapeseed and Sunflower Oils. J Food Nutr Res, **45** (3), 104 (2006).

23. J. H. AHN, Y. P. KIM, E. M. SEO, Y. K. CHOI, H. S. KIM: Antioxidant Effect of Natural Plant Extracts on the Microencapsulated High Oleic Sunflower Oil. J Food Eng, **84**, 327 (2008).
24. J. H. AHN, Y. P. KIM, H. S. KIM: Effect of Natural Antioxidants on the Lipid Oxidation of Micro-encapsulated Seed Oil. Food Control, **23**, 528 (2012).
25. M. R. SAZEGAR, A. BANAKAR, N. BAHRAMI, A. BAHRAMI, M. BAGHBANI, P. NEMA-TOLAHI, M. MOTTAGHI: The Antioxidant Activity of Chamomile (*Matricaria chamomilla* L.) Extract in Sunflower Oil. World Appl Sci J, **9** (8), 873 (2010).
26. G. BUDRYN, E. NEBESNY, D. ZYZELEWICZ: Oxidative Stability of Lard and Sunflower Oil Supplemented with Coffee Extracts under Storage Conditions. Int J Fats Oils, 62 (2), 155 (2011).
27. A. MARIOD, B. MATTHÄUS, I. H. HUSSEIN: Antioxidant Activities of Extracts from *Combretum hartmannianum* and *Guiera senegalensis* on the Oxidative Stability of Sunflower Oil. Emir J Agric Sci, **18** (2), 20 (2006).
28. P. M. ANGELO, N. JORGE: Antioxidant Evaluation of Coriander Extract and Ascorbyl Palmitate in Sunflower Oil under Thermoxidation. J Am Oil Chem Soc, **85** (11), 1045 (2008).
29. L. B. MOKGOPE: Cowpea Seeds Coats and Their Extracts. Phenolic Composition and Use as Anti-oxidants in Sunflower Oil. Thesis for the Degree of MInstAgrar, Faculty of Natural and Agricultural Sciences, University of Pretoria, Pretoria (South Africa), 2007.
30. S. F. RADWAN, A. M. EBTESAM, M. B. AMANY: Use Crude Olive Leaf Juice as a Natural Anti-oxidant for the Stability of Sunflower Oil during Heating. Int J Food Sci Tech, **42** (1), 107 (2007).
31. Z. RAFIEE, S. M. JAFARI, M. ALAMI, M. KHOMEIRI: Antioxidant Effect of Microwave-assisted Extracts of Olive Leaves on Sunflower Oil. J Agr Sci Tech, **14**, 1497 (2012).
32. S. EINAFSHAR, H. POORAZRANG, R. FARHOOSH, S. M. SEIEDI: Antioxidant Activity of the Essential Oil and Methanolic Extract of Cumin Seed (*Cuminum cyminum*). Eur J Lipid Sci Technol, **114** (2), 168 (2012).
33. A. SIDDIQ, F. ANWAR, M. MANZOOR, A. FATIMA: Antioxidant Activity of Different Solvent Extracts of *Moringa oleifera* Leaves under Accelerated Storage of Sunflower Oil. Asian J Plant Sci, **4** (6), 630 (2005).
34. I. NIKLOVA, S. SCHMIDT, K. HABALOVA, S. SEKRETAR: Effect of Evening Primrose Extracts on Oxidative Stability of Sunflower and Rapeseed Oils. Eur J Lipid Sci Technol, **103** (5), 299 (2001).
35. J. P. MEHTA, C. R. FULTARIYA, P. H. PARMAR, S. H. VADIA, B. A. GOLAKIYA: Evaluation of Phenolic Content and Antioxidant Capacity of *Eleusine coracana* (L.). E-J Chem, **9** (4), 2089 (2012).
36. S. IQBAL, M. I. BHANGER: Stabilization of Sunflower Oil by Garlic Extract during Accelerated Storage. Food Chem, **100** (1), 246 (2007).
37. L. ZAHRADNIKOVA, S. SCHMIDT, S. SEKRETAR, L. JANAC: Determination of the Antioxidant Activity of *Ginkgo biloba* Leaves Extract. J Food Nutr Res, **46**, 15 (2007).
38. M. A. POIANA: Enhancing Oxidative Stability of Sunflower Oil during Convective and Microwave Heating Using Grape Seed Extract. Int J Mol Sci, **13**, 9240 (2012).
39. J. YIN, E. M. BECKER, M. L. ANDERSEN, L. H. SKIBSTED: Green Tea Extract as Food Antioxi-dant. Synergism and Antagonism with α-tocopherol in Vegetable Oils and Their Colloidal Systems. Food Chem, **135** (4), 2195 (2012).
40. N. BABOVIC, I. ZIZOVIC, S. SAICIC, J. IVANOVIC, S. PETROVIC: Oxidative Stabilization of Sunflower Oil by Antioxidant Fractions from Selected Lamiaceae herbs. Chem Ind Chem Eng Q, **16** (4), 287 (2010).
41. A. E. ABDALLA, J. P. ROOZEN: Effect of Plant Extracts on the Oxidative Stability of Sunflower Oil and Emulsion. Food Chem, **64** (3), 323 (1999).
42. H. MEFTAHIZADE, E. SARGSYAN, H. MORADKHANI: Investigation of Antioxidant Capacity of *Melissa officinalis* L. Essential Oils. J Med Plant Res, **4** (14), 1391 (2010).
43. R. S. MOUSAVI, M. GHAVAMI, M. GHARACHORLOO, L. NATEGHI, P. MAHASTI: Examina-tion of the Effect of Mint and Basil Extracts on Sunflower Oil Stability. Adv Environ Biol, **6** (7), 1891 (2012).

44. J. TSAKNIS, S. LALAS: Extraction and Identification of Natural Antioxidant from *Sideritis euboea* (Mountain Tea). J Agric Food Chem, **53**, 6375 (2005).

45. H. S. YIM, F. Y. CHYE, P. Y. HENG, C. W. HO: Oxidative Stability of Sunflower Oil Supplemented with Medicinal Split Gill Mushroom, *Schizophyllum commune* Fr:Fr. Extract during Accelerated Storage. Int J Med Mushrooms, **13** (4), 357 (2011).

46. M. MONFARED, A. KAMKAR, S. G. KHALIGH, A. J. JAVAN, F. ASADI, A. A. BASTI: Antioxidative Effects of Iranian *Urtica dioica* L. Extracts on the Oxidation of Sunflower Oil. J Med Plant Res, **5** (18), 4438 (2011).

47. F. AMMARI, D. J. RIMBAUD-BOUVERESSE, N. BOUGHANMI, D. N. RUTLEDGE: Study of the Heat Stability of Sunflower Oil Enriched in Natural Antioxidants by Different Analytical Techniques and Front-face Fluorescence Spectroscopy Combined with Independent Components Analysis. Talanta, **15** (99), 323 (2012).

48. N. ERKAN, G. AYRANCI, E. AYRANCI: Lipid Oxidation Inhibiting Capacities of Black Seed Essential Oil and Rosemary Extract. Eur J Lipid Sci Technol, **114** (2), 175 (2012).

49. F. ANWAR, A. JAMIL, S. IQBAL, M. A. SHEIKH: Antioxidant Activity of Various Plant Extracts under Ambient and Accelerated Storage of Sunflower Oil. Int J Fats Oils, **57** (2), 189 (2006).

50. M. E. ABD-ELGHANY, M. S. AMMAR, A. E. HEGAZY: Use of Olive Waste Cake Extract as a Natural Antioxidant for Improving the Stability of Heated Sunflower Oil. World Appl Sci J, **11** (1), 106 (2010).

51. M. WRONIAK, M. LUBIAN: Assessing the Oxidative Stability of Cold Pressed Rapeseed and Sunflower Oils with Oregano Extract Added Using the Rancimat and Schaal Oven Tests. ZNTJ, **15** (4), 80 (2008).

52. M. BUDINC, Z. R. VRBASKI, J. TURKULO, E. DIMIC: Oxidative Stability of Feed Fats. Lipid/Fett, **97** (9), 355 (1995).

53. E. MAFORIMBO: Evaluation of Capsicum as a Source of Natural Antioxidant in Preventing Rancidity in Sunflower Oil. J Food Technol Africa, **7** (2), 68 (2002).

54. M. RAHIMIPANAH, M. HAMEDI, M. MIRZAPOUR: Antioxidant Activity and Phenolic Contents of Persian Walnut (*Juglans regia* L.) Green Husk Extract. Afr J Food Sci Technol, **1** (4), 105 (2010).

55. M. MIRZAPOUR, M. HAMEDI, M. RAHIMIPANAH: Sunflower Oil Stabilization by Persian Walnut Leaves Extract during Oven Storage Test. Food Sci Technol Res, **16** (5), 443 (2010).

56. A. GRAMZA-MICHALOWSKA, B. STACHOWIAK: The Antioxidant Potential of Carotenoid Extract from *Phaffia rhodozyma*. Acta Sci Pol Technol Aliment, **9** (2), 171 (2010).

57. K. MORTEZA-SEMNANI, M. SAEEDI, S. SHAHANI: Antioxidant Activity of the Methanolic Extracts of Some Species of *Phlomis* and *Stachys* on Sunflower Oil. Afr J Biotechnol, **5** (24), 2428 (2006).

58. S. IQBAL, S. HALEEM, M. AKHTAR, M. ZIA-UL-HAQ, J. AKBAR: Efficiency of Pomegranate Peel Extracts in Stabilization of Sunflower Oil under Accelerated Conditions. Food Res Int, **41** (2), 194 (2008).

59. F. M. A. REHAB: Improvement the Stability of Fried Sunflower Oil by Using Different Levels of Pomposia (*Syzyygium cumini*). Electron J Environ Agric Food Chem, **9**, 396 (2010).

60. M. F. OSMAN, E. A. TAHA: Antioxidant Activity of Water Extract of Propolis from Different Regions in Kafr El-Sheikh Governorate. Alex J Fd Sci Technol, Special Volume Conference, **83** (2008).

61. S. A. S. CHATHA, A. I. HUSSAIN, J. U. R. BAJWA, M. SAGIR: Antioxidant Activity of Different Solvent Extracts of Rice Bran at Accelerated Storage of Sunflower Oil. J Food Lipids, **13**, 424 (2006).

62. K. L. NYAM, Y. N. TEH, C. P. TAN, L. KAMARIAH: *In vitro* Antioxidant Activities of Extract and Oil from Roselle (*Hibiscus sabdariffa* L.) Seed against Sunflower Oil Autoxidation. Mal J Nutr, **18** (2), 265 (2012).

63. A. RIZNER-HRAS, M. HADOLIN, Z. KNEZ, D. BAUMAN: Comparison of Antioxidative and Synergistic Effects of Rosemary Extract with α-tocopherol, Ascorbyl Palmitate and Citric Acid in Sunflower Oil. Food Chem, **71** (2), 229 (2000).

64. G. KALANTZAKIS, G. BLEKAS: Effect of Greek Sage and Summer Savory Extracts on Vegetable Oil Thermal Stability. Eur J Lipid Sci Technol, **108** (10), 842 (2006).

65. M. H. H. KHODAPARAST, A. HAGHDOOST, G. G. MOVAHHED: New Source of Butein in Root of *Salvia leriinfolia* (N o w r o o z a k). Am-Euras J Agric Environ Sci, **4** (6), 731 (2008).

66. A. A. MOHDALY, I. SMETANSKA, M. F. RAMADAN, M. A. SARHAN, A. MAHMOUD: Antioxidant Potential of Sesame (*Sesamum indicum*) Cake Extract in Stabilization of Sunflower and Soybean Oils. Ind Crop Prod, **34** (1), 952 (2011).

67. NASIRULLAH, R. B. LATHA: Storage Stability of Sunflower Oil with Added Natural Antioxidant Concentrate from Sesame Seed Oil. J Oleo Sci, **58** (9), 453 (2009).

68. F. E. SIKWESE, K. G. DUODU: Antioxidant Effect of a Crude Phenolic Extract from *Sorghum Bran* in Sunflower Oil in the Presence of Ferric Ions. Food Chem, **104** (1), 324 (2007).

69. A. de LEONARDIS, V. MACCIOLA, A. di ROCCO: Oxidative Stabilization of Cold-pressed Sunflower Oil Using Phenolic Compounds of the Same Seeds. J Sci Food Agric, **83** (6), 523 (2003).

70. T. CAPCANARI: Incorporation of Sweet Pepper Extracts to Improve Thermal Stability of Vegetable Oil Mixtures. Food Environ Saf, **10** (2), 13 (2011).

71. P. DZOMBA, E. TOGAREPI, C. MUSEKIWA, C. J. CHAGWIZA: Improving Oxidative Stability of Soy and Sunflower Oil Using *Temnocalyx obovatus* Extracts. Afr J Biotechnol, **11** (50), 11099 (2012).

72. Z. ZABOROWSKA, K. PRZYGONSKI, A. BILSKA: Antioxidative Effect of Thyme (*Thymus vulgaris*) in Sunflower Oil. Acta Sci Pol Technol Aliment, **11** (3), 283 (2012).

73. N. ALIGIANNIS, S. MITAKU, E. TSITSA-TSARDIS, C. HARVALA, I. TSAKNIS, S. LALAS, S. HAROUTOUNIAN: Methanolic Extract of *Verbascum macrurum* as a Source of Natural Preservatives against Oxidative Rancidity. J Agric Food Chem, **51** (25), 7308 (2003).

74. H. Y. CHEN, Y. C. LIN, C. L. HSIEH: Evaluation of Antioxidant Activity of Aqueous Extract of Some Selected Nutraceutical Herbs. Food Chem, **104** (4), 1418 (2007).

75. R. S. FARAG, K. H. El-KHAWAS: Influence of Gamma-irradiation and Microwaves on the Antioxidant Property of Some Essential Oils. Int J Food Sci Nutr, **49** (2), 109 (1998).

76. A. N. ASSIMOPOULOU, S. N. ZLATANOS, V. P. PAPAGEORGIOU: Antioxidant Activity of Natural Resins and Bioactive Triterpenes in Oil Substrates. Food Chem, **92** (4), 721 (2005).

77. M. B. HASHEMI, M. NIAKOUSARI, M. J. SAHARKHIZ, M. H. ESKANDARI: Stabilization of Sunflower Oil with *Carum copticum* B e n t h & H o o k Essential Oil. JFST, (2011).

78. S. A. RAZA, A. REHMAN, A. ADNAN, F. QURESHI: Comparison of Antioxidant Activity of Essential Oil of *Centella asiatica* and Butylated Hydroxyanisole in Sunflower Oil at Ambient Conditions. Biharean Biologist, **3** (1), 71 (2009).

79. S. Y. A. Al-DALAIN, A. H. Al-FRAIHAT, E. T. Al-KASSASBEH: Effect of Aromatic Plant Essential Oils on Oxidative Stability of Sunflower Oil during Heating and Storage. Pak J Nutr, **10** (9), 864 (2011).

80. A. MARIOD, B. MATTHÄUS, K. EICHNER, I. H. HUSSEIN: Improving the Oxidative Stability of Sunflower Oil by Blending with *Sclerocarya birrea* and *Aspongopus viduatus* Oils. J Food Lipids, **12**, 150 (2005).

81. A. KAMKAR, A. J. JAVAN, F. ASADI, M. KAMALINEJAD: The Antioxidative Effect of Iranian *Mentha pulegium* Extracts and Essential Oil in Sunflower Oil. Food Chem Toxicol, **48** (7), 1796 (2010).

82. S. FILIP, J. HRIBAR, R. VIDRIH: Influence of Natural Antioxidants on the Formation of Trans Fatty Acids during Heat Treatment of Sunflower Oil. Eur J Lipid Sci Technol, **113** (2), 224 (2011).

83. M. B. HASHEMI, M. NIAKOUSARI, M. J. SAHARKHIZ, M. H. ESKANDARI: Effect of *Satureja khuzestanica* Essential Oil on Oxidative Stability of Sunflower Oil during Accelerated Storage. Nat Prod Res, **26** (15), 1458 (2012).

84. M. G. MIGUEL, M. FALCATO-SIMÕES, A. C. FIGUEIREDO, J. M. G. BARROSO, L. G. PEDRO, L. M. CARVALHO: Evaluation of the Antioxidant Activity of *Thymbra capitata*, *Thymus mastichina* and *Thymus camphoratus* Essential Oils. J Food Lipids, **12**, 181 (2005).

85. M. B. HASHEMI, M. NIAKOUSARI, M. J. SAHARKHIZ, M H. ESKANDARI: Influence of *Zataria multiflora* B o i s s. Essential Oil on Oxidative Stability of Sunflower Oil. Eur J Lipid Sci Technol, **113** (12), 1520 (2011).

86. C. V. SARMANDAL: Cancer, Heart and Other Chronic Diseases: Some Preventive Measures to Control Lipid Peroxidation through Choice of Edible Oils. I Res J Biological Sci, **1** (6), 68 (2012).

87. S. KHATOON, J. HEMAVATHY, C. V. SARMANDAL, A G. GOPALAKRISHNA: Physico-chemical Characteristics of Selected Vegetable Oil Blends for Use as Health Oils. JOTAI, **35** (2), 63 (2003).

88. R. F. M. ALI, A. M. El-ANANY: Physicochemical Studies on Sunflower Oil Blended with Cold Pressed Tiger Nut Oil, during Deep Frying Process. J Food Process Technol, **3**, 176 (2012).

89. R. S. FARAG, M. A. S. El-AGAIMY, A. B. S. El-HAKEEM: Effects of Mixing Canola and Palm Oils with Sunflower Oil on the Formation of Trans Fatty Acids during Frying. FNS, **1**, 24 (2010).

90. A. G. ABDEL-RAZEK, S. M. El-SHAMI, M. H. El-MALLAH, M. M. M. HASSANIEN: Blending of Virgin Olive Oil with Less Stable Edible Oils to Strengthen Their Antioxidative Potencies. Aust J Basic Appl Sci, **5** (10), 312 (2011).

91. M. M. M. HASSANIEN, A. G. ABDEL-RAZEK: Improving the Stability of Edible Oils by Blending with Roasted Sesame Seed Oil as a Source of Natural Antioxidants. J Appl Sci Res, **8** (8), 4074 (2012).

92. F. ANWAR, A. I. HUSSAIN, S. IQBAL, M. I. BHANGER: Enhancement of the Oxidative Stability of Some Vegetable Oils by Blending with *Moringa oleifera* Oil. Food Chem, **103**, 1181 (2007).

93. R. NAZARUDDIN, N. MAHZAD, J. IRWANDI: Oxidative Stability of Blend Oil during Deep-fat Frying of Potato Chips. Pak J Nutr, **11** (9), 730 (2012).

94. C. POPOVICI, T. CAPCANARI, O. DESEATNICOVA, R. STURZA: Study of Quality Indices of Functional Vegetal Oil Mixture. The Annals of the University Dunarea de Jos of Galati, Fascicle VI – Food Technology, **34** (1), 18 (2009).

95. J. K. MOSER, S. F. VAUGHN: Antioxidant Activity of Phytochemicals from Dried Distillers Grain Oil. J Am Oil Chem Soc, **86**, 1026 (2009).

96. A. SHARIF, R. FARHOOSH, M. H. H. KHODAPARAST, M. H. T. KAFRANI: Antioxidant Activity of Bene Hull Oil Compared with Sesame and Rice Bran Oils during the Frying Process of Sunflower Oil. J Food Lipids, **16** (3), 394 (2009).

97. M. A. SAHARI, D. ATAII, M. HAMEDI: Characteristics of Tea Seed Oil in Comparison with Sunflower and Olive Oils and Its Effect as a Natural Antioxidant. J Am Oil Chem Soc, **81** (6), 585 (2004).

98. A. S. S. MAHMOUD, M. H. M. ALY: Thermal Stability of Some Commercial Natural and Synthetic Antioxidants and Their Mixtures. J Food Lipids, **9**, 277 (2002).

99. L. NYSTRÖM, T. ACHRENIUS, A.-M. LAMPI, R. A. MOREAU, V. PIIRONEN: A Comparison of the Antioxidant Properties of Steryl Ferulates with Tocopherol at High Temperatures. Food Chem, **101**, 947 (2007).

100. M. D. PAVLOVIC, M. PUCAREVIC, V. MICOVIC, M. ZIVIC, S. ZLATANOVIC, S. GOR-JANOVIC, J. GVOZDENOVIC: Influence of Sunflower Oil Qualities and Antioxidants on Oxidative Stability on Whey-based Salad Dressings. Acta Chim Slov, **59**, 42 (2012).

101. E. MARINOVA, A. TONEVA, N. YANISHLIEVA: Synergistic Antioxidant Effect of α-tocopherol and Myricetin on the Autoxidation of Triacylglycerols of Sunflower Oil. Food Chem, **106** (2), 628 (2008).

102. S. REGE, S. MOMIN, S. WADEKAR, A. PRATAP, D. BHOWMICK: Effect of Demethoxycurcumin and Bisdemethoxycurcumin on Antioxidant Activity of Curcumin in Refined Sunflower Oil. J Food Process Pres, (2012).

103. S. NAZ, S. T. H. SHERAZI, F. N. TALPUR: Changes of Total Tocopherol and Tocopherol Species during Sunflower Oil Processing. J Oil Fat Industries, **88** (1), 127 (2012).

104. K. A. WARNER, J. K. MOSER: Frying Stability of Purified Mid-oleic Sunflower Oil Triacylglycerols with Added Pure Tocopherols and Tocopherol Mixtures. J Am Oil Chem Soc, **86** (12), 1199 (2009).

105. D. MOZAFFARIAN, R. MICHA, S. WALLACE: Effects on Coronary Heart Disease of Increasing Polyunsaturated Fat in Place of Saturated Fat: A Systematic Review and Meta-analysis of Randomized Controlled Trials. PLoS Med, **7** (3), e1000252 (2010).

106. A. ESMAILLZADEH, L. AZADBAKHT: Different Kinds of Vegetable Oils in Relation to Individual Cardiovascular Risk Factors among Iranian Women. Br J Nutr, **105** (6), 919 (2011).

107. L. HOOPER, C. D. SUMMERBELL, R. THOMPSON, D. SILLS, F. G. ROBERTS, H. J. MOORE, G. DAVEY-SMITH: Reduced or Modified Dietary Fat for Preventing Cardiovascular Disease. Cochrane Database of Systematic Reviews, (5) (2012).

108. C. E. RAMSDEN, J. R. HIBBELN, S. F. MAJCHRZAK, J. M. DAVIS: *n*–6 Fatty Acid-specific and Mixed Polyunsaturate Dietary Interventions Have Different Effects on CHD Risk: A Meta-analysis of Randomized Controlled Trials. Br J Nutr, **104** (11), 1586 (2010).

109. P. GUALLAR-CASTILLÓN, F. RODRÍGUEZ-ARTALEJO, E. LOPEZ-GARCIA, L. M. LEÓN-MUÑOZ, P. AMIANO, E. ARDANAZ, L. ARRIOLA, A. BARRICARTE, G. BUCKLAND, M.-D. CHIRLAQUE, M. DORRONSORO, J.-M. HUERTA, N. LARRAÑAGA, P. MARIN, C. MARTÍNEZ, E. MOLINA, C. NAVARRO, J. R. QUIRÓS, L. RODRÍGUEZ, M. J. SANCHEZ, C. A. GONZÁLEZ, C. MORENO-IRIBAS: Consumption of Fried Foods and Risk of Coronary Heart Disease: Spanish Cohort of the European Prospective Investigation into Cancer and Nutrition study. BMJ, **344**, e363 (2012).

110. M. A. ALLMAN-FARINELLI, K. GOMES, E. J. FAVALORO, P. PETOCZ: A Diet Rich in High-oleic-acid Sunflower Oil Favorably Alters Low-density Lipoprotein Cholesterol, Triglycerides, and Factor VII Coagulant Activity. J Am Diet Assoc, **105** (7), 1071 (2005).

111. A. NEMATI, A. NAGHIZADEH-BAGHI, M. H. DEHGAN, H. ALIMOHAMMADI-ASL, G. H. ETTEHAD, H. SADEGHI: The Effect of Sunflower Oil Intake on Coagulating Factors in Healthy Males Individuals. Res J Biol Sci, **2** (6), 650 (2007).

112. P. OUBIÑA, F. J. SÁNCHEZ-MUNIZ, S. RÓDENAS, C. CUESTA: Eicosanoid Production, Thrombogenic Ratio, and Serum and LDL-peroxides in Normo- and Pypercholesterolaemic Postmenopausal Women Consuming Two Oleic Acid-rich Diets with Different Content of Minor Components. Br J Nutr, **85**, 41 (2001).

113. M. VÁZQUEZ-VELASCO, E. L. DÍAZ, R. LUCAS, S. GÓMEZ-MARTÍNEZ, S. BASTIDA, A. MARCOS, F. J. SÁNCHEZ-MUNIZ: Effects of Hydroxytyrosol-enriched Sunflower Oil Consumption on CVD Risk Factors. Br J Nutr, **105** (10), 1448 (2011).

114. E. L. ASHTON, J. D. BEST, M. J. BALL: Effects of Monounsaturated Enriched Sunflower Oil on CHD Risk Factors Including LDL Size and Copper-induced LDL Oxidation. J Am Coll Nutr, **20** (4), 320 (2001).

115. E. K. KABAGAMBE, A. BAYLIN, A. ASCHERIO, H. CAMPOS: The Type of Oil Used for Cooking Is Associated with the Risk of Nonfatal Acute Myocardial Infarction in Costa Rica. J Nutr, **135** (11), 2674 (2005).

116. H. CAMPOS, A. BAYLIN, W. C. WILLETT: α-Linolenic Acid and Risk of Nonfatal Acute Myocardial Infarction. Circulation, **118** (4), 339 (2008).

117. C. M. AGUILERA, M. D. MESA, M. C. RAMIREZ-TORTOSA, M. T. NESTARES, E. ROS, A. GIL: Sunflower Oil Does Not Protect against LDL Oxidation as Virgin Olive Oil Does in Patients with Peripheral Vascular Disease. Clin Nutr, **23** (4), 673 (2004).

118. B. SUDHAKAR, P. KALAIARASI, K. S. Al-NUMAIR, G. CHANDRAMOHAN, R. K. RAO, K. V. PUGALENDI: Effect of Combination of Edible Oils on Blood Pressure, Lipid Profile, Lipid Peroxidative Markers, Antioxidant Status, and Electrolytes in Patients with Hypertension on Nifedipine Treatment. Saudi Med J, **32** (4), 379 (2011).

119. H. J. MURFF, X. O. SHU, H. LI, G. YANG, X. WU, H. CAI, W. WEN, Y. T. GAO, W. ZHENG: Dietary Polyunsaturated Fatty Acids and Breast Cancer Risk in Chinese Women: A Prospective Cohort Study. Int J Cancer, **128** (6), 1434 (2011).

120. A. K. ZAINEDDIN, K. BUCK, A. VRIELING, J. HEINZ, D. FLESCH-JANYS, J. LINSEISEN, J. CHANG-CLAUDE: The Association between Dietary Lignans, Phytoestrogen-rich Foods, and Fiber Intake and Postmenopausal Breast Cancer Risk: A German Case-control Study. Nutr Cancer, **64** (5), 652 (2012).

121. G. LIETZ, C. J. HENRY, G. MULOKOZI, J. K. MUGYABUSO, A. BALLART, G. D. NDOSSI, W. LORRI, A. TOMKINS: Comparison of the Effects of Supplemental Red Palm Oil and Sunflower Oil on Maternal Vitamin A Status. Am J Clin Nutr, **74** (4), 501 (2001).

122. L. F. EICHENFIELD, A. McCOLLUM, P. MSIKA: The Benefits of Sunflower Oleodistillate (SOD) in Pediatric Dermatology. Pediatr Dermatol, **26** (6), 669 (2009).

123. F. SCHÄFER, S. E. ADAMS, J A. NICHOLSON, T. F. COX, M. McGRADY, F. MOORE: *In vivo* Evaluation of an Oral Health Toothpaste with 0.1% Vitamin E Acetate and 0.5% Sunflower Oil (with Vitamin F). Int Dent J, **57** (S2), 119 (2007).

124. R. TOMASCH, K. H. WAGNER, I. ELMADFA: Antioxidative Power of Plant Oils in Humans: the Influence of Alpha- and Gamma-tocopherol. Ann Nutr Metab, **45** (3), 110 (2001).

125. L. MÜLLER, K. THEILE, V. BÖHM: *In vitro* Antioxidant Activity of Tocopherols and Tocotrienols and Comparison of Vitamin E Concentration and Lipophilic Antioxidant Capacity in Human Plasma. Mol Nutr Food Res, **54**, 731 (2010).

126. A. BAYLIN, M. K. KIM, A. DONOVAN-PALMER, X. SILES, L. DOUGHERTY, P. TOCCO, H. CAMPOS: Fasting Whole Blood as a Biomarker of Essential Fatty Acid Intake in Epidemiologic Studies: Comparison with Adipose Tissue and Plasma. Am J Epidemiol, **162** (4), 373 (2005).

127. E. EDER, M. WACKER, U. LUTZ, J. NAIR, X. FANG, H. BARTSCH, F. A. BELAND, J. SCHLAT-TER, W. K. LUTZ: Oxidative Stress Related DNA Adducts in the Liver of Female Rats Fed with Sunflower-, Rapeseed-, Olive- or Coconut Oil Supplemented Diets. Chem Biol Interact, **159** (2), 81 (2006).

128. J. L. QUILES, J. R. HUERTAS, M. BATTINO, M. C. RAMÍREZ-TORTOSA, M. CASSINELLO, J. MATAIX, M. LOPEZ-FRIAS, M. MAÑAS: The Intake of Fried Virgin Olive or Sunflower Oils Differentially Induces Oxidative Stress in Rat Liver Microsomes. Br J Nutr, **88** (1), 57 (2002).

129. V. RUIZ-GUTIÉRREZ, C. M. VÁZQUEZ, C. SANTA-MARIA: Liver Lipid Composition and Antioxidant Enzyme Activities of Spontaneously Hypertensive Rats after Ingestion of Dietary Fats (Fish, Olive and High-oleic Sunflower Oils). Bioscience Rep, **21** (3), 271 (2001).

130. A. WALCZEWSKA, B. DZIEDZIC, T. STEPIEN, E. SWIATEK, D. NOWAK: Effect of Dietary Fats on Oxidative–Antioxidative Status of Blood in Rats. J Clin Biochem Nutr, **47** (1), 18 (2010).

131. L. NUNES-MASI, A. ROQUE-MARTINS, J. C. ROSA-NETO, C. L. DO AMARAL, A. RABELLO-CRISMA, M. A. RAMIREZ-VINOLO, E. A. de LIMA JÚNIOR, S. M. HIRABARA, R. CURI: Sunflower Oil Supplementation Has Proinflammatory Effects and Does Not Reverse Insulin Resistance in Obesity Induced by High-fat Diet in C57BL/6 Mice. J Biomed Biotechnol, (2012).

132. A. C. POLETTO, G. F. ANHÊ, P. EICHLER, H. K. TAKAHASHI, D. T. FURUYA, M. M. OKAMOTO, R. CURI, U. F. MACHADO: Soybean and Sunflower Oil-induced Insulin Resistance Correlates with Impaired GLUT4 Protein Expression and Translocation Specifically in White Adipose Tissue. Cell Biochem Funct, **28** (2), 114 (2010).

133. R. J. DÍAZ, M. D. YAGO, V. E. MARTÍNEZ, J. A. NARANJO, M. A. MARTÍNEZ, M. MAÑAS: Comparison of the Effects of Dietary Sunflower Oil and Virgin Olive Oil on Rat Exocrine Pancreatic Secretion *in vivo*. Lipids, **38** (11), 1119 (2003).

134. R. J. NICOLOSI, B. WOOLFREY, T. A. WILSON, P. SCOLLIN, G. HANDELMAN, R. FISHER: Decreased Aortic Early Atherosclerosis and Associated Risk Factors in Hypercholesterolemic Hamsters Fed a High- or Mid-oleic Acid Oil Compared to a High-linoleic Acid Oil. J Nutr Biochem, **15**, 540 (2004).

135. M. F. RAMADAN, M. M. AFIFY-AMER, S. S. El-SAADANY, R. ABD El-FATAH El-MASRY, A. El-SAID AWAD: Changes in Lipid Profile by Vegetable Oil Blends Rich in Polyunsaturated Fatty Acids in Rats with Hypercholesterolemia. Food Sci Technol Int, **15** (2), 119 (2009).
136. S. GORINSTEIN, H. LEONTOWICZ, M. LEONTOWICZ, A. LOJEK, M. CÍŽ, R. KRZEMINSKI, Z. ZACHWIEJA, Z. JASTRZEBSKI, E. DELGADO-LICON, O. MARTIN-BELLOSO, S. TRA-KHTENBERG: Seed Oils Improve Lipid Metabolism and Increase Antioxidant Potential in Rats Fed Diets Containing Cholesterol. Nutr Res, **23**, 317 (2003).
137. R. di BENEDETTO, L. ATTORRI, F. CHIAROTTI, A. EUSEPI, A. di BIASE, S. SALVATI: Effect of Micronutrient-enriched Sunflower Oils on Plasma Lipid Profile and Antioxidant Status in High-fat-fed Rats. J Agric Food Chem, **58** (9), 5328 (2010).
138. N. D. SONI, U. CHOUDHARY, P. SHARMA, A. DUBE: To Study the Effect of Diet Supplementation with Coconut Oil, Mustard Oil and Sunflower Oil on Blood Lipids in Rabbit. Ind J Clin Biochem, **25** (4), 441 (2010).
139. R. I. BELLO, C. GÓMEZ-DÍAZ, M. I. BURÓN, P. NAVAS, J. M. VILLALBA: Differential Regulation of Hepatic Apoptotic Pathways by Dietary Olive and Sunflower Oils in the Ageing Rat. Exp Gerontol, **41** (11), 1174 (2006).
140. Z. B. ZULLYT-RODRÍGUEZ, R. GONZÁLEZ-ÁLVAREZ, D. GUANCHE, N. MERINO, F. HERNÁNDEZ-ROSALES, S. MENÉNDEZ-CEPERO, Y. ALONSO-GONZÁLEZ, S. SCHULZ: Antioxidant Mechanism Is Involved in the Gastroprotective Effects of Ozonized Sunflower Oil in Ethanol-induced Ulcers in Rats. Mediators Inflamm, (2007).
141. G. J. KAPADIA, M. A. AZUINE, H. TOKUDA, M. TAKASAKI, T. MUKAINAKA, T. KONOSHIMA, H. NISHINO: Chemopreventive Effect of Resveratrol, Sesamol, Sesame Oil and Sunflower Oil in the Epstein-Barr Virus Early Antigen Activation Assay and the Mouse Skin Two-stage Carcinogenesis. Pharmacol Res, **45** (6), 499 (2002).
142. M. P. THOMSON, C. S. ANTICEVIC, B. H. RODRÍGUEZ, V. V. SILVA: *In vitro* Antifungal Susceptibility, *in vivo* Antifungal Activity and Security from a Natural Product Obtained from Sunrise Oil (AMO3) against Dermatophytes. Rev Chilena Infectol, **28** (6), 512 (2011).
143. R. O. DAVID, F. J. SÁNCHEZ-MUNIZ, S. BASTIDA, J. BENEDI, M. J. GONZÁLEZ-MUÑOZ: Gastric Emptying and Short-term Digestibility of Thermally Oxidized Sunflower Oil Used for Frying in Fasted and Nonfasted Rats. J Agric Food Chem, **58** (16), 9242 (2010).
144. M. A. ABOKI, M. MOHAMMED, S. H. MUSA, B. S. ZURU, H. M. ALIYU, M. GERO, I. M. ALIBE, B. INUWA: Physicochemical and Anti-microbial Properties of Sunflower (*Helianthus annuus* L.) Seed Oil. IJST, **2** (4), 151 (2012).
145. F. HERNÁNDEZ, D. HERNÁNDEZ, Z. ZULLYT, M. DÍAZ, O. ANCHETA, S. RODRIGUEZ, D. TORRES: *Giardia duodenalis*: Effects of an Ozonized Sunflower Oil Product (Oleozon®) on *in vitro* Trophozoites. Exp Parasitol, **121** (3), 208 (2009).
146. C. SOLER-RIVAS, F. R. MARÍN, S. SANTOYO, M. R. GARCÍA-RISCO, F. J. SEÑORÁNS, G. REGLERO: Testing and Enhancing the *in vitro* Bioaccessibility and Bioavailability of *Rosmarinus officinalis* Extracts with a High Level of Antioxidant Abietanes. J Agric Food Chem, **58** (2), 1144 (2010).
147. A. K. MISHRA, A. MISHRA, P. CHATTOPADHYAY: Herbal Cosmetics for Photo-protection from Ultraviolet B Radiation: A Review. Trop J Pharm Res, **10** (3), 351 (2011).
148. J. KANNER: Dietary Advanced Lipid Oxidation Endproducts Are Risk Factors to Human Health. Mol Nutr Food Res, **51** (9), 1094 (2007).
149. K. ESPOSITO, D. GIUGLIANO: Diet and Inflammation: A Link to Metabolic and Cardiovascular Diseases. Eur Heart J, **27** (1), 15 (2006).
150. P. L. LUTSEY, L. M. STEFFEN, J. STEVENS: Dietary Intake and the Development of the Metabolic Syndrome: the Atherosclerosis Risk in Communities Study. Circulation, **117** (6), 754 (2008).
151. A. JOYCE, S. DIXON, J. COMFORT, J. HALLETT: Reducing the Environmental Impact of Dietary Choice: Perspectives from a Behavioral and Social Change Approach. J Environ Public Health, (2012).
152. S. SIVASANKARAN: The Cardio-protective Diet. Indian J Med Res, **132** (5), 608 (2010).

153. Y. ADKINS, D. S. KELLEY: Mechanisms Underlying the Cardioprotective Effects of Omega-3 Polyunsaturated Fatty Acids. JNB, **21**, 781 (2010).

154. V. S. MALIK, F. B. HU: Popular Weight-loss Diets: from Evidence to Practice. Nat Clin Pract Cardiovasc Med, **4** (1), 34 (2007).

155. A. ZAMPELAS, A. G. KAFATOS: Olive Oil Intake in Relation to Cardiovascular Diseases. Int J Fats Oils, **24** (55), 24 (2004).

156. H. M. ROCHE: Olive Oil, High-oleic Acid Sunflower Oil and CHD. Br J Nutr, **85**, 3 (2001).

157. M.-J. OLIVERAS-LÓPEZ, G. BERNÁ, E. M. CARNEIRO, H. LÓPEZ-GARCÍA de la SER- RANA, F. MARTÍN, M. C. LÓPEZ: An Extra-virgin Olive Oil Rich in Polyphenolic Compounds Has Antioxidant Effects in Of1 Mice. J Nutr, **138**, 1074 (2008).

158. D. M. MAESTRI, V. NEPOTE, A. L. LAMARQUE, J. A. ZYGADLO: Natural Products as Anti- oxidants. In: Phytochemistry: Advances in Research (Ed. Filippo Imperato). Research Signpost, Kerala, 2006, 105–135.

159. M. G. MIGUEL: Antioxidant and Anti-inflammatory Activities of Essential Oils: A Short Review. Molecules, **15**, 9252 (2010).

160. S. BORRA, P. M. KRIS-ETHERTON, J. G. DAUSCH, S. YIN-PIAZZA: An Update of Trans-fat Reduction in the American Diet. J Am Diet Assoc, **107** (12), 2048 (2007).

161. S. FILIP, R. VIDRIH: Trans Fatty Acids and Human Health. In: The Cardiovascular System – Physi- ology, Diagnostics and Clinical Implications (Ed. Dr. David Gaze). InTech, 2012, 53–58. Available from: http://www.intechopen.com/books/the-cardiovascular-system-physiology -diagnostics-and- clinical-implications/trans-fatty-acids-and-human-health.

162. A. A. CARELLI, I. C. FRANCO, G. H. CRAPISTE: Effectiveness of Added Natural Antioxidants in Sunflower Oil. Int J Fats Oils, **56** (4), 303 (2005).

163. L. FENGJUAN, T. WENJUAN, K. ZHANFANG, W. CHI-WAI: Tocotrienol Enriched Palm Oil Prevents Atherosclerosis through Modulating the Activities of Peroxisome Proliferators-activated Receptors. Atherosclerosis, **211** (1), 278 (2010).

164. Z. REBLOVA, P. OKROUHLA: Ability of Phenolic Acids to Protect α-tocopherol. Czech J Food Sci, **28** (4), 290 (2010).

165. C. G. BEDDOWS, C. JAGAIT, M. J. KELLY: Preservation of Alpha-tocopherol in Sunflower Oil by Herbs and Spices. Int J Food Sci Nutr, **51** (5), 327 (2000).

166. EFSA: Scientific Opinion of the Panel on Food Additives, Flavourings, Processing Aids and Materi- als in Contact with Food on a Request from the Commission on Mixed Tocopherols, Tocotrienol Tocopherol and Tocotrienols as Sources for Vitamin E. EFSA J, **640**, 1 (2008).

167. J. BARDHAN, R. CHAKRABORTY, U. RAYCHAUDHURI: The 21st Century Form of Vitamin E-tocotrienol. Curr Pharm Des, **17** (21), 2196 (2011).

168. B. HALLIWELL, J. RAFTER, A. JENNER: Health Promotion by Flavonoids, Tocopherols, To- cotrienols, and Other Phenols: Direct or Indirect Effects? Antioxidant or Not? Am J Clin Nutr, **81** (1), 268S (2005).

169. V. RUBALYA, P. NEELAMEGAM: Antioxidant Potential in Vegetable Oil. Res J Chem Environ, **16** (2), 87 (2012).

170. G. BJELAKOVIC, D. NIKOLOVA, L. L. GLUUD, R. G. SIMONETTI, C. GLUUD: Antioxidant Supplements for Prevention of Mortality in Healthy Participants and Patients with Various Diseases. Cochrane Database of Systematic Reviews, (3) (2012).

171. N. GOUGOULIAS: Comparative Study on the Polyphenol Content and Antioxidant Activity of Some Medicinal Plants. Oxid Commun, **35** (4), 1001 (2012).

172. D. A. KOSTIC, D. S. DIMITRIJEVIC, G. S. STOJANOVIC, S. S. MITIC, M. N. MITIC: Phenolic Composition and Antioxidant Activity of Fresh Fruit Extracts of Mulberries from Serbia. Oxid Commun, **36** (1), 4 (2013).

173. M. N. MITIC, M. V. OBRADOVIC, D. A. KOSTIC, A. N. PAVLOVIC, J. M. BRCANOVIC: Phenolic Compounds and Antioxidant Capacities of Dried Raspberry from Serbia, Extracted with Different Solvents. Oxid Commun, **35** (3), 674 (2012).

174. M. POP-SCHWERIN, C. L. SCHWERIN, A. X. LUPEA, A. GHARIBEH-BRANIC, A.-M. CHIS-PANA: Evaluation of Antioxidant Activity of Some *Vaccinium* Extracts and Their Application for the Inhibition of Oxidation Process in Vegetable Oil. Oxid Commun, **33** (1), 175 (2010).

175. M. GHARACHORLOO, M. GHAVAMI, F. JAMDAR: Stabilising Activities of Acetone and Ethanolic Extracts of Turmeric on Canola and Sunflower Seed Oils. Oxid Commun, **35** (4), 1021 (2012).

176. D. KRUZLICOVA, M. DANIHELOVA, M. VEVERKA: Quantitative Structure-antioxidant Activity Relationship of Quercetin and Its New Synthesised Derivatives. Nova Biotechnologica et Chimica, **11** (1), 37 (2012).

177. L. ALVARADO-SOTO, R. RAMIREZ-TAGLE: NICS: A Possible New Criterion to Evaluate the Structure–Antioxidant Activity Relationship of Phenolic Compound. Oxid Commun, **34** (3), 516 (2011).

178. B. LUCIC, D. AMIC, N. TRINAJSTIC: Antioxidant QSAR Modeling as Exemplified on Polyphenols. Methods Mol Biol, **477**, 207 (2008).

179. D. AMIC, D. DAVIDOVIC-AMIC, D. BESLO, V. RASTIJA, B. LUCIC, N. TRINAJSTIC: SAR and QSAR of the Antioxidant Activity of Flavonoids. Curr Med Chem, **14**, 827 (2007).

180. A. I. KHLEBNIKOV, I. A. SCHEPETKIN, N. G. DOMINA, L. N. KIRPOTINA, M. T. QUINN: Improved Quantitative Structure–Activity Relationship Models to Predict Antioxidant Activity of Flavonoids in Chemical, Enzymatic, and Cellular Systems. Bioorg Med Chem, **15** (4), 1749 (2007).

181. A. SCHIAVONE, J. NERY, J. A. CHOQUE-LOPEZ, M. D. BAUCELLS, A. C. BARROETA: Dietary Lipid Oxidation and Vitamin E Supplementation Influence *in vivo* Erythrocyte Traits and Postmortem Leg Muscle Lipid Oxidation in Broiler Chickens. Can J Anim Sci, **90** (2), 197 (2010).

182. A. BELENGUER, P. G. TORAL, P. FRUTOS, G. HERVAS: Changes in the Rumen Bacterial Community in Response to Sunflower Oil and Fish Oil Supplements in the Diet of Dairy Sheep. J Dairy Sci, **93** (7), 3275 (2010).

183. P. G. TORAL, Y. CHILLIARD, L. BERNARD: Short Communication: *in vivo* Deposition of [1-(13)C]vaccenic Acid and the Product of its Δ9-desaturation, [1-(13)C]rumenic Acid, in the Body Tissues of Lactating Goats Fed Oils. J Dairy Sci, **95** (11), 6755 (2012).

184. A. KHOL-PARISINI, R. van den HOVEN, S. LEINKER, H. W. HULAN, J. ZENTEK: Effects of Feeding Sunflower Oil or Seal Blubber Oil to Horses with Recurrent Airway Obstruction. Can J Vet Res, **71** (1), 59 (2007).

185. M. MARTÍN-POLVILLO, G. MÁRQUEZ-RUIZ, M. C. DOBARGANES: Oxidative Stability of Sunflower Oils Differing in Unsaturation Degree during Long-term Storage at Room Temperature. J Am Oil Chem Soc, **81** (6), 577 (2004).

186. S. MARMESAT, L. VELASCO, M. V. RUIZ-MÉNDEZ, J. M. FERNÁNDEZ-MARTÍNEZ, C. DO-BARGANES: Thermostability of Genetically Modified Sunflower Oils Differing in Fatty Acid and Tocopherol Compositions. Eur J Lipid Sci Technol, **110**, 776 (2008).

187. D. SKORIC, S. JOCIC, Z. SAKAC, N. LECIC: Genetic Possibilities for Altering Sunflower Oil Quality to Obtain Novel Oils. Can J Physiol Pharmacol, **86** (4), 215 (2008).

188. D. SKORIC: Possible Uses of Sunflower in Proper Human Nutrition. Med Pregl, **62** (Suppl. 3), 105 (2009).

189. L. VELASCO-VARO, J. M. FERNÁNDEZ-MARTÍNEZ, B. PEREZ-VICH: United States Patent Application 2011 0061138 (2011).

190. M. de LORGERIL, P. SALEN: New Insights into the Health Effects of Dietary Saturated and Omega-6 and Omega-3 Polyunsaturated Fatty Acids. BMC Med, **10**, 50 (2012).

191. L. HODSON, C. M. SKEAFF, B. A. FIELDING: Fatty Acid Composition of Adipose Tissue and Blood in Humans and Its Use as a Biomarker of Dietary Intake. Prog Lipid Res, **47** (5), 348 (2008).

192. A. COLIN, J. REGGERS, V. CASTRONOVO, M. ANSSEAU: Lipids, Depression and Suicide. L'Encéphale, **29** (1), 49 (2003).

SECONDARY LIPID OXIDATION PRODUCTS OF OIL IN WHITE MUSTARD SEEDS (*Sinapis albae semen*)

D. PAUNOVIC[a], T. S. KNUDSEN[b]*, B. ZLATKOVIC[a], M. ANTIC[a,b]

[a]*Faculty of Agriculture, University of Belgrade, 6 Nemanjina Street, 11 080 Belgrade, Serbia*
[b]*Department of Chemistry, Institute of Chemistry, Technology and Metallurgy, University of Belgrade, 12 Njegoseva Street, P.O. Box 473, 11 001 Belgrade, Serbia*
E-mail: tsolevic@chem.bg.ac.rs

ABSTRACT

In this study secondary lipid oxidation products of oil in white mustard seeds were analysed. Ground white mustard seeds were extracted by solvent extraction and the extract was analysed by gas chromatographic–mass spectrometric instrumental analysis. (Semi)volatile compounds different from fatty acids represented less than 1% of all compounds present in the extract. Except from the naturally occurring flavour and aroma compounds, a whole series of saturated and unsaturated aldehydes with 1 or 2 double bonds was identified in the extract. It was shown that most of them can be useful indicators of lipid oxidation in white mustard seeds. Additionally, it was shown that these unsaturated aldehydes, when present in high concentrations, can be indicators of an early stage of lipid oxidation in this plant.

Keywords: oilseeds, lipid oxidation, degradation, extraction/separation, GC/MS.

AIMS AND BACKGROUND

Oil seeds are rich source of lipids, and most of them are characterised by high content of unsaturated fatty acids[1,2]. When seeds are damaged, lipid degradation reactions can occur and this process proceeds at different rates in seeds from different plant species[3]. Acyl lipid constituents, such as oleic, linoleic and linolenic acids, having one or more double bounds within the fatty acid molecule, can easily be oxidised via an autocatalytic process consisting of a free radical mechanism. On the other hand, lipid degradation reactions can occur as enzyme-catalysed oxidation, mediated by the enzyme lipoxygenase, which is very specific for the substrate, having as the best substrate linoleic acid (18:2). In both cases oxidation reactions provide position-specific

---

* For correspondence.

hydroperoxides that may be decomposed to produce various secondary degradation products[4].

Major secondary degradation products of oil oxidation reactions are aldehydes, ketones, alcohols, hydrocarbons and carboxylic acid[5]. The exact composition of these compounds varies depending on the fatty acid composition of the fat/oil containing source material and environmental conditions. From the point of view of food quality, the most important is generation of aliphatic aldehydes because they are major contributors to unpleasant odours and flavours in food products[6]. Moreover, due to their low odour threshold and observed rise in their concentration during storage, these compounds are often used as indicators of the degree of oxidation of food products[7].

Depending on the variety, mustard seeds contain 30–50% of oil with high content of unsaturated fatty acids: oleic, linoleic, linolenic and erucic[1,8]. This composition of lipids makes them highly susceptible to various degradation reactions. However, literature lacks information on oxidation products of oil in mustard seeds. In the present study, we report our investigation on secondary lipid oxidation products in white mustard seeds (*Sinapis albae semen*).

This investigation is based on the solvent extraction of the ground white mustard seeds and gas chromatographic–mass spectrometric (GC–MS) instrumental analysis of the total profile of (semi)volatiles in the white mustard seeds with a particular emphasis on the secondary lipid oxidation products of oil in this material. The results obtained here were compared with previously reported results of an analysis of non-oxidised white mustard seeds[9].

EXPERIMENTAL

Aiming at identifying the secondary lipid oxidation products of oil in white mustard seeds, commercially available air-dried and ground seeds of this plant (*Sinapis albae semen*) were analysed in details.

The ground seeds were extracted in a Soxhlet extraction system for 10 h using methylene-chloride (b.p. 38°C) as a solvent. All analyses were done in triplicates. With each set of samples a solvent blank was passed through the extraction and GC–MS analytical procedure.

The extracts were analysed by gas chromatography - mass spectrometry (GC–MS) techniques. An Agilent 7890N gas chromatograph fitted with a HP5-MS capillary column (temperature range: 40°C for 9 min, then 4°C/min to 65°C for 0 min, then 9°C/min to 285°C for 3 min) with helium as the carrier gas (flow rate 1.5 cm^3/min) was used. The GC was coupled to a Hewlett–Packard 5972 MSD operated at 70 eV in the 45–550 scan range. All analyses of the investigated samples were conducted in a full scan mode. The most relevant peaks were identified by comparison of their retention indices with literature data and on the basis of their total mass spectra, by comparison with mass spectra databases (NIST/ EPA/NIH Mass spectral library

NIST2000, Wiley/ NBS Registry of Mass spectral Data 7th Ed., electronic versions). Retention indices were calculated relative to C_7–C_{29} alkanes on the HP-5MS column, according to the Kovats equation[10].

Relative abundances of the identified compounds were calculated from chromatographic peak areas without correction factors.

All analyses were done in triplicates and the results are expressed as mean ± standard deviation.

Considering the fact that the data about the time of storage of the seeds, temperature, humidity and the pressure of the storage were not available to the authors, the influence of these and other atmospheric parameters on mustard seed autoxidation will not be discussed in this paper.

RESULTS AND DISCUSSION

As already stated, aliphatic aldehydes are major contributors to unpleasant odours and flavours in food products[6]. Due to their low odour threshold and observed rise in their concentration during storage these compounds are often used as indicators of the degree of oxidation of food products[7]. For the purpose of monitoring the extent of lipid oxidation, commonly measured compounds include pentanal, hexanal, and 2,4-decadienal[11]. However, some results indicated that the degree of oxidation is better reflected by the total profile of volatiles rather than the presence of a selected compound[12].

In this study we present the results of an analysis of the total profile of volatiles in white mustard seeds with a particular emphasis on the secondary lipid oxidation products of oil in this material.

Figure 1 shows total ion current (TIC) chromatogram of the extract from the investigated white mustard seeds. The chromatogram is characterised by a broad and prominent 'hump' of an unresolved complex mixture (UCM) of fatty acids, comprising more than 99% of the all compounds in the extract. The most abundant compounds in the sample are oleic, linoleic, linolenic, eicosenoic and erucic acids.

(Semi)volatile compounds different from fatty acids represent less than 1% of all compounds present in the extract (Fig. 1). However, these low abundant compounds are the main responsible for flavour and aroma of white mustard seeds. Sixteen (semi) volatile compounds were identified in the mustard seeds investigated (Fig. 2, Table 1). One of the most abundant compounds in this range of retention times was (4-hydroxy-phenyl)acetonitrile, the main degradation product of myrosinase catalysed degradation of 4-hydroxybenzylglucosinolate (sinalbin)[13]. (4-Hydroxyphenyl)acetonitrile is only slightly volatile but contributes significantly to the sharp pungent taste of mustard. Additionally, 4 compounds which were proven to be aroma-emitting constituents in white mustard seeds (limonene, phenylacetaldehyde, phenylethylalcohol and geranyl acetate)[9] were identified in the range of (semi)volatile compounds (Fig. 2, Table 1).
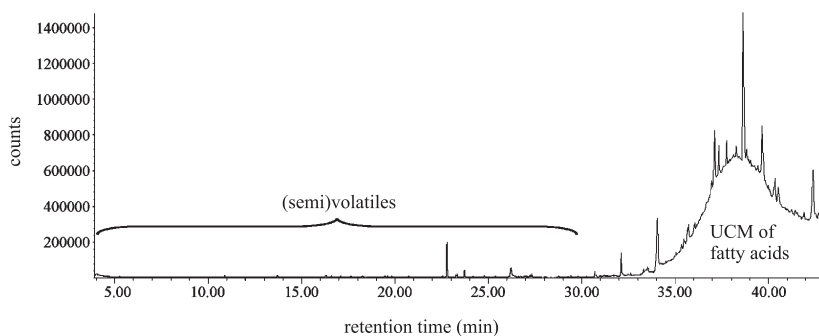
Fig. 1. TIC chromatogram of the extract from the analysed white mustard seeds
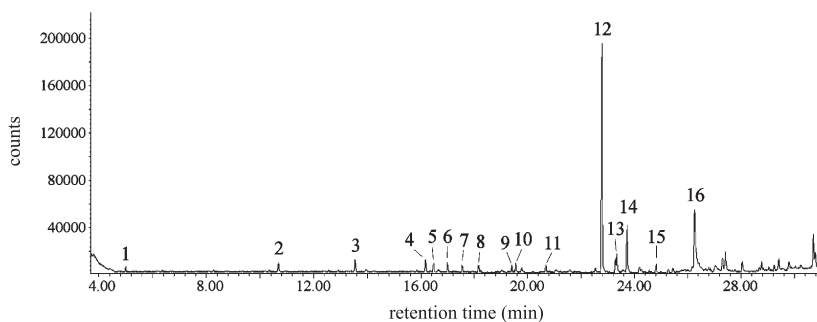

Fig. 2. Enlarged part of the TIC chromatogram of the extract showing only (semi)volatile compounds (identification of the compounds is given in Table 1)

Table 1. Identification and relative abundances of (semi)volatiles in the white mustard seeds

No	RI*	Compound	Peak area (%)
1	800	hexanal	0.013 ± 0.001
2	907	heptanal	0.019 ± 0.001
3	957	(*E*)-2-heptenal	0.023 ± 0.001
4	1005	octanal	0.022 ± 0.001
5	1012	(*E,E*)-2,4-heptadienal	0.019 ± 0.001
6	1025	limonene	0.016 ± 0.001
7	1043	phenylacetaldehyde	0.013 ± 0.001
8	1057	(*E*)-2-octenal	0.015 ± 0.001
9	1102	nonanal	0.014 ± 0.001
10	1114	phenylethylalcohol	0.018 ± 0.001
11	1162	(*E*)-2-nonenal	0.012 ± 0.001
12	1265	(*E*)-2-decenal	0.212 ± 0.004
13	1297	(*E,E*)-2,4-decadienal	0.033 ± 0.001
14	1321	(*E,E*)-2,4-dodecadienal	0.050 ± 0.001
15	1388	geranylacetate	0.018 ± 0.001
16	1480	(4-hydroxyphenyl)acetonitrile	0.141 ± 0.003

*The Kovats retention index (RI) on HP-5MS column.

672

Besides these natural flavour compounds, a whole series of saturated and unsaturated aldehydes with 1 or 2 double bonds was identified in the sample investigated (Fig. 2, Table 1): C_6, C_7, C_8 and C_9 alkanals; C_7, C_8, C_9 and C_{10} 2-enals and C_7, C_{10} and C_{12} 2,4-dienals. Almost all of them are characteristic secondary oxidation products of oleic, linoleic and linolenic acids[6]. However, some of them can also be present in small amounts in fresh oilseeds[4], and therefore, their identification requires further explanation.

Aldehyde hexanal has been for years considered a linoleic acid originating indicator of oxidation of the fat/oil containing material[11]. However, numerous researches showed that determination of changes in the content of hexanal is usable mainly in the evaluation of the quality of meat products, and that for vegetable oils the determination of nonanal would be more advisable[7]. Moreover, it was proven that the autoxidation of 2,4-decadienal yields hexanal and other volatiles which coincide with those obtained from linoleic acid, and that saturated aldehydes are mainly produced in a tertiary reaction, e. g. during the autoxidation of 2,4-decadienal[6]. Additionally, previously reported results of an analysis of non-oxidised white mustard seeds[9] showed that hexanal, when present in low amounts, is a natural aroma-emitting constituent in white mustard seeds. Accordingly, it can be concluded that hexanal can be an useful indicator of oxidation of oil in mustard seeds, but only if it is present in concentrations higher than naturally occurring in this plant and if the oxidation is additionally confirmed by the presence of other oxidation-indicative compounds.

Except from hexanal, 3 other saturated aldehydes are identified in the sample investigated: heptanal, octanal and nonanal. Previous analysis of mustard seeds[9] showed that in non-oxidised white mustard seeds heptanal is present only in trace amount while octanal and nonanal were absent. Based on these results, but also considering the fact that C_7–C_9 alkanals are characteristic secondary oxidation products of oleic, linoleic and linolenic acids[6], it can be concluded that octanal and nonanal, when they are present in white mustard seeds, and heptanal, when it is present in an amount higher than traces, can be considered indicators of the oxidation of oil in this plant.

Four (E)-2-alkenals were identified in the sample investigated (Fig. 2, Table 1). According to Grosch (1987) (Ref. 14) these 2-alkenals, being secondary lipid oxidation products, can be used as indicators to determine their fatty acid precursors in the sample. On the basis of these findings, it can be concluded that the presence of C_7–C_{10} (E)-2-alkenals in the sample indicates not only that the oxidation of oil in this sample has already started, but also that these white mustard seeds contained a significant amount of oleic and linoleic acid. These results are in an agreement with the previously published analysis which showed that C_7, C_9 and C_{10} (E)-2-alkenals are absent from non-oxidised white mustard seeds[9], as well as with the previously determined fatty acids profile of mustard seeds[1,8].

Based on the peak areas, 2-alkenals are the most abundant volatile compounds in this sample, with (E)-2-decenal as the most abundant (Fig. 2, Table 1). It is well known that 2-alkenals and 2,4-alkadienals are oxidised substantially faster than the

unsaturated fatty acids, giving hexanal and other saturated volatiles which can, over a long enough period of time, enrich the oxidation products and become predominant[6]. Accordingly, it can be concluded that high concentration of 2-alkenals indicates that the investigated sample is in the early stage of lipid oxidation. Moreover, according to the high abundance of (*E*)-2-decenal in these oxidised white mustard seeds, and its absence from non-oxidised seeds[9], it might be presumed that this compound might be useful as an indicator of the degree of oxidation of white mustard oil.

Finally, in the sample investigated, three (*E,E*)-2,4-dienals were identified in significant amounts (Fig. 2, Table 1). Their presence confirms the previous conclusion about the early lipid oxidation stage of this sample. This conclusion is in accordance with the previous results of Miyazawa and Kawata (Ref. 9), who showed that (*E,E*)-2,4-heptadienal and (*E,E*)-2,4-decadienal were absent from non-oxidised white mustard seeds while (*E,E*)-2,4-undecadienal was present in trace amount only. Additionally, the presence of (*E,E*)-2,4-heptadienal and (*E,E*)-2,4-decadienal in the sample investigated points to linolenic and linoleic acid as their precursor[6], proving again previously determined fatty acids profile of mustard seeds[1,8].

However, it should be stressed that the origin of (*E,E*)-2,4-undecadienal in this sample remains unclear. As a potential secondary lipid oxidation product, this compound is difficult to be traced to its precursor fatty acids. However, this compound was identified in trace amount in non-oxidised white mustard seeds[9], and in higher amount in the white mustard seeds analysed in this study whose (semi)volatiles composition is proven to be oxidation-altered. It might be possible that (*E,E*)-2,4-undecadienal is a specific indicator of the oxidation of oil in this plant. Nevertheless, this assumption has yet to be proven.

ACKNOWLEDGEMENTS

REFERENCES

1. R. J. MAILER: Oilseeds Overview. In: Encyclopedia of Grain Science (Eds H. Corke, C. E. Walker, C. Wrigley). Elsevier Ltd., 2004, 380–386.
2. K. GEORGIEVA, P. PETKOV, Y. DENEV: Study and Classification of Vegetable Oils Using the Fourier Transform Infrared Spectroscopy. Oxid Commun, **36**, 85 (2013).
3. D. STAJNER, M. KRALJEVIC-BALALIC, M. MILOSEVIC, M. VUJAKOVIC, M. ZLOKOLICA: Stress Resistance in Seeds. Oxid Commun, **25**, 596 (2002).
4. F. YILDIZ: Advances in Food Biochemistry. CRC Press, Copyright © Taylor & Francis Group LLC, 2010.
5. E. N. FRANKEL: Chemistry of Autoxidation. Mechanism Products and Flavor Significance. In: Flavor Chemistry of Fats and Oils (Eds D. B. Min, T. H. Smouse). Champaign, Ill., American Oil Chemists' Society, 1985, 1–34.
6. H.-D. BELITZ, W. GROSCH, P. SCHIEBERLE: Food Chemistry. 4 ed. Springer Verlag, Berlin, Heidelberg, 2009.

7. B. PLUTOWSKA, W. WARDENCKI: Aromagrams – Aromatic Profiles in the Appreciation of Food Quality. Food Chem, **101**, 845 (2007).

8. S. SAMMAN, J. W. Y. CHOW, M. J. FOSTER, Z. I. AHMAD, J. L. PHUYAL, P. PETOCZ: Fatty Acid Composition of Edible Oils Derived from Certified Organic and Conventional Agricultural Methods. Food Chem, **109**, 670 (2008).

9. M. MIYAZAWA, J. KAWATA: Identification of the Main Aroma Compounds in Dried Seeds of *Brassica hirta*. J Nat Med, **60**, 89 (2006).

9. E. KOVATS: Gas-chromatographische Charakterisierung organischer Verbindungen. Teil 1: Retentionsindices aliphatischer Halogenide, Alkohole, Aldehyde und Ketone. Helv Chim Acta, **41**, 1915 (1958).

11. S. S. NIELSEN: Food Analysis. 4 ed. Springer, New York, Dordrecht, Heidelberg, London, 2010.

12. S. M. van RUTH, J. P. ROOZEN, F. J. H. M. JANSEN: Aroma Profiles of Vegetable Oils Varying in Fatty Acid Composition versus Concentrations of Primary and Secondary Lipid Oxidation Products. Nahrung, **44**, 318 (2000).

13. S. BUSKOV, J. HASSELSTRØM, C. E. OLSEN, H. SØRENSEN, J. C. SØRENSEN, S. SØRENSEN: Supercritical Fluid Chromatography as a Method of Analysis for the Determination of 4-hydroxy-benzylglucosinolate Degradation Products. J Biochem Biophys Methods, **43**, 157 (2000).

14. W. GROSCH: Low-MW Products of Hydroperoxide Reactions. In: Autoxidation of Unsaturated Lipids (Ed. H. W. S. Chan). Academic Press, London, 1987, 95–139.

SERUM HOMOCYSTEINE, FOLATE, VITAMIN B12 LEVELS AND OXIDATIVE LIPID AND PROTEIN DAMAGE MARKERS IN DEPRESSIVE PATIENTS. THE EFFECT OF SERTRALINE TREATMENT

U. G. BEKMEZCI[a], A. ARICIOGLU[a]*, N. EREN[b], A. CUMAOGLU[c], N. YUKSEL[b]

[a]*Department of Medical Biochemistry, Faculty of Medicine, Gazi University, 06 500 Besevler, Ankara, Turkey*
E-mail: *aysela@gazi.edu.tr*
[b]*Department of Psychiatry, Faculty of Medicine, Gazi University, Ankara, Turkey*
[c]*Department of Biochemistry, Faculty of Pharmacy, Erciyes University, Kayseri, Turkey*

ABSTRACT

Previous studies have supported an association between low levels folate, vitamin B12 levels and elevated homocysteine levels as possible predictors of depression. Hyperhomocysteinemia induces free radical production, leading to alteration of oxidative lipid and protein modifications. Vitamin supplementation or antidepressants may reduce risk factors underlying depression. The aims of this study were to determine serum levels of protein carbonylation, lipid peroxidation, homocysteine, folic acid and vitamin B12 in depressive patients and to compare them with healthy controls; and to investigate the effects of sertraline (50 mg/day) treatment during 45 days. 23 depressed patients and 23 healthy controls participated in this study. Serum protein carbonylation was determined by spectrophotometric measurement of 2,4-dinitrophenylhydrason formation. Malondialdehyde levels were determined by spectrophotometric measurement of colour which was the reaction between thiobarbituric acid and malondialdehyde. Serum homocysteine levels were measured by HPLC, and vitamin B12 and folate levels – by radioimmunoassay. There was no remarkable difference in protein carbonylation, malondialdehyde formation, homocysteine, vitamin B12 and folate levels between healthy control group and depressed patients. Sertraline treatment caused a significant decrease in malondialdehyde levels. The findings suggest that sertraline treatment caused decreasing in oxidative stress by lowering lipid peroxidation in depressed patients.

Keywords: protein carbonylation, lipid peroxidation, homocysteine, vitamin B12, folate.

---

* For correspondence.

AIMS AND BACKGROUND

There is an increasing interest in hyperhomocysteinemia as a risk factor for neuropsychiatric disorders such as major depression[1,2]. Homocysteine is a thiol-containing amino acid that is formed by de-methylation of methionine, which uses as cofactors folate,vitamin B6 and vitamin B12. Therefore, a decrease in folate, vitamin B12 and vitamin B6 can induce a significant increase in plasma homocysteine levels[3]. Oxidation of homocysteine to homocysteine sulphinic acid and homocysteic acid can induce the production of reactive oxygen species (ROS) and promote oxidative stress. Neurotoxic effect of homocysteine may be mediated through increased ROS levels. Homocysteine may promote excitotoxicity and lead to increased neuronal cell death. Homocysteine sulphinic acid and homocysteic acids are putative neurotransmitters and endogenous agonists of N-methyl-D-aspartate (NMDA) receptors. NMDA receptors are a subgroup of excitatory glutaminergic receptors involved in synaptic trasmission and important in a mechanism of neurotoxicity called excitotoxicity. Activation of NMDA receptors resuls in a rise in intracellular calcium, consequent release of cellular proteases and eventual cell death[4]. The other ROS-produced mechanism in depressive patient is activated immune cells. Recent studies have shown that major depression is accompanied by increased number of peripheral blood mononuclear cells[5]. There is some evidence that activation of immune cells is releated to overproduction of ROS (Ref. 6). Extensive production of ROS leads to lipid peroxidation in biological membranes and causes loss of fluidity in cell membranes leading to cell death especially in neuronal cells[7,8]. Many researchers have focused on the relationship of oxidants and antioxidant systems in depression patients in the last dacade. The results of several reports suggest that lower antioxidant defences against lipid peroxidation exist in patients with depression[9,10]. Under oxidative stress, many enzymes and other structural proteins can be modified by reactive free radicals with direct formation of oxidised amino acids which can lead to the formation of protein carbonyl derivatives such as toxic aldehydes and ketones. Accumulation of modified derivatives can impair the cellular functions and cause loss of catalytic and structural integrity. Also the best known marker of oxidative protein damages is metal-catalysed protein oxidation characterised by protein carbonyl content[11,12]. Homocysteine can interact with transitions metals such as copper and result in potentiation of oxidative toxicity and neuronal cell death[13]. Vitamin supplementation maybe reduces lipid and protein oxidation by decreasing homocysteine levels in serum or neuronal tissues. In contrast, high dose vitamin supplementation can induce disfunction in nervous system[14]. Sertraline is a well-known selective serotonin re-uptake inhibitor. The antidepressant effect of sertraline presumed to be linked to its ability to inhibit the neuronal re-uptake of serotonin. Its neuroprotective and antioxidant actions have been reported in neurodegenerative diseases[15].

Based on the above findings, in the present study have been determined the serum levels of protein carbonylation, malondialdehyde formation, homocyteine, folate and

vitamin B 12 levels in depressive patients and their healthy control match, and the possible role of the sertraline treatment in depressive patients.

EXPERIMENTAL

Patients. In this study 46 subjects participated, 23 major depressed and 23 healthy control subjects. Patients who applied to the Psychiatry Department in Medical Faculty Gazi University, Ankara, Turkey were selected. All participants were aged between 20 and 62 years, average 38 years. Patients were utilised as having major depression according to the DSM-IV criteria[16] and they were required to have a score of at least 16 at baseline on the 17-item Hamilton depression rating scale[17]. Depressed patients were treated with sertraline 50 mg/day during 45 days. Venous blood samples were drawn into tube at the beginning of the day treatment and at the end of treatment and centrifuged at 3000 rpm 10 min to obtain serum. This study was carried out at Gazi University, Department of Medical Biochemistry, after having permission from local ethic committee.

Determination of oxidative stress markers. Protein carbonyl levels were measured spectrophotometrically using the method of Levine et al.[18] Protein carbonyl groups react with 2,4-dinitrophenylhydrazine (DNPH) to generate chromophoric dinitrophenylhydrazones. DNPH was dissolved in 2.5 M HCl, and after the DNPH reaction, proteins were precipitated with an equal volume of 20% (w/v) trichloroacetic acid and washed 3 times with 1 ml of ethyl acetate/ethanol mixture (1:1). Washings were achieved by mechanical disruption of pellets in the washing solution and re-pelleting by centrifugation at 6000 rpm for 10 min. Finally, the precipitates were dissolved in 6 M guanidine-HCl solution and the absorbances were measured at 370 nm, using the molar extinction coefficient of DNPH, $e = 2.2 \times 10^4$ M^{-1} cm^{-1}.

Malondialdehyde (MDA), an end product of unsaturated fatty acid peroxidation, can react with thiobarbituric acid (TBA) to form a pink coloured complex called thiobarbituric acid-reactive substance (TBARS). TBA reactivity was assayed by the method of Yoshioka et al.[19] The absorbance of the TBARS were read at 532 nm using a spectrophotometer.

Determination of homocysteine levels. Homocysteine levels were determined by reversed-phase high performance liquid chromatography (HPLC) coupled to a fluorescence detector (ImmuChrom, Bensheim, Germany). The albumin-bound and oxidised homocysteine was reduced and converted into a fluorescence probe in one step. The quantification was performed using a delivered plasma calibrator and the concentration was calculated via the internal standard method.

Determination of folate and vitamin B12 levels. Serum levels of vitamin B 12 and folate were tested with a commercial radioimmunoassay kit (Smul TRAK-SNB, USA) that allows the simultaneous determination of both vitamins.

Statistical analysis. Statictical analyses were evaluated by a computerised statistic program, SPSS 11.5 for Windows. The normal distribution of the variables was analysed by means of the Shapiro-Wilk test. Group mean differences were examined by means of *t*-test or Mann Whitney U-test. Differences in groups, prior (1st day) to and after treatment (45th day) were analysed by the Wilcoxon signed rank test. All results were expressed as the arithmetic mean±standart deviation.

RESULTS AND DISCUSSION

The main characteristics of all oxidative damage markers, homocysteine levels and vitamin contents are presented in Table 1. Slight but not statistically (*p*>0.05) significant differences between control group and depressive patient group were observed. So in our study we did not observe hyperhomocysteinemia and altered vitamin levels in patients when compared with those of healthy controls. Sertraline treatment significantly (*p*=0.004) decreased malondialdehyde levels in patients.

Table 1. Effect of sertralin treatment in 45 days on serum levels of protein carbonyl group (nmol/mg protein), malondialdehyde (nmol/mg), homocysteine (μmol/l), vitamin B12 (pg/ml) and folate (ng/ml) in depressed patients and their healty control match

Oxidative damage markers	Healthy controls		Depressed patients	
	1st day	45th day	1st day	45th day
Protein carbonyl	3.4±0.39	3.3±0.27	3.5±0.43	3.5±0.47
Malondialdehyde	3.9±0.69	3.9±0.80	4.3±0.89	3.3±0.64*
Homocysteine	14.3±4.36	15.3±4.81	14.4±3.97	14.2±4.03
Vitamin B12	357.8±191.62	327.3±173.44	312.1±119.29	304.1±123.06
Folate	7.7±2.52	7.3±2.53	8.3±3.56	8.0±3.29

*p<0.05 versus 1st days depressed patients.

Major depression is a mood disorder characterised by physiologic changes such as a sense of inadequacy, despondency, decreased activity, pessimism, anhedonia and sadness as these symptoms severely disrupt and adversely affect the person life. Biochemical changes are arranged by hyperhomocysteinemia and hypovitaminosis (decresed folate, vitamin B12 and B6 contents) in homocysteine metabolism in major depression. The elevated levels of homocysteine may occur due to a deficiency in vitamins that are necessary for the metabolism of homocysteine[20]. On the other hand, oxidative stress is the imbalance between oxidants/antioxidants systems implicated in the pathophysiology of several neuropsychiatric diseases, including major depressive disorder[21]. Oxidative stress leads to lipid peroxidation. Malondialdehyde, as an end-product of lipid peroxidation, is one of the most extensively studied indices of lipid peroxidation and thus oxidative stress[22]. Several studies have reported increased levels of malondialdehyde in depressive patients when compared with healthy controls[9,10,23,24]. But we found unchanged malondialdehyde levels in depressive patients when compared with those of healthy controls. It may be related to limited number of participants

in our expertice or different assay protocols. On the other hand, we believe that this is the first study investigating plasma levels of carbonyl-modified proteins which are markers of oxidative damage in depressive patients, in which we did not find any significant differences between the depressive patients and the control groups. This unchanged oxidative stress may be associated with unchanged homocysteine levels in depressive patients. In this study depression in patients did not increase homocysteine levels. At the same time, many publications have reported increased plasma levels of homocyteine in major depression[25-27]. However Fava et al.[28] has reported unchanged plasma vitamin B12 and homocyseine levels in major depression. In the same study it was reported that the antidepressant fluoxetine could not affect the same parameters[28]. In our study we measured unchanged vitamin B12 and folate levels in patients in comparison to controls. Several studies have reported unchanged vitamin B12 levels, although some of them have reported unchanged vitamin B12 and decreased folate levels in major depression[29]. Also sertraline is a selective serotonin re-uptake inhibitor and its antioxidant effects have been emphasised in neurodegenerative disorders. In our study sertraline treatment could not alter homocyteine and vitamin levels, but decreased malondialdehyde levels in major depressive patients. Several publications have shown that antidepressant drug treatment could normalise oxidative stress markers[23,24,30].

The present findings demonstrated the effects of sertraline treatment on oxidative stress markers, homocysteine levels and vitamin B12 and folic acid levels in depression. In future studies there is a need to include higher number of participants in order to obtain statistically more significant results. However, sertraline may be used to decrease the harmful effects of peroxidative lipid damage in depressive patients.

REFERENCES

1. P. SACHDEV: Homocysteine and Neuropsychiatric Disorders. Rev Bras Psiquiatr, **26**, 50 (2004).
2. S. REUTENS, P. SACHDEV: Homocysteine in Neuropsychiatric Disorders of the Elderly. Int J Geriatr Psychiatry, **17**, 859 (2002).
3. P. GU, L. F. DEFINA, D. LEONARD, S. JOHN, M. F. WEINER, E. S. BROWN: Relationship between Serum Homocysteine Levels and Depressive Symptoms. Cooper Center Longitudinal Study. J Clin Psychiatry, **73**, 691 (2012).
4. S. A. LIPTON, W. K. KIM, Y. B. CHOI, S. KUMAR, D. M. D'EMILIA, P. V. RAYUDU, D. R. ARNELLE, J. S. STAMLER: Neurotoxicity Associated with Dual Actions of Homocysteine at the N-methyl-d-aspartate Receptor. Proc Natl Acad Sci, **11**, 5923 (1997).
5. M. MAES, J. LAMBRECHTS, E. BOSMANS, J. JACOBS, E. SUY, C. VANDERVORST, C. de JONCKHEERE, B. MINNER, J. RAUS: Evidence for a Systemic Immune Activation during Depression, Results of Leukocyte Enumeration by Flow Cytometry in Conjunction with Monoclonal Antibody Staining. Psychol Med, **22**, 45 (1992).

6. Y. Y. LEE, J. S. PARK, J. S. JUNG, D. H. KIM, H. S. KIM: Anti-inflammatory Effect of Ginsenoside Rg5 in Lipopolysaccharide-stimulated BV2 Microglial Cells. Int J Mol Sci, **14**, 9820 (2013).

7. J. M. C. GUTTERIDGE: Lipid Peroxidation and Antioxidants as Biomarkers of Tissue Damage. Clin Chem, **41**, 1819 (1995).

8. S. YAGER, M. J. FORLENZA, G. E. MILLER: Depression and Oxidative Damage to Lipids. Psychoneuroendocrinology, **35**, 1356 (2010).

9. A. SARANDOL, E. SARANDOL, S. S. EKER, S. ERDINC, E. VATANSEVER, S. KIRLI: Major Depressive Disorder Is Accompanied with Oxidative Stress: Short-term Antidepressant Treatment Does Not Alter Oxidative–Antioxidative Systems. Hum Psychopharmacol Clin Exp, **22**, 67 (2007).

10. M. BILICI, H. EFE, M. A. KÖROGLU, H. A. UYDU, M. BEKAROGLU, O. DEGER: Antioxidative Enzyme Activities and Lipid Peroxidation in Major Depression: Alterations by Antidepressant Treatments. J Affect Disord, **64**, 43 (2001).

11. A. HACISEVKI, B. BABA, A. GONENC, S. ASLAN: Protein Carbonyl Contents Is the Most General and Well-used Biomarker of Severe Oxidative Stress. Oxid Commun, **35** (2), 413 (2012).

12. I. DALLE-DONNE, D. GIUSTARINI, R. COLOMBO, R. ROSSI, A. MILZANI: Protein Carbonylation in Human Diseases. Trends Mol Med, **9**, 169 (2003).

13. A. R. WHITE, X. HUANG, M. F. JOBLING, C. J. BARROW, K. BEYREUTHER, C. L. MASTERS, A. I. BUSH, R. CAPPAI: Homocysteine Potentiates Copper- and Amyloid Beta Peptide-mediated Toxicity in Primary Neuronal Cultures: Possible Risk Factors in the Alzheimer's-type Neurodegenerative Pathways. J Neurochem, **76**, 1509 (2001).

14. A. SINISCALCHI, F. MANCUSO, L. GALLELLI, F. G. IBBADU, N. B. MERCURI, G. de SARRO: Increase in Plasma Homocysteine Levels Induced by Drug Treatments in Neurologic Patients. Pharmacol Res, **52**, 367 (2005).

15. P. KUMAR, A. KUMAR: Possible Role of Sertraline against 3-nitropropionic Acid Induced Behavioral, Oxidative Stress and Mitochondrial Dysfunctions in Rat Brain. Prog Neuropsychopharmacol Biol Psychiatry, **33**, 100 (2009).

16. American Psychiatric Association: Diagnostic and Statistical Manual of Mental Disorders. 4th ed. American Psychiatric Press, Washington, DC, 1994.

17. M. HAMILTON: A Rating Scale for Depression. J Neurol Neurosurg Psychiatry, **23**, 56 (1960)

18. R. L. LEVINE, D. GARLAND, C. N. OLIVER, A. AMICI, I. CLIMENT, A. G. LENZ, B. AHN, S. SHALTIEL, E. R. STADTMAN: Determination of Carbonyl Content in Oxidatively Modified Proteins. Meth Enzymol, **186**, 464 (1990).

19. T. YOSHIOKA, K. KAWADA, T. SHIMADA, M. MORI: Lipid Peroxidation in Maternal and Cord Blood and Protective Mechanism against Activated-oxygen Toxicity in the Blood. Obstet Gynecol, **135**, 372 (1979).

20. T. BOTTIGLIERI, M. LAUNDY, R. CRELLIN, B. K. TOONE, M. W. CARNEY, E. H. REYNOLDS: Homocysteine, Folate, Methylation, and Monoamine Metabolism in Depression. J Neurol Neurosur Ps, **69**, 228 (2000).

21. J. A. PASCO, C. G. NICHOLSON, N. G. FELICITY, J. M. HENRY, L. J. WILLIAMS, A. MARK, M. A. KOTOWICZ, J. M. HODGE, S. DODD, F. KAPCZINSKI, S. CLARISSA, C. S. GAMA, M. BERK: Oxidative Stress May Be a Common Mechanism Linking Major Depression and Osteoporosis. Acta Neuropsychiatr, **20**, 112 (2008)

22. A. C. GASPAROVIC, M. JAGANJAC, B. MIHALJEVIC, S. B. SUNJIC, N. ZARKOVIC: Assays for the Measurement of Lipid Peroxidation. Methods Mol Biol, **965**, 283 (2013).

23. S. D. KHANZODE, G. N. DAKHALE, S. S. KHANZODE, A. SAOJI, R. PALASODKAR: Oxidative Damage and Major Depression: The Potential Antioxidant Action of Selective Serotonin Reuptake Inhibitors. Redox Rep, **8**, 365 (2003).

24. M. E. OZCAN, M. GULEC, E. OZEROL, R. POLAT, O. AKYOL: Antioxidant Enzyme Activities and Oxidative Stress in Affective Disorders. Int Clin Psychopharmacol, **19**, 89 (2004).

25. R. J. R. FRAGUAS, G. I. PAPAKOSTAS, D. MISCHOULON, T. BOTTIGLIERI, J. ALPERT, M. FAVA: Anger Attacks in Major Depressive Disorder and Serum Levels of Homocysteine. Biol Psychiatry, **60**, 270 (2006).
26. O. P. ALMEIDA, K. McCAUL, G. J. HANKEY, P. NORMAN, K. JAMROZIK, L. FLICKER: Homocysteine and Depression in Later Life. Arch Gen Psychiatry, **65**, 1286 (2005).
27. J. M. KIM, R. STEWART, S. W. KIM, S. J. YANG, I. S. SHIN, J. S. YOON: Predictive Value of Folate, Vitamin B12 and Homocysteine Levels in Late-life Depression. Br J Psychiatry, **192**, 268 (2007)
28. M. FAVA, J. S. BORUS, J. E. ALPERT, A. A. NIERENBERG, J. F. ROSENBAUM, T. BOTTIGLIERI: Folate, Vitamin B12, and Homocysteine in Major Depressive Disorder. Am J Psychiatry, **154**, 426 (1997)
29. G. I. PAPAKOSTAS, T. PETERSEN, B. D. LEBOWITZ, D. MISCHOULON, J. L. RYAN, A. A. NIERENBERG, T. BOTTIGLIERI, J. E. ALPERT, J. F. ROSENBAUM, M. FAVA: The Relationship between Serum Folate, Vitamin B12, and Homocysteine Levels in Major Depressive Disorder and the Timing of Improvement with Fluoxetine. Int J Neuropsychopharmacol, **8**, 523 (2005).
30. H. HERKEN, A. GUREL, B. SELEK: Adenosine Deaminase, Nitric Oxide, Superoxide Dismutase, and Xanthine Oxidase in Patients with Major Depression: Impact of Antidepressant Treatment. Arch Med Res, **38**, 247 (2007).

REDOX REACTIONS OF SODIUM TETRAHYDROBORATE AND TRANSITION METAL IONS. I. FORMATION OF NICKEL(0)

M. DASGUPTA, M. K. MAHANTI*

Department of Chemistry, North-Eastern Hill University, 793 022 Shillong, India
E-mail: *mkmahanti@gmail.com*

ABSTRACT

The reaction between nickel(II) chloride and sodium tetrahydroborate in buffered aqueous solution has been investigated. At pH = 8.0, the product was nickel boride (Ni_2B), while at pH = 12.0, the products were nickel boride (Ni_2B) and metallic nickel (Ni(0)). A plausible mechanism has been suggested.

Keywords: sodium tetrahydroborate, nickel(II), nickel(0).

AIMS AND BACKGROUND

The reactions of hydroborate ion with transition metal compounds usually resulted either in the reduction of metal to a lower oxidation state and possibly the formation of a hydride compound, or the formation of a diborane derivative[1,2]. Solutions of sodium tetrahydroborate ($NaBH_4$) in water or methanol were found to be effective for the conversion of aldehydes and ketones into the corresponding alcohols[3]. The reaction between ketones and sodium tetrahydroborate in isopropanol solvent has also been reported[4]. There have been earlier reports on the reaction of $NaBH_4$ with cobalt ions[5], and iron(II) and iron(III) ions[6], resulting in the corresponding metal ions. The present investigation highlights the reaction of nickel(II) ions with $NaBH_4$, in buffered aqueous medium. It has been observed that the pH of the medium is important in determining the final product(s), showing that subtle changes in reaction conditions could have unusual outcomes. Thus, a novel method for the preparation of metallic nickel (Ni(0)) is reported.

EXPERIMENTAL

Materials. Sodium tetrahydroborate ($NaBH_4$, Loba Chemical Co.) was kept under vacuum. The purity of $NaBH_4$ was checked by infrared analysis (FT-IR spectrophoto-

---

* For correspondence.

meter). Two sharp peaks were obtained at 2290 and 1120 cm^{-1}, both being character-istic for NaBH$_4$. These peaks have been assigned[7] as follows:

(i) 2290 cm^{-1}: (B–H)$_{assym}$ stretching; (ii) 1120 cm^{-1} : BH$_2$ deformation.

The (B–H)$_{assym}$ stretching mode was further split (2380 and 2290 cm^{-1}). It was suggested that the splitting was a consequence of the inability of the tetrahedral anion to rotate freely in the crystal lattice[8]. Nickel(II) chloride, ammonium hydroxide and ammonium perchlorate were E. Merck samples.

Product analysis. (a) *At pH = 8.0*. Nickel(II) chloride (1.0 mol dm^{-3}, taken in 50 ml of 0.5 mol dm^{-3} NH$_4$OH) was mixed with NaBH$_4$ (1.0 mol dm^{-3}, taken in 5.0 mol dm^{-3} NH$_4$OH), and the reaction mixture allowed to stand at 30°C for 48 h, under nitrogen. Black coloured particles were precipitated. The mixture was filtered. The precipitate was taken in 50 ml water, boiled for 1 h to dissolve any free boric acid or borate. The precipitate was filtered and washed with hot water until the washings were free from adhering boric acid or borate. The precipitate was dried. The filtrate was analysed for the presence of borate, described in (c). A known weight of the precipitate (0.5123 g) was taken in 100 ml water, and 5 ml of concentrated H$_2$SO$_4$ were added. On heating, the precipitate dissolved, and the solution turned light-green in colour. Water (100 ml) was added, the solution heated to 70°C, and the nickel present was precipitated as the nickel dimethylglyoxime [Ni(DMG)] complex. The precipitate was washed, dried and weighed. The Ni(DMG) precipitate was found to contain 0.4600 g of nickel, corresponding to 89.79% of nickel in the product (Ni$_2$B). This value compared fa-vourably, within the limits of experimental error, with the theoretical percentage of nickel present in Ni$_2$B (91.57%); (b) *At pH = 12.0*. The precipitation was carried out as in (a) above, except that the pH was maintained at 12.0. Apart from the expected Ni$_2$B (94.65% Ni, gravimetric estimation), shining silver-white flakes, supposedly metallic nickel, were distinctly visible. The shining white particles were found to form a mirror on the walls of the reaction vessel. An electron micrograph of the final product (magnification 50 times, taken at 20°C, Jeol SM-350F), showed the presence of metallic crystals against a background of amorphous nickel boride.

Analysis of the metallic mirror. The metallic mirror was washed with cold water, and the adhering particles removed. The mirror was washed with ethanol and dried. The mirror particles were scratched and collected. The mirror particles (0.2142 g) were precipitated as the Ni(DMG) complex, as described in (a) above, and found to contain 0.2104 g of nickel, which corresponded to 98.2% of nickel (as against 100% of pure nickel).
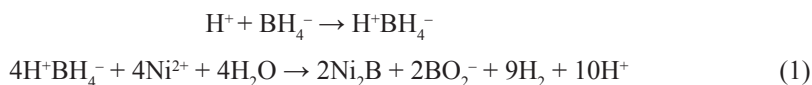
Oxidation state of nickel in the mirror particles. The nickel in the mirror form (Ni(0)) was oxidised to Ni^{2+} using an excess of ferric ammonium sulphate (FAS) solution, and the unreacted FAS estimated iodometrically. The quantity of Fe^{3+} solution consumed due to the oxidation of Ni^0 was thus determined, and compared with the standard value, so as to establish the oxidation state of nickel.

The mirror particles (0.0221 g) were treated with 15 ml of 0.1 mol dm^{-3} of FAS solution and 5 ml of concentrated H_2SO_4 solution, and allowed to stand until complete dissolution. Sodium carbonate solution (0.1 mol dm^{-3}, 5 ml) was added, and the quantity of Fe^{3+} consumed for the oxidation of Ni(0) was estimated, iodometrically, and found to be 0.0419 g (theoretical value, 0.0421 g). This confirmed that the oxidation state of nickel was zero (Ni(0)).

(c) *Analysis of the filtrate obtained in* (a) *and* (b). The filtrate was slowly evaporated in a porcelain dish. It was then digested with concentrated HCl, and evaporated to dryness to obtain the residue, which was recrystallised from hot water. A small portion of the recrystallised product (0.2 g) was taken in a porcelain dish, and mixed with concentrated H_2SO_4 (2 ml) to make a paste. Methanol (3 ml) was added, the solution heated and the vapours ignited. A green-edged flame confirmed the presence of borate. The IR spectrum of the product obtained was identical with that of boric acid.

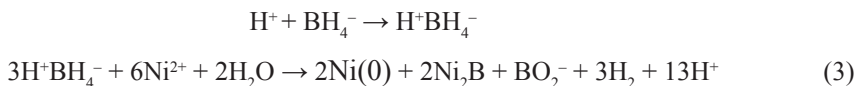*Mechanism.* The mechanistic pathway could be represented as follows:
   (a) *At pH = 8.0*

$$H^+ + BH_4^- \rightarrow H^+BH_4^-$$

$$4H^+BH_4^- + 4Ni^{2+} + 4H_2O \rightarrow 2Ni_2B + 2BO_2^- + 9H_2 + 10H^+ \tag{1}$$

The overall stoichiometric reaction is:

$$4BH_4^- + 4Ni^{2+} + 4H_2O \rightarrow 2Ni_2B + 2BO_2^- + 9H_2 + 6H^+. \tag{2}$$

   (b) *At pH = 12.0*

$$H^+ + BH_4^- \rightarrow H^+BH_4^-$$

$$3H^+BH_4^- + 6Ni^{2+} + 2H_2O \rightarrow 2Ni(0) + 2Ni_2B + BO_2^- + 3H_2 + 13H^+ \tag{3}$$

The overall stoichiometric reaction is:

$$3BH_4^- + 6Ni^{2+} + 2H_2O \rightarrow 2Ni(0) + 2Ni_2B + BO_2^- + 3H_2 + 10H^+. \tag{4}$$

There have been earlier reports regarding the existence of an intermediate boron compound, BH_3OH^-, formed during the reaction of ketones with $NaBH_4$ (Refs 9 and 10). In an earlier communication, we had established that the boron intermediate, BH_3OH^-, was indeed formed during the reaction between sodium tetrahydroborate and sodium bismuthate, and we had provided chemical and spectral evidence for its formation[11]. If such an intermediate does get formed, then there is a possibility of further hydrolysis to yield species such as $BH(OH)_2^-$, BH_2OH, $BH(OH)_2$ and H_3BO_3. Hence, $NaBH_4$ would ultimately get converted to borate, via the formation of such intermediate boron compounds.

CONCLUSIONS

Nickel (II) reacts with sodium tetrahydroborate, in buffered aqueous solution, giving nickel boride (Ni_2B) at pH = 8.0, while at pH = 12.0, the products were nickel boride (Ni_2B) and metallic nickel (Ni^0). This novel redox reaction highlights the importance of pH in determining the reaction products.

REFERENCES

1. A. P. GINSBERG: Diborane Derivatives of Transition Metal Ions. Adv Transition Metal Chem, **1**, 111 (1965).
2. M. L. H. GREEN, D. J. JONES: Hydride Complexes of the Transition Metals. Adv Inorg Chem Radiochem, **7**, 215 (1965).
3. S. W. CHAIKIN, W. G. BROWN: Reduction of Aldehydes, Ketones and Acid Chlorides by Sodium Borohydride. J Am Chem Soc, **71**, 122 (1955).
4. H. C. BROWN, E. J. MEAD, B. C. SUBBA RAO: A Study of Solvents for Sodium Borohydride and the Effect of Solvent and the Metal Ion on Borohydride Reductions. J Am Chem Soc, **77**, 6209 (1955).
5. G. N. GLAVEE, K. J. KLABUNDE, C. M. SORENSEN, G. C. HADJIPANAYIS: Sodium Borohydride Reduction of Cobalt Ions in Nonaqueous Media. Formation of Ultrafine Particles (Nanoscale) of Cobalt Metal. Inorg Chem, **32**, 474 (1993).
6. G. N. GLAVEE, K. J. KLABUNDE, C. M. SORENSEN, G. C. HADJIPANAYIS: Chemistry of Sodium Borohydride Reduction of Iron (II) and Iron (III) Ions in Aqueous and Non-aqueous Media. Formation of Nanoscale Fe, FeB, and Fe_2B Powders. Inorg Chem, **34**, 28 (1995).
7. W. C. PRICE, H. C. LONGUETT-HIGGINS, B. RICE, T. F. YOUNG: The Vibrational Spectra of Some Metal Borohydrides. J Chem Phys, **17**, 217 (1949).
8. T. C. WADDINGTON: Infrared Spectra of Metal Tetrahydroborates. J Chem Soc, 4783 (1958).
9. J. GOUBEAU, H. KALFASS: Die Reaktion Natriumborhydrid und Wasser. Z Anorg Allgem Chem, **299**, 160 (1959).
10. J. A. GARDINER, J. W. COLLATT: Kinetics of the Stepwise Hydrolysis of Tetrahydroborate Ion. J Am Chem Soc, **87**, 1692 (1965).
11. S. DASGUPTA, M. K. MAHANTI : Evidence for the Boron Intermediate BH_3OH^-, in the Oxidation of Sodium Tetrahydroborate by Sodium Bismuthate. Oxid Commun, **29**, 618 (2006).

REDOX REACTIONS OF SODIUM TETRAHYDROBORATE AND TRANSITION METAL IONS. III. FORMATION OF SILVER METAL

M. DASGUPTA, M. K. MAHANTI*

Department of Chemistry, North-Eastern Hill University, 793 022 Shillong, India
E-mail: *mkmahanti@gmail.com*

ABSTRACT

The reaction between silver(II) and sodium tetrahydroborate in aqueous acidic solution has been investigated. The final product obtained was metallic silver, Ag (0), characterised by chemical methods.

Keywords: sodium tetrahydroborate, silver(II), silver(0).

AIMS AND BACKGROUND

Diverse organic[1] and inorganic[2] substrates have been oxidised by silver(II). The Ag(II)/Ag(I) couple has a high reduction potential (+2.00 V) in 1.0 mol dm^{-3} perchloric acid[3]. The oxidation of Fe^{2+}, Mn^{2+}, Co^{2+}, Ce^{3+}, and V^{4+} by Ag(II) revealed a wide range of reduction potentials and self-exchange rates[4,5]. The oxidation of HgI by Ce^{4+} ions as well as the oxidations of Ce(III), Cr(III), V(IV), hydrazine[6] and oxalate[7] by peroxydisulphate were all catalysed by Ag(I) ions.

The reactions of the tetrahydroborate ion with transition metal compounds usually resulted either in the reduction of metal to a lower oxidation state, or the formation of a tetrahydroborate or a diborane derivative[8,9]. Sodium tetrahydroborate in water or methanol solution has been used for the conversion of aldehydes and ketones to the corresponding alcohols[10,11]. There have been earlier reports on the reactions of sodium tetrahydroborate with cobalt ions[12], and iron(II) and iron(III) ions[13], resulting in the formation of the corresponding metal ions. We report here a novel reaction of silver(II) ions with sodium tetrahydroborate, in aqueous acidic medium, resulting in the formation of silver metal, Ag(0).

EXPERIMENTAL

Materials. Sodium tetrahydroborate ($NaBH_4$, Loba Chemical Co.) was kept under vacuum. The purity of $NaBH_4$ was checked by infrared analysis (FT-IR spectrophoto-

---

* For correspondence.

meter). Two sharp peaks were obtained at 2290 and 1120 cm^{-1}, both being characteristic for NaBH$_4$, and were assigned[14] as follows:

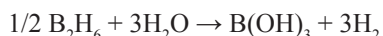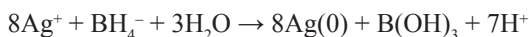(i) 2290 cm^{-1}: (B–H)$_{asym}$ stretching; (ii) 1120 cm^{-1}: BH$_2$ deformation.

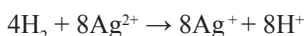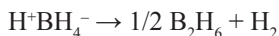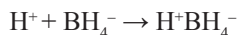The (B–H)$_{assym}$ stretching mode was further split (2380 and 2290 cm^{-1}). It was suggested that the splitting was a consequence of the inability of the tetrahedral anion to rotate freely in the crystal lattice[15]. Tetrakis(pyridine)silver(II) peroxodisulphate, [Ag(py)$_4$]S$_2$O$_8$, was prepared by the standard procedure[16], and was used as the source of Ag (II). Perchloric acid (E. Merck) was used.

Product analysis. (a) A solution of NaBH$_4$ (2×10^{-3} mol dm^{-3}) in 100 ml of water was mixed with a solution containing the Ag(II) complex (2×10^{-3} mol dm^{-3}), taken in 0.5 mol dm^{-3} HClO$_4$, and the mixture allowed to stand at 30ºC for 24 h, under nitrogen. Greyish coloured particles were precipitated along with a thin layer of shining silver mirror formed on the walls of the reaction vessel. The mixture was filtered. The precipitate was washed with 50 ml water, boiled for 1 h to dissolve any free boric acid or borate. The precipitate was filtered and washed with hot water until the washings were free from adhering boric acid or borate. The precipitate was dried. The filtrate was analysed for the presence of borate, described below; (b) A known weight of the precipitate (0.5187 g) was taken, converted to AgCl by the standard method[17], and gravimetrically estimated as AgCl. The weight of AgCl was 0.6682 g, corresponding to 0.5029 g of silver. This value compared favourably, within the limits of experimental error, with the theoretical percentage of silver present in the final product (theoretically, 100%; experimentally obtained by this method, 96.9%. This confirmed that the silver was present in the final product as Ag(0).
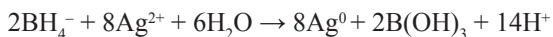
Analysis of the filtrate. The filtrate was slowly evaporated in a porcelain dish near to dryness. It was then digested with concentrated HCl, and again evaporated to dryness to obtain the residue, which was recrystallised from hot water. The recrystallised product (0.2 g) was taken in a porcelain dish, and mixed with concentrated H$_2$SO$_4$ (2 ml) to make a paste. Methanol (3 ml) was added, the solution heated and the vapours ignited. A green-edged flame confirmed the presence of borate, confirmed by IR analysis.

Mechanism. Molecular hydrogen reacted homogeneously with metal ions in solution, converting them to a lower oxidation state[18–20]. Acidic solutions of Ag^{2+} ions were converted to metallic silver by a variety of reagents[21–23]. Aqueous solutions of AgClO$_4$ were reduced by hydrogen to the metal, via a homolytic cleavage of hydrogen[24].

In the present investigation, the reaction sequence was represented as:

$$H^+ + BH_4^- \rightarrow H^+BH_4^-$$

$$H^+BH_4^- \rightarrow 1/2\ B_2H_6 + H_2$$

$$4H_2 + 8Ag^{2+} \rightarrow 8Ag^+ + 8H^+$$

$$8Ag^+ + BH_4^- + 3H_2O \rightarrow 8Ag(0) + B(OH)_3 + 7H^+$$

$$1/2\ B_2H_6 + 3H_2O \rightarrow B(OH)_3 + 3H_2$$

The overall stoichiometric reaction was as follows:

$$2BH_4^- + 8Ag^{2+} + 6H_2O \rightarrow 8Ag^0 + 2B(OH)_3 + 14H^+$$

CONCLUSIONS

Silver(II) reacts with sodium tetrahydroborate, in acidic medium, to give silver(0), which has been characterised.

ACKNOWLEDGEMENT

REFERENCES

1. C. BAIOCCHI, G. BOVIO, E. MENTASTI: Kinetics and Mechanisms of Oxidation of Organic Compounds by Silver (II) Species. Part VI. Iminodiacetic Acid and N-methyliminodiacetic Acid. Int Chem Kinet, **14**, 1017 (1982).
2. A. K. INDRAYAN, S. K. MISHRA, Y. K. GUPTA: Kinetics and Mechanism of Oxidation of Hypophosphorus Acid with Silver (II) in Aqueous Perchloric Acid Solution. Inorg Chem, **20**, 450 (1981).
3. G. BIEDERMANN, F. MAGGIO, V. ROMANO, R. ZINGALES: On the Formal Potential of the Ag^{2+}/Ag^+ Couple in 6.5 M $HClO_4$ Medium at 5°C. Acta Chem Scand A, **35**, 287 (1981).
4. P. ARSELLI, C. BAIOCCHI, E. MENTASTI, J. S. COE: Kinetics of Silver (II) Oxidation of Metal Cations. J Chem Soc Dalton T, 475 (1984).
5. W. C. E. HIGGINSON, D. R. ROSSEINSKY, B. STEAD, A. G. SYKES: Kinetics of Some Oxidation-reduction Reactions between Metal Cations in Aqueous Solution. Disc Faraday Soc, **29**, 49 (1960).
6. W. H. CONE: The Reduction of Peroxydisulfate by Cerous Ion, Catalyzed by Silver Nitrate. J Am Chem Soc, **67**, 78 (1945).
7. J. M. ANDERSON, J. K. KOCHI: Silver (I) Catalyzed Oxidative Decarboxylation of Acids by Peroxydisulfate. Role of Silver (II). J Am Chem Soc, **92**, 1951 (1970).
8. A. P. GINSBERG: Diborane Derivatives of Transition Metal Ions. Adv Transit Metal Chem, **1**, 111 (1965).
9. M. L. H. GREEN, D. J. JONES: Hydride Complexes of the Transition Metals. Adv Inorg Chem Radiochem, **7**, 215 (1965).
10. S. W. CHAIKIN, W. G. BROWN: Reduction of Aldehydes, Ketones and Acid Chlorides by Sodium Borohydride. J Am Chem Soc, **71**, 122 (1955).
11. H. C. BROWN, E. J. MEAD, B. C. SUBBA RAO: A Study of Solvents for Sodium Borohydride and the Effect of Solvent and the Metal Ion on Borohydride Reductions. J Am Chem Soc, **77**, 6209 (1955).
12. G. N. GLAVEE, K. J. KLABUNDE, C. M. SORENSEN, G. C. HADJIPANAYIS: Sodium Borohydride Reduction of Cobalt Ions in Nonaqueous Media. Formation of Ultrafine Particles (Nanoscale) of Cobalt Metal. Inorg Chem, **32**, 474 (1993).
13. G. N. GLAVEE, K. J. KLABUNDE, C. M. SORENSEN, G. C. HADJIPANAYIS: Chemistry of Sodium Borohydride Reduction of Iron(II) and Iron(III) Ions in Aqueous and Nonaqueous Media. Formation of Nanoscale Fe, FeB, and Fe_2B Powders. Inorg Chem, **34**, 28 (1995).

14. W. C. PRICE, H. C. LONGUETT-HIGGINS, B. RICE, T. F. YOUNG: The Vibrational Spectra of Some Metal Borohydrides. J Chem Phys, **17**, 217 (1949).
15. T. C. WADDINGTON: Infrared Spectra of Metal Tetrahydroborates. J Chem Soc, 4783 (1958).
16. G. PASS, H. SUTCLIFFE: Practical Inorganic Chemistry. Chapman and Hall, London, 1974, p. 79.
17. A. I. VOGEL: A Textbook of Quantitative Analysis. ELBS, 1985, p. 479.
18. E. PETERS, J. HALPERN: Homogeneous Catalytic Activation of Molecular Hydrogen by Cupric Perchlorate. J Phys Chem, **59**, 793 (1955).
19. J. HALPERN, E. R. MacGREGOR, E. PETERS: The Nature of the Activated Intermediate in the Homogeneous Catalytic Activation of Hydrogen by Cupric Salts. J Phys Chem, **60**, 1455 (1956).
20. G. J. KORINEK, J. HALPERN: Kinetics of the Reaction of Molecular Hydrogen with Mercuric and Mercurous Perchlorate in Aqueous Solution. J Phys Chem, **60**, 285 (1956).
21. A. H. WEBSTER, J. HALPERN: Homogeneous Catalytic Activation of Molecular Hydrogen in Aqueous Solution by Silver Salts. II. High Temperature Hydrogenation and Exchange Studies. J Phys Chem, **61**, 1239 (1957); A. H. WEBSTER, J. HALPERN: Homogeneous Catalytic Activation of Molecular Hydrogen in Aqueous Solution by Silver Salts. III. Precipitation of Metallic Silver from Solutions of Various Silver Salts. J Phys Chem, **61**, 1245 (1957).
22. R. J. KLINE, C. J. KERSHNER: The Oxidation of Uranium (IV) Acetate by Silver Acetate in Liquid Ammonia. Inorg Chem, **5**, 932 (1966).
23. J. HALPERN: Homogeneous Catalytic Hydrogenation: A Retrospective Account. J Organomet Chem, **200**, 133 (1980) and references therein.
24. A. H. WEBSTER, J. HALPERN: Homogeneous Catalytic Activation of Molecular Hydrogen in Aqueous Solution by Silver Salts. J Phys Chem, **60**, 280 (1956).

A NEW SYSTEM FOR THE DETERMINATION OF SELENIUM USING SPECTROPHOTOMETRY

B. NARAYANA*, K.VEENA

Department of Post-graduate Studies and Research in Chemistry, Mangalore University, 574 199 Mangalagangotri, India
E-mail: nbadiadka@yahoo.co.uk

ABSTRACT

A simple, rapid, selective and sensitive method is described for the spectrophotometric determination of selenium. The method is based on the oxidation of 4-hydrazinyl-8-(trifluoromethyl) quinoline (HTQ) and coupling reaction. Selenium oxidises 4-hydrazinyl-8-(trifluoromethyl) quinoline to its diazonium salt. The diazonium salt is then coupled with 4-chloro-2-nitrophenol (CNP) or chloroacetyl catechol (CAC) or resorcinol (RES) to form corresponding azo dye. The Beer law is obeyed in the concentration range of 5.00–13.00 μg ml^{-1} of selenium for HTQ–CNP system, 1.00–7.00 μg ml^{-1} of selenium for HTQ–CAC system and 0.60–2.00 μg ml^{-1} of selenium for HTQ–RES system. Molar absorptivity and the Sandell sensitivity for each system were calculated. The method has been applied to the determination of selenium in water samples, soil samples and plant material.

Keywords: 4-hydrazinyl-8-(trifluoromethyl) quinoline, 4-chloro-2-nitrophenol, chloroacetyl catechol, resorcinol, spectrophotometry.

AIMS AND BACKGROUND

The determination of selenium is of considerable interest because of its contrasting biological effects. Selenium is a toxic element as well as a trace element present in animals and humans. High concentration of selenium causes pulmonary edema, abdominal pain, jaundice, chronic gastrointestinal diseases, hair loss and fatigue in humans[1] and its deficiency causes Keshan and Kaschin Beck diseases in humans, which are frequently reported in China[2]. It also plays a major role in the life cycle of plants, which absorb organoselenium compounds accumulated in the soils of semiarid areas and may poison livestock that graze on them. Selenium enters into natural water through seepage from seleniferrous soil and industrial waste. Water drained from such

---

* For correspondence.

a soil may cause severe environmental pollution and wide life toxicity. Selenium is also reported to be present in cigarette paper, tobacco[3] and various cosmetic samples[4]. It is an essential nutrient at trace level but toxic in excess[5]. Selenium has both beneficial and harmful effects. Low doses of selenium are needed to maintain good health. However, exposure to high levels can cause adverse health effects.

The toxicity, availability and environmental mobility of selenium are very much dependent on its chemical forms[6]. Selenium can occur in different oxidation states in organic and inorganic forms. In many environmental, matrices, e.g. natural water, soils, etc. the predominent oxidation states of selenium are Se(IV) and Se(VI). Precise knowledge of the amounts of selenium and its compounds present in a system is, therefore, required for accurate assessment of the environmental and biological impact of selenium. This has resulted in an increasing need for analytical methods suitable for their determination at trace levels. Selenium is incorporated into proteins to make selenoproteins, which are important antioxidant enzymes. The antioxidant properties of selenoproteins help to prevent cellular damage from free radicals. Free radicals are natural by-products of oxygen metabolism that may contribute to the development of chronic diseases such as cancer and heart disease[7,8]. Other selenoproteins help to regulate thyroid function and play a role in the immune system[9–11]. Because of its significance, several analytical methods have been reported for the determination of selenium. These methods include X-ray fluorescence[12], chromatography[13], hydride generation inductively coupled plasma atomic emission spectrometry[14], catalytic kinetic method[15] and spectrophotometry[16–22]. Spectrophotometric determination of selenium using potassium iodide and starch, ethyl acetoacetate and azure B as reagents was reported by our group[20–22].

The present work reports a simple, rapid, selective and sensitive spectrophotometric method for the determination of selenium. The method is based on the oxidation of 4-hydrazinyl-8-(trifluoromethyl)quinoline and coupling reaction. The developed method has been successfully applied to the determination of the selenium in water samples, soil samples and plant material.

EXPERIMENTAL

Apparatus. All absorbance values were measured using a Shimadzu UV-2550 UV-vis. spectrophotometer with 1-cm matching cells.

Reagents. All chemicals used were of analytical reagent grade, and doubly distilled water was used in the preparation of all solutions in the experiments. Standard selenium(IV) stock solution (1000 µg ml^{-1}) was prepared and the stock solution was diluted as needed. 4-hydrazinyl-8-(trifluoromethyl)quinoline (1%), chloroacetyl catechol (1%), 4-chloro-2-nitrophenol (1%), resorcinol (1%), HCl (2M), NaOH (2M) were also used.

Procedures. Aliquots of sample containing 5.00–13.00 µg ml^{-1} of selenium for HTQ–CNP system, 1.00–7.00 µg ml^{-1} of selenium for HTQ–CAC system and 0.60–2.00 µg ml^{-1} of selenium for HTQ–RES system, respectively, was transferred into a series of 10-ml calibrated flasks. To each of the flasks, 1 ml of 4-hydrazinyl-8-(trifluoromethyl) quinoline and 1 ml of 2M HCl solutions were added. Each mixture was allowed to stand for 5 min, followed by the addition of 1 ml of 1% 4-chloro-2-nitrophenol or chloroacetyl catechol or resorcinol and 1 ml of 2M NaOH solution, and then again allowed to stand for 5 min, with occasional shaking to complete the reaction. After dilution to 10 ml with water, the absorption spectra of the coloured dye was measured at 435 or 498 or 410 nm against the corresponding reagent blank and the calibration graphs were constructed.

Determination of selenium in soil samples. A known weight of a soil sludge sample was placed in a 50-ml beaker and extracted with concentrated HCl (10 ml). The extract was boiled for 10 min to convert any selenium(VI) to selenium(IV), cooled, diluted to 25 ml with distilled water and suitable aliquots of the sample solution were analysed. All the tested samples gave negative results. To these samples a known amount of the selenium was added and analysed for selenium by the proposed method and compared with reference method[16].

Determination of selenium in water samples. Each filtered water samples were analysed for selenium. All the tested samples gave negative results. To these samples a known amount of the selenium was added and analysed for selenium by the proposed method and compared with reference method[16].

Determination of selenium in plant material. A sample of vegetable (5 g) was digested with HNO$_3$ (10 ml) for 20 min. After cooling, perchloric acid (0.5 ml) was added and heating was continued for another 10 min. Water (10 ml) and HCl (5 ml) were added to the cooled residue and this was then boiled for 10 min to convert selenium(VI) to selenium(IV). The solution was centrifuged and transferred in to a 50-ml calibrated flask and suitable aliquots of the sample solution were analysed. All the tested samples gave negative results. To these samples, a known amount of the selenium was added and analysed for selenium by the proposed method and also with the reference method[16].

Determination of selenium in water samples, soil samples and plant material are given in Tables 1–3.

Table 1. Determination of selenium in water samples, soil samples and plant material (HTQ–CNP system)

Sample	Se(IV) added ($\mu g\ ml^{-1}$)	Reference method		Proposed method		t-test[b]	F-test[c]
		Se(IV) found ($\mu g\ ml^{-1} \pm$ SD)[a]	recovery (%)	Se(IV) found ($\mu g\ ml^{-1} \pm$ SD)[a]	recovery (%)		
Water	6.00	6.01 ± 0.02	100.16	6.01 ± 0.05	100.16	0.447	6.25
sample	8.00	7.98 ± 0.02	99.75	7.98 ± 0.03	99.75	1.491	2.25
Soil	6.00	6.04 ± 0.05	100.67	5.97 ± 0.03	99.50	2.236	2.78
sample	8.00	8.01 ± 0.02	100.12	7.95 ± 0.04	99.37	2.795	4.00
Plant mate-	6.00	5.98 ± 0.03	99.67	6.02 ± 0.03	100.30	1.490	1.00
rial	8.00	7.98 ± 0.03	99.75	7.99 ± 0.03	99.87	0.745	1.00

[a] Mean ± standard deviation (n=5); [b] tabulated t-value for 5 degrees of freedom at 95% probability level is 2.31; [c] tabulated F-value for (4,4) degrees of freedom at 95% probability level is 6.39.

Table 2. Determination of selenium in water samples, soil samples and plant material (HTQ–CAS system)

Sample	Se(IV) added ($\mu g\ ml^{-1}$)	Reference method		Proposed method		t-test[b]	F-test[c]
		Se(IV) found ($\mu g\ ml^{-1} \pm$ SD)[a]	recovery (%)	Se(IV) found ($\mu g\ ml^{-1} \pm$ SD)[a]	recovery (%)		
Water	4.00	4.01 ± 0.02	100.25	3.99 ± 0.04	99.75	0.559	4.00
sample	6.00	6.01 ± 0.02	100.16	5.96 ± 0.03	99.33	2.980	2.25
Soil	4.00	4.02 ± 0.02	100.50	4.01 ± 0.02	100.25	1.118	1.00
sample	6.00	6.04 ± 0.05	100.67	5.98 ± 0.03	99.66	1.490	2.78
Plant mate-	4.00	4.01 ± 0.02	100.25	3.98 ± 0.02	99.50	2.236	1.00
rial	6.00	5.98 ± 0.03	99.67	5.97 ± 0.04	99.50	1.677	1.78

[a] Mean ± standard deviation (n=5); [b] tabulated t-value for 5 degrees of freedom at 95% probability level is 2.31; [c] tabulated F-value for (4,4) degrees of freedom at 95% probability level is 6.39.

Table 3. Determination of selenium in water samples, soil samples and plant material (HTQ–RES system)

Sample	Se(IV) added ($\mu g\ ml^{-1}$)	Reference method		Proposed method		t-test[b]	F-test[c]
		Se(IV) found ($\mu g\ ml^{-1} \pm$ SD)[a]	recovery (%)	Se(IV) found ($\mu g\ ml^{-1} \pm$ SD)[a]	recovery (%)		
Water	1.00	1.02 ± 0.01	102.00	0.98 ± 0.02	98.00	2.236	4.00
sample	2.00	1.98 ± 0.03	99.00	1.99 ± 0.02	99.50	1.118	2.25
Soil	1.00	1.06 ± 0.02	106.00	0.97 ± 0.03	97.00	3.354	2.25
sample	2.00	1.98 ± 0.03	99.00	2.01 ± 0.03	100.50	0.745	1.00
Plant ma-	1.00	0.99 ± 0.04	99.00	0.99 ± 0.04	99.0	0.559	1.00
terial	2.00	1.98 ± 0.02	99.00	1.96 ± 0.04	98.0	2.236	4.00

[a] Mean ± standard deviation (n=5); [b] tabulated t-value for 5 degrees of freedom at 95% probability level is 2.31; [c] tabulated F-value for (4,4) degrees of freedom at 95% probability level is 6.39.

RESULTS AND DISCUSSION

Absorption spectra. The method is based on the oxidation of 4-hydrazinyl-8-(trifluoromethyl) quinoline and coupling reaction. Selenium oxidises 4-hydrazinyl-8-(trifluoromethyl)quinoline to its diazonium salt in an acid medium. The diazonium salt is then coupled with 4-chloro-2-nitrophenol or chloroacetyl catechol or resorcinol in an alkaline medium which were measured at 435, 498 and 410 nm, respectively. The reactions are described in the Scheme. Diazotisation and coupling reactions are found to be temperature dependent. Diazotisation is carried out at 0–5 °C and coupling reaction is carried out at room temperature, above 30 °C there is a decrease in the intensity of the colour. The absorption spectra of the coloured species of azo dyes are presented in Fig. 1. The reagent blanks had negligible absorption at these wavelengths. Under the optimised conditions, although the colour developed instantaneously, 5 min were allowed, in order to obtain the maximum and constant absorbance in all coloured derivatives.
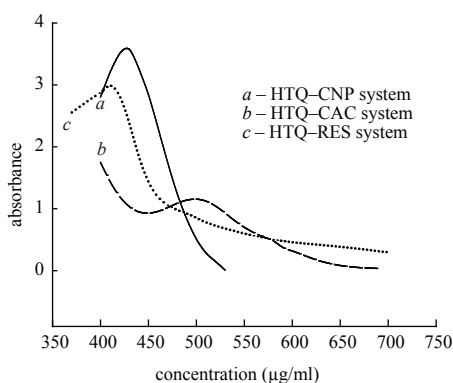

Fig. 1. Absorption spectra of HTQ–CNP, HTQ–CAS and HTQ–RES system

Oxidation of 4-hydrazinyl-8-(trifluoromethyl)quinoline by selenium(IV) is most effective in acid medium. It is found that absorbance at 435, 498 or 410 nm is maximum when concentration of HCl during the oxidation reaction is 2 M and further increase in acid concentration does not affect the absorbance. A volume of 1 ml of 1% 4-hydrazinyl-8-(trifluoromethyl)quinoline solution was required for maximum absorbance and it was found that addition of 1 ml of chloroacetyl catechol or resorcinol or 4-chloro-2-nitrophenol reagents provides maximum absorbance. The use of larger excess of reagent produced no further increase in the absorbance.

Comparison to the spectrophotometric method with earlier methods is shown in Table 4.
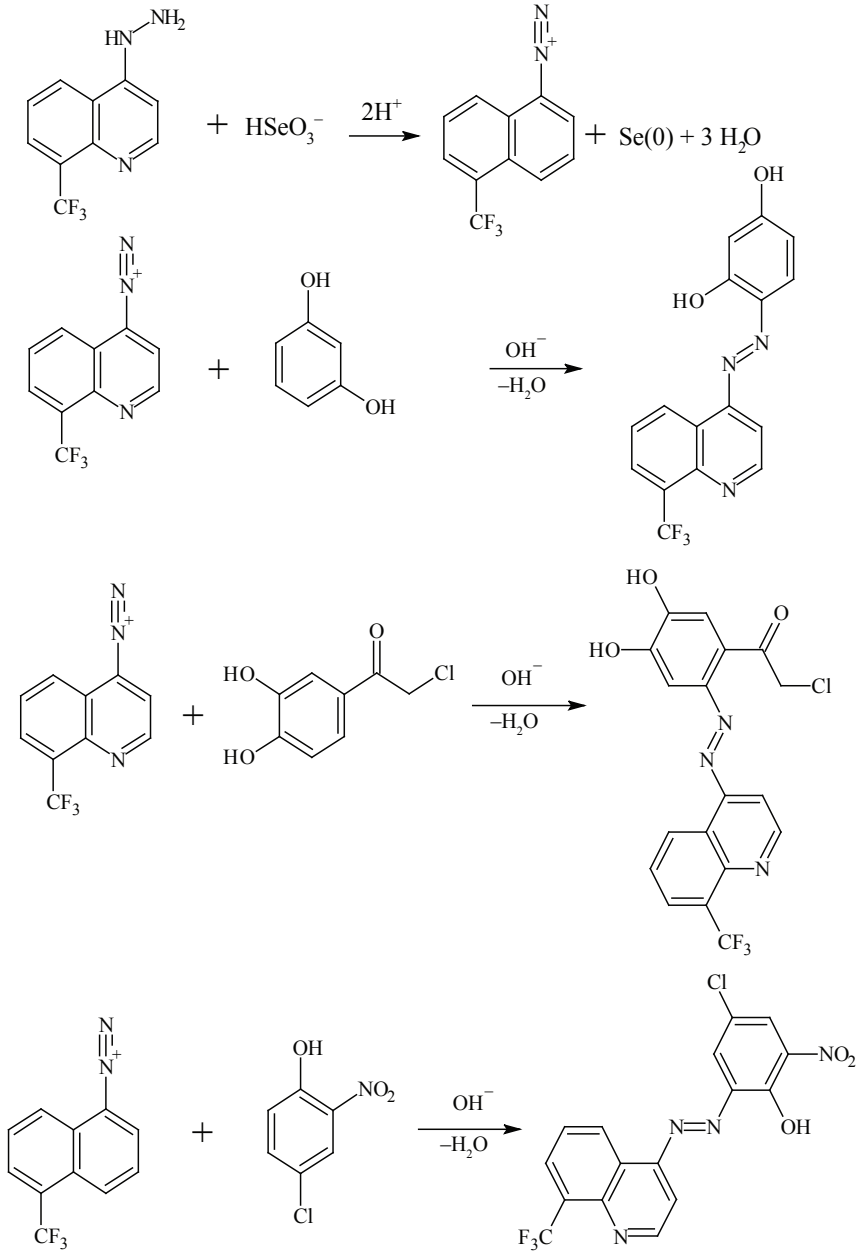
Scheme

Table 4. Comparison of the spectrophotometric method with earlier methods

Reagent	Molar absorptivity (l mol^{-1}cm^{-1})	The Beer law range (µg ml^{-1})	The Sandell sensitivity (µg cm^{-2})
Hexamethyleneimine car-bodithioate[17]	4.42×10³	0.50–4.00	0.016
(4′-Bromophenyl)-4,4,6-trimethyl-(1H,4H)-pyrimidine-2-thiol[18]	1.10×10⁴	2.00–14.00	0.068
Hydroiodic acid[19]	1.00×10⁴	5.00–120.00	0.007
Potassim iodide and starch[20]	1.40×10⁴	2.00–12.00	0.005
PHS–AA (Ref. 21)	1.02×10⁴	0.50–20.00	0.008
PHS–EAA (Ref. 21)	1.18×10⁴	1.00–24.00	0.007
Proposed method			
HTQ–CNP	1.37×10⁴	5.00–13.00	0.005
HTQ–CAC	2.80×10³	1.00–7.00	0.028
HTQ–RES	0.93×10⁴	0.60–2.00	0.008

PHS – phenyl hydrazine-*p*-sulphonic acid; AA – acetyl acetone; EAA – ethyl acetoacetate.

Analytical data. The adherence to the Beer law is studied by measuring the absorbance values of solutions varying selenium concentration. A straight line graph is obtained by plotting absorbance against concentration of selenium. The calibration graphs are described by the following equation: $Y = a + bX$ (where Y is absorbance, a – intercept, b – slope and X – concentration in µg ml^{-1}) obtained by the method of least square. All the optimisation steps were carried out with a chosen selenium concentration. The Beer law is obeyed in the concentration range of 5.00–13.00 µg ml^{-1} of selenium for HTQ–CNP system, 1.00–7.00 µg ml^{-1} of selenium for HTQ–CAC system and 0.60–2.00 µg ml^{-1} of selenium for HTQ–RES system. The molar absorptivity, the Sandell sensitivity, slope, intercept, detection limit and quantitation limit for HTQ–CNP system and HTQ–CAC system are found to be 2.76 × 10³ l mol^{-1} cm^{-1}, 0.028 µg cm^{-2}, 0.041, 0.052, 0.080 µg ml^{-1}, 0.244 µg ml^{-1}; 1.37 × 10⁴ l mol^{-1} cm^{-1}, 5.70 × 10^{-3} µg cm^{-2}, 0.093, 0.159, 0.035 µg ml^{-1}, 0.108 µg ml^{-1}; while that for HTQ–RES system is found to be 0.93 × 10⁴ l mol^{-1} cm^{-1}, 8.40 ×10^{-3} µg cm^{-2}, 0.115, 0.016, 0.028 µg ml^{-1}, 0.086 µg ml^{-1}, respectively. Adherence to the Beer law for the determination of selenium are given in Figs 2–4.
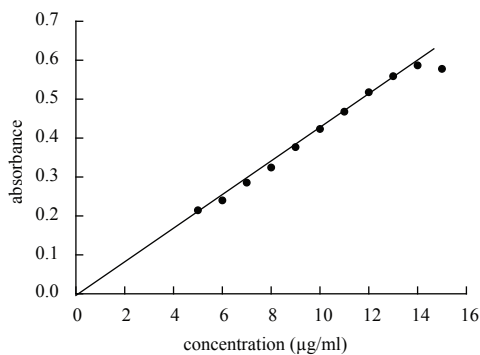
Fig. 2. Adherence to the Beer law for the determination of selenium (HTQ–CNP system)
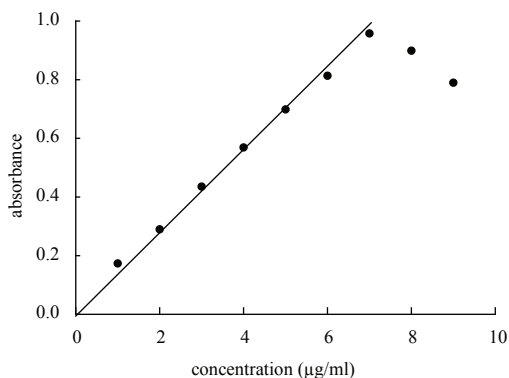
Fig. 3. Adherence to the Beer law for the determination of selenium (HTQ–CAC system)

Fig. 4. Adherence to the Beer law for the determination of selenium (HTQ–RES system)

Effect of diverse ions. The effect of various non-target species on the determination of selenium is investigated. The tolerance limits of interfering species are established at those concentrations that do not cause more than ± 2% error in absorbance values of selenium with fixed concentration. The present method is based on the oxida-

tion of 4-hydrazinyl-8-(trifluoromethyl)quinoline with selenium, then coupled with coupling reagents. Therefore, strong oxidising or reducing species are expected to interfere. The results indicated that Fe(III) showed severe interference. However, the tolerance level of this ion may be increased by the addition of NaF. The results are given in Table 5.
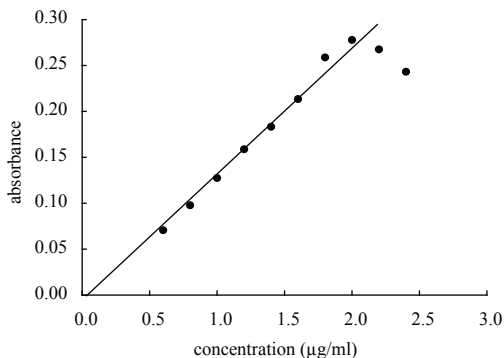
Table 5. Effect of diverse ions on the determination of selenium

Foreign ion	Tolerance limit
Using 4-chloro-2-nitro phenol as a reagent	
Citrate, oxalate, tartarate, acetate, K^+, Na^+	>2000
Mg^{2+}, Ca^{2+}, Mn^{2+}, Ni^{2+}, Ba^{2+}, Zn^{2+}, Al^{3+}	>700
Fe^{3+}*	25
Using chloroacetyl catechol as a reagent	
Citrate, oxalate, tartarate, acetate, K^+, Na^+	>1000
Mg^{2+}, Ca^{2+}, Mn^{2+}, Ni^{2+}, Ba^{2+}, Zn^{2+}, Al^{3+}	>1000
Fe^{3+}*	25
Using resorcinol as a reagent	
Citrate, oxalate, tartarate, acetate, K^+, Na^+	>1500
Mg^{2+}, Ca^{2+}, Mn^{2+}, Ni^{2+}, Ba^{2+}, Zn^{2+}, Al^{3+}	>500
Fe^{3+}*	25

*Masked by masking agents.

Applications. The reagents used in the present study, HTQ–CNP, HTQ–CAC and HTQ–RES are sensitive and selective reagents for the spectrophotometric determination of selenium. Compared to other existing methods, the developed method retains the specific interaction of selenium with HTQ–CNP, HTQ–CAC and HTQ–RES to form colour derivatives, and good sensitivity is achieved at room temperature without the need for extraction. The proposed method has significant advantages over the reported method in terms of sensitivity[17] and is also comparable with other spectrophotometric methods[18–20]. Accurate and reproducible results are obtained with permissible standard deviation. It is also found that, as shown in Tables 1, 2 and 3, there is no significant difference between the proposed method and a previously reported method[16], indicating that the proposed method is as accurate and precise as the reported method. The proposed method has been applied to the determination of selenium in water samples, soil samples and plant material. The performances of the proposed method are compared statistically in terms of the student *t*-test and the variance ratio *F*-test. At 95% confidence level, the calculated *t* and *F* values do not exceed the theoretical values for the 2 methods.

CONCLUSIONS

The developed method is comparable with the reported methods[17–20]. The developed method does not involve any stringent reaction conditions and offers the advantages of colour stability about more than 2 h. The low value of the standard deviation indicates the accuracy and precision of the method. The proposed method has been successfully applied to the determination of trace amounts of selenium in water samples, soil samples and plant material.

ACKNOWLEDGEMENT

REFERENCES

1. M. I. SMITH, K.W. FRANKE, B.B WESTFALL: The Selenium Problem in Relation to Public Health. Pub Health Rep, **51**, 1496 (1936).
2. J. TAN, Y. HUANG, J. WALTER: Selenium in Geo-ecosystem and Its Relation to Endemic Diseases in China. Air Soil Pollut, **57**, 59 (1991).
3. P. W. WEST, A. D. SHENDRIKAR: Air Sampling Methods for the Determination of Selenium. Anal Chim Acta, **89**, 403 (1977).
4. J. R. SHAPIRA: Organic Selenium Compounds. Their Chemistry and Biology. Wiley Interscience, New York, 1971, p. 703.
5. R. W. ANDREWS, D. C. JOHNSON: Determination of Se(IV) by Anodic Stripping Voltametry in Flow System with Ion-exchange Separation. Anal Chem, **47**, 294 (1975).
6. R. L. TATKEN, R. J. LEWIS: Registry of Toxic Effects of Chemical Substances. US Dept. Health and Human Services, Cincinnati, Ohio, 1983.
7. S. B. GOLDHABER: Trace Element Risk Assessment: Essentiality versus Toxicity. Regul Toxicol Pharm, **38**, 232 (2003).
8. G. F. COMBS, W. P GRAY: Chemopreventive Agents: Selenium. Pharmacol Ther, **79**, 179 (1998).
9. O. A. LEVANDER: Nutrition and Newly Emerging Viral Diseases: An Overview. J Nutr, **127**, 948S (1997).
10. J. R. ARTHUR: The Role of Selenium in Thyroid Hormone Metabolism. Can J Physiol Pharmacol, **69**, 1648 (1991).
11. B. CORVILAIN, A .O. CONTEMPRE, P. LONGOMBE, C. GOYENS, F. GERVY-DECOSTER, J. B. LAMY, VANDERPAS, J. E DUMONT: Selenium and the Thyroid: How the Relationship was Established. Am J Clin Nutr, **57**, 244S (1993).
12. V. BETHEL, V. HAMM, A. KOCHEL: The Determination of Trace Elements in Blood Serum by Total-reflection X-ray Fluorescence Analysis. Fresenus J Anal Chem, **335**, 855 (1989).
13. J. W .YOUNG, G. D. CHRISTIAN: Gas-chromatographic Determination of Selenium. Anal Chim Acta, **65**, 127 (1973).
14. R. BYE: Considerations on the Different Oxidation States of Antimony, Arsenic and Selenium in the Determination of the Elements by Hybride Generation-atomic Spectrometry. Talanta, **37**, 1029 (1990).

15. A. A. ENSAFI, M. SABERI LEMRASKI: Highly Sensitive Spectrophotometric Reaction Rate Method for the Determination of Selenium Based on the Catalytic Reduction of Sulfonazo by Sulfide. Anal Lett, **37**, 2469 (2004).
16. H. D. REVANASIDDAPPA, T. N. KIRAN KUMAR: A Facile Sensitive Method for the Spectrophotometric Determination of Selenium. Anal Sci, **17**, 1309 (2001).
17. M. N. PATHARE, A. D. SAWANT: Extractive Spectrophotometric Determination of Se(IV) Using Sodium Salt of Hexamethyleneiminecarbodithioate. Anal Lett, **28**, 317 (1995).
18. G. B. KOLEKAR, M. A. ANUSE: Extractive Spectrophotometric Determination of Selenium (IV) Using 1-(4′-bromophenyl)-4,4,6-trimethyl(1H,4H)-pyrimidine-2-thiol from Alloys and Pharmaceutical Samples. Res J Chem Environ, **2**, 9 (1998).
19. G .A. El-HAFEEZ MOSTAFA, S. El-SYED GHAZY: Indirect Spectrophotometric Determination of Small Amounts of Selenium(IV) and Arsenic(V) by Simple Extraction Using Flotation Columns. Anal Sci, 1189 (2001).
20. B. NARAYANA, M. MATHEW, N. G. BHAT, N. V. SREEKUMAR: Spectrophotometric Determination of Selenium Using Potassium iodide and Starch as Reagents. Microchim Acta, **141**, 175 (2003).
21. T. CHERIAN, B. NARAYANA: A New System for the Spectrophotometric Determination of Trace Amount of Selenium. Indian J Chem Technol, **13**, 222 (2006).
22. M. MATHEW, B. NARAYANA: An Easy Spectrophotometric Determination of Selenium Using Azure B as a Chromogenic Reagent. Indian J Chem Technol, **13**, 459 (2006).

NEW REAGENTS FOR THE SPECTROPHOTOMETRIC DETERMINATION OF CHROMIUM

B. NARAYANA*, K.VEENA

Department of P. G. Studies and Research in Chemistry, Mangalore University, 574 199 Mangalagangotri, India
E-mail: *n_badiadka@yahoo.co.uk*

ABSTRACT

A simple, rapid and sensitive method is described for the spectrophotometric determination of chromium using crystal violet (CV) and rhodamine B (RB) as reagents. The method is based on the reaction of chromium(VI) with potassium iodide in acid medium to liberate iodine. The liberated iodine bleaches the colour of rhodamine B or crystal violet and their absorbance was measured at 550 or 582 nm, respectively, against the reagent blank. Chromium(III) is also determined after it is oxidised to chromium(VI) by bromine water. The Beer law is obeyed in the concentration range of 1.00–8.00 μg ml^{-1} of chromium for chromium–rhodamine B system and 0.80–2.00 μg ml^{-1} of chromium for chromium–crystal violet system. Molar absorptivity and the Sandell sensitivity for each system were calculated. The method has been successfully applied to the determination of chromium in water samples, soil samples and dietary supplements.

Keywords: chromium, spectrophotometry, crystal violet and rhodamine B.

AIMS AND BACKGROUND

Chromium is an essential nutrient required for normal sugar and fat metabolism and works primarily by potentiating the action of insulin. It is present in the entire body but with the highest concentrations in the liver, kidneys, spleen and bone. Chromium exists in the environment as chromium(III) and chromium(VI) oxidation states. Chromium(III) is an essential nutrient for maintaining normal physiological function[1] whereas chromium(VI) is toxic[2]. Hexavalent chromium compounds are both skin and pulmonary sensitisers, producing a generalised irritation of the conjunctiva and mucous membranes, nasal perforations[3] and a contact dermatitis. The determination of micro-amounts of chromium in soils and other naturally occurring materials are

---

* For correspondence.

of considerable interest because of the contrasting biological effects of its 2 common oxidation states, chromium(III) and chromium(VI) and also the growing interest in environmental problems. It is known that an increase in the content in soils makes them infertile and toxic effects depend to some extent on the chromium oxidation state. On the other hand, the introduction of salts into soils have some positive effects due to activation of some biochemical processes[4].

Many methods have been reported for the quntitative determination of chromium. The analytical technique varies from inductively coupled plasma-atomic emission spectroscopy[5], complexometric[6], HPLC (Ref. 7) and spectrophotometry[8,9]. The determination of chromium using different reagents was reported by our group[10–14].

The present work reports a simple and sensitive method for the spectrophotometric determination of chromium. The method has been applied to the determination of chromium in water samples, soil samples and dietary supplements.

EXPERIMENTAL

Materials and methods. All absorbance values were measured using a Shimadzu UV 2550 UV-vis. spectrophotometer with 1-cm matching cells. All chemicals used were of analytical grade and distilled water was used for preparing reagent solutions. A standard chromium(VI) and chromium(III) solutions (1000 µg ml^{-1}) were prepared and the stock solutions were diluted as needed. Suitable volume of these solutions was diluted to obtain the working concentration. Potassium iodide (2%), crystal violet (0.05%) and rhodamine B (0.01%) were also used.

Procedure. Aliquots of sample solution containing 1.00–8.00 µg ml^{-1} of chromium(VI) for chromium–CV system and 0.80–2.00 µg ml^{-1} of chromium(VI) for chromium–RO system, respectively, were transferred into a series of 10-ml calibrated flasks. To this potassium iodide (1 ml) and hydrochloric acid (1 ml) were added and the mixture was gently shaken until the appearance of yellow colour indicating the liberation of iodine. Then, rhodamine B (0.5 ml) or crystal violet (0.5 ml) was added followed by the addition of 2ml of acetate buffer (pH = 4) solution. The contents were diluted to the mark with distilled water and mixed well. The absorbance of the coloured species was measured at 550 or 615 nm against the reagent blank. For the determination of Cr(III), suitable volume of an aliquot of sample solution of chromium(III) was transferred into a series of 10-ml calibrated flasks. A volume of 0.5 ml saturated bromine water and 0.5 ml of 4.5 M KOH solution were added to each flask and allowed to stand for 5 min. Then 0.5 ml of 2.5 M sulphuric acid and 0.5 ml of 5% sulphosalicylic acid were added and then above procedure for chromium(VI) was followed. The absorbance of the resulting solution was measured at 550 or 615 nm against the reagent blank.

Determination of chromium in water samples. Each filtered environmental water samples were analysed for chromium. All the tested samples gave negative results. To these samples known amounts (not more than 1.00–8.00 µg ml^{-1} of chromium for

chromium–RB system, 0.80–2.00 µg ml^{-1} of chromium for chromium–CV system) were spiked and analysed for chromium by the proposed methods and also by the reference methods[13].

Determination of chromium in soil samples. About 1 g of the soil sample (spiked with known amount of chromium samples) was weighed and placed in a 50-ml beaker and extracted with 5 ml of 1% sodium carbonate. The extract was filtered and made up to 100 ml in a standard flask. Suitable aliquot of the solution was transferred to a 10-ml calibrated flask and chromium content was determined directly according to the proposed methods and also by the reference methods[13].

Chromium determination in pharmaceutical samples. Samples of the finely ground multivitamin-multimineral tablets (Aristo Pharmaceuticals Ltd.) containing chromium(III) were treated with 5 ml of concentrated nitric acid, and the mixtures were evaporated to dryness. The residue was leached with 5 ml of 0.5 mol l^{-1} H$_2$SO$_4$. The solution was diluted to a known volume with water. Suitable aliquots of the sample solution were analysed according to the procedure for chromium(III) determinarion. The results of the determination of chromium in water samples, soil samples and dietary supplements are given in Tables 1 and 2.

Table 1. Determination of chromium in water samples, soil samples and dietary supplements (using rhodamine B as a reagent)

Samples	Chromium added (µg ml^{-1})	Standard method		Proposed method		*t*-test[b]	*F*-test[c]
		chromium found[a] (µg ml^{-1})	relative error (%)	chromium found[a] (µg ml^{-1})	relative error (%)		
Sample 1	1.00	0.99±0.02	1.00	0.98±0.02	2.00	2.24	1.00
	2.00	1.98±0.02	1.00	2.01±0.03	0.50	0.75	2.25
Soil samples	1.00	0.98±0.02	2.00	0.97±0.03	3.00	2.24	2.25
	2.00	1.97±0.04	1.50	1.97±0.06	1.50	1.12	2.25
Tablets	chromium certified in mg	chromium found in mg		chromium found in mg			
	0.20	0.199±0.04	0.50	0.199±0.03	0.50	0.07	1.78

[a] Mean ± standard deviation (*n*=5); [b] tabulated *t*-value for 5 degrees of freedom at 95% probability level is 2.31; [c] tabulated *F*-value for (4,4) degrees of freedom at 95% probability level is 6.39; Tablets – Chromoplex (Label claim, 0.2 mg per tablet) Aristo Pharmaceuticals Ltd., India.

Table 2. Determination of chromium in water samples, soil samples and dietary supplements (using crystal violet as a reagent)

Samples	Chromium added (μg ml^{-1})	Standard method		Proposed method		t-test[b]	F-test[c]
		chromium found[a] (μg ml^{-1})	relative error(%)	chromium found[a] (μg ml^{-1})	relative error (%)		
Sample1	0.80	0.806±0.006	0.75	0.796±0.006	0.50	1.49	1.00
	1.00	0 .990±0.020	1.00	0.980±0.020	2.00	2.24	1.00
Soil samples	0.80	0.796±0.006	0.50	0.803±0.004	0.38	1.68	2.25
	1.00	0.980±0.020	2.00	1.02±0.030	2.00	1.49	2.25
Tablets	chromium certified in mg	chromium found in mg		chromium found in mg			
	0.20	0.197±0.010	1.50	0.199±0.006	0.50	0.37	2.78

[a] Mean ± standard deviation (n=5); [b] tabulated t-value for 5 degrees of freedom at 95% probability level is 2.31; [c] tabulated F-value for (4,4) degrees of freedom at 95% probability level is 6.39; Tablets – Chromoplex (Label claim, 0.2 mg per tablet) Aristo Pharmaceuticals Ltd., India.

RESULTS AND DISCUSSION

Absorption spectra. The method is based on the reaction of chromium(VI) with potassium iodide in acid medium to liberate iodine. The liberated iodine bleaches the colour of rhodamine B or crystal violet. The decrease in absorbance at 550 or 615 nm is directly proportional to the chromium(VI) concentration. The absorption spectrum of the coloured species of rhodamine B or crystal violet are presented in Fig. 1*a,b* and the reaction system is presented in the Scheme.
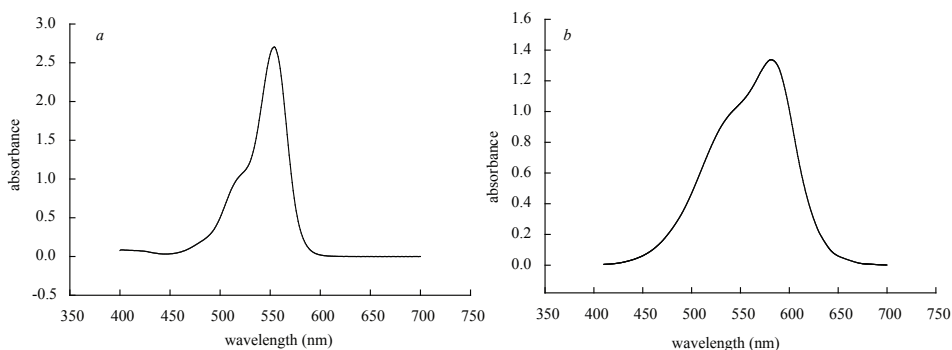

Fig. 1. Absorption spectra of coloured species of rhodamine B (*a*) and crystal violet (*b*)

Effect of iodide concentration and acidity. The liberation of iodine from KI in an acid medium is quantitative. The appearance of yellow colour indicates the liberation of

iodine. Although any excess of iodine in the solution will not interfere. It is found that 1 ml of each 2% KI and 2M HCl are sufficient for the liberation of iodine from iodide by chromium(VI) and 0.5 ml of rhodamine B or crystal violet were sufficient for the decoulorisation reaction. The bleached reaction systems were found to be stable for more than 1 h for each chromium–rhodamine B and chromium–crystal violet systems.

Effect of diverse ions. The effect of various of ions at microgram levels on the determination of chromium is examined. The tolerance limits of interfering species are established at those concentrations that does not cause more than ±2% error in absorbance values of chromium with fixed concentration. The results are shown in Table 3.

Table 3. Effect of diverse ions on the determination of chromium

Foreign ion	Tolerance limit ($\mu g\ ml^{-1}$)
Oxalate, tartrate, acetate, citrate	>2000
Ba^{2+}, Cd^{2+}, Ca^{2+}, Ni^{2+}	1000
Mg^{2+}, Mn^{2+}, Al^{3+}	1000
EDTA	>1500
Na^+, Cl^-	800

Analytical data. In this method adherence to the Beer law is studied by measuring the absorbance values of solutions varying chromium concentration. A straight line graph is obtained by plotting absorbance against concentration of chromium. The Beer law is obeyed in the concentration range of 1.00–8.00 $\mu g\ ml^{-1}$ of chromium for chromium–rhodamine B system and 0.80–2.00 $\mu g\ ml^{-1}$ of chromium for chromium–crystal violet system. Molar absorptivity, the Sandell sensitivity, slope, detection limit and quantitation limit for each system were found to be 1.62×10^4 l mol^{-1} cm^{-1}, 0.003 $\mu g\ cm^{-2}$, 0.201, 0.082 and 0.248 $\mu g\ ml^{-1}$; 4.49×10^4 l mol^{-1} cm^{-1}, 8.00×10^4 $\mu g\ cm^{-2}$, 0.834, 0.019 and 0.059 $\mu g\ ml^{-1}$, respectively. Adherences to the Beer law for the determination of above methods are shown in Fig. 2*a, b*.
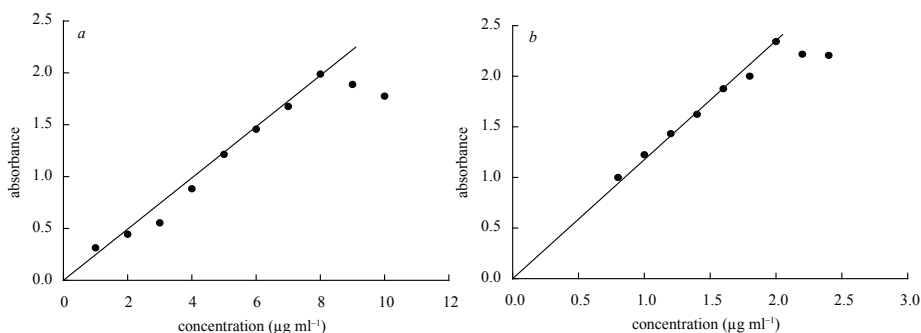
Fig. 2. Adherence to the Beer law for the determination of chromium using rhodamine B (*a*) and crystal violet (*b*) as reagents

Comparison of the proposed method with the reported method is shown in Table 4.

Table 4. Comparison of the spectrophotometric method with reported methods

Reagent (l mol^{-1} cm^{-1})	Molar absorptivity	Remarks
Variamine blue[15]	8.12×10^3	low sensitivity
Citrazinic acid[16]	2.12×10^4	less stable
Chitin[17]	3.50×10^4	required solvents for the extraction
Perphenazine[18]	1.87×10^4	colour is stable up to 30 min only
Proposed method using		
Crystal violet	6.44×10^4	colour is stable up to 2 h
Rhodamine B	1.62×10^4	less interference, facile, sensitive and non-extractive

S c h e m e

$$Cr_2O_7^{2-} + 6\,I^- + 14H^+ \longrightarrow 2Cr^{3+} + 3I_2 + 7H_2O$$

crystal violet (blue colour)   crystal violet (leuco form)

rhodamine B (coloured)   rhodamine B (colourless)
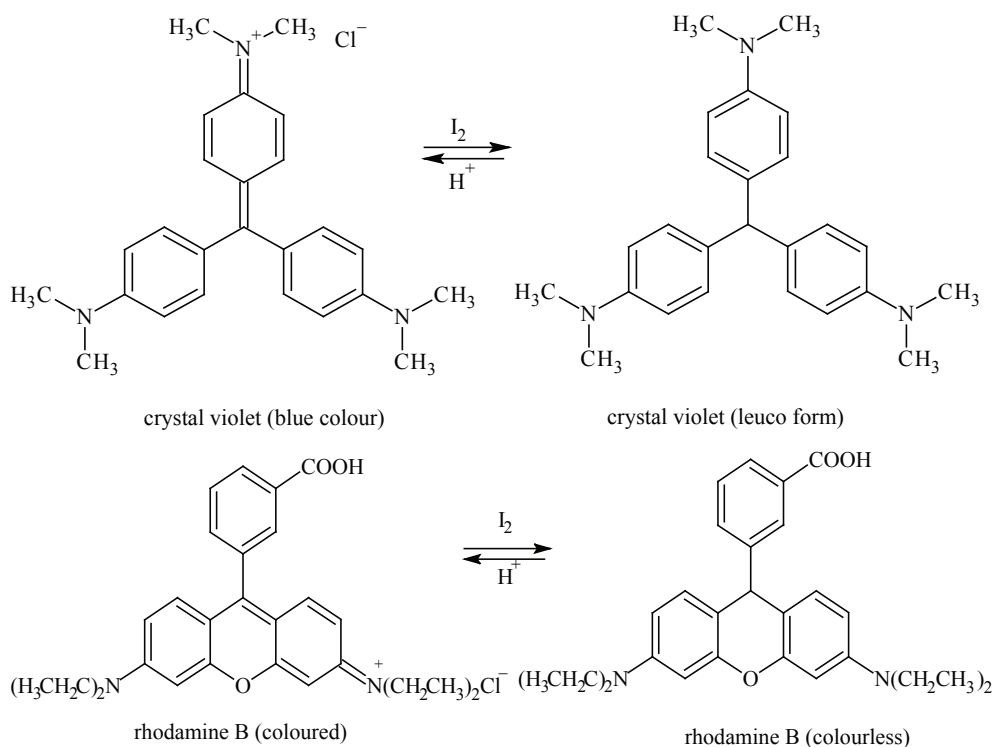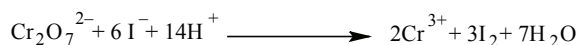
Applications. The proposed method has the advantage of simplicity, sensitivity, rapidity and will compete with most of the spectrophotometric methods available in literature. Accurate and reproducible results are obtained with permissible standard deviation. The low values of standard deviation indicated the high accuracy of the method. The precision and accuracy of the method were studied by analysing the sample solution containing known amounts of the cited reagents within the Beer law limit. The proposed method can be used for the determination of chromium in water samples, soil samples and dietary supplements.

CONCLUSIONS

The proposed method has significant advantage over the reported method[15–18]. No extraction step is required and hence, the use of organic solvents, which are generally toxic pollutants, is avoided. Determination of Cr(IV) and Cr(III) individually make the method more versatile. The results of the parallel determination with the standard method confirm the precision and accuracy of the method.

ACKNOWLEDGEMENT

REFERENCES

1. J. VERSIEK, R. CORNELIS: Normal Levels of Trace Elements in Human Blood Plasma or Serum. Anal Chim Acta, **116**, 217 (1980).
2. J. M. ECKERT, R. J. JUDD, P. A. LAY, A. D. SYMONS: Response of Chromium(V) to the Diphenylcarbazide Spectrophotometric Method for the Determination of Chromium(VI). Anal Chim Acta, **255**, 31 (1991).
3. E. LINDBERG, G. HEDENSTIERNA: Chrome Plating: Symptoms, Findings in the Upper Airways and Effects on Lung Function. Arch Environ Health, **38**, 367 (1983).
4. M. KAMBUROVA: Spectrophotometric Determination of Chromium(VI) with Methylene Blue. Talanta, **40**, 713 (1993).
5. S. HIRATA, Y. UMEZAKI, M. IKEDA: Determination of Chromium(III), Titanium, Vanadium, Iron(III) and Aluminium by Inductively Coupled Plasma Atomic Emission Spectrometry with an On-line Preconcentrating Ion-exchange Column. Anal Chem, **58**, 2602 (1986).
6. A. I. VOGEL: A Textbook of Quantitative Inorganic Analysis. 5th ed. Longmans, London, 1989, p. 448.
7. A. IMRAN, Y. A. HASSAN: Speciation of Arsenic and Chromium Metal Ions by Reversed Phase High Performance Liquid Chromatography. Chemosphere, **48**, 275 (2002).
8. S. BALASUBRAMANIAN, V. PUGALENTHI: Determination of Total Chromium in Tannery Waste Water by Inductively Coupled Plasma-atomic Emission Spectrometry, Flame Atomic Absorption Spectrometry and UV-vis. Spectrophotometric Methods. Talanta, **50**, 457 (1999).
9. M. I. C. MONTEIRO, I. C. S. FRAGA, A. V. YALLOUZ, N. M. M. OLIVEIRA, S. H. RIBEIRO: Determination of Total Chromium Traces in Tannery Effluents by Electrothermal Atomic Absorption

Spectrometry, Flame Atomic Absorption Spectrometry and UV-vis. Spectrophotometric Methods. Talanta, **58**, 629 (2002).

10. K. VEENA, B. NARAYANA B: A New Facile and Sensitive Method for the Spectrophotometric Determination of Chromium. Eurasian J Anal Chem, **3**, 410 (2009).

11. K. SUNIL, B. NARAYANA: Facile and Sensitive Spectrophotometric Determination of Chromium. Anal Lett, **41**, 2374 (2008).

12. T. CHERIAN, B. NARAYANA: Spectrophotometric Determination of Chromium Using Saccharin. Indian J Chem Technol, **12**, 596 (2005).

13. B. NARAYANA, T. CHERIAN: Rapid Spectrophotometric Determination of Trace Amounts of Chromium Using Variamine Blue as a Chromogenic Reagent. J Braz Chem Soc, **16**, 197 (2005).

14. B. NARAYANA, T. CHERIAN: Spectrophotometric Determination of Trace Amounts of Chromium by the Oxidation of Azure B. Oxid Commun, **28**, 923 (2005).

15. F.A.S. FABIYI, A. Z. DONNIO: Determination of Nano Amounts of Chromium. Synth React Inorg Met, **37**, 809 (2007).

16. H. D. REVANASIDDAPPA, T. N. KIRAN KUMAR: Spectrophotometric Determination of Trace Amounts of Chromium with Citrazinic Acid. J Anal Chem, **56**, 1084 (2001).

17. S. HOSHI, K. KONUMA, M. SUGAWARA, M. UTO, K. AKATSUK: A Simple and Rapid Spectrophotometric Determination of Trace Chromium(VI) after Preconcentration as Its Colored Complex on Chitin. Talanta, **47**, 659 (1998).

18. A. A. MOHAMMED, M. F. El-SHAHAT: Spectrophotometric Determination of Chromium and Vanadium. Anal Sci, **16**, 151 (2000).

ROLE OF OXIDATION TEMPERATURE AND ACID SOLUTION COMPONENT IN CARBON NANOTUBE PURIFICATION PROCESS

M. MOJTAHEDZADEH[a]*, M. ELYASSI[b], F. ZAMANI[b], S. A. SEBT[b]

[a]*Isotope Research Group, Agricultural Medical and Industrial Research School, Nuclear Science and Technology Research Center Institute (NSTRI), Karaj, Iran*
E-mail: *mmojtahedzaleh@nrcam.org*; *mmojtahedfr@yahoo.com*
[b]*Plasma Physics Research Centre, Islamic Azad University, P. O. Box, 14665-678 Tehran, Iran*

ABSTRACT

Three purification methods using 2-stage purification consisting of oxidation and acid washing have been developed that provide the removal of carbon impurities and metal catalyst from multiwall carbon nanotubes (MWCNTs) prepared by thermal chemical vapour deposition (TCVD) technique. Different samples were characterised by scanning electron microscopy (SEM), energy dispersion X-ray (EDX), X-ray diffraction (XRD), the Raman spectroscopy and a thermogravimetric analyser (TGA). The results show that both oxidation temperature and the acid ratio in solution have strong effect on the purification degree. Increasing the reaction time during acid reflux treatment damages MWCNT structure and makes it more susceptible towards air oxidation.

Keywords: carbon nanotubes, purification, acid treatment, oxidation.

AIMS AND BACKGROUND

Since discovery of carbon nanotubes (CNTs) in 1991 (Ref. 1), there is extensive interest in CNTs due to the unique electric, thermal and mechanical properties. Carbon nanotubes are expected to be useful in many different fields, such as effective field emission characteristics[2,3], capability for the storage of large amount of hydrogen[4–6], high modulus[7,8], and structural diversities that make it possible for the band gap engineering[9,10].

However, in order to obtain the optimum performance of carbon nanotubes in various applications, high-purity carbon nanotubes will be required. The impurities typically found in as-prepared carbon nanotubes are the metals that were used as

---

* For correspondence.

catalysts for growth, amorphous carbon, graphitic shells, carbon nanoparticles, C_{60} and other fullerenes.

All purification methods attempt to remove the metal and unwanted carbon without affecting the carbon nanotubes. Different purification methods have been reported to date[11–14]. The purification of CNTs is usually a complicated process consisting of several stages.

The metal is typically present as nanoparticles with a carbon coating that varies from disordered carbon layers to graphitic shells. Gas phase oxidation can remove the more disordered carbon layer which permits removal of this metal with an acid wash.

In this work, 3 purification methods for purifying carbon nanotubes are described and compared together finally to have an idea about the definition of a cleaning procedure that provides additional removal of metal and non-nanotube carbons from carbon nanotube samples.

EXPERIMENTAL

The pristine carbon nanotubes were produced by thermal chemical vapour deposition method (CVD) (Ref. 15). They were then refluxed in deionised water for approximately 3 h. The refluxed CNTs were dried in an oven at 80°C for 24 h. After drying, 2 samples were collected and purified at different conditions. The purification process combines a 2-stage gas phase oxidation process, followed by a wash in HCl/HNO_3 solution. The oxidation process and afterwards the acid washing conditions are given in Table 1.

Table 1. Oxidation temperatures and acid treatment in purification process for different samples

Sample	Purification methods
As-prepared	(a) initial carbon nanotubes
	(b) water refluxed in deionised water for 3 h
	(c) dried in oven for 24 h at 80°C
1	(d) (c) heated at 300°C for 1 h in O_2/Ar (O_2 = 10 sccm, Ar = 200 sccm), 1atm
	(e) (d) heated at 450°C for 1 h in O_2/Ar (O_2 = 10 sccm, Ar = 200 sccm), 1atm
	(f) (e) treated by ultrasound for 30 min with HNO_3/HCl = 1/3
	(g) (f) filtered and washed with deionised water to pH=6
2	(d′) (c) heated at 300°C for 1 h in O_2/Ar (O_2 = 10 sccm, Ar = 200 sccm), 1atm
	(e′) (d′) heated at 500°C for 1 h in O_2/Ar (O_2 = 10 sccm, Ar = 200 sccm), 1atm
	(f′) (e′) treated by ultrasound for 30 min with HNO_3/HCl = 3/1
	(g′) (f′) filtered and washed with deionised water to pH=6
3	(h′) (g′) refluxed the purified sample 2 with HNO_3/HCl = 3/1 for 16 h
	(i′) (h′) filtered and washed with deionised water to pH=6

The oxidation was performed in a quartz resistance furnace at ambient pressure in a mixture of Ar (=200 standard cm³ per min (sccm)) and O_2 (=10 sccm), for 1 h at selected temperatures.

Sample 1 was heated first at 300ºC and subsequently at 450ºC, each of them fixed for 1 h. On the other hand, this process was carried out for the same time at 300 and 500ºC for sample 2. After oxidation, each sample was treated by ultrasound with 35 kHz frequency for 30 min in a solution of HCl (37%) and HNO_3 (65%) at different ratio in order to remove the metal catalysts and summarised in Table 1. After that, the samples were filtered and washed with deionised water for several times until the collected water achieve a pH of 6 and then dried in oven at 120ºC for 24 h.

To investigate the effect of kinetics in catalyst dissociation, part of sample 2 (named as sample 3) was refluxed in a solution of HCl and HNO_3 (HNO_3:HCl = 3:1) for 16 h and subsequently filtered, washed and dried as before.

In order to evaluate the effectiveness of the above procedure, samples before and after purification were characterised by scanning electron microscopy (SEM, XL–30, Philips) and energy dispersion X-ray (EDX).

The Raman scattering spectra were recorded with a Lab Ram HR800, a Jobin Yvon spectrometer, a 532 nm Nd:Yag laser was used as excitation source with a resolution of 4 cm⁻¹. Thermal analysis of the carbon nanotube samples was performed in a thermogravimetric analyser (TGA) in flowing air atmosphere (60 cm³ min⁻¹). Approximately 2 mg of sample were heated in an open platinum crucible up to 900ºC at rate of 10ºC min⁻¹. X-ray diffraction (XRD, PW1800, Philips) patterns were obtained using a CuKα radiation.

RESULTS AND DISCUSSION

Figure 1 shows SEM images of the CNTs before and after purification. In Fig. 1*a*, any CNT bundles can be observed on the surface of the pristine sample, probably due to the coverage of the surface with carbon impurities and catalyst particles. On the contrary, after purification processes the carbon nanotube bundles can be easily observed on the surface in samples 1 and 2 (Fig. 1*b,c*). Comparing Fig. 1*b* with Fig. 1*c*, it may be concluded that the surface cleanliness and the carbon nanotube density of sample 2 are higher than of sample 1.

The XRD patterns of different samples are shown in Fig. 2. It is obvious from this figure that the intensity of graphitic carbon peak of sample 1 has been increased in comparison with as-prepared sample. Although more carbon graphitic peaks are observable in sample 2, indicating a better elimination of non-carbon nanotubes, more peaks concerning catalyst impurities like Co and Mo are present too by comparison with sample 1. According to Fig. 2, the intensity of carbon graphite peak of sample 3 decreases and no catalyst signal can be seen. The comparison of sample 1 pattern with that of sample 2 shows that both oxidation temperature and applied acid ratio play an important role in purification process. Knowing that oxidation step is essen-

tially used to remove the non-carbon nanotubes and acid treatment for elimination of catalyst impurities[12], from XRD results and referring to Table 1 we concluded that it is more effective to perform oxidation at 500°C rather than at 450°C and acid treatment with HNO_3 : HCl ratio equal to 1: 3. At this ratio more catalysts have been removed from as-prepared CNTs. The decrease of carbon graphite peak intensity in sample 3 compared with samples 1 and 2 can be explained by the degradation of CNT structure. In reality, extension of acid treatment time apparently dissolves most of the catalytic particles and also begins to destroy the CNTs. This effect has been also reported in Ref. 16.
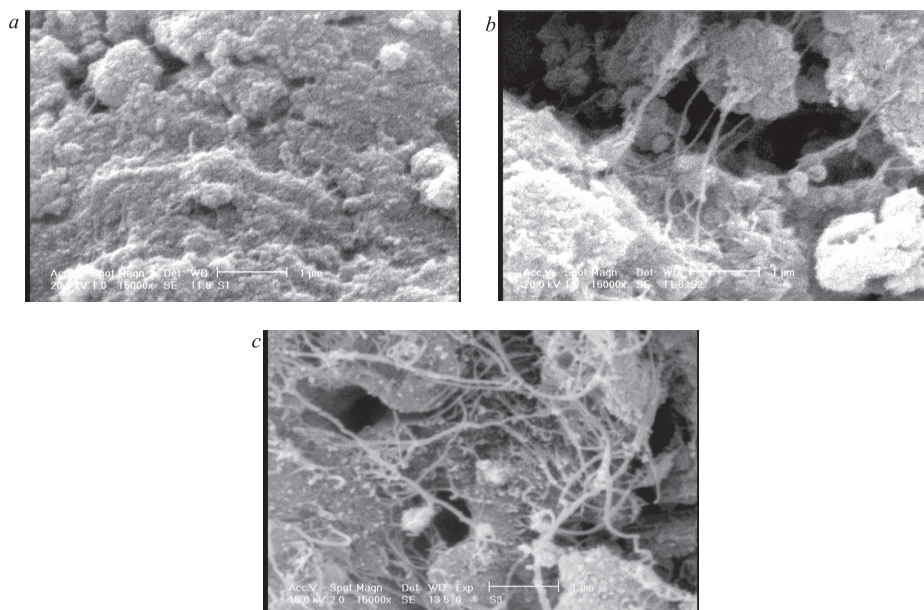

Fig. 1. SEM images of CNTs: before purification (*a*), sample 1 (*b*) and sample 2 (*c*) after purification.
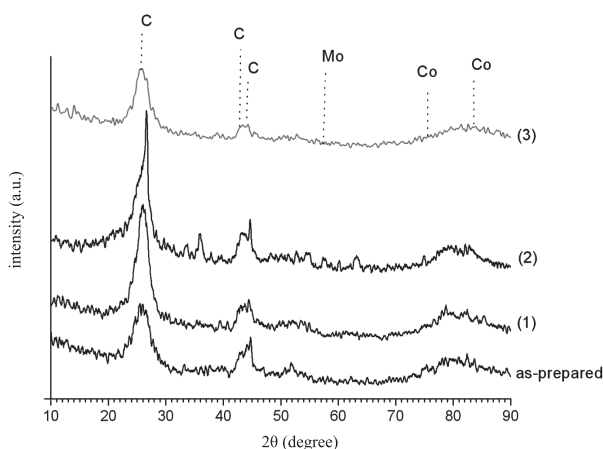

Fig. 2. XRD analysis of unpurified CNTs and purified samples 1, 2 and 3

713

Our explanation about the importance of acid ratio has been subsequently supported by EDS analysis results in Fig. 3. The results are summarised in Table 2 in terms of weight percent. This analysis clarified that the principal elements in the unpurified CNTs are Co and Mo. As we can observe from Table 2 the amount of catalyst impurities in sample 2 is two times higher than in sample 1 which is consistent with XRD results as discussed above.
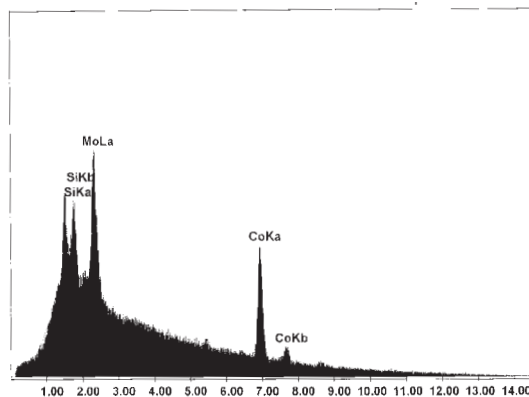
Fig. 3. EDX analysis of unpurified CNTs. Carbon signal is not shown because of detection limit of measurement apparatus and signal of Si comes from sample holder

Table 2. EDS results of initial CNTs (as-prepared) and purified samples

Sample	Co (wt. %)	Mo (wt.%)
As-prepared	61	30
1	21	11
2	43	21
3	22	5

The last point concerning EDS and XRD analysis is related to the difference between the results of samples 2 and 3. The amount of catalysts has been considerably decreased with the increase of solubility time in the same solution (Table 1), which is probably due to the kinetics of the reaction.

Figure 4 shows the Raman spectra of the carbon nanotubes from 250 to 3000 cm^{-1} before and after purification. The spectra essentially show 3 peaks at about 1350 (D band), 1600 (G band) and 2650 cm^{-1} (G′ band), respectively. The G band corresponds to the symmetric E_{2g} vibrational mode in graphite-like materials, the D band is assigned to an A_{1g} mode due to the finite size of nanometer order of the crystalline domains and to the high density of twisty tubes[17] and the G′ band can be interpreted as an overtone of the D band and is due to 2-phonon, second-order Raman scattering process.

714

Fig. 4. The Raman spectra of CNTs for the sample before purification and samples 1 and 2 after purification process according to Table 1

The intensity ratio of I_G/I_D is known to depend on the structural properties of CNTs (Ref. 18). The larger this ratio, the better the structural quality of the sample. The intensity ratio (I_G/I_D) for different samples is given in Table 3. As shown in Table 3, this ratio increases in purified samples relative to the as-prepared. It 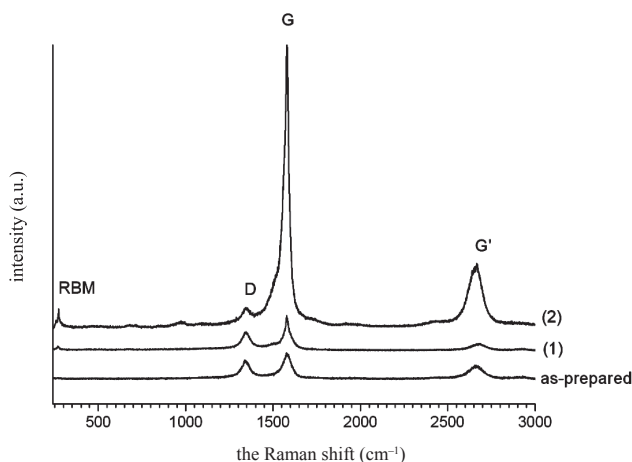suggests that the applied purification process has impact on CNT structure and quality. In the case of sample 2 oxidised at 300 and 500°C and then treated in the (HNO_3: HCl = 3: 1) solution we observe not only a maximum I_G/I_D of 15, but also a sharp peak at about 260 cm⁻¹ clearly appears. This peak in low frequency domain called radial breathing mode (RBM) frequency is resulted from the A$_g$ symmetry in MWCNTs. The presence of the RBM frequency provides an indication of a presence of MWCNTs within the samples. To explain the results obtained by SEM and the Raman analysis, we propose that the as-prepared sample consists of CNTs (mainly multiwall) covered by the catalyst particles and carbon impurities. As pointed out above, the purification process applied to sample 1 removes essentially the metal impurities but there is always the carbon impurities such as amorphous carbon (Fig. 1b) attached to the tube-wall as for raw materials. The consequence of the carbon impurity attachment on the tube-wall is a softening of vibrational E$_{2g}$ modes, and nearly prohibits observation of RBM modes associated to the MWCNTs present in the sample. In the case of sample 2, the purification process, most notably oxidation at 500°C, is predominated by elimination of the carbon impurity from the tube-walls rather than metallic impurities as a consequence of acid washing. Then, less intercarbon bond in CNT is affected by impurities leading to an enhancement of tangential and breathing vibrational modes. Figure 5 shows the Raman spectrum of sample 3 which is similar to that of sample 2 with a difference in I_G/I_D ratio which decreases about 3 times (I_G/I_D = 3.2). The decrease of CNT quality in accordance with XRD results is may be due to the partial destruction of CNTs after a long period of acid washing.

715

Table 3. The ratio of I_G/I_D calculated from the Raman results in as-prepared CNTs and purified samples

Sample	I_G/I_D
As-prepared	1.2
1	1.8
2	15.0
3	3.2
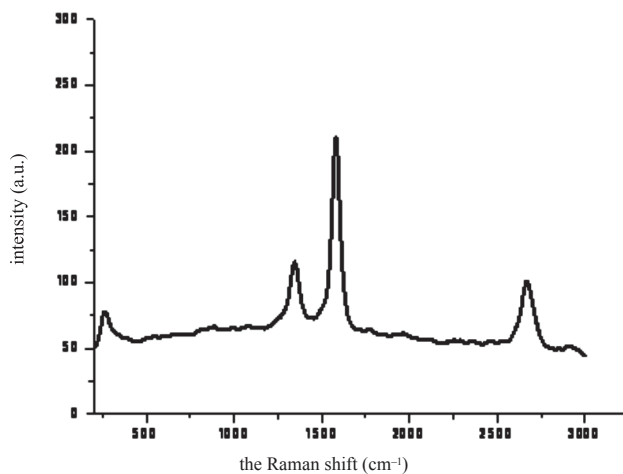
Fig. 5. The Raman spectrum of sample 3

Thermogravimetric analysis of the as-prepared and purified samples is shown in Fig. 6. The weight loss of as-prepared MWCNTs starts at about 400°C and a significant loss is observed at 530–700°C. The weight loss at 550 - 700°C can be ascribed to the MWCNT combustion while the weight loss below 550°C is due to the removal of carbon impurities by oxidation[16]. The weight remaining at >700°C (~30 wt. %) is probably due to the presence of catalytic metals introduced in the synthesis, in accordance with the literature report in Ref. 19.

Since about 25 wt. % of as-prepared sample are consumed below 550°C, and about 30 wt. % remained above 700°C, the purity of raw CNTs may be conservatively estimated to be about 45 wt. %. The TGA curves of purified samples exhibit a weight loss region at 450°C for sample 1 and 500°C for sample 2, while the major weight losses for samples 1 and 2 are at 550–610 and 600–650°C, respectively. The comparison of starting temperatures of weight loss of 3 samples together (400, 450 and 500°C for samples as-prepared, 1 and 2, respectively) inferred that sample 2 is more stable at temperatures below 550°C due to less contamination of the product by amorphous carbon and other carbon impurities probably because of adopted oxidation temperature. This suggestion is consistent well with the Raman spectra shown in Fig.

4. In the case of samples 1 and 2, the metal weights remaining at the high temperature are about 10 and 18 wt.%, respectively. From this result we can conclude that the rate of metal dissolution in $HNO_3:HCl = 1:3$ solution is approximately 2 times higher than that in $HNO_3: HCl = 3:1$ solution. The residual metal wt. % ratio in different samples measured by TGA presents the same trend as obtained by EDS (Table 1). As pointed out previously, in sample 1 less than 5 wt. % are consumed below 550°C, and less than 10 wt.% remain above 550°C, the final purity of sample 1 is conservatively estimated to be >85 wt.%, and in the case of sample 2 the mentioned values are changed to less than 2 wt.% below 550°C, less than 18 wt.% above 550°C and the final purity >80 wt.% is calculated.
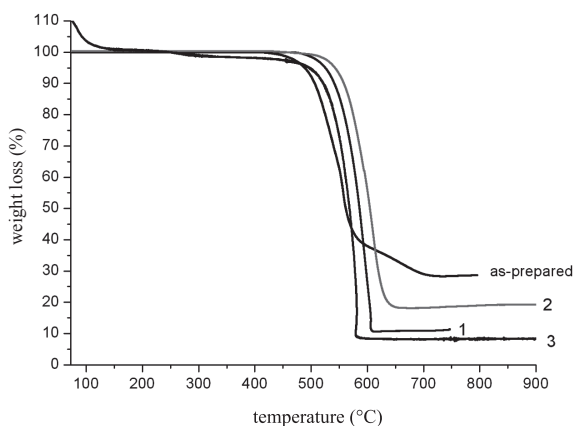
Fig. 6. TGA curves of as-prepared MWCNTs and purified MWCNT samples 1, 2 and 3 according to Table 1

The TGA data for sample 3 shown in Fig. 6 exhibit 2 weight loss regions < 100°C and 250–300°C, though the more intense weight loss is at 550–600°C. The weight loss at < 100°C is attributed to the release of water from MWCNT (Ref. 19). The small weight loss at 250–300°C may be due to the formation of damages on the surfaces of the MWCNTs and production of carboxyle, aldehyde, and other oxygen-containing functional groups which are more susceptible to air oxidation. Dillon et al.[16] have reported similar trend when they refluxed the crude soot synthesised by a laser vaporisation method for 16 h in 3 M HNO_3. As discussed above we can conservatively estimate a final purity of 80 wt.% for sample 3, knowing that less than 15 wt.% are consumed below 550°C, and less than 5 wt.% remain above 550°C. The low value of metal contamination in sample 3 obtained by TGA was predictable using EDX results (Table 2).

CONCLUSIONS

In this study 3 purification processes have been developed which result in > 80% pure MWCNTs. They combine the water reflux and 2-stage gas phase oxidation process fallowed by acid ultrasonic treatment.

The TGA and Raman spectroscopy results show that the CNTs in sample 1 are oxidised at 300°C and then 450°C, each for 1 h in mixture of argon and oxygen (Ar =200 sccm, O_2=10 sccm) at atmospheric pressure is more contaminated by carbon impurities than in sample 2 which is oxidised at 300°C and then 500°C at the same conditions. On the other hand, acid treatment applied to sample 1 (HNO_3: HCl = 1: 3) presents a dissolution rate of metallic impurities 2 times higher than that of sample 2 (HNO_3: HCl = 3: 1). To compensate the low rate of dissolution by method 2 for dissolving the metal particles an increase of the reaction time (sample 3; 16 h) in the solution (HNO_3: HCl = 3: 1) has been adopted. According to the analysis results, although the amount of metal particles reduces considerably in sample 3 compared with sample 2, it is more susceptible towards air oxidation due to the MWCNT degradation.

REFERENCES

1. S. IIJIMA: Helical Microtubules of Graphitic Carbon. Nature, **354**, 56 (1991).
2. S. FAN, M. G. CHAPLINE, N. R. FRANKLIN, T. W. TOMBLER, A. M. CASSELL, H. DAI: Self-oriented Regular Arrays of Carbon Nanotubes and Their Field Emission Properties. Science, **283**, 512 (1999).
3. P. G. COLLINS, A. ZETTL: Unique Characteristics of Cold Cathode Carbon Nanotube-matrix Field Emitter. Phys Rev B, **55**, 9391 (1997).
4. H. WU, D. WEXLER, A. RANJBARTOREH, H. LIU, G. WANG: Chemical Processing of Double-walled Carbon Nanotubes for Enhanced Hydrogen Storage. Hydrogen Energy, **35**, 6345 (2010).
5. A. ZOLFAGHARI, P. POURHOSSEIN, H. Z. JOOYA: The Effect of Temperature and Topological Defects on H2 Adsorption on Carbon Nanotubes. Hydrogen Energy, **36**, 13250 (2011).
6. H. WU, D. WEXLER, H. LIU: Effects of Different Palladium Content Loading on the Hydrogen Storage Capacity of Double-walled Carbon Nanotubes. Hydrogen Energy, **37**, 5686 (2012).
7. B. I. YAKOBSON, C. J. BRABEC, J. BERNHOLC: Nanomechanics of Carbon Tubes: Instabilities beyond Linear Response. Phys Rev Lett, **76**, 2511 (1996).
8. J. P. SALVETAT, G. A. D BRIGGS, J. M. BONARD, R. R. BACSA, A. J. KULIK, T. STOCKLI, N. A. BURNHAM, L. FORRÓ: Elastic and Shear Moduli of Single-walled Carbon Nanotube Ropes. Phys Rev Lett, **82**, 944 (1999).
9. J. W. MINTMIRE, B. I. DUNLAP, C. T. WHITE: Are Fullerene Tubules Metallic? Phys Rev Lett, **68**, 631 (1992).
10. N. HMADA, S. SAWADA, A. OSHIYAMA: New One-dimensional Conductors: Graphitic Micro-tubules. Phys Rev Lett, **68**, 1579 (1992).
11. L. STOBINSKI, B. LESIAK, L. KOVER, J. TOTH, S. BINIAK, G. TRYKOWSKI, J. JUDEK: Multiwall Carbon Nanotubes Purification and Oxidation by Nitric Acid Studied by the FTIR and Electron Spectroscopy Methods. J Alloy Compd, **501** (1), 77 (2010).
12. J. BARKAUSKAS, I. STANKEVICIENE, A. SELSKIS: A Novel Purification Method of Carbon Nanotubes by High-temperature Treatment with Tetrachloromethane. Sep Purif Technol, **71** (3), 331 (2010).
13. X. LING, Y. WEI, L. ZOU, S. XU: The Effect of Different Order of Purification Treatments on the Purity of Multiwalled Carbon Nanotubes. Appl Surf Sci, **276**, 159 (2013).

14. Ch. HE, Y. HAO, H. ZENG, T.TANG, J. XING, J. CHEN: A New Purification Method for Carbon Nanotubes and Associated Atomic Force Microscope Force–distance Curve Analysis. Sep Purif Technol, **81** (2), 174 (2011).

15. A. RASHIDI, A. HORRI, B. A. MOHAJERI, A. SARAIE, S. JOZANI, K. J. NAKHAEIPOR: US20080274277 Patent, June 2008.

16. A. C. DILLON, T. GENNETT, K. M. JONES, J. L. ALLEMAN, P. A. PARILLA, M. J. HEBEN: A Simple and Complete Purification of Single-walled Carbon Nanotube Materials. Adv Mater, **11**, 1354 (1999).

17. Y. S. JUNG, D. Y. JEON: Surface Structure and Field Emission Property of Carbon Nanotubes Grown by Radio Frequency Plasma-enhanced Chemical Vapor Deposition. Appl Surf Sci, **193**, 129 (2002).

18. J. P. CHENG, X. B. ZHANG, F. LIU, J. P. TU, H. M. LU, Y. L. SUN, F. CHEN LONG: Bundles of Aligned Carbon Nanofibers Obtained by Vertical Floating Catalyst Method. Mater Chem Phys, **87**, 241 (2004).

19. M. ZHANG, A. SMITH, W. GROSKI: Carbon Nanotube–Chitosan System for Electrochemical Sensing Based on Dehydrogenase Enzymes. Anal Chem, **76**, 5045 (2004).

OXIDATION OF VALINE AND 2-AMINOISOBUTYRIC ACID BY DITELLURATOCUPRATE(III) IN ALKALINE MEDIUM. A KINETIC AND MECHANISTIC STUDY

JINHUAN SHAN*, YI LI, JIN HAN, ZIWEI ZHANG

College of Chemistry and Environmental Science, Hebei University, Baoding, 071 002 Hebei, China
E-mail: *shanjinhuaner@yahoo.com.cn*

ABSTRACT

Oxidation of valine and 2-aminoisobutyric acid by ditelluratocuprate(III) (DTC) in alkaline medium had been studied spectrophotometrically in the temperature range of 10 to 30°C. It was found that the reaction was pseudo-first order in DTC and fractional order in valine, whereas $1 < n_{ap} < 2$ in 2-aminoisobutyric acid. The pseudo-first order rate constant, k_{obs}, decreased with an increase in $[OH^-]$ and $[TeO_4^{2-}]$. There was negative salt effect. The rate of valine oxidation was higher than that of 2-aminoisobutyric acid in alkaline medium. A plausible mechanism involving pre-equilibriums before the rate-controlling step and a free radical mechanism was proposed based on the kinetic study. The rate equations derived from the mechanism can explain all experimental phenomena. In addition, the activation parameters at 298.2 K along with rate constants of the rate-determining step were computed by the slow step of the mechanism.

Keywords: oxidation, kinetics, ditelluratocuprate(III), valine, 2-aminoisobutyric acid.

AIMS AND BACKGROUND

Recently, studies on the transition metals in a higher oxidation state have been the most active area. Transition metals generally can be stabilised by chelation with polydentate ligands, such as ditelluratocuprate(III) (Refs 1 and 2), diperiodatocuprate(III) (Refs 3 and 4), diperiodatoargentate(III) (Refs 5 and 6), ditelluratoargentate(III) (Ref. 7), diperiodatonickelate(IV) (Ref. 8) are good oxidants in a medium with an appropriate pH. As a kind of oxidation reagents, those complexes have been used widely in kinetic studies. Now, Cu(III) complex has been used in many biological systems involving electron-transfer processes[9] and organic mixture qualitative analysis[10].

---

* For correspondence.

Because Cu(III) is in the higher oxidation state and the reaction is complicated, it is of significance to carry out a further study on this kind of reaction system. In the present paper, oxidation of valine and 2-aminoisobutyric acid by ditelluratocuprate (III) in alkaline medium is reported.

Both valine and 2-aminoisobutyric acid are white powders and soluble in water. Moreover, valine and 2-aminoisobutyric acid are important amino acids in the human body and they have been used widely in synthesis of intermediate for medicine and organic raw material. In addition, valine can be used as drug to accelerate the wound healing.

EXPERIMENTAL

Materials. All the reagents used were A.R. grade and doubly distilled water was used throughout the work. Ditelluratocuprate(III) (DTC) was prepared and standardised by the method reported by Chandra and Yadava[11,12]. The purity of the complex was checked by comparing UV-vis. spectrum with literature data, which showed a characteristic absorption peak at 405 nm. KNO_3 and KOH were used to maintain ionic strength and alkaliniy of the reaction, respectively. Besides, solutions of DTC and reductants were always freshly prepared before using.

Kinetics measurements and apparatus. The kinetics was followed under pseudo-first order conditions, solution (2 ml) containing required concentration of DTC, OH⁻, TeO_4^{2-} and ionic strength and reductant solution (2 ml) of requisite concentration were mixed at the desired temperature. The progress of the reaction was followed by measuring the decrease in absorbance of DTC at 405 nm. The kinetic measurements were performed on a UV-vis. spectrophotometer (TU-1900, Beijing Puxi Inc., China), which had a cell holder kept at constant temperature (± 0.1ºC) by circulating water from a thermostat (DC-2010, Baoding Xinhua Inc., China). It was verified that there was negligible interference from other reagents at this wavelength.

RESULTS

Product analysis. Under the kinetic conditions the product of oxidation was identified as ketone formate, ketone and NH_3 by its characteristic spot test[13].

Evaluation of pseudo-first order rate constants. Under the conditions of [reductant]$_0$ >> [Cu(III)]$_0$, the plots of ln ($A_t - A_\infty$) versus time were straight lines ($r \geq 0.999$) (Fig. 1), indicating the order in DTC to be unity. The pseudo-first order rate constants, k_{obs}, were evaluated by using equation ln ($A_t - A_\infty$) = $- k_{obs}t + b$ (constant). The k_{obs} values were the average value of at least 3 independent experiments, and reproducibility was within $\pm 5\%$.
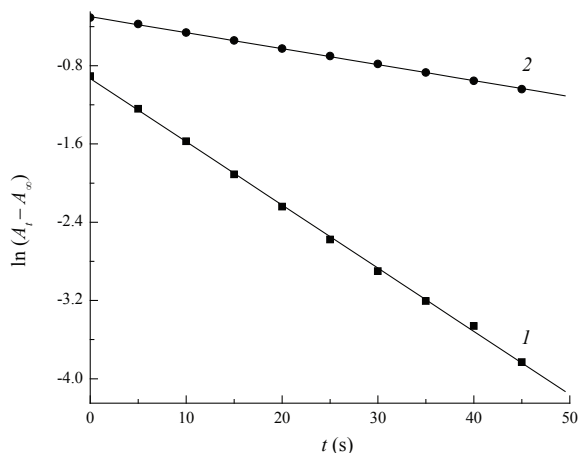
Fig. 1. Plot of ln $(A_t - A_\infty)$ versus time at T=293.2 K
[DTC] = 8.96×10^{-5} mol l^{-1}; [TeO$_4^{2-}$] = 1.00×10^{-3} mol l^{-1}; [OH$^-$] = 1.00×10^{-2} mol l^{-1}; μ = 2.10×10^{-2} mol l^{-1}; [reductant] = 3.00×10^{-3} mol l^{-1}
1 – [valine]: k_{obs}=6.46×10^{-2} s^{-1}; *2* – [2-aminoisobutyric acid]: k_{obs}=1.63×10^{-2} s^{-1}

Rate dependence on the [*reductant*]. The [reductant] was varied in the range of 1.00 to 5.00×10^{-3} mol l^{-1} at different temperatures keeping all other [reactants] constant. The orders n_{ap} were found to be fractional in valine and $1 < n_{ap} < 2$ in 2-aminoisobutyric acid form the slopes of ln k_{obs} versus ln[reductant]. Besides, the k_{obs} value increased with increasing [reductant]. Both the plot of k_{obs}^{-1} versus [valine]$^{-1}$ and the plot of [2-aminoisobutyric acid]/k_{obs} versus [2-aminoisobutyric acid]$^{-1}$ were straight lines ($r \geq 0.997$) (Figs 2 and 3).
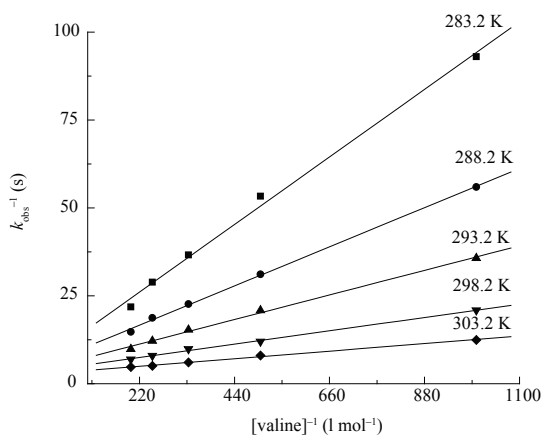
Fig. 2. Plots of k_{obs}^{-1} versus [valine]$^{-1}$ ($r \geq 0.998$)
[DTC]=8.96×10^{-5} mol l^{-1}; [TeO$_4^{2-}$]=1.00×10^{-3} mol l^{-1}; [OH$^-$]=1.00×10^{-2} mol l^{-1}; μ=2.10×10^{-2} mol l^{-1}
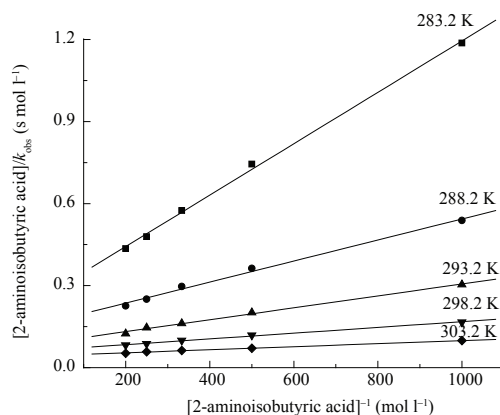
Fig. 3. Plots of [2-aminoisobutyric acid]/k_{obs} versus [2-aminoisobutyric acid]$^{-1}$ ($r \geq 0.997$)
[DTC]=8.96×10^{-5} mol l^{-1}; [TeO$_4^{2-}$]=1.00×10^{-3} mol l^{-1}; [OH$^-$]=1.00×10^{-2}mol l^{-1}; μ=2.10×10^{-2} mol l^{-1}

Rate dependence on [OH^-]. The effect of [OH$^-$] on the reaction had been studied in the range of 0.50 to 2.50×10^{-2} mol l^{-1} at constant [DTC], [reductant], [TeO$_4^{2-}$], μ and temperature. It was found that k_{obs} decreased with increasing [OH$^-$]. The plot of k_{obs}^{-1} versus [OH$^-$]$\times 10^2$ was linear with a positive intercept (Fig. 4).
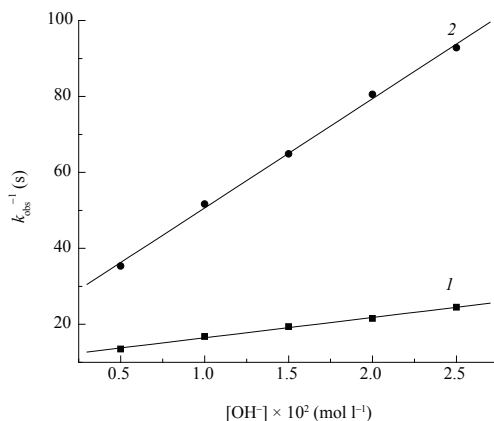
Fig. 4. Plots of k_{obs}^{-1} verus [OH$^-$] $\times 10^2$ at 293.2 K ($r \geq 0.998$)
[DTC]=8.96×10^{-5} mol l^{-1}; [TeO$_4^{2-}$]=1.00×10^{-3} mol l^{-1}; μ=3.80×10^{-2} mol l^{-1}; [reductant]=3.00×10^{-3} mol l^{-1}
1 – [valine]; *2* – [2-aminoisobutyric acid]

Rate dependence on [TeO_4^{2-}]. The [TeO$_4^{2-}$] was varied from 0.5 to 2.5×10^{-3} mol l^{-1} range at constant [DTC], [reductant], [OH$^-$], μ and temperature. The k_{obs} values increased with the decreasing concentration of TeO$_4^{2-}$. The order with respect to TeO$_4^{2-}$ was found to be a negative fraction, which revealed that TeO$_4^{2-}$ was produced

in equilibrium before the rate-controlling step. A plot of k_{obs}^{-1} versus $[TeO_4^{2-}]$ was a straight line (Fig. 5).
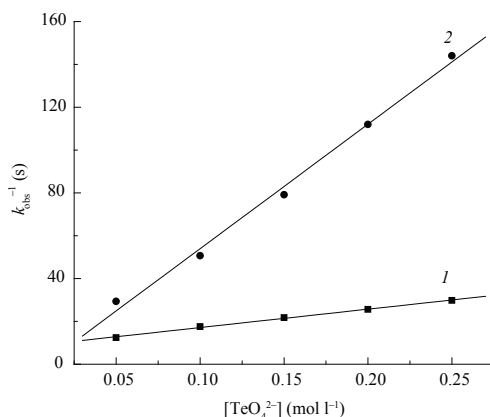
Fig. 5. Plots of k_{obs}^{-1} versus [TeO_4^{2-}] at 293.2 K ($r \geq 0.997$)
[DTC] = 8.96×10^{-5} mol l^{-1}; [OH$^-$] =1.00×10^{-2} mol l^{-1}; μ=3.80×10^{-2} mol l^{-1}; [reductant]=3.00×10^{-3} mol l^{-1}
1 – [valine]; *2* – [2-aminoisobutyric acid]

Rate dependence on ionic strength μ. The effect of ionic strength on the reaction was studied in the rang of 2.00 to 10.00×10^{-2} mol l^{-1} at constant [DTC], [reductant], [OH$^-$], $[TeO_4^{2-}]$ and temperature. The experimental results indicated that the rate constant k_{obs} decreased with increase in ionic strength μ (Table 1), which showed that there was negative salt effect consistent with the common regulation of the kinetics[14].

Table 1. Influence of variation of ionic strength μ on k_{obs} at 293.2 K
[Reductant]=3.00×10^{-3} mol l^{-1}; [DTC]=8.96×10^{-5} mol l^{-1}; [OH$^-$]= 1.00×10^{-2} mol l^{-1}; $[TeO_4^{2-}]$=1.00×10^{-3} mol l^{-1}

$\mu \times 10^2$ (mol l^{-1})		2.00	4.00	6.00	8.00	10.00
$k_{obs} \times 10^3$ (s^{-1})	valine	63.22	56.65	53.51	50.01	47.94
	2-aminoisobutyric acid	25.82	22.80	21.21	18.99	17.24

Free radical detection. To study the possible presence of free radicals during the reaction, a known amount of acrylamide was added under the protection of nitrogen atmosphere. A polymerisation reaction clearly occurred which indicated that free radical intermediates may be produced in the oxidation by DTC. And blank experiments in reaction system gave no polymeric suspensions.

DISCUSSION

In alkaline medium, the electric dissociation equilibrium of telluric acid was given earlier (here pK_w=14) as follows:

$$H_5TeO_6^- + OH^- \rightleftharpoons H_4TeO_6^{2-} + H_2O, \lg \beta_1 = 3.049 \tag{1}$$

$$H_4TeO_6^{2-} + OH^- \rightleftharpoons H_3TeO_6^{3-} + H_2O, \lg \beta_2 = -1 \tag{2}$$
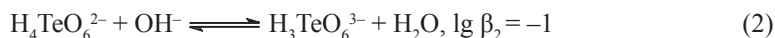
The distribution of all species of tellurate in aqueous alkaline solution can be calculated from equilibria (1)–(2). In alkaline medium such as $[OH^-] = 0.001$, $[H_4TeO_6^{2-}]:[H_5TeO_6^-]:[H_3TeO_6^{3-}]=1000:89:1$, so in the concentration of OH^- range used in this work $H_5TeO_6^-$ and $H_3TeO_6^{3-}$ can be neglected, the main tellurate species was $H_4TeO_6^{2-}$.

The rate constant k_{obs} decrease with an increase of $[OH^-]$ showed that there was a hydrolysis equilibrium before the rate-determining step. The plot of $1/k_{obs}$ versus $[TeO_4^{2-}]$ was a straight line with a positive intercept indicating a dissociation equilibrium in which the Cu(III) losses a tellurate ligand $H_4TeO_6^{2-}$ from its coordination sphere forming an active specie monotelluratocuprate (III) complex (MTC). In addition, the plots of k_{obs}^{-1} versus $[valine]^{-1}$ and of $[2\text{-aminoisobutyric acid}]/k_{obs}$ versus $[2\text{-aminoisobutyric acid}]^{-1}$ were straight lines providing that they had different order along with reaction mechanism. In alkaline solution studied, $(H_2TeO_6)_4^-$ protonated easily and it coordinated with central ion formed $[Cu(H_4TeO_6)_2]^-$

According to the above discussion, two plausible mechanisms of oxidation were proposed as follows:

Mechanism I – with respect to valine:
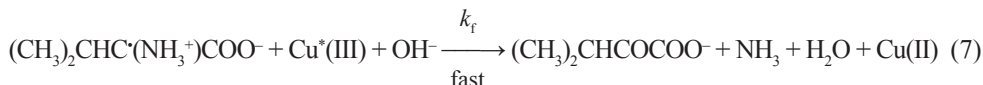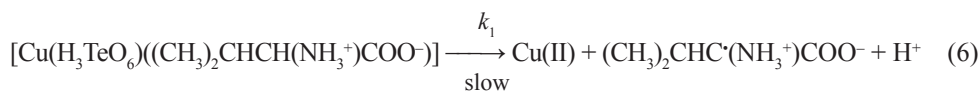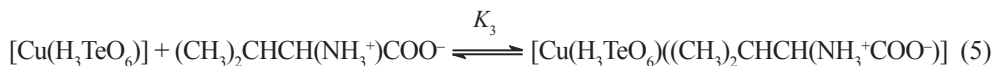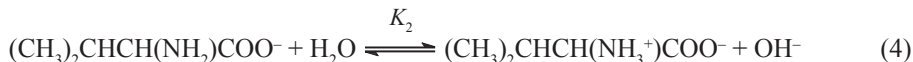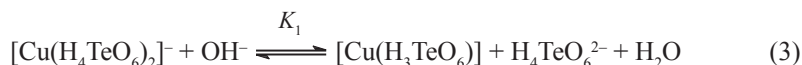
$$[Cu(H_4TeO_6)_2]^- + OH^- \xrightarrow{K_1} [Cu(H_3TeO_6)] + H_4TeO_6^{2-} + H_2O \tag{3}$$

$$(CH_3)_2CHCH(NH_2)COO^- + H_2O \xrightarrow{K_2} (CH_3)_2CHCH(NH_3^+)COO^- + OH^- \tag{4}$$

$$[Cu(H_3TeO_6)] + (CH_3)_2CHCH(NH_3^+)COO^- \xrightarrow{K_3} [Cu(H_3TeO_6)((CH_3)_2CHCH(NH_3^+COO^-)] \tag{5}$$

$$[Cu(H_3TeO_6)((CH_3)_2CHCH(NH_3^+)COO^-)] \xrightarrow[\text{slow}]{k_1} Cu(II) + (CH_3)_2CHC^\cdot(NH_3^+)COO^- + H^+ \tag{6}$$

$$(CH_3)_2CHC^\cdot(NH_3^+)COO^- + Cu^*(III) + OH^- \xrightarrow[\text{fast}]{k_f} (CH_3)_2CHCOCOO^- + NH_3 + H_2O + Cu(II) \tag{7}$$

Cu*(III) stands for any kind of which Cu^{3+} existed in equilibrium. The total concentration of Cu(III) can be written (subscripts T and e stand for total concentration and at equilibrium, respectively) as follows:

$$[Cu(III)]_T = [Cu(H_4TeO_6)_2]_e^- + [Cu(H_3TeO_6)]_e + [Cu(H_3TeO_6)((CH_3)_2CHCH(NH_3^+)COO^-)]_e$$

Since reaction (6) is the rate-determining step, the rate of disappearance of $[Cu(III)]_T$ is represented as:

$$-\frac{d[Cu(III)]_T}{dt} = \frac{2k_1K_1K_2K_3[(CH_3)_2CHCH(NH_2)COO^-]Cu(III)}{[H_4TeO_6^{2-}] + K_1[OH^-] + K_1K_2K_3[(CH_3)_2CHCH(NH_2)COO^-]} = k_{obs}Cu(III) \quad (8)$$

$$k_{obs} = \frac{2k_1K_1K_2K_3[(CH_3)_2CHCH(NH_2)COO^-]}{[H_4TeO_6^{2-}] + K_1[OH^-] + K_1K_2K_3[(CH_3)_2CHCH(NH_2)COO^-]}. \quad (9)$$

Re-arranging of equation (9) leads to equations (10)–(12):

$$\frac{1}{k_{obs}} = \frac{1}{2k_1} + \frac{[H_4TeO_6^{2-}] + K_1[OH^-]}{2k_1K_1K_2K_3} \frac{1}{[(CH_3)_2CHCH(NH_2)COO^-]} \quad (10)$$

$$\frac{1}{k_{obs}} = \frac{1}{2k_1} + \frac{[H_4TeO_6^{2-}]}{2k_1K_1K_2K_3[(CH_3)_2CHCH(NH_2)COO^-]}$$

$$+ \frac{[OH^-]}{2k_1K_1K_2K_3[(CH_3)_2CHCH(NH_2)COO^-]} \quad (11)$$

Mechanism II – with respect to 2-aminoisobutyric acid:
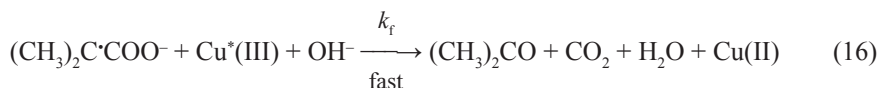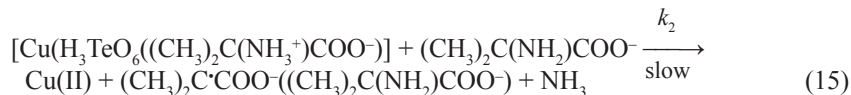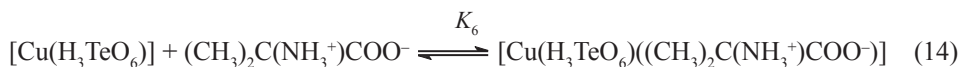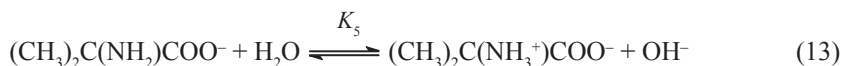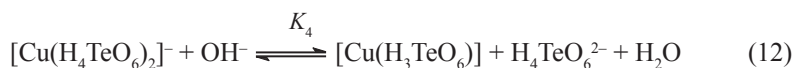
$$[Cu(H_4TeO_6)_2]^- + OH^- \xrightleftharpoons{K_4} [Cu(H_3TeO_6)] + H_4TeO_6^{2-} + H_2O \quad (12)$$

$$(CH_3)_2C(NH_2)COO^- + H_2O \xrightleftharpoons{K_5} (CH_3)_2C(NH_3^+)COO^- + OH^- \quad (13)$$

$$[Cu(H_3TeO_6)] + (CH_3)_2C(NH_3^+)COO^- \xrightleftharpoons{K_6} [Cu(H_3TeO_6((CH_3)_2C(NH_3^+)COO^-)] \quad (14)$$

$$[Cu(H_3TeO_6((CH_3)_2C(NH_3^+)COO^-)] + (CH_3)_2C(NH_2)COO^- \xrightarrow[\text{slow}]{k_2}$$
$$Cu(II) + (CH_3)_2C^{\cdot}COO^-((CH_3)_2C(NH_2)COO^-) + NH_3 \quad (15)$$

$$(CH_3)_2C^{\cdot}COO^- + Cu^*(III) + OH^- \xrightarrow[\text{fast}]{k_f} (CH_3)_2CO + CO_2 + H_2O + Cu(II) \quad (16)$$

Cu*(III) stands for any kind of which Cu^{3+} existed in equilibrium. The total concentration of Cu(III) can be written (subscripts T and e stand for total concentration and at equilibrium, respectively) as follows:

$$[Cu(III)]_T = [Cu(H_4TeO_6)_2]_e^- + [Cu(H_3TeO_6)]_e + [Cu(H_3TeO_6((CH_3)_2C(NH_3^+)COO^-)]_e.$$

Since reaction (16) is the rate-determining step, the rate of disappearance of $[Cu(III)]_T$ is represented as:

$$-\frac{d[Cu(III)]_T}{dt} = \frac{2k_2K_4K_5K_6[(CH_3)_2C(NH_2)COO^-]Cu(III)}{[H_4TeO_6^{2-}] + K_4[OH^-] + K_4K_5K_6[(CH_3)_2C(NH_2)COO^-]} = k_{obs}Cu(III) \quad (17)$$

$$k_{obs} = \frac{2k_2K_4K_5K_6[(CH_3)_2CH(NH_2)COO^-]}{[H_4TeO_6^{2-}] + K_4[OH^-] + K_4K_5K_6[(CH_3)_2C(NH_2)COO^-]} . \quad (18)$$

Rearranging equation (18) leads to equations (19)–(20):

$$\frac{[(CH_3)_2C(NH_2)COO^-]}{k_{obs}} = \frac{1}{2k_2} + \frac{[H_4TeO_6^{2-}] + K_4[OH^-]}{2k_2K_4K_5K_6} \frac{1}{[(CH_3)_2C(NH_2)COO^-]} \quad (19)$$

$$\frac{1}{k_{obs}} = \frac{1}{2k_2[(CH_3)_2C(NH_2)COO^-]} + \frac{[H_4TeO_6^{2-}]}{2k_2K_4K_5K_6[(CH_3)C(NH_2)COO^-]^2}$$

$$+ \frac{[OH^-]}{2k_2K_5K_6[(CH_3)C(NH_2)COO^-]^2} \quad (20)$$

Equations (8) and (17) suggest that the order with respect to Cu(III) is unity. Equations (9) and (18) showed that the order in valine and 2-aminoisobutyric acid were found to be fractional and $1 < n_{ap} < 2$, respectively. From equations (10) and (19), the rate constants of the rate-determining step at different temperatures were determined by the intercept of the plots k_{obs}^{-1} versus [valine]$^{-1}$ and the plots of [2-aminoisobutyric acid]/k_{obs} versus [2-aminoisobutyric acid]$^{-1}$, respectively, which were straight lines. Equations (11) and (20) showed that the plots of k_{obs}^{-1} versus $[TeO_4^{2-}]$ should be linear and the plots of k_{obs}^{-1} versus $[OH^-]$ should also be straight lines. The rate equations derived from the 2 plausible mechanisms were consistent with our experimental results. Hence activation energy and the thermodynamic parameters were evaluated at 298.2 K by the method given earlier (Table 2).

Table 2. Rate constants (k) and the activation parameters for the rate-determining step at 298.2 K

T (K)		283.2	288.2	293.2	298.2	303.2
$k \times 10^2$ (s^{-1})	valine	7.30	9.04	11.71	13.57	17.72
k (mol^{-1}l s^{-1})	2-aminoisobutyric acid	1.96	3.14	5.68	7.93	11.59
Thermody-namic activa-tion param-eters	valine	E_a (kJ mol^{-1}) = 31.07, ΔH^* (kJ mol^{-1}) = 28.67, ΔS^*(J K^{-1} mol^{-1})= −165.22				
	2-aminoisobutyric acid	E_a (kJ mol^{-1}) = 64.05, ΔH^* (kJ mol^{-1}) = 61.61, ΔS^* (J K^{-1} mol^{-1})= −21.25				

The plots of ln$k$ versus 1/T have the following intercept (a) slope (b) and relative coefficient (r): for valine: $a = 10.59$, $b = -3741.63$, $r = -0.997$ and for 2-aminoisobutyric acid: $a = 27.91$, $b = -7704.01$, $r = -0.996$.

CONCLUSIONS

Through the comparative study of oxidation of valine and 2-aminoisobutyric acid by ditelluratocuprate(III), we found that the rate constants of the rate-determining step and the activation parameters for reductants had a great difference. The values of the activation parameters with respect to 2-aminoisobutyric acid were larger than that of valine, which indicated a higher reactivity of valine than that of 2-aminoisobutyric acid. The reason was that the steric stability of 2-aminoisobutyric acid was larger than that of valine, which indicated that the latter could easier react with Cu(III) than the former. The above conclusion was consistent with the experimental results.

REFERENCES

1. J. H. SHAN, Y. P. LIU, H. X. SHEN, J. Y. ZHANG, Y. F. YANG: Kinetics and Mechanism of Oxidation of 3-phenoxy-1,2-propanediol by Ditelluratocuprate(III) in Alkaline Medium. Int J Chem, **2**, 3 (2011).
2. J. H. SHAN, Y. P. LIU, J. Y. ZHANG: Kinetics and Mechanism of Oxidation of 1-methoxy-2-propanol and 1-ethoxy-2-propanol by Ditelluratocuprate(III) in Alkaline Medium. Chin J Chem, **29**, 4 (2011).
3. K. M. NAIK, S. T. NANDIBEWOOR: Kinetic and Mechanistic Study of Oxidation of Succinamide by Diperiodatocuprate(III). Oxid Commun, **35**, 545 (2012).
4. J. H. SHAN, X. Q.WANG, N. ZHAO: Kinetics and Mechanism of Oxidation of Sarcosine by Diperiodatocuprate(III) Complex in Alkaline Medium. Chin J Chem, **7**, 28 (2010).
5. R. H. RAGUNATHARADDI, P. S. NAGARAJ, T. N. SHARANAPPA: Mechanistic Investigation on the Oxidation of Ampicillin Drug by Diperiodatoargentate (III) in Aqueous Alkaline Medium. J Phys Org Chem, **3**, 22 (2009).
6. I. G. JAYANT, R. S. SANJEEVARADDI, T. N. SHARANAPPA: Oxidation of Xylitol by a Silver(III) Periodate Complex in the Presence of Osmium(VIII) as a Homogeneous Catalyst. Catal Sci Technol, **2** (2012).
7. J. H. SHAN, C. H. YIN, L. LIU, Y. P. LIU: Kinetics and Mechanism of Oxidation of 1-methoxy-2-propanol and 1-ethoxy-2-propanol by Ditelluratoargentate(III) in Alkaline Medium. Asian J Chem, **11**, 24 (2012).

8. J. H. SHAN, H. X. SHEN, H. Y. WANG, X. Q. WANG: Kinetics and Mechanism of Oxidation of L-lysine and L-ornithine by Dihydroxydiperiodationickelate(IV) in Alkaline Liquids. Oxid Commun, **35** (2012).

9. F. FEIGL: Spot Tests in Organic Analysis. Elsevier Publishing Co. New York, 1956, p. 208.

10. K. B. REDDY, B. SETHURAM, T. N. RAO: Kinetics of Oxidative Deamination and Decarboxylation of Some Amino Acids by Diperiodatocuprate(III) in Alkaline Medium. Indian J Chem, **20A** (1981).

11. S. CHANDRA, K. L. YADAVA: Oxidation of Some Sugar with Copper(III). Talanta, **15** (1968).

12. P. K. JAISWAL, K. L. YADAVA: Determination of Sugar and Organic Acids with Periodato Complex of Cu(III). Indian J Chem, **11** (1973).

13. F. FEIGL: Spot Tests in Organic Analysis. Elsevier Publishing Co. New York, 1966, p. 196.

14. J. J. JIN: Kinetics Principle of Chemical Reaction in Liquid Phase. Science Technique Press, Shanghai, 1966, p. 186.

EXPRESSION OF ANTIOXIDANT ACTIVITIES OF SOD, APX AND EST ISOENZYMES IN GERMINATING PEANUT SEED AND SEEDLING

SHENGJUAN JIANG*, XIAOLONG ZHANG, CHANGMAO CAO

College of Life Science, Anhui Science and Technology University, 233 100 Anhui Fengyang, China
E-mail: *jiangsjahstu@126.com*

ABSTRACT

Seed germination is a complex multi-stage developmental process accompanied with many distinct metabolic and physiological changes. To ascertain the variations of the isoenzymes, the activities of superoxide dismutase (SOD), ascorbate peroxidase (APX) and esterase (EST) were measured. All assayed enzymes were present in the embryos and cotyledons. The activities of test enzymes increased with the course of germination, except SOD in the embryos. The activity levels of EST in cotyledons remained similar to their levels in embryos, showing that the enzyme played fundamental role in the two parts of seed. The result also showed that SOD probably provided the first line of defense against the toxic effects of elevated levels of reactive oxygen species (ROS) in the early germination process, since they had higher levels of activity compared with other enzymes. As the germination continued, many new isoforms of SOD and APX appeared gradually in embryos and cotyledons of peanut seeds. It was speculated that the SOD and APX isoenzymes were related to ever-changing ROS-controlling network resulted from the metabolism changes during germination and seedling.

Keywords: *Arachis hypogaea*, isoenzymes, germination, superoxide dismutase, ascorbate peroxidase, esterase.

AIMS AND BACKGROUND

Seed germination is a complex multi-stage developmental process accompanied with many distinct metabolic, cellular and physiological changes. Germination is the process through which dormancy is broken, and the mechanism remains largely unknown[1]. Germination begins with the uptake of water by dry quiescent seeds. The appearance of

---

* For correspondence.

the radicle marks the end of germination and the beginning of seedling period[2]. Upon imbibition, the dry quiescent seeds take up water and rapidly resume many fundamental metabolic activities such as respiration and protein synthesis[3]. In the germination course, the oxygen uptake increases, and mitochondrial energy metabolism becomes active. The seedling depends on the aerobic respiration to acquire energy until it grows leaves. Reactivation of mitochondrial metabolism and the respiration results in the production of reactive oxygen species (ROS) which can lead to many damages, such as lipid peroxidation[4]. Germination and seedling establishment are critical phases in the life of a plant and they are very vulnerable to ROS stress. The protection against ROS harms is required during the seed imbibition, germination and seedling stage[5]. Plants have evolved a battery of enzymes that can efficiently destroy ROS radicals, including superoxide dismutase (SOD) and ascorbate peroxidase (APX). SOD (EC 1.15.1.1) is the most effective intracellular enzyme which is ubiquitous in all aerobic organisms and in all sub-cellular compartments prone to ROS mediated oxidative stress[6]. SOD catalyses the dismutation of two superoxide radicals and water into H_2O_2 and O_2. So it removes O^{2-} and hence decreases the risk of OH· formation[7]. APX (EC 1.11.1.11) catalyses the transfer of electrons from ascorbate to peroxides, producing dehydroascorbate and water to detoxify peroxides such as hydrogen peroxide. APX has a higher affinity for H_2O_2 and it is thought to play the most essential role in protecting cells in higher plants. SOD and APX constitute the part of water–water cycle. The balance between SOD and APX activity in cells is considered to be crucial for determining the steady state level of O^{2-} and H_2O_2 (Ref. 8).

Peanut (*Arachis hypogaea*) is well known for its balanced nutrient contents[9]. It accumulates large amounts of oils during the development of their seeds[10]. During the germination, the lipids are aroused and begin to metabolise. Esterase (EST) (EC 3.1.1.1), involved in the metabolism of the lipids, is an important hydrolase enzyme that split esters into an acid and an alcohol in a chemical reaction with water. In order to metabolise the lipids, the peanut seeds need much more oxygen than other seeds. So the oxidisation pressure in peanut seed is severer.

Most studies of antioxidant enzyme activities during seed germination have evaluated the changes caused by stresses, such as ageing[11], metal toxicity[12] and drought conditions[13]. There are few studies which are concerned with the esterase and the antioxidant isoenzymes, such as SOD and APX, during peanut seed germination. In this paper, the activities of SOD, APX and EST were studied to distinguish their differential expressions in different tissues and different germination courses.

EXPERIMENTAL

Plant materials. Peanut (*Arachis hypogaea*) seeds were kept by our laboratory at −80°C. After sterilised with 70% (v/v) ethanol for 40–60 s and followed with treatment of 5% (v/v) sodium hypochlorite (NaOCl) for 20 min on the surface, the seeds were washed with sterile water to remove residual NaOCl.

Seed germination and protein extraction. The seeds were spread onto 2 layers of moistened Whatman No 1 filter paper on a mesh tray and germinated under aseptic conditions at 25°C in the dark. Seeds were taken at 12, 24, 36, 48, 60, 72, 84, and 96 h following the imbibition. The sterilised seeds were straightway used as a control and considered to be the 0 h sample. Each treatment was replicated 3 times.

The cotyledons and the embryos (including the embryonic root and embryonic shoot of the seedling) were collected individually, frozen by liquid nitrogen and stored at –70°C before the preparation of the enzyme solutions. Peanut proteins were extracted from seeds by a modification of the Kang et al. method[14]. In brief, 500 mg of seed tissues with 5 ml of 20 mM *tris*-HCl (pH 8.2) were stirred at 4°C for 30 min, and then the aqueous fraction was collected by centrifugation (3000 rpm) for 5 min at 4°C. The aqueous phase was transferred into fresh chilled Eppendorf tube and subsequently subjected to 2 additional 15-min centrifugations (12 000 rpm) at 4°C to remove residual traces of oil and insoluble particles. The extracts were prepared freshly every time. Soluble seed protein at each time point was measured by the Bradford method and tested by SDS-PAGE (SDS polyacrylamide gel electrophoresis). Each experiment was replicated 3 times. The state analyses of the protein contents were performed by using SPSS statistics software (SPSS Statistics 18, Release. 18.0.0. 2009. Chicago: SPSS Inc.).

Native PAGE and activity staining. For all the enzymes, the solutions were subjected to native PAGE with 10% polyacrylamide gel at 4°C. The detections of SOD and APX were performed by following the method of Shri et al.[12] Activity staining for EST was carried out with a modification of the Carvalho method[15]. The gel equilibrated with water and 100 mM phosphate buffer (pH 6.4) for 5 min, individually. Esterase activity was visualised by submerging the gels in a solution of 200 ml of 100 mM phosphate buffer (pH 6.4) containing 200 mg of α-naphthyl acetate, 200 mg of Fast Blue RR salt, and 10 ml of acetone for 30–60 min with gentle agitation at 37°C. Similar results were obtained in at least 4 independent experiments.

RESULTS

Protein content. During the germination and seedling stages, the concentration of the soluble proteins varied very much because many enzymes came to express by the activation of the seed imbibition. The contents of the protein were measured by the Bradford method (Table 1). The results showed that the contents of protein increased with the time in the embryos and cotyledons. The protein amount of 60 h in the embryos was highest. The possible reason might be that some insoluble proteins became the soluble forms after the imbibition induction. The soluble proteins in the cotyledons increased slowly, implying that the stored proteins gradually began the catabolic process.

Table 1. Soluble protein contents in embryos and cotyledons of germinating peanut seeds and seedling

	Time (h)								
	0	12	24	36	48	60	72	84	96
Embryos (mg/ml)	8.05 ±0.07[i]	15.07 ±0.04[h]	19.08 ±0.03[g]	24.44 ±0.08[c]	20.07 ±0.04[f]	31.88 ±0.05[a]	20.41 ±0.07[e]	24.16 ±0.05[d]	28.48 ±0.03[b]
Cotyledons (mg/ml)	4.05 ±0.09[h]	10.67 ±0.11[g]	14.16 ±0.07[f]	17.25 ±0.06[e]	19.99 ±0.01[b]	19.15 ±0.02[d]	19.52 ±0.02[c]	19.10 ±0.05[d]	20.45 ±0.04[a]

Each observation is a mean±SD. The protein content of different germinating time was compared with respective 0 h sample of embryos and cotyledons in the stat analyses. Values with different superscripts differ significantly ($p<0.05$) ($n=3$).

Activity staining. The data presented in Fig. 1 referred to the expression patterns of SOD, APX and EST isoenzymes isolated from the embryos and cotyledons of the germinating seeds for 0, 12, 24, 36, 48, 60, 72, 84 and 96 h.
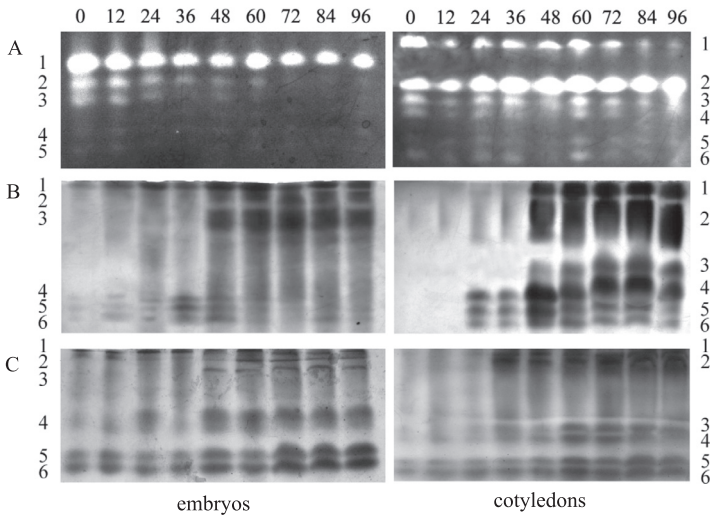
Fig. 1. Activity staining of the isoenzymes of SOD (A), APX (B) and EST (C) in embryos and cotyledons of germinating 0, 12, 24, 36, 48, 60, 72, 84 and 96 h peanut seeds. The top numbers mean the germinating times. The different isoforms are numbered from cathode to anode. The digit (1, 2, 3, 4, 5 and 6) on the left and right means different isoenzymes from the embryos and cotyledons, respectively. One hundred micrograms of protein was loaded in each lane. The similar results were obtained in at least 4 independent experiments

Five and six isoforms of SOD were identified in peanut embryos and in peanut cotyledons, respectively, by native PAGE with activity staining (Fig. 1A). In the embryos, the five SOD isoenzymes were present in all tested time points. SOD 2 and 3 became weaker and weaker with the time. SOD 1 was relatively intense and stable, however, SOD 4 and 5 remained very weak in all tested periods. In peanut cotyledons, all the 6 isoenzymes were present in the test time points. SOD 1 became weaker and

weaker with the time, while the activity of SOD 2 became stronger and stronger. The activities of other isoforms did not fluctuate with the time. Further analyses of the electrophoretic mobility showed that SOD isoform 1 in the cotyledons was the new synthesised band when it was compared with the isoforms in embryos.

Native gel electrophoresis combined with specific activity staining revealed a total number of six APX forms in peanut embryos (Fig. 1B). All isoforms were present in embryos from 48 to 96 h. The isoforms 3 remained intense after it appeared. The similar pattern was found in cotyledons. APX showed a total number of six forms in cotyledons. APX activity was not detected in 0 and 12 h samples. APX isoform 4, 5 and 6 appeared at 24 h sample. The activity of APX isoform 4 increased markedly at 48 h and then remained stable. New isoforms of APX (1, 2 and 3) were synthesised in cotyledons at 48 h and the activity of isoform 2 kept strong. Further analyses showed that five APX isoforms (1, 2, 4, 5 and 6) in cotyledons displayed the same electrophoretic mobility with the isoforms (1, 3, 4, 5 and 6) in embryos.

The electrophoretic pattern of EST showed that a total number of six isoforms existed not only in embryos, but also in cotyledons (Fig. 1C). EST 3 and 4 in the embryos were different with those in the cotyledons by comparisons of the relative electrophoretic mobility. The other EST isoforms in the embryos and cotyledons had similar relative electrophoretic mobility. The enhancements of the intensities of bands 5 and 6 were observed particularly after 48 h in embryos and after 60 h in cotyledons.

DISCUSSION

The imbibition of seeds leads to an increase in the water content inside the cells and initiates a sequence of events, including the respiration and the mobilisation of the cotyledon reserves to the embryo. Those metabolic processes contribute to the release of ROS (Ref. 16). All living organisms produce ROS during normal metabolic processes as by-products or signal transducers. A slight alteration in the homeostatic state of intracellular ROS level signals the cell to modulate its metabolism[17]. The ROS homeostasis results from a shift of the balance between ROS release and the activation of antioxidation system[8].

Peanut, a representative of the oil bearing crop, has many food reserves in the seed. The cotyledons contain the nutrients and food reserves that supply the needs of the seedlings during germination[18]. In the germination course, the mobilisation of the reserves becomes faster[3] and leads to the increase of the protein contents of the embryo. Our measurement of the soluble proteins in the seed showed that the proteins in embryos were relatively abundant. The reason might be that the rich oil in cotyledon influenced the protein extraction amounts of the cotyledons. Our results showed that the isoenzymes in cotyledon had more isoforms on the whole. The results implies that embryo and cotyledon reveal different metabolic activity during the germination and

the seedling stages. This polymorphism also implicates the isozymes perform diverse functions in a broad range of physiological processes[19].

In our experiments, all of these enzymes were present in embryos and cotyledons with different isoenzymes and the synthesis of SOD, APX and EST enzymes were activated to different extent. The activity levels of EST in cotyledons remained similar to their levels in embryos, showing that the enzyme played fundamental roles in the two parts of seed. The whole activity of APX was higher in the cotyledons than in the embryos, indicating that APX preferred to protect cotyledons cells by eliminating ROS. The activities of APX and EST in cotyledons and embryos tended to increase substantially with the experimental time, possibly reflecting a further increase of ROS production. The number and activity of SOD isozymes in embryos decreased with the time, probably implying that in the germination (before 36 h), SOD was the main antioxidant enzymes involved in the scavenging of ROS. So SOD provides the first line of defense against the toxic effects of elevated levels of ROS (Ref. 7). The isoforms with the same electrophoretic mobility in different tissues might perform the similar and vital functions. Many new isoforms of SOD, APX and EST appeared gradually in embryos and cotyledons of peanut seeds as the germination continued. It is speculated that the antioxidant isoenzymes are related to ever-changing ROS-controlling network resulted from the metabolism changes during germination and seedling. In brief, our work fully indicates the pioneer roles of SOD and the fundamental functions of APX and EST, which supplements the researches on isoenzymes in the germination stage.

Isoenzymes exist widely and have plenty of biological functions in a lot of tissues and organisms. Isozymes meet the metabolic special needs, and provide unique metabolic regulation in different tissues and different developmental stages[20]. At the same time, their expressions are under the control of different developmental and environmental stimuli[7]. In the germination and seedling stages, many proteins express, interact and constitute the regulatory networks in the seeds[1]. Germination of *Arabidopsis* seeds can be blocked by a translational inhibitor, but not by a RNA polymerase II inhibitor[21], which implies the importance of the protein translation and regulation. As the members of the network, the isozymes might have the coordinative expression and regulatory mechanisms, however, relatively little is known about them. In our work, the individual expression of the isoenzymes was studied, and it was the fundamental work to research the interactions and regulation mechanisms of them. With the rapid development of proteomics, metabonomics and systems biology, the researches on the isoenzymes would make mighty achievements.

has been approved by all co-authors. The authors have no conflict of interest. We also appreciate comments and suggestions made by editors and anonymous reviewers.

REFERENCES

1. S. PENFIELD, J. KING: Towards a Systems Biology Approach to Understanding Seed Dormancy and Germination. Proc Biol Sci (The Royal Society), **276**, 3561 (2009).
2. D. PRVULOVIC, R. KASTORI, I. KADAR: Effects of Selenium from the Seed on Antioxidant Defense System in Triticale Aestivum Seedlings. Oxid Commun, **33**, 436 (2010).
3. Y. Q. AN, L. LIN: Transcriptional Regulatory Programs Underlying Barley Germination and Regulatory Functions of Gibberellin and Abscisic Acid. BMC Plant Biology, **11**, 105 (2011).
4. D. STOKANOVIC, A. RISTIC-PETROVIC, V. ZIVKOVIC, V. STOKANOVIC, I. PESIC, D. RANCIC, S. LJUBISAVLJEVIC, T. CVETKOVIC, D. PAVLOVIC: The Role of Oxidative Stress in the Etiopathology of Male Infertility. Oxid Commun, **35**, 1038 (2012).
5. R. BACZEK-KWINTA, M. ZACZYNSKI: Antioxidant Aspect of Thermal Hardening of Maize Seedlings. Oxid Commun, **32**, 685 (2009).
6. D. TODOROVA, I. SERGIEV, I. MOSKOVA, V. ALEXIEVA, M. HALL: Oxidative Stress Provoked by Low and High Temperatures in Wild Type and Ethylene-insensitive Mutant Eti5 of *Arabidopsis thaliana* (L.) H e y n h. Oxid Commun, **35**, 651 (2012).
7. S. S. GILL, N. TUTEJA: Reactive Oxygen Species and Antioxidant Machinery in Abiotic Stress Tolerance in Crop Plants. Plant Physiol Bioch (Societe francaise de physiologie vegetale), **48**, 909 (2010).
8. Y. P. LEE, K. H. BAEK, H. S. LEE, S. S. KWAK, J. W. BANG, S. Y. KWON: Tobacco Seeds Simultaneously Over-expressing Cu/Zn-superoxide Dismutase and Ascorbate Peroxidase Display Enhanced Seed Longevity and Germination Rates under Stress Conditions. J Exp Bot, **61**, 2499 (2010).
9. S. JIANG, S. WANG, Y. SUN, Z. ZHOU, G. WANG: Molecular Characterization of Major Allergens Ara h 1, 2, 3 in Peanut Seed. Plant Cell Reports, **30**, 1135 (2011).
10. K. GALLARDO, R. THOMPSON, J. BURSTIN: Reserve Accumulation in Legume Seeds. Comptes rendus biologies, **331**, 755 (2008).
11. P. REVILLA, A. BUTRON, V. M. RODRIGUEZ, R. A. MALVAR, A. ORDAS: Identification of Genes Related to Germination in Aged Maize Seed by Screening Natural Variability. J Exp Bot, **60**, 4151 (2009).
12. M. SHRI, S. KUMAR, D. CHAKRABARTY, P. K. TRIVEDI, S. MALLICK, P. MISRA, D. SHUKLA, S. MISHRA, S. SRIVASTAVA, R. D. TRIPATHI, R. TULI: Effect of Arsenic on Growth, Oxidative Stress, and Antioxidant System in Rice Seedlings. Ecotox Environ Safe, **72**, 1102 (2009).
13. P. GONG, J. ZHANG, H. LI, C. YANG, C. ZHANG, X. ZHANG, Z. KHURRAM, Y. ZHANG, T. WANG, Z. FEI, Z. YE: Transcriptional Profiles of Drought-responsive Genes in Modulating Transcription Signal Transduction, and Biochemical Pathways in Tomato. J Exp Bot, **61**, 3563 (2010).
14. I. H. KANG, P. SRIVASTAVA, P. OZIAS-AKINS, M. GALLO: Temporal and Spatial Expression of the Major Allergens in Developing and Germinating Peanut Seed. Plant Physiol, **144**, 836 (2007).
15. V. M. D. CARVALHO, R. M. MARQUES, A. S. LAPENTA, M. D. F. P. S. MACHADO: Functional Classification of Esterases from Leaves of *Aspidosperma polyneuron* M. A r g. (Apocynaceae). Genet Mol Biol, **26**, 195 (2003).
16. L. WOJTYLA, M. GARNCZARSKA, T. ZALEWSKI, W. BEDNARSKI, L. RATAJCZAK, S. JURGA: A Comparative Study of Water Distribution, Free Radical Production and Activation of Antioxidative Metabolism in Germinating Pea Seeds. J Plant Physiol, **163**, 1207 (2006).
17. A. GUL, M. A. RAHMAN, S. HAMID: Biochemistry of Antioxidants and Their Role in Oxidative Stress Caused by Free Radicals. Oxid Commun, **33**, 682 (2010).

18. D. O. GONZALEZ, L. O. VODKIN: Specific Elements of the Glyoxylate Pathway Play a Significant Role in the Functional Transition of the Soybean Cotyledon during Seedling Development. BMC Genomics, **8**, 468 (2007).

19. M. HERNANDEZ, N. FERNANDEZ-GARCIA, P. DIAZ-VIVANCOS, E. OLMOS: A Different Role for Hydrogen Peroxide and the Antioxidative System under Short and Long Salt Stress in *Brassica oleracea* Roots. J Exp Bot, **61**, 521 (2010).

20. L. de GARA, V. LOCATO, S. DIPIERRO, M. C. de PINTO: Redox Homeostasis in Plants. The Challenge of Living with Endogenous Oxygen Production. Resp Physiol Neurobi, **173** Suppl, S13 (2010).

21. M. KIMURA, E. NAMBARA: Stored and Neosynthesized mRNA in *Arabidopsis* Seeds: Effects of Cycloheximide and Controlled Deterioration Treatment on the Resumption of Transcription during Imbibition. Plant Mol Biol, **73**, 119 (2010).

ROLE OF THE OXIDATIVE STRESS AND ANTIOXIDANTS IN THE DEVELOPMENT OF PSEUDOEXFOLIATION SYNDROME

Z. YILDIRIM[a]*, N. I. UCGUN[b], F. YILDIRIM[c]

[a]*Etimesgut Public Health Laboratory, 06 770 Ankara, Turkey*
E-mail: *zyildirim2004@yahoo.com*
[b]*Second Ophthalmology Clinic, Ankara Numune Education and Research Hospital, 06 100 Ankara, Turkey*
[c]*Duatepe Government Hospital, Clinic of Internal Medicine, 06 900 Polatli, Ankara, Turkey*

ABSTRACT

The aim of the study was to investigate the role of oxidant/antioxidant status and protein oxidation in the development of pseudoexfoliation (PSX) syndrome. The activities of serum superoxide dismutase (SOD), glutathione peroxidase (GPx) and the levels of serum malondialdehyde (MDA), advanced oxidation protein products (AOPP), glutathione (GSH), and vitamin C were measured in 20 patients with PSX and in 20 control subjects without PSX.

The serum MDA and AOPP levels were significantly increased in PSX group when compared to the control group ($p<0.05$). The serum GSH levels and SOD, GPx activities were significantly decreased in the PSX group when compared to the control group ($p<0.05$). It was shown that in the study groups the serum vitamin C levels were unchanged ($p>0.05$). These results support the hypothesis that decreased antioxidant defense system and increased oxidative stress may be important for the development of PSX syndrome.

Keywords: PSX syndrome, oxidative stress, antioxidants, protein oxidation.

AIMS AND BACKGROUND

Pseudoexfoliation (PSX) syndrome is an age-related disease in which abnormal fibril-lar extracellular material is progressively produced and accumulated in intraocular tissues. PSX fibers were identified in connective-tissue portions of many visceral organs such as the heart, lung, gall bladder, kidney, and cerebral meninges. Its ocular manifestations include all structures of the anterior segment, as well as conjunctiva

---

* For correspondence.

and orbital structures. Glaucoma occurs more commonly in eyes of patients with PSX than in those without it. It is suggested that PSX is the most common identifiable cause of glaucoma. Patients with PSX are also predisposed to develop angle-closure glaucoma, and glaucoma in PSX patients has a more serious clinical progress and worse prognosis than primary open-angle glaucoma. PSX syndrome may affect up to 30% of the population older than 60 with a worldwide distribution[1,2].

Accumulation of white material on the anterior lens surface is the most constant diagnostic feature of PSX. The classic pattern consists of 3 different zones that become visible when the pupil is fully dilated. Next to the lens, PSX material is most prominent at the pupillary border. Other important findings of PSX are pigment loss from the iris sphincter and its deposition on anterior chamber structures[1].

Physicians should be alerted by the presence of PSX because of the increased complication risk of intraocular surgery, most commonly zonular dialysis, capsular rupture and vitreous loss during cataract extraction[2].

It is suggested that PSX syndrome is a systemic disorder and associated preliminarily with transient ischemic attacks, stroke, the Alzheimer disease, dementia, systemic hypertension and myocardial infarction[1].

PSX syndrome is also associated with ocular ischemia, iris hypoperfusion, anterior chamber hypoxia, and with a decreased ocular and retroocular micro- and macrovascular blood flow occurring both in patients with and without glaucoma[3,4].

One of the greatest challenges in oxidation research today is the determination of oxidative stress *in vivo*. Because proteins are ubiquitous in all cells and tissues and are susceptible to oxidative modifications, they can serve as useful markers of oxidative stress. The presence of oxidised proteins have been reported in numerous disease conditions[5].

Oxidative stress is one of the initiating factors for the development of cataracts, the most important cause of visual impairment at advanced age. A significant proportion of lenses and aqueous humor taken from cataract patients showed elevated H_2O_2 levels, which can cause lens opacification[6–8].

It is now well known that free radicals and antioxidants enzymes play role in ageing, and oxidative damage has been demonstrated to play major role in ocular disease. Increasing evidence indicates that oxidative stress plays a key role in pathogenesis of PSX syndrome[1]. The pathogenesis and mechanisms underlying open PSX and the subsequent progression of PSX and exfoliative glaucoma (XFG) remain unknown[1].

Our purpose was to investigate the role of protein and lipid peroxidation, and role of antioxidants in the development of PSX syndrome. Therefore, we measured the activities of superoxide dismutase (SOD) and glutathione peroxidase (GPx) enzymes and serum levels of malondialdehyde (MDA), advanced oxidation protein products (AOPP), glutathione (GSH), and vitamin C in patients with PSX and control subjects without PSX.

EXPERIMENTAL

Subjects. In this study 20 nuclear cataract patients with PSX, 10 men and 10 women (mean±SD; 72.18±9.10 years, (50–90)) were included. The control group (nuclear cataract patients without PSX) included 20 individuals, 10 men and 10 women (mean±SD; 64.95±11.23 years, (36–80)). There were no statistically significant differences between the groups in terms of age and sex. Patients with other ophthalmic conditions (e.g. glaucoma, uveitis, progressive retinal disease) and systemic diseases (e.g. diabetes, arthritis, coronary arterial disease, periferic vascular disease) were excluded.

All subjects both in the control group and the patient group filled out a questionnaire giving the following information: age, gender, no smoking habits, no supplements such as vitamins and/or antioxidants. Human Ethics Committee rules were satisfied.

All patients underwent a comprehensive ophthalmic examination and were examined prior to surgery after pupillary dilation for the presence of exfoliation material. Only patients who exhibited exfoliation material upon the lens or pupil were included. Grade 2–3 nuclear cataract patients were included in the study if visual acuity was 1–4 Snellen lines. All patients included in this study had intraocular pressure lower than 20 mm Hg.

The serum samples before the operation during cataract surgery were obtained. Blood samples were drawn from the patients and the controls after the overnight fasting, then centrifuged as soon as possible at $2000 \times g$ for 10 min at 4°C. Serum samples were stored at −70°C until the analyses are carried out.

Methods. AOPP levels were measured by a spectrophotometric method (Schimadzu UV 1601 spectrophotometer, Schimadzu, Tokyo, Japan) in the presence of potassium iodide at 340 nm (Ref. 9) and calibrated with chloramine-T solutions. AOPP levels were expressed in micromoles chloramine-T equivalents per l.

Lipid peroxidation was estimated using the thiobarbituric acid reactive substances (TBARS) test as described previously[10]. Briefly, TBARS formation was quantitated using 1,1,3,3-tetraethoxypropane as standard, and the absorbances of the TBARS were read at 532 nm using a Schimadzu UV 1601 spectrophotometer, Schimadzu, Tokyo, Japan.

The GSH levels were determined as R–SH (Ref. 11) 0.5 ml of each sample was mixed with 1 ml of a solution containing 100 mM Tris-HCl (pH 8.2), 1% sodium dodecyl sulfate, and 2 mM ethylenediaminotetraacetic acid. The mixture was incubated for 5 min at 25°C and centrifuged to remove any precipitate. 5,5-dithiobis (2-nitrobenzoic acid) (DTNB) 0.3 mM was then added to each reaction volume and incubated for 15 min at 37°C. The absorbance of each sample was determined at 412 nm. The R–SH levels were calculated assuming a molar extinction coefficient of 13 000 mol^{-1} cm^{-1} at 412 nm.

The SOD activity measurements were carried out by inhibiting the SOD activity by nitroblue tetrazolium reduction. Xanthine-xanthine oxidase was used as a superoxide generator, and 1 IU was defined as the quantity of SOD required to produce 50% inhibition[12].

The GPx activity was determined spectrophotometrically as described in literature[13]. The reaction mixture containing 50 mM phosphate buffer pH 7.4, 7.7 unit GSH reductase, 5 mM GSH, and crude extract was preincubated for 5 min at 37ºC. Thereafter, 20 µl nicotinamide adenine dinucleotide phosphate, reduced form (NADPH) (0.3 mM) solution, was added and the hydroperoxide-independent consumption of NADPH was monitored for about 5 min. The overall reaction was started by adding 20 µl of prewarmed hydroperoxide solution (0.025 mM) and decrease in absorption at 340 nm was monitored.

The total ascorbate was determined by the modified Roe and Kuether method[14]. Serum samples were added to trichloroacetic acid solution and centrifuged at $3000 \times g$ for 10 min. 2,4-dinitrophenylhydrazine-thiourea-copper sulphate reagent was added to the serum sample tubes. The contents of each tube were mixed, capped with parafilm, and placed in a water bath 37ºC for 4 h. The tubes were removed and cooled in ice water. Ice-cold 65% sulphuric acid solution was added and mixed thoroughly. The mixture was allowed to stand at room temperature for 30 min, and absorbance was read in a Schimadzu UV 1601 model spectrophotometer at 515 and 520 nm, respectively. The lower limit of detection for vitamin C was 0.05 µmol/l.

Statistical analysis. Data were presented as the mean±SD. Statistical analyses were carried out by the Mann-Whitney *U*-test (SPSS for Windows 11.5; SPSS, Chicago, IL, USA). $p < 0.05$ was taken as significant.

RESULTS AND DISCUSSION

This study included a total of 40 subjects who were equally divided into 2 groups; PSX group and control group. The mean age was 72.18±9.10 (50–90) (10 men, 10 women) years in the PSX group and 64.95±11.23 (36–80) (10 men, 10 women) years in the control group. All groups were matched for age and gender and no statistically significant difference was observed. The serum MDA and AOPP levels were significantly higher in the PSX group when compared to the control group ($p < 0.05$) (Table 1). The serum GSH levels and SOD, GPx activities were significantly lower in the PSX group when compared to the control group ($p < 0.05$) (Table 1). It was shown that in the study group the serum vitamin C levels were unchanged ($p > 0.05$) (Table 1).

Table 1. Serum superoxide dismutase (SOD), glutathione peroxidase (GPx) activities and malondialdehyde (MDA), advanced oxidation protein products (AOPP), glutathione (GSH), and vitamin C levels in PSX patients and the control group (mean±SD)

Groups	PSX group (n=20)	Control group (n=20)
SOD (U/ml)	8.65±1.64*	10.16±4.44
	(5.87–10.94)	(0.22–16.45)
GPx (U/ml)	13.10±6.60*	23.25±17.55
	(5.04–27.91)	(0.62–75.80)
MDA (nmol/l)	8.82±3.15*	5.47±1.71
	(4.95–16.12)	(2.50–9.08)
AOPP (µmol/l)	226.99±47.59*	187.05±43.65
	(151.75–339.34)	(131.07–278.31)
GSH (nmol/ml)	262.05±73.98*	369.65±62.22
	(163.51–380.47)	(284.22–523.6)
Vitamin C (µmol/l)	2.83±1.29	2.78±1.19
	(0.90–5.14)	(0.62–5.57)

*$p < 0.05$, as compared to the control group.

The eye is an exceptional organ because of its continuous exposure to environmental chemicals, radiation, and atmospheric oxygen[15]. These oxidative stress has been implicated in the possible pathophysiology of different ocular diseases, such as cataract, age-related macular degeneration, glaucoma, uveits, and PSX syndrome[15]. Several ocular degenerative disorders have been studied, and evidences of oxidative stress were demonstrated in terms of markers of lipid peroxidation, activity of antioxidant enzymes, and the levels of low-molecular weight antioxidants[16].

The lenses are often under the threat of oxidative stress. Biochemical evidence demonstrates that proteins and lipids undergo oxidative damage by free radicals. The proteins are important as the contents of cytoplasm within the fibre cells and lipoproteins are important in the cell membranes of the lens cells. Free radicals are neutralised by the antioxidant enzymes and by the antioxidant vitamins. Therefore it should be helpful to enhance the antioxidant status of the eye by nutritional means to promote eye health and to prevent cataracts[17].

There are several studies on relationships between oxidative stress and the progression of PSX syndrome[2,6,13,18].

Because MDA has been found to be elevated in various diseases it is thought to be related to free radical damage, determination of serum MDA levels is still the most commonly applied assay for lipid peroxidation in biomedical sciences[18]. It was demonstrated that the serum MDA levels were higher in PSX subjects[19], and Gartaganis et al.[20] found high levels of TBARS in aqueous humor of patients with PSX, reflecting free radical damage to lipid peroxides. In the present study it was determined that the serum MDA levels were significantly higher in the PSX group when compared to the control group, as in agreement with previous studies[19,20].

The complete chemical composition of PSX material remains unknown in spite of extensive research. An overproduction and abnormal metabolism of glycosaminoglycans have been proposed as the major changes in PSX. The protein components of PSX contain both noncollagenous basement membrane components and elastic fiber system such as fibrillium[1,2]. Regardless of etiology, typical PSX fibres have been shown electron microscopically in close association with the pre-equatorial lens epithelium, the non-pigmented ciliary epithelium, the iris pigment epithelium, the corneal endothelium, the trabecular endothelium, and with almost all cell types of the iris stroma, such as fibrocytes, melanocytes, vascular endothelial cells, pericytes, and smooth muscle cells[1,2].

Biochemical analyses are impeded by insufficient amounts of available material, by the insolubility of the material and by lack of experimental models. Indirect histochemical and immunohistochemical evidence suggests a complex glycoprotein/proteoglycan-structure which is composed of a protein core surrounded by glycoconjugates, probably glycosaminoglycans, also forming the amorphous ground substance[21,22]. PSX material is resistant to degradation by most enzymes including collagenase, trypsin, pepsin, and papain[23].

AOPP measurements reflect free radical generation and the degree of protein oxidation[9,24]. In the present study it was determined that the serum AOPP levels were significantly higher in the PSX group when compared to the control group. It was demonstrated that the aqueous humour and serum protein carbonyl (PC) levels were higher in patients with PSX compared to control[3]. Therefore, this study demonstrated that protein oxidation, a useful oxidative stress marker, increased in PSX syndrome, suggesting increased oxidative stress. These findings becomes more important when PSX is considered as an age-related disease.

Antioxidant enzymes are considered to be a primary defense system preventing biological macromolecules from oxidative damage. SOD is an antioxidant key enzyme in the metabolism of oxygen free radicals[25]. Ucakhan et al.[26] showed an increase in SOD activity in the lens capsule of patients with PSX. However, Yagci et al.[18] showed a decrease in serum SOD activity. In the present study it was determined that the serum SOD activities were significantly lower in the PSX group when compared to the control group.

The free radicals are produced continuously and are detoxified by the antioxidant defense system enzymes SOD, GPx, and CAT. Some authors measured a greatly reduced total antioxidative capacity of aqueous humor in PSX eyes with and without glaucoma, together with a decreased activity of antioxidative enzymes, such as CAT and GPx[22,27]. The reduced antioxidative enzymes, for example microsomal glutathione-S-transferase (mGST-1), in anterior segment tissues seem to confirm a defective protection against oxidative stress[2]. In the present study it was determined that the serum GPx activities were significantly lower in the PSX group when compared to the control group.

GSH is also one of the major defense systems in the retina. A high concentration of GSH is present in most living cells and is known to be involved in responses to various stresses. Redox situation of cells is linked to the protection by GSH in reduced state. It protects retina from the toxic effects of ROS (Ref. 28).

Gartaganis et al.[20] found low levels of GSH in aqueous humor of patients with PSX. In the present study it was determined that the serum GSH levels were significantly lower in the PSX group when compared to the control group.

There is increasing evidence that cellular stress conditions, as oxidative stress and ischemia constitute major mechanisms involved in the pathobiology of PSX syndrome[6]. Greatly reduced levels of ascorbic acid, the most effective free radical scavenger in the eye, and concomitantly increased levels of oxidative stress markers suggest a faulty antioxidative defence system and increased oxidative stress in the anterior chamber of PSX eyes[6].

Ascorbic acid may be reduced in the aqueous humour of patients PSX suggesting a role for free radical-induced oxidative damage in PSX pathobiology[6].

Yilmaz et al.[19] reported much lower antioxidant, serum vitamin C concentrations in PSX subjects. There are other studies demonstrating significantly lower concentrations of ascorbic acid in the aqueous humour of patients with PSX when compared with control groups with PSX (Refs 6 and 18). In the present study it was determined that in the study groups the serum vitamin C levels were unchanged. It is observed that there is no effect of vitamin C on the development of PSX syndrome according to the results of vitamin C in the study.

The loss of the antioxidant protection and the impairment of the protein redox status in the lens of PSX patients may be important factors associated with the onset of ocular complications during ageing. Oxidative events are of great importance in PSX complications and, particularly in the lens may have a role in the pathogenesis of PSX as exihibited in this study.

CONCLUSIONS

In conclusion, our findings indicate that free radical action together with a depleted antioxidant defense system may represent important molecular mechanisms in the development of PSX. Further in-depth studies including both serum and aqueous humour parameters are required to investigate and support our findings.

ACKNOWLEDGEMENTS

REFERENCES

1. R. RITCH, U. SCHLOTZER-SCHREHARDT: Exfoliation Syndrome. Surv Ophthalmol, **45**, 265 (2001).
2. U. SCHLOTZER-SCHREHARDT, G. O. NAUMANN: Ocular and Systemic Pseudoexfoliation Syndrome. Am J Ophthalmol, **141**, 921 (2006).
3. N. YUKSEL, V. L. KARABAS, A. ARSLAN, A. DENIRCI, Y. CAGLAR: Ocular Hemodynamics in Pseudoexfoliation Syndrome and Pseudoexfoliation Glaucoma. Ophthalmol, **108**, 1043 (2001).
4. O. OCAKOGLU, N. KOYLUOGLU, A. KAYIRAN, N. TAMCELIK, S. OZKAN: Microvascular Blood Flow of the Optic Nerve Head and Peripapillary Retina in Unilateral Exfoliation Syndrome. Acta Ophthalmol, **82**, 49 (2004).
5. R. YAGCI, I. ERSOZ, M. ERDURMUS, A. GUREL, S. DUMAN: Protein Carbonyl Levels in the Aqueous Humour and Serum of Patients with Pseudoexfoliation Syndrome. Eye, **22**, 128 (2008).
6. G. G. KOLIAKOS, A. G. KONSTAS, U. SCHLOTZER-SCHREHARDT, G. HOLLO, I. E. KAT-SIMBRIS, N. GEORGIDIS, R. RITCH: 8-Isoprostaglandin F_2a and Ascorbic Acid Concentration in the Aqueuos Humour of Patients with Exfoliation Syndrome. Br J Ophthalmol, **87**, 353 (2003).
7. G. LAGANOVSKA, A. MARTINSONS, B. PITRANS, B. WIDNER, D. FUCHS: Kynurenine and Neopterin in the Aqueous Humour of the Anterior Chamber of the Eye and in Serum of Cataract Patients. Adv Exp Med Biol, **527**, 367 (2003).
8. C. DELCOURT, I. CARRIERE, M. DELAGE, B. DESCOMPS, J. P. CRISTOL, L. PAPOZ: Associations of Cataract with Antioxidant Enzymes and Other Risk Factors: the French Age-related Eye Diseases (POLA) Prospective Study. Ophthalmol, **110**, 2318 (2003).
9. V. WITKO-SARSAT, M. FRIEDLANDER, C. CAPEILLERE-BLANDIN, T. NGUYEN-KHOA, A. T. NGUYEN, J. ZINGRAFF, P. JUNGERS, B. DESCAMPS-LATSCHA: Advanced Oxidation Protein Products as a Novel Marker of Oxidative Stress in Uremia. Kidney Int, **49**, 1304 (1996).
10. T. YOSHIOKA, K. KAWADA, T. SHIMADA, M. MORI: Lipid Peroxidation in Maternal and Cord Blood and Protective Mechanism against Activated-oxygen Toxicity in the Blood. Am J Obstet Gynecol, **135**, 372 (1979).
11. H. KURTEL, D. N. GRANGER, P. TSO M. B. GRISHAM: Vulnerability of Intestinal Interstitial Fluid to Oxidant Stress. Am J Physiol, **263**, 573 (1992).
12. Y. SUN, L. W. OBERLEY, Y. LI: A Simple Method for Clinical Assay of Superoxide Dismutase. Clin Chem, **34**, 497 (1988).
13. D. E. PAGLIA, W. N. VALENTINE: Studies on the Quantitative and Qualitative Characterization of Erytrocyte Glutathione Peroxidase. J Lab Clin Med, **70**, 158 (1967).
14. L. W. MAPSON: The Estimation of Dehydro-L-ascorbic Acid when Present in Low Concentration in Tissues, by the Roe and Kuether Procedure. Ann N Y Acad Sci, **92**, 284 (1961).
15. S. E. OHIA, C. A. OPERE, A. M. LEDAY: Pharmacological Consequences of Oxidative Stress in Ocular Tissues. Mutat Res, **579**, 22 (2005).
16. B. HALLIWELL, J. GUTTERIDGE: Free Radicals in Biology and Medicine. 3rd ed. Oxford University Press Inc, New York, 1989, 1–35.
17. G. G. KOLIAKOS, A. G. KONSTAS, U. SCHLOTZER-SCHREHARDT, T. BUFIDIS, N. GEORGIADIS, A. RINGVOLD: Ascorbic Acid Concentration Is Reduced in the Aqueuos Humour of Patients with Exfoliation Syndrome. Am J Ophthalmol, **134**, 879 (2002).
18. R. YAGCI, A. GUREL, I. ERSOZ, U. C. KESKIN, I. F. HEPSEN, S. DUMAN, R. YIGITOGLU: Oxidative Stress and Protein Oxidation in Pseudoexfoliation Syndrome. Curr Eye Res, **31**, 1029 (2006).
19. A. YILMAZ, U. ADIGUZEL, L. TAMER, O. YILDIRIM, O. OZ, H. VATANSEVER, B. ERCAN, U. DEGIRMENCI, U. ATIK: Serum Oxidant/Antioxidant Balance in Exfoliation Syndrome. Clin Experiment Ophthalmol, **33**, 63 (2005).

20. S. P. GARTAGANIS, C. D. GEORGAKOPOULOS, N. E. PATSOUKIS, S. S. GOTSIS, V. S. GARTAGANIS, C. D. GEORGIOU: Glutathione and Lipid Peroxide Changes in Pseudoexfoliation Syndrome. Curr Eye Res, **8**, 647 (2005).
21. M. DAVANGER: On the Interfibrillar Matrix of the Pseudo-exfoliation Material. Acta Ophthalmol (Copenh), **56**, 233 (1978).
22. M. DAVANGER: Studies on the Pseudo-exfoliation Material: A Review. Albrecht Von Graefes Arch Klin Exp Ophthalmol, **208**, 65 (1978).
23. J. H. SELAND: Histopathology of the Lens Capsule in Fibrillopathia Epitheliocapsularis (FEC) or so-called Senile Exfoliation or Pseudoexfoliation. An Electron Microscopic Study. Acta Ophthalmol (Copenh), **57**, 477 (1979).
24. C. J. ALDERMAN, S. SHAH, J. C. FOREMAN, B. M. CHAIN, D. R. KATZ: The Role of Advanced Oxidation Protein Products in Regulation of Dendritic Cell Function. Free Radic Biol Med, **32**, 377 (2002).
25. J. J. ENGHILD, I. B. THOGERSEN, T. D. OURY, Z. VALNICKOVA, P. HOJRUP, J. D. CRAPO: The Heparin-binding Domain of Extracellular Superoxide Dismutase Is Proteolytically Processed Intracellularly during Biosynthesis. J Biol Chem, **274**, 14818 (1994).
26. O. O. UCAKHAN, F. KAREL, A. KANPOLAT, E. DEVRIM, I. DURAK: Superoxide Dismutase Activity in the Lens Capsule of Patients with Pseudoexfoliation Syndrome and Cataract. J Cataract Refract Surg, **32**, 618 (2006).
27. L. ZORIC, D. MIRIC, S. MILENKOVIC, P. JOVANOVIC, G. TRAJKOVIC: Pseudoexfoliation Syndrome and Its Antioxidative Protection Deficiency as Risk Factors for Age-related Cataract. Eur J Ophthalmol, **16**, 268 (2006).
28. M. PENNINCKX: A Short Review on the Role of Glutathione in the Response of Yeasts to Nutritional, Environmental, and Oxidative Stresses. Enzyme Microb Technol, **26**, 737 (2000).

CoMFA AND CoMSIA ANALYSES OF CARBONIC ANHYDRASE II INHIBITORS

(*Dedicated to the memory of Prof. Padmakar V. Khadikar*)

S. SINGH*, A. DAS MANIKPUR, P. V. KHADIKAR

QSAR and Cheminformatics Laboratory, Department of Chemistry, Bareilly College, Bareilly, India
E-mail: shalinisingh_15@yahoo.com

ABSTRACT

Quantitative structure–activity relationship (3D-QSAR) analyses were performed on a set of 30 substituted benzene-sulphonamides for the estimation of their human CAII binding constant (lg *K*). Both comparative molecular field analysis (CoMFA) and comparative molecular similarity indices analysis (CoMSIA) models using database alignment gave good internal predictions with cross-validated analyses. The results are critically discussed using a variety of statistical parameters. Results indicate that the CoMFA and CoMSIA models could be reliable model which may be used in the design of novel carbonic anhydrase inhibitors as leads.

Keywords: CoMFA , CoMSIA, 3D-QSAR, carbonic anhydrase II.

AIMS AND BACKGROUND

Carbonic anhydrases (CAs, EC 4.2.1.1) are ubiquitous metallo-enzymes present in prokaryotes and eukaryotes. They are encoded by 4 distinct evolutionarily unrelated gene families: the α-CAs (present in vertebrates, bacteria, algae, and cytoplasm of green plants), the β-CAs (predominantly in bacteria, algae, and chloroplasts both of mono- as well as dicotyledons, the γ-CAs (mainly in archaea and some bacteria), and the δ-CAs present in some marine diatoms, respectively[1,2]. In mammals, 15 different α-CA isozymes or CA-related proteins (CARP) were described, with very different catalytic activity, sub-cellular localisation, tissue distribution, and susceptibility and are inhibited by sulphonamides[1–5]. There are several cytosolic forms: CAI–III, CAVII and CAXIII, 4 membrane-bound isozymes: CAIV, CAIX, CAXII, and CAXIV, two mitochondrial forms (CAVA and CAVB), as well as a secreted CA isozyme (in saliva and milk) CAVI. The carbonic anhydrase-related proteins (CARPs) are CAVIII,

---

* For correspondence.

CAX and CAXI. These enzymes catalyse a very simple physiological reaction, the inter-conversion between carbon dioxide and the bicarbonate ion, and are thus involved in crucial physiological processes connected with respiration and transport of CO_2/bicarbonate between metabolising tissues and lungs, pH and CO_2 homeostasis/ electrolyte secretion in a variety of tissues/organs, biosynthetic reactions (such as gluconeogenesis, lipogenesis, and ureagenesis), bone resorption, calcification, tumorigenicity, and many other physiologic/pathologic processes[1,2]. CAII inhibitors have a wide range of applications as diuretics, antiepileptic, as agents for the treatment of glaucoma, gastro-duodenal ulcers, certain neurological disorders, motions, altitude sickness and modulators of cancer chemotherapy[3,4]. The development of topical CA inhibitors for the treatment of glaucoma, dorzolamide and brinzolamide, has renewed the pharmacological interest for this enzyme[3,4]. The synthesis and testing of a wide variety of new drugs, which could inhibit CA secretory activity is a continual goal in the medicinal chemistry. However, very little work is performed on CoMFA and CoMSIA analysis of this class of compounds. This has prompted us to undertake the present work. Supuran and Khadikar have carried out an exhaustive 2-D QSAR studies on carbonic anhydrase inhibitors and activators using topological indices. However, they have not performed 3D CoMFA and CoMSIA analysis. This was the main objective of the present work. Since, isozyme CAII is known for decades to be physiologically important, we have undertaken the present investigation in that we have modelled binding constant (lg K) of benzene sulphonamides to human CAII using famous 3-D QSAR comparative molecular field analysis (CoMFA) and comparative molecular similarity indices analysis (CoMSIA). Carbonic anhydrase II (CAII) [E.C. 4.2.1.1] is an ubiquitous and physiologically highly relevant isoform. It is a highly efficient catalyst for the reversible hydration of carbon dioxide through a 2-step, zinc-hydroxide mechanism described by equations (A) and (B) below:

$$Zn^{2+}-OH + CO_2 \rightleftharpoons Zn^{2+} + HCO_3^- \qquad (A)$$

$$Zn^{2+} + H_2O \rightleftharpoons H^+ + Zn^{2+}-OH^- \qquad (B)$$
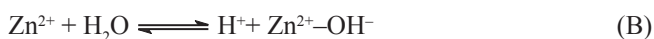
CAII can also hydrate aldehydes and hydrolyse some esters. It is a well characterised enzyme whose 3-dimensional structure has been determined by X-ray crystallography in the absence and presence of inhibitors[2–4]. The active site of human CAII (hCAII) contains a catalytically essential zinc ion in tetrahedral geometry. The metal ion is coordinated by 3 imidazolic nitrogen atoms belonging to His94, His96 and His119 and 1 oxygen atom from a water molecule/hydroxyl ion. At physiological pH, aromatic and heterocyclic unsubstituted sulphonamides ($R-SO_2NH_2$), which are known to inhibit CAs, have an ionised sulphonamide group (pK_a 6 ~ 10). Upon binding, the sulphonamide group displaces the water from the zinc coordination sphere. Substitution of the $R-SO_2NH_2$ hydrogen substantially decreases the CA inhibitory activity due to steric hindrance. The aromatic side chains of sulphonamide inhibitors interact with many amino acid residues in the binding site (e.g. Phe131, Leu141, Val143, and Ala145) and stabilise the interaction. Unsubstantiated amides ($R-CONH_2$)

such as urethane, phenyl carbamate are a second, albeit much less potent, class of known CA-II inhibitors. It contrast to sulphonamides, the CA inhibitors anions such as SCN^-, ClO_4^-, I^- are also weak CAII inhibitors with K (inhibition constant) values of $8 \sim 30$ M, since they only coordinate zinc and lack other stabilising interactions. In summary, a negativity charged Zn ion coordinator and suitable hydrophobic moieties are thought to be the important structural requirement of CAII inhibitors.

EXPERIMENTAL

MOLECULAR MODELLING

3-dimensional quantitative structure–activity relationship (QSAR) studies have been found to be of great importance to design and develop potent drugs. QSAR greatly helps to modify the structures of the compounds leading to the compounds of high therapeutic value[6–8]. The structure details of the substituted benzene-sulphonamides and biological activities data were obtained from literature[9–13]. The values of lg K used as the biological activity characteristics in the 3D QSAR study are given in Table 1.

Three-dimensional structure building and modelling were performed using the Sybyl 7.2 program package 55 on a personal computer Dell Precision Workstation 370 dt. Molecular building was done with molecular sketch program. Geometry optimisation was carried out using MAXMIN molecular mechanics and tripos force field Gasteiger–Huckle charge supplied Sybyl 7.2, with the convergence criterion CoMFA and CoMSIA analyses. QSAR models were randomly derived from a training set of 20 molecules. An external test set consisting of 9 molecules was used to validate the CoMFA and CoMSIA. The most active molecule **11** was used as the template molecule for alignment. A common substructure-based alignment adopted in the present study is attempted to align molecules to the template molecule on a common backbone. The best fit conformation and sub-structure used for alignment are shown in Figs 1 and 2.

Table 1. Structural details of benzene sulphonamides and their binding constants in lg units
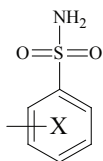
Com. No	X	lg K
1	H	6.69
2	4-Me	7.09
3	4-Et	7.53
4	4-nPr	7.77
5	4-nBu	8.30
6	4-nAm	8.86
7	4-COOMe	7.98
8	4-COOEt	8.50
9	4-COO-n-Pr	8.77
10	4-COO-n-Bu	9.11
11	4-COO-n-Am	9.39
12	4-COO-n-He	9.39
13	4-CONHMe	7.08
14	4-CONHEt	7.53
15	4-CoNH-n-Pr	8.08
16	4-CONH-n-Bu	8.49
17	4-CONH-n-Am	8.75
18	4-CONH-n-He	8.88
19	4-CONH-n-Hp	8.93
20	3-COOMe	5.87
21	3-COOEt	6.21
22	3-COOPr	6.44
23	3-COOBu	6.95
24	3-COOAm	6.86
25	2-COOMe	4.41
26	2-COOEt	4.80
27	2-COOPr	5.28
28	2-COOBu	5.76
29	2-COOAm	6.18

Note: Am – pentyl; He – hexyl; Hp – heptyl; Me – methyl; Et – ethyl; Pr – propyl; Bu – butyl; lg K - binding constant of the benzene sulphonamide to human CAII.
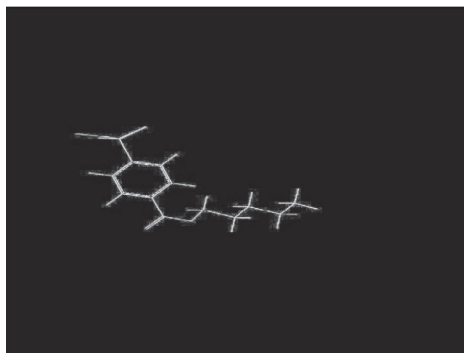
Fig. 1. Best fit conformation
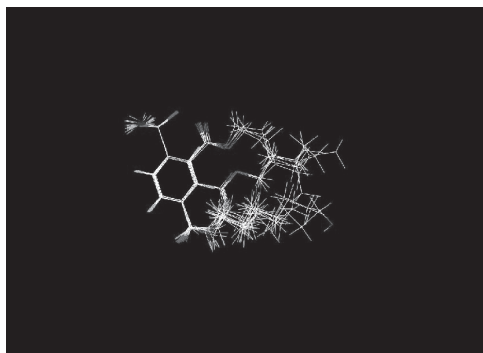
Fig. 2. Alignment of molecule by database

CoMFA ANALYSIS

The CoMFA analysis of the afore-mentioned molecules was carried out on the steric and electrostatic fields using field with default values. The steric and electrostatic CoMFA potential fields were calculated at each lattice interaction of a regularly spaced grid of 2.0 Å. The steric and electrostatic fields were calculated separately for each molecule using sp^3 carbon atom probe with charge of +1, respectively, with Tripos force field (default probe atom in Sybyl) and energy cut-off values of 30 kcal/mol for both steric and electrostatic fields.

CoMSIA ANALYSIS

The CoMSIA descriptors were derived with the same lattice box, which was used in CoMFA calculation. Five CoMSIA similarity index fields available within Sybyl (steric, electrostatic, hydrophobic, hydrogen bond donor, and hydrogen bond acceptor) were evaluated using the probe atom. The Gaussian type distance dependence was between the grid point and each atom of molecule and default value of 0.3 was used as attenuation factor.

Partial least square (PLS) method[14] was applied to generate 3D-QSAR models. The PLS algorithm with the leave-one-out[15] cross-validation method was employed to choose the optimum number of components and to assess the statistical significance of each model. All cross-validation PLS analyses were performed with a column filters values of 2.0. The cross-validated coefficient, q^2, was calculated using the following equation:

$$q^2\,(r^2_{cv}) = 1 - \frac{\sum (Y_{pred} - Y_{obs})^2}{\sum (Y_{obs} - Y_{mean})^2}\,, \tag{1}$$

where Y_{pred}, Y_{obs}, and Y_{mean} are predicted, actual, and mean values of the target inhibitory activity (A), respectively.

The optimum number of components was chosen which gave less standard error of prediction and high r^2_{cv}. In addition, the r^2_{cv} and number of components, the conventional correlation coefficient r^2 and its standard error were also computed for model. The predictive r^2 (r^2_{pred}) value was calculated using the following equation:

$$r^2_{pred} = SD\text{-}PRESS/SD \tag{2}$$

where SD is the sum of squared deviations between biological activity of the test set and mean activity of training set molecules, and PRESS – the sum of squared deviations between the actual and the predicted activity values for every molecule in the test set.

In addition, r^2_{cv}, r^2_{pred} and the number of components, the conventional correlation coefficient r^2 and its standard error were also computed for model. The CoMFA and CoMSIA results were graphically interpreted by field contribution maps using the STDEV * COEFF: field type. The boot strapping procedure was used to validate each model. This is a procedure in which 10 times random selection out of the original set of 10 objects are performed several times, to simulate different sampling from a larger set of objects. In each run some objects may not be included in the PLS analysis (same method to determine q^2), whereas some other might be included more than once confident intervals for each term can be estimated from such a procedure, giving an independent measure of the stability of the PLS model.

RESULTS AND DISCUSSION

The CoMFA and CoMSIA approaches were used to estimate binding constant (lg K) of the benzene sulphonamides under present study. CoMFA steric and electrostatic field with 2 regions in CoMFA (never region) and steric cut of each any row (energy cut-off values of 30 kcal/mol for both steric and electrostatic and grid spacing was 2.0 Å) and obtained 2 models offers different fields. CoMSIA offers 5 different fields – steric, electrostatic, hydrophobic, H-bond donor and H-bond acceptor, which were calculated at each lattice interactions of a regularly spaced grid of 2.0 Å. A probe

atom with radius 1.0 Å, +1 charge, hydrophobicity+1.0, and H-bond donor and acceptor properties of +1.0 was used to calculate steric, electrostatic, hydrophobic, and H-bond donor and acceptor fields. Table 2 summarises the predicted results obtained from the CoMFA and CoMSIA models.

Table 2. CoMFA and CoMSIA results (statistical data for QSAR models using CoMFA and CoMSIA along with database alignment)

CoMFA (comparative molecular field analysis)		
Region	steric cut of each any row	never
Field	steric and electrostatic	steric and electrostatic
q^2	0.895	0.948
S_{PRESS}	0.521	0.391
ONC	3	5
r^2_{nv}	0.980	0.998
SD	0.227	0.071
F	262.228	1646.157
R^2_{bs}	0.983	0.999
SD_{bs}	0.010	0.001
r^2_{cv}	0.895	0.949
Fraction		
S	0.747	0.596
E	0.253	0.404
r^2_{pred}	**0.770**	**0.845**

CoMSIA (comparative molecular similarity indices analysis)					
Field	S	H	HA	HD	E
q^2	0.871	0.926	0.704	0.593	0.85
S_{PRESS}	0.616	0.468	0.874	1.024	0.880
ONC	5	5	3	3	11
r^2_{nv}	0.970	0.986	0.891	0.832	0.998
SD	0.299	0.207	0.684	0.658	0.097
F	89.126	190.334	24.061	26.383	395.497
R^2_{bs}	0.999	0.996	0.821	0.846	0.999
SD_{bs}	0.007	0.002	0.088	0.082	0.001
r^2_{cv}	0.775	0.919	0.700	0.592	0.790
r^2_{pred}	**0.775**	**0.641**	**0.954**	**0.504**	**0.003**

Note: S – steric; H – hydrophobic; HA – hydrogen-bond acceptor; DA – hydrogen-bond donor; E – electrostatic; q^2 – cross-validated correlation Loo (leave-one-out); S_{press} – standard error of prediction, ONC – optimum number of components; r^2_{nv} – no validation of correlation coefficient – standard error of estimate by n; F – the Fisher value; R^2_{bs} – correlation coefficient of boot strapping; R^2_{sd} – standard error of estimate from bootstrapping; SD_{bs} – standard deviation of boot strapping; r^2_{cv} – cross-validated correlation coefficient; r^2_{pred} – correlation coefficient of the prediction test set.

The results obtained from the PLS analysis are summarised in Table 2. A perusal of Table 2 shows that leave-one-out cross-validated value q^2 is 0.948 at 5 components and non-cross validated r^2 is 0.998. Out of 29 compounds, 20 compounds were considered to form the training set, the predicted binding activity lg K value for each training set of compounds and the residual values are shown in Table 3.

Table 3. Experimental and predicted lg K values for the training set of molecules using CoMFA analysis

Comp. No	Never			Steric cut of each any row	
	lg K_{obs}	lg K_{est}	lg K_{res}	lg K_{est}	lg K_{res}
1	6.69	6.600	0.090	6.356	0.334
2	7.09	7.215	−0.125	7.047	0.043
3	7.53	7.495	0.035	7.267	0.263
4	7.77	7.770	0.000	7.613	0.157
6	8.86	8.798	0.148	8.956	−0.096
8	8.50	8.412	0.088	8.095	0.405
9	8.77	8.859	−0.089	8.611	0.159
11	9.39	9.417	0.522	9.279	0.111
12	9.39	9.478	−0.088	9.489	−0.099
13	7.08	7.164	−0.084	7.134	−0.054
15	8.08	8.047	0.033	8.242	−0.162
16	8.49	8.464	0.026	8.746	−0.256
18	8.93	8.884	0.046	9.098	−0.168
19	8.93	8.877	0.016	8.932	−0.002
22	6.44	6.455	−0.015	6.822	−0.382
24	6.86	6.877	−0.017	6.986	−0.126
25	4.41	4.448	0. 353	4.684	−0.274
26	4.80	4.763	0.037	4.773	−0.027
28	5.76	5.758	0.002	5.817	−0.057
29	6.18	6.169	0.035	6.007	0.173

The excellent CoMFA model in region 'never' yielded a q^2 value of 0.948 with 5 components. A value of q^2 of 0.5 is generally considered as an indication that the model is internally predictive. Thus, the q^2 values obtained in the present case are excellent: 0.998 to validate the model. The boot strapping function was used to determine the error in r^2 (r^2_{boot}) and (SEE$_{boot}$) of the model. In the never region of CoMFA we obtained r^2_{bs} =0.999, SD$_{bs}$ =0.001 of steric cut-off. The binding constants (lg K) for 9 compounds were predicted from the corresponding external test set. The afore-mentioned 9 compounds were used to validate CoMFA analysis. The models

obtained have a very good predictive r^2 (r^2_{pred}) of 0.845 for never region and models have excellent external and internal prediction. All the statistical features are summarised in Table 2. The observed and estimated binding constant (lg K) values of test set are shown in Table 4.

Table 4. Observed and estimated lg K values along with their residue (difference between observed and estimated lg K) for test set of molecules using CoMFA analysis molecule

Comp. No	lg K_{obs}	lg K_{est}	lg K_{res}
5	8.30	8.213	0.087
7	7.98	7.505	0.475
10	9.11	8.971	0.139
14	7.53	7.815	−0.285
17	8.75	8.708	0.042
20	5.87	6.980	−1.11
21	6.21	6.067	0.143
23	6.95	6.175	0.775
27	5.28	5.447	−0.167

CoMSIA ANALYSIS

Five CoMSIA models were generated using the same training set and test set. The cross-validated q^2 values of these 5 models are shown in supporting information. Each model with individual fields of the steric, hydrophobic, hydrogen bond acceptor, donor were taken into account; the q^2 and predictive r^2 (for external validation) are excellent. The statistical parameters associated with all these models are shown in Table 2. The predicted binding lg K and the residual values for training and test set of compounds are given in Tables 5 and 6, respectively. We observed that except the electrostatic field (which is with poor predictive r^2), all models have excellent prediction potential.

Table 5. Observed and estimated lg K values and their residue (residue – difference between observed and estimated lg K) for training set of molecules using CoMSIA analysis (steric, hydrophobic, hydrogen-bond acceptor, hydrogen-bond donor, electrostatic)

Comp. No	lg K_{obs}	lg K_{est}	lg K_{res}	lg K_{est}	lg K_{res}	lg K_{est}	lg K_{res}	lg K_{est}	lg K_{res}	lg K_{est}	lg K_{res}
		S		H		HA		HD		E	
1	6.69	6.498	0.192	6.604	0.086	7.629	−0.939	7.479	−0.789	6.798	−0.108
2	7.09	7.031	0.059	6.827	0.263	7.607	−0.517	7.495	−0.405	6.993	0.097
3	7.53	7.408	0.122	7.286	0.244	7.614	−0.084	7.497	0.033	7.431	0.099
4	7.77	7.783	−0.013	8.014	−0.244	7.628	0.142	7.567	0.203	7.867	−0.097
6	8.86	8.823	0.037	9.092	−0.232	7.728	1.132	7.708	1.152	8.862	−0.002
8	8.50	7.927	0.573	8.159	0.341	8.602	−0.102	9.205	−0.705	8.487	0.013
9	8.77	8.584	0.186	8.825	−0.055	8.609	0.161	8.947	−0.177	8.758	0.012
11	9.39	9.528	−0.138	9.380	0.010	8.534	0.856	8.671	0.719	9.303	0.087
12	9.39	9.331	0.059	9.323	0.067	8.640	0.750	9.275	0.115	9.491	−0.101
13	7.08	7.564	−0.484	7.220	−0.140	8.594	−1.514	8.166	−1.086	7.106	−0.026
15	8.08	8.342	−0.262	8.246	−0.166	8.564	−0.484	8.093	−0.013	8.103	−0.023
16	8.49	8.719	−0.229	8.559	−0.069	8.553	−0.063	8.105	0.385	8.549	−0.059
18	8.93	8.998	−0.068	8.817	0.113	8.534	0.396	8.121	0.809	8.824	0.106
19	8.93	8.733	0.197	8.888	0.042	8.864	0.066	8.972	−0.042	8.931	−0.001
22	6.44	7.031	−0.591	6.621	−0.181	6.674	−0.234	6.637	−0.197	6.432	0.008
24	6.86	6.742	0.118	6.759	0.101	6.542	0.318	6.873	−0.013	6.862	−0.002
25	4.41	6.634	−2.224	4.613	−0.203	4.518	−0.108	4.880	−0.47	4.404	0.006
26	4.80	4.834	−0.034	4.659	0.141	5.445	−0.645	5.570	−0.77	4.775	0.025
28	5.76	4.495	1.265	5.972	−0.212	5.461	0.299	5.364	0.396	5.779	−0.019
29	6.18	5.775	0.405	6.085	0.095	5.608	0.572	5.327	0.853	6.198	−0.018

Table 6. CoMSIA actual and predicted lg K values using the test set of molecules (steric, hydrophobic, acceptor, donor, electrostatic)

Comp. No	lg K_{obs}	lg K_{est}	lg K_{res}	lg K_{est}	lg K_{res}	lg K_{est}	lg K_{res}	lg K_{est}	lg K_{res}	lg K_{est}	lg K_{res}
		S		H		HA		HD		E	
1	8.30	8.493	−0.193	8.836	−0.536	7.352	0.948	7.112	1.188	8.037	0.263
2	7.98	7.451	0.529	7.470	0.510	8.423	−0.443	9.055	−1.075	6.814	1.166
3	9.11	8.823	0.287	9.116	−0.006	8.574	0.536	9.156	−0.046	9.209	−0.099
4	7.53	8.101	−0.571	9.230	−1.7	8.695	−1.165	9.299	−1.769	6.349	1.181
6	8.75	8.652	0.098	10.001	−1.251	8.472	0.278	8.614	0.136	6.898	1.852
8	5.87	7.341	−1.471	6.016	−0.146	6.790	−0.92	6.837	−0.967	3.168	2.702
9	6.21	6.396	−0.186	6.347	−0.137	6.613	−0.403	6.877	−0.667	6.142	0.068
11	6.95	6.952	−0.002	5.430	1.520	6.793	0.157	7.046	−0.096	6.456	0.494
12	5.28	4.740	0.540	6.070	−0.79	5.379	−0.099	5.265	0.015	5.963	−0.683

The q^2 values in the training set associates with the CoMSIA as well as CoMFA models are similar. However, the CoMFA models have better internal predictive power than the CoMSIA models. The model (never region) of CoMFA has a very good predictive power. In CoMSIA except electrostatic model, all models have excellent predictive ability. After consideration both of the internal and external predictive powers of the models, the best CoMFA and CoMSIA models were selected for the construction of the coefficient contour maps. The CoMFA contour map with never region is shown in Fig. 3. The Figure shows the steric field: A (sterically favourable for the activity) and B (sterically unfavourable for the activity) contours represent 80 and 20% level contribution, respectively. The D (negative charge favourable for activity) and C (the negative charge unfavourable for activity) contours in the CoMFA electrostatic field contours represent 80 and 20% level contribution, respectively.

Fig. 3. Steric contour map: **A** contours (80% contribution) refer to sterically favoured regions and **B** contours (20% contribution) are sterically unfavoured; **C** contours (80% contribution) refer to regions where positively charged substituents are favoured; D contours (20% contribution) indicate regions where negatively charged substituents are favoured

The contours map of the CoMFA with a very big region of **A** suggests that the steric bulky groups are favourable in this region, and increases with the binding constant lg K. The most potent compounds fall in this region. This is confirmed by the high binding constants (lg K) of compounds **9**, **10**, **11** and **12**. In view of this, we argue that binding constant (lg K) for CAII will increase when a bulky group is present in this region. At this stage it is worth mentioning that in the CoMFA models the **B** region is not allowed. The presence of a hetero-atom falls in a **D** favourable region suggesting that the negative charge increases the lg K values. This was confirmed by the fact that compounds **13** to **19** fall in this region. The very big **C** region in the CoMFA contours suggests that the positive charge will increase the binding constant (lg K). In the electrostatic region the influence of the hydrogen bond acceptor, carbonyl

amide as a part of this field is considered, so the carbonyl amide could be a part of the electrostatic fields and help the exhibition of the binding constant (lg K).

The CoMSIA contour maps are shown in Figs 4 and 5. CoMSIA analysis was also selected to construct contours maps. The contours maps of CoMSIA models represent the CoMSIA steric field. The **A** region suggests that the introduction of the bulky group in this region will increase the binding constant (lg K). This was confirmed by the unsubstituted benzene sulphonamide which has low binding constant (lg K). Also the entire potent compounds fall in this region. A very small **B** region in hydrophobic maps suggests that the carbon atoms increase the lg K values. A very big **A** region in hydrophobic group indicates that addition of the hydrophobic group will decrease the binding constant (lg K). In the CoMSIA contour maps of hydrogen-bond acceptor, **A** region in the 4-substituted benzene sulphonamide; the oxygen group increases the binding constant (lg K). **B** region in the hydrogen-bond acceptor group is unfavourable for the exhibition of the binding constant (lg K). From the results and discussion made above we argue that all the 2-substituted benzene sulphonamide compounds fall in this region, and that binding constant (lg K) decreases. Also, in 4-substituted benzene sulphonamides the presence of hydrogen-bond acceptor group like oxygen is not favourable in this region. The donor and acceptor contours show that the very big **A** region is favourable for the hydrogen-bond donor region meaning that the donor group like CO is favourable for the exhibition of binding constant (lg K).

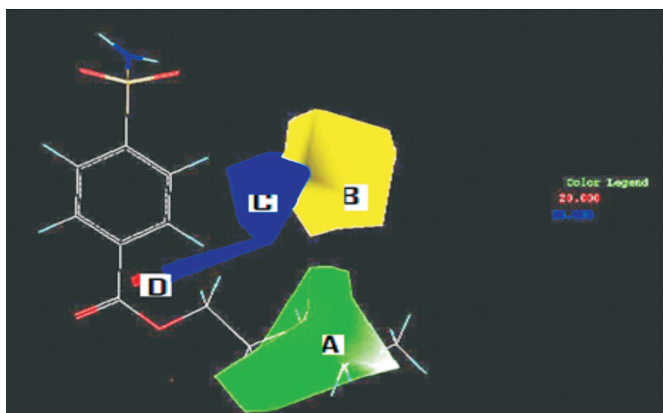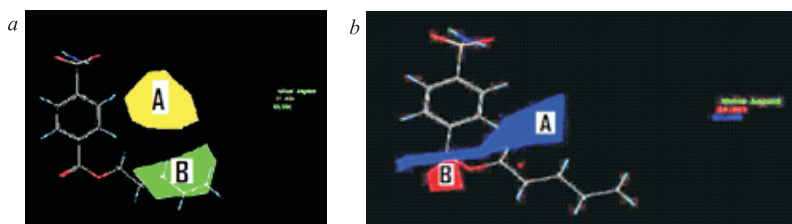**Fig. 4**. Steric contour map (*a*): **A** contours (80% contribution) refer to sterically favoured regions, and **B** counters (20% contribution) are sterically unfavoured; electrostatic contour map (*b*): **A** (contours (80% contribution) refer to regions where positively charged substituent are favoured and **B** contours (20% contribution) indicate regions where negatively charged substituent are favoured
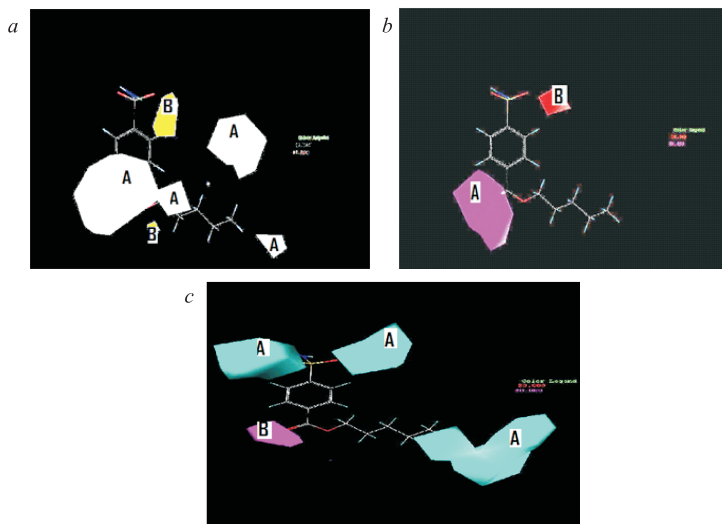
Fig. 5. Hydrophobic contour map (*a*): **A** contours (20% contribution) refer to regions where hydrophilic substituent are favoured, and **B** contours (80% contribution) indicate regions where hydrophobic substituent are favoured; hydrogen-bond acceptor or contour map (*b*): **A** (80% contribution) favourable contours refer to areas where hydrogen-bond donors on the receptor promote the affinity, and **B** (unfavourable); hydrogen-bond donor contour map (*c*): **A** contours (80% contribution) indicate regions where hydrogen-bond acceptor groups on the receptor increase activity, and **B** (unfavourable)

CONCLUSIONS

From the afore-mentioned results and discussion we draw the following conclusions:

1. On the basis of alignment of the molecule, good internal predictive 3D QSAR models can be derived.

2. Each model validated using an external test set of 9 compounds showed excellent predictive r^2, with combination of diverse descriptors.

3. Seven models were generated from CoMFA and CoMSIA. The obtained CoMFA and CoMSIA models provided statistically significant correlation and predictive ability and could be potentially helpful in the design of novel and more potent carbonic anhydrase inhibitors.

ACKNOWLEDGEMENT

REFRENCES

1. C. T. SUPURAN: Physiologic and Pathologic Processes in the Organism. In: Carbonic Anhydrase and Modulation of Physiologic and Pathologic Processes in the Organism (Ed. I. Pucas). Helicon Press, Timisoara, 1994, p. 111.
2. U. F. MANSOOR, Y. R. ZHANG, G. M. BLACKBURN: The Design of New Carbonic Anhydrase Inhibitors. In: The Carbonic Anhydrase - New Horizons (Eds W. R. Chegwidden, Y. Edwards, N. Carter). Birkhauser Verlag, Basel, 2000, 437–460.
3. W. R. CHEGWIDDEN, N. D. CARTER, Y. H. EDWARDS (Eds): The Carbonic Anhydrases – New Horizons. Birkhauser Verlag, Basel-Boston-Berlin, 2000.
4. B. W. CLARE, C. T. SUPURAN (Eds): Carbonic Anhydrases, Its Inhibitors and Activators. CRC Press, Boca Raton, FI, USA, 2004.
5. A. PHADNI, A. S. SHARMA, V. SHARMA, P. V. KHADIKAR: QSAR Study on Carbonic Anhydrase Inhibition Activity and Related Parameters Using SO_2NH_2 NMR Chemical Shift and Topological Indices. Oxid Commun, **35** (4), 920 (2012).
6. S. SINGH: A Comparative Molecular Field (CoMFA) Studies on Carbonic Anhydrase Inhibitor hCA IX-Tumor-Associated (Hypoxia). Lett Drug Des Discov (Bentham Science), **8**, 877 (2011).
7. S. SINGH: A Comparative Molecular Field Analysis (CoMFA) Studies on [1,2,4] triazolo [1,5-a] pyrimidines, a Class of Anticancer Agents, Inhibition of Tubulin. Oxid Comm, **34** (3), 650 (2011).
8. S. SINGH, C. T. SUPURAN: 3D-QSAR CoMFA Studies on Sulphonamide Inhibitors of the Rv3588c β-carbonic Anhydrase from *Mycobacterium tuberculosis* and Design of not yet Synthesized New Molecules. J Enzym Inhib Med Ch (in press).
9. J. SINGH, S. SINGH, M. LAKHWANI, A. K. JOSHI, P. V. KHADIKAR, C. T. SUPURAN, B. W. CLARE: Development of Quantity Structure Activity Relationship for the Inhibitors of Human Carbonic Anhydrase II Using Topological Indices and Their Combination with Quantum Theoretical Descriptors. J Med Chem Res, **15**, 156 (2006).
10. P. V. KHADIKAR, O. DEEB, A. JABER, J. SINGH, M. LAKHWANI: Development of Quantity Structure Activity Relationship for a Set of Human Carbonic Anhydrase Inhibitors: Use of Quantum and Chemical Descriptors. Lett Drug Design Disco, **3**, 622 (2006).
11. P. V. KHADIKAR, M. DIUDEA, J. SINGH, P. JOHN, A. SHRIVASTAVA, S. SINGH, S. KAR-MARKAR, M. LAKHWANI, P. THAKUR: Use of PI Index in Computer Aided Designing of Bioactive Compounds. Curr Bioact Comp, **2**, 19 (2006).
12. P. V. KHADIKAR, S. KARMARKAR, V. K. AGRAWAL, J. SINGH, A. SHRIVASTAVA, I. LUKO-VITS, M. V. DIUDEA: Szeged Index-Applications for Drug Modeling. Drug Design and Discovery, **2**, 606 (2005).
13. A. T. BALABAN, P. V. KHADIKAR, C. T. SUPURAN, A. THAKUR, M. THAKUR: Study on Supramolucular Complexing Ability vis-à-vis Estimation of p$K\alpha$ of Substituted Sulphonamides. Bioorg Med Chem Lett, **15**, 3966 (2005).
14. P. GELADI: Notes on the History and Nature of Partial Least Squares (PLS) Modeling. J Chemon, **2**, 246 (1988).
15. R. D. CRAMER III, J. D. BUNCE, D. E. PATTERSON: Cross-validation, Boot Strapping, and Partial Least Squares Compared with Multiple Regression in Conventional QSAR. Quant Struct Act Relat, **7**, 18 (1988).

QSAR STUDY ON 1,4-DIHYDROPYRIDINE AS CALCIUM CHANNEL ANTAGONISTS

J. SINGH[a], B. SHAIK[b], S. K. SHUKLA[b], M. SHARMA[c], S. SINGH[c], V. K. AGRAWAL[b]*

[a]*Department of SHM, Amrapali Institute of Technology & Sciences, Shiksha Nagar, Lamachaur, 263 139 Haldwani,Uttara Khand, India*
E-mail: *jyotisingh.dtu@gmail.com*
[b]*Department of Applied Science, National Institute of Technical Teachers Training & Research, Shamla Hills, 462 002 Bhopal, India*
E-mail: *apsvka@yahoo.co.in*; *basheerulla.81@gmail.com*
[c]*Chemistry Department, Govt. K. N. PG College, Sant Ravidas Nagar, UP, India*

ABSTRACT

A quantitative structure–activity relationship (QSAR) study has been performed on 1,4-dihydropyridine analogues as calcium channel antagonists to understand the structural features influencing the activity of these analogues towards the hypertension. The results showing that lg $1/IC_{50}$ activity could be modelled using topological as well as some other parameters, viz. AlogP, BAC, Jhete, W, MR, POL. The predictive ability of the models was checked by cross-validation method.

Keywords: calcium channel antagonists, QSAR, topological modelling, dihydropyridines.

AIMS AND BACKGROUND

Hypertension is a common problem being experienced by most of the people all over the world. Because of its promising depressor effect and relatively good tolerability[1], calcium channel antagonists (CCA) are experimentally verified drugs for treatment of hypertension. The most commonly used CCA are derivatives of 1,4-dihydropyridines (1,4-DHPs). The general structure of 1,4-DHPs is given in Fig. 1. These drugs are having some important features like renal protection, weak anti-platelet, regression of left ventricular pressure and vascular hypertrophy, anti-ischemic and anti-atherogenic activity[2–4].

---

* For correspondence.
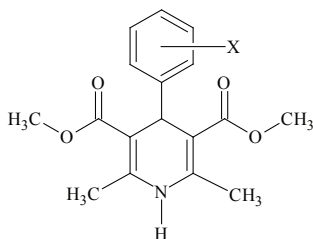
Fig. 1. General structure of 1,4-dihydropyridines (1,4-DHPs)

The mechanisms of these drugs reveal that they act directly on the voltage-dependent calcium channels present in the cell membrane and blocks the flux of calcium ions effectively from the extra cellular medium to the cell cytoplasm.

We have successfully modelled the antihypertensive activity of 2-aryl-imino-imidazolidines and a series of alkyl N-[diphenyl alkyl] aminoalkyl-4-aryl-1,4-dihydro-2,6-dimethyl pyridine-3,5 di-carboxylats using topological indices as well as physicochemical parameters[5,6].

QSAR is a good tool for modelling, which suggests structural modifications also. Therefore, quantitative structure–property/activity relationship (QSPR/QSAR) study has been proposed for modelling the lg $1/IC_{50}$ of 1,4-DHP (Fig. 1). In the recent past also we have successfully used several topological and physicochemical parameters independently and simultaneously for modelling biological activities of drug molecules in recent past[7–21].

The aim of this study is to model lg $1/IC_{50}$ activity of 1, 4-DHP with diverse structures and establish a new and accurate QSAR model using topological and physicochemical parameters. The use of proposed models would narrow the search for future drug molecules.

EXPERIMENTAL

Parameters used. The independent parameters used in the present investigation include following topological indices: Weiner (W), Balaban (J), the Balaban hetero atom type indices (JhetZ, Jhetm, Jhetv, Jhete, Jhetp), the Balaban centric index (BAC), the Ghose - Crippen octanol water partition coefficeint (AlogP), connectivity indices ($^0\chi$, $^1\chi$, $^2\chi$, $^3\chi$, $^0\chi^V$, $^1\chi^V$, $^2\chi^V$ and $^3\chi^V$). These parameters have been calculated using DRAGON software[22]. Apart from topological indices we have also used few physicochemical parameters. These, parameters include molecular weight (MW), molar refractivity (MR), molar volume (MV), parachor (PC), index of refraction (IR), density (*d*), polarisability (POL). These parameters have been calculated by Chemsketch software provided by ACD labs[23].

Drug activity (*dependent parameter*). The drug activity is measured in terms of IC_{50} (the molar concentration of the drug required to inhibit 50%) of the contraction of

guinea pig ileum induced by methyl-furmethide). Its log value has been used as dependent parameter and the same has been modelled. These values have been taken from the work of Costa et al.[24]

RESULTS AND DISCUSSION

The structural details of 1,4-DHP along with the lg $1/IC_{50}$ values are reported in Table 1. 45 such derivatives have been undertaken in this study. A perusal of this Table shows that the variation in activity is difficult to explain on the basis of substitution at various positions. However, the minimum activity (3.0) belongs to compound **45** (Table 1) having substitution of OMe at 2, 4, 5 position. Similarly the highest activity (8.890) belongs to compound **1** (Table 1) having –Br at position 3. Neither substitution having more electronegative group, nor electron rich groups could explain this variation. Therefore, topological indices will be used for modelling the lg $1/IC_{50}$ value of these compounds.

Table 1. Experimental activities (lg $1/IC_{50}$) of 1,4-dihydropyridine calcium channel antagonists

Compd. No	X	lg $1/IC_{50}$	AlogP
1	2	3	4
1	3′-Br	8.890	3.673
2	2′-CF$_3$	8.820	3.764
3	2′-Cl	8.660	3.399
4	3′-NO$_2$	8.400	2.835
5	2′-CH=CH$_2$	8.350	3.703
6	2′-NO$_2$	8.290	2.835
7	2′-Me	8.220	3.348
8	2′-Et	8.190	3.745
9	2′-Br	8.120	3.673
10	2′-CN	7.800	2.917
11	3′-Cl	7.800	3.399
12	3′-F	7.680	3.021
13	H	7.680	2.881
14	3′-CN	7.460	2.917
15	3′-I	7.380	4.139
16	2′-F	7.370	3.021
17	2′-I	7.330	4.139
18	2′-OMe	7.240	2.357
19	3′-CF$_3$	7.130	3.764
20	3′-Me	6.960	3.348
21	2′-OEt	6.960	2.700
22	3′-OMe	6.720	2.357
23	3′-NMe$_2$	6.050	3.146

1	2	3	4
24	3′-OH	6.000	2.597
25	3′-NH$_2$	5.700	2.098
26	3′-OAc	5.220	2.380
27	3′-OCOPh	5.200	4.293
28	2′-NH$_2$	4.400	2.098
29	4′-F	6.890	3.021
30	4′-Br	5.400	3.673
31	4′-I	4.640	4.139
32	4′-NO$_2$	5.500	2.835
33	4′-NMe$_2$	4.000	3.146
34	4′-CN	5.460	2.917
35	4′-Cl	5.090	3.399
36	2′,6′-Cl$_2$	8.720	3.917
37	F$_5$	8.360	3.579
38	2′-F,6′-Cl	8.120	3.539
39	2′,3′-Cl$_2$	7.720	3.917
40	2′-Cl,5′-NO$_2$	7.520	3.353
41	3′,5′-Cl$_2$	7.030	3.917
42	2′-OH,5′-NO$_2$	7.000	2.550
43	2′,5′-Me$_2$	7.000	3.816
44	2′,4′-Cl$_2$	6.400	3.917
45	2′,4′,5′-(OMe)$_3$	3.000	1.310

The calculated parameters using Dragon[22] and Chemsketch[23] softwares are reported in Tables 2 and 3.

The correlation matrix showing inter-correlation among biological activity and various descriptors is reported in Table 4. A perusal of this table shows that certain topological indices possess strong colinearity such pair of descriptors are given below: J-JhetZ, J-Jhetm, J-Jhetv, J-Jhete, J-JhetP, Jhetz-Jhetv, Jhetz-Jhete, Jhetz-JhetP, Jhetm-Jhetv, Jhetm-Jhete, Jhetm-JhetP, Jhetv-Jhete, Jhetv-JhetP, Jhete-JhetP, $^0\chi$–$^1\chi$, $^0\chi$–$^2\chi$, $^0\chi$–$^3\chi$, $^1\chi$–$^2\chi$, $^1\chi$–$^3\chi$, $^1\chi$–PC, $^2\chi$–$^3\chi$, $^0\chi^V$–$^1\chi^V$, $^0\chi^V$–$^2\chi^V$, $^0\chi^V$–$^3\chi^V$, $^0\chi^V$–MR , $^0\chi^V$–PC, $^0\chi^V$–MV, $^1\chi^V$–$^2\chi^V$, $^1\chi^V$–$^3\chi^V$, $^1\chi^V$–MR, $^1\chi^V$–MV, $^1\chi^V$–PC, $^2\chi^V$–$^3\chi^V$, $^2\chi^V$–MW, $^2\chi^V$–MR, $^2\chi^V$–POL, $^3\chi^V$–MUU, $^3\chi^V$–MR, $^3\chi^V$–PC, $^3\chi^V$–POL, MW–d, MR–MV, MR–PC, MR–POL, MV–PC, PV–POL, PC–POL, IR–ST.

Table 2. Calculated values of topological and connectivity indices

Compd. No	W	J	JhetZ	Jhetm	Jhetv	Jhete	Jhetp	BAC	$^0\chi$	$^1\chi$	$^2\chi$	$^3\chi$	$^0\chi^V$	$^1\chi^V$	$^2\chi^V$	$^3\chi^V$
1	2	3	4	5	6	7	8	9	10	11	12	13	14	15	16	17
1	1044	2.337	2.867	2.868	2.379	2.826	2.31	58	17.146	10.900	9.725	8.070	14.984	7.802	6.089	4.246
2	1409	2.479	2.979	2.984	2.398	2.974	2.279	95	19.646	12.128	11.614	8.975	14.654	7.643	5.704	4.148
3	1028	2.375	2.895	2.896	2.394	2.867	2.327	58	17.146	10.917	9.619	8.221	14.154	7.393	5.547	4.131
4	1328	2.343	2.883	2.882	2.317	2.879	2.216	78	18.723	11.811	10.624	8.791	14.283	7.409	5.471	3.985
5	1153	2.399	2.924	2.923	2.475	2.921	2.401	63	17.853	11.455	9.810	8.535	14.304	7.523	5.452	4.098
6	1280	2.434	2.974	2.974	2.373	2.971	2.267	78	18.723	11.828	10.550	8.774	14.283	7.415	5.434	4.015
7	1028	2.375	2.857	2.857	2.394	2.855	2.319	58	17.146	10.917	9.619	8.221	14.020	7.326	5.475	4.070
8	1153	2.399	2.868	2.868	2.433	2.866	2.362	63	17.853	11.455	9.810	8.535	14.727	7.887	5.671	4.318
9	1028	2.375	2.906	2.908	2.406	2.863	2.336	58	17.146	10.917	9.619	8.221	14.984	7.808	5.994	4.509
10	1153	2.399	2.905	2.904	2.453	2.902	2.378	63	17.853	11.455	9.810	8.535	13.967	7.300	5.318	3.963
11	1044	2.337	2.856	2.857	2.368	2.83	2.302	58	17.146	10.900	9.725	8.070	14.154	7.387	5.610	3.988
12	1044	2.337	2.839	2.841	2.316	2.835	2.223	58	17.146	10.900	9.725	8.070	13.398	7.009	5.174	3.753
13	926	2.314	2.795	2.795	2.316	2.792	2.239	45	16.276	10.506	9.091	7.743	13.097	6.910	5.029	3.704
14	1185	2.333	2.840	2.840	2.405	2.838	2.334	63	17.853	11.438	9.894	8.494	13.967	7.294	5.356	3.920
15	1044	2.337	2.870	2.871	2.385	2.819	2.320	58	17.146	10.900	9.725	8.070	15.555	8.088	6.419	4.424
16	1028	2.375	2.876	2.878	2.339	2.873	2.244	58	17.146	10.917	9.619	8.221	13.398	7.015	5.140	3.787
17	1028	2.375	2.910	2.911	2.412	2.855	2.347	58	17.146	10.917	9.619	8.221	15.555	8.094	6.302	4.770
18	1153	2.399	2.909	2.909	2.329	2.906	2.239	63	17.853	11.455	9.810	8.535	14.428	7.439	5.360	4.021
19	1473	2.365	2.871	2.875	2.328	2.866	2.217	95	19.646	12.112	11.683	9.032	14.654	7.637	5.742	4.118
20	1044	2.337	2.821	2.821	2.368	2.819	2.295	58	17.146	10.900	9.725	8.070	14.020	7.320	5.533	3.946
21	1302	2.396	2.906	2.905	2.282	2.903	2.187	68	18.560	11.955	10.190	8.670	15.135	8.026	5.589	4.101
22	1185	2.333	2.844	2.844	2.289	2.841	2.203	63	17.853	11.438	9.894	8.494	14.428	7.433	5.395	3.998
23	1328	2.343	2.843	2.843	2.343	2.84	2.257	78	18.723	11.811	10.624	8.791	15.467	7.938	6.108	4.291
24	1044	2.337	2.835	2.834	2.333	2.832	2.253	58	17.146	10.900	9.725	8.070	13.467	7.044	5.214	3.775

to be continued

1	2	3	4	5	6	7	8	9	10	11	12	13	14	15	16	17
25	1044	2.337	2.829	2.829	2.352	2.826	2.273	58	17.146	10.900	9.725	8.070	13.597	7.109	5.289	3.815
26	1517	2.302	2.840	2.840	2.195	2.837	2.1	83	19.430	12.294	11.116	8.721	15.336	7.933	5.785	4.024
27	2604	1.755	2.199	2.199	1.649	2.197	1.57	58	22.543	14.867	13.097	11.076	17.723	9.593	6.947	4.982
28	1028	2.375	2.865	2.865	2.377	2.862	2.297	58	17.146	10.917	9.619	8.221	13.597	7.115	5.247	3.878
29	1060	2.304	2.806	2.808	2.295	2.802	2.204	58	17.146	10.900	9.713	8.153	13.398	7.009	5.170	3.774
30	1060	2.304	2.832	2.833	2.355	2.794	2.287	58	17.146	10.900	9.713	8.153	14.984	7.802	6.086	4.303
31	1060	2.304	2.835	2.836	2.36	2.787	2.296	58	17.146	10.900	9.713	8.153	15.555	8.088	6.416	4.493
32	1376	2.265	2.803	2.802	2.267	2.799	2.17	78	18.723	11.811	10.612	8.852	14.283	7.409	5.467	4.008
33	1376	2.265	2.766	2.766	2.291	2.763	2.209	78	18.723	11.811	10.612	8.852	15.467	7.938	6.104	4.314
34	1217	2.275	2.783	2.783	2.363	2.78	2.294	63	17.853	11.438	9.882	8.562	13.967	7.294	5.352	3.944
35	1060	2.304	2.822	2.823	2.345	2.797	2.279	58	17.146	10.900	9.713	8.153	14.154	7.387	5.607	4.026
36	1134	2.439	3.002	3.003	2.477	2.947	2.419	73	18.016	11.328	10.156	8.626	15.210	7.877	6.068	4.519
37	1538	2.539	3.140	3.149	2.423	3.133	2.273	130	20.627	12.577	11.566	10.525	14.600	7.444	5.602	4.103
38	1134	2.439	2.983	2.985	2.422	2.953	2.335	73	18.016	11.328	10.156	8.626	14.454	7.499	5.661	4.189
39	1149	2.405	2.966	2.968	2.453	2.914	2.396	73	18.016	11.328	10.125	8.813	15.210	7.877	6.047	4.697
40	1447	2.415	2.996	2.996	2.405	2.97	2.31	95	19.593	12.222	11.152	9.284	15.340	7.893	5.989	4.417
41	1166	2.369	2.927	2.929	2.427	2.878	2.37	73	18.016	11.294	10.371	8.308	15.210	7.865	6.194	4.226
42	1447	2.415	2.975	2.975	2.374	2.972	2.268	95	19.593	12.222	11.152	9.284	14.653	7.549	5.619	4.104
43	1151	2.402	2.891	2.891	2.451	2.889	2.378	73	18.016	11.311	10.253	8.563	14.942	7.737	5.979	4.317
44	1166	2.373	2.931	2.933	2.430	2.882	2.373	73	18.016	11.311	10.253	8.541	15.210	7.871	6.128	4.407
45	1763	2.465	3.050	3.050	2.342	3.047	2.238	111	21.008	13.336	11.334	10.069	17.090	8.491	6.068	4.618

Table 3. Calculated physicochemical parameters

Compd. No	MW	MR	MV	PC	IR	ST	*d*	POL
1	380.233	89.040	276.600	703.400	1.557	41.800	1.374	35.300
2	369.335	86.330	293.900	714.300	1.499	34.800	1.256	34.220
3	335.782	86.250	272.300	689.500	1.546	41.000	1.232	34.190
4	346.335	87.900	272.200	709.400	1.558	46.000	1.271	34.840
5	327.374	92.280	286.300	719.900	1.557	39.900	1.143	36.580
6	346.335	87.900	272.200	709.400	1.558	46.000	1.271	34.840
7	315.364	86.180	276.700	690.600	1.535	38.800	1.139	34.160
8	329.390	90.900	293.200	730.700	1.532	38.500	1.123	36.030
9	380.233	89.040	276.600	703.400	1.557	41.800	1.374	35.300
10	326.347	86.460	261.600	700.000	1.574	51.200	1.240	34.270
11	335.782	86.250	272.300	689.500	1.546	41.000	1.232	34.190
12	319.328	81.350	264.600	659.700	1.526	38.600	1.206	32.250
13	301.337	81.350	260.400	652.400	1.537	39.300	1.157	32.250
14	326.347	86.460	261.600	700.000	1.574	51.200	1.240	34.270
15	427.234	94.260	282.500	726.300	1.581	43.600	1.512	37.370
16	319.328	81.350	264.600	659.700	1.526	38.600	1.206	32.250
17	427.234	94.260	282.500	726.300	1.581	43.600	1.512	37.370
18	331.363	88.030	284.400	711.000	1.531	39.000	1.164	34.900
19	369.335	86.330	293.900	714.300	1.499	34.800	1.256	34.220
20	315.364	86.180	276.700	690.600	1.535	38.800	1.139	34.160
21	345.390	92.670	300.900	751.000	1.528	38.800	1.147	36.730
22	331.363	88.030	284.400	711.000	1.531	39.000	1.164	34.900
23	344.405	95.670	298.400	757.000	1.554	41.400	1.154	37.920
24	317.336	83.240	258.800	667.600	1.556	44.200	1.225	32.990
25	316.352	85.590	262.700	680.300	1.565	44.900	1.204	33.930
26	359.373	92.700	298.000	756.200	1.534	41.400	1.205	36.740
27	421.443	113.000	343.800	890.000	1.571	44.800	1.225	44.790
28	316.352	85.590	262.700	680.300	1.565	44.900	1.204	33.930
29	319.328	81.350	264.600	659.700	1.526	38.600	1.206	32.250
30	380.233	89.040	276.600	703.400	1.557	41.800	1.374	35.300
31	427.234	94.260	282.500	726.300	1.581	43.600	1.512	37.370
32	346.335	87.900	272.200	709.400	1.558	46.000	1.271	34.840
33	344.405	95.670	298.400	757.000	1.554	41.400	1.154	37.920
34	326.347	86.460	261.600	700.000	1.574	51.200	1.240	34.270
35	335.782	88.250	272.300	689.500	1.546	41.000	1.232	34.190
36	370.227	91.140	284.300	726.600	1.554	42.600	1.302	36.130
37	391.289	81.320	281.400	689.100	1.489	35.900	1.390	32.240
38	353.773	86.240	276.500	696.800	1.536	40.200	1.279	34.190
39	370.227	91.140	284.300	726.600	1.554	42.600	1.302	36.130
40	380.780	92.800	284.200	746.600	1.566	47.600	1.339	36.780
41	370.227	91.140	284.300	726.600	1.554	42.600	1.302	36.130
42	362.334	89.780	270.700	724.600	1.577	51.300	1.338	35.590
43	329.390	91.000	292.900	728.900	1.533	38.300	1.124	36.070
44	370.227	91.140	284.300	726.600	1.554	42.600	1.302	36.130
45	391.415	101.390	332.400	828.200	1.522	38.500	1.177	40.190

Table 4. Correlation matrices

	lg 1/IC$_{50}$	W	J	JhetZ	Jhetm	Jhetv	Jhete	JhetP	BAC	$^0\chi$	$^1\chi$	$^2\chi$	$^3\chi$
lg 1/IC$_{50}$	1												
W	−0.306	1											
J	0.386	−0.526	1										
JhetZ	0.347	−0.438	0.977	1									
Jhetm	0.349	−0.435	0.977	1.000	1								
Jhetv	0.389	−0.739	0.887	0.855	0.853	1							
Jhete	0.329	−0.403	0.981	0.989	0.988	0.826	1						
JhetP	0.369	−0.778	0.821	0.788	0.785	0.989	0.746	1					
BAC	−0.039	0.502	0.404	0.499	0.503	0.110	0.532	−0.002	1				
$^0\chi$	−0.211	0.948	−0.238	−0.142	−0.138	−0.513	−0.102	−0.583	0.742	1			
$^1\chi$	−0.259	0.984	−0.383	−0.296	−0.293	−0.635	−0.254	−0.687	0.598	0.978	1		
$^2\chi$	−0.175	0.928	−0.293	−0.203	−0.198	−0.543	−0.173	−0.610	0.708	0.969	0.930	1	
$^3\chi$	−0.178	0.918	−0.240	−0.138	−0.134	−0.491	−0.105	−0.557	0.709	0.960	0.947	0.901	1
$^0\chi^V$	−0.324	0.685	−0.329	−0.214	−0.213	−0.403	−0.269	−0.382	0.347	0.653	0.682	0.620	0.629
$^1\chi^V$	−0.275	0.706	−0.462	−0.365	−0.363	−0.507	−0.419	−0.473	0.215	0.626	0.683	0.608	0.607
$^2\chi^V$	−0.209	0.453	−0.350	−0.241	−0.239	−0.280	−0.337	−0.228	0.154	0.399	0.409	0.438	0.388
$^3\chi^V$	−0.116	0.454	−0.233	−0.129	−0.128	−0.194	−0.220	−0.149	0.193	0.426	0.445	0.410	0.466
AlogP	0.391	−0.012	−0.175	−0.147	−0.141	0.041	−0.245	0.094	−0.133	−0.052	−0.074	0.066	−0.003
MW	−0.104	0.418	−0.155	−0.015	−0.011	−0.193	−0.111	−0.187	0.319	0.427	0.401	0.453	0.435
MR	−0.406	0.693	−0.528	−0.442	−0.444	−0.533	−0.479	−0.487	0.120	0.583	0.668	0.542	0.553
MV	−0.310	0.770	−0.336	−0.278	−0.276	−0.512	−0.281	−0.516	0.383	0.739	0.778	0.699	0.691
PC	−0.387	0.830	−0.459	−0.370	−0.371	−0.563	−0.382	−0.549	0.327	0.766	0.829	0.711	0.722
IR	−0.196	−0.083	−0.345	−0.289	−0.295	−0.048	−0.350	0.042	−0.429	−0.219	−0.135	−0.231	−0.197
ST	−0.150	0.060	−0.219	−0.154	−0.160	−0.032	−0.168	0.009	−0.138	−0.002	0.046	−0.039	0.007
d	0.101	−0.075	0.071	0.193	0.197	0.153	0.083	0.163	0.100	−0.039	−0.098	0.019	0.004
POL	−0.395	0.695	−0.523	−0.437	−0.439	−0.531	−0.473	−0.486	0.125	0.587	0.672	0.546	0.557

Continuation of Table 4

	$^0\chi^V$	$^1\chi^V$	$^2\chi^V$	$^3\chi^V$	AlogP	MW	MR	MV	PC	IR	ST	d	POL
$^0\chi^V$	1												
$^1\chi^V$	0.975	1											
$^2\chi^V$	0.904	0.904	1										
$^3\chi^V$	0.895	0.891	0.916	1									
AlogP	0.294	0.382	0.594	0.536	1								
MW	0.792	0.766	0.853	0.812	0.502	1							
MR	0.927	0.947	0.821	0.813	0.220	0.620	1						
MV	0.887	0.882	0.691	0.706	0.151	0.527	0.850	1					
PC	0.932	0.935	0.744	0.757	0.110	0.578	0.958	0.922	1				
IR	0.154	0.193	0.297	0.261	0.113	0.227	0.345	−0.196	0.150	1			
ST	−0.010	0.003	0.017	0.015	−0.150	0.045	0.140	−0.317	0.073	0.844	1		
d	0.284	0.255	0.497	0.437	0.473	0.787	0.108	−0.109	0.006	0.407	0.280	1	
POL	0.929	0.949	0.821	0.815	0.218	0.623	0.999	0.852	0.960	0.345	0.141	0.111	1

Table 5. Regression parameters and quality of correlations along with their cross-validated parameters

Model No	Parameters used	$A_i =(1$----$6)$	B	SE	R^2	R^2_{adj}	F-ratio	$Q = R$/SE	PRESS/SSY	R^2_{CV}	S_{PRESS}	PSE
1	AlogP	1.0081(±0.2926)	3.6861	0.1758	0.2334	0.2137	11.872	2.7481	3.2851	−2.2851	1.2170	1.1870
2	AlogP	1.7957(±0.2834)	13.7751	0.1398	0.5276	0.5028	21.223	5.1957	0.8952	0.1047	0.9678	0.9317
	$^2\chi^v$	−2.2218(±0.4566)										
3	AlogP	1.8441(±0.2507)	0.8690	0.1235	0.6412	0.6121	22.040	6.4838	0.5595	0.4404	0.8548	0.8120
	Jhete	3.7738(±1.1028)										
	$^2\chi^v$	−1.8773(±0.4157)										
4	AlogP	2.1117(±0.2583)	−22.26291	0.1126	0.7093	0.6770	21.964	7.4796	0.4097	0.5902	0.7619	0.7308
	W	−0.0120(±0.0026)										
	$^1\chi$	4.3824(±0.9245)										
	$^2\chi^v$	−2.2708(±0.4704)										
5	AlogP	1.8253(±0.1669)	−42.7405	0.0875	0.8293	0.8050	34.018	10.4075	0.2057	0.7942	0.6061	0.5600
	BAC	−0.1526(±0.0202)										
	Jhete	20.9749(±2.4959)										
	MR	−0.1931(±0.0282)										
	W	0.0095(±0.0013)										
6	AlogP	1.8069(±0.1588)	−40.2915	0.0832	0.8504	0.8240	32.205	11.0838	0.1759	0.8240	0.5758	0.5243
	BAC	−0.1463(±0.0194)										
	Jhete	20.0432(±2.4092)										
	MR	−0.8400(±0.2971)										
	POL	1.6454(±0.7527)										
	W	0.0090(±0.0013)										

According to Randic[25], these co-linearities are present in most of the first generation indices. However, this discrepancy is removed in the higher generation indices derived later on.

As mentioned before, it is forbidden to use those descriptors simultaneously which are highly correlated when biological activities are modelled. But as discussed elsewhere the Randic recommendation[25] will be followed in such cases. Accordingly one should not discard the descriptors which are highly correlated as their removal will also deprive the contribution of information contents of deleted descriptor.

The data was subjected to regression analysis[26] which resulted into several correlations. Such correlations and their respective statistical qualities are reported in Table 5.

However, during the process of regression analysis[26] it has been observed that compounds **1, 4, 23** and **31** are serious outliers, hence they were deleted from the data set and the entire process of regression analysis was repeated. We do not have convincing reasons why they behave differently but a drastic improvement in the statistics has been observed after they are deleted from the data set. The Models obtain after deleting 4 outliers are given below.

1-parametric model before deleting outliers:

$$\lg 1/IC_{50} = 0.8500\ (\pm 0.3050)\ \text{AlogP} + 4.1821 \tag{1}$$

$n = 45$, SE$= 0.1893$, $R^2 = 0.1530$, $R^2_{adj} = 0.1333$, F-ratio$= 7.768$, $Q = 2.0663$

1-parametric model after deleting outliers:

$$\lg 1/IC_{50} = 1.0081(\pm 0.2926)\ \text{AlogP} + 3.6861 \tag{2}$$

$n = 41$, SE$= 0.1758$, $R^2 = 0.2334$, $R^2_{adj} = 0.2137$, F-ratio$= 11.872$, $Q = 2.7481$

2-parametric model before deleting outliers:

$$\lg 1/IC_{50} = 1.7301(\pm 0.3081)\ \text{AlogP} - 2.3172\ (\pm 0.4819)\ ^2\chi^V + 14.5678 \tag{3}$$

$n = 45$, SE$= 0.1538$, $R^2 = 0.4537$, $R^2_{adj} = 0.4277$, F-ratio $= 17.440$, $Q = 4.3795$

2-parametric model after deleting outliers:

$$\lg 1/IC_{50} = 1.7957(\pm 0.2834)\ \text{AlogP} - 2.2218\ (\pm 0.4566)\ ^2\chi^V + 13.7751 \tag{4}$$

$n = 41$, SE$= 0.1398$, $R^2 = 0.5276$, $R^2_{adj} = 0.5028$, F-ratio$= 21.223$, $Q = 5.1957$

3-parametric model before deleting outliers:

$$\lg 1/IC_{50} = 1.7801\ (\pm 0.2830)\ \text{AlogP} + 3.7728\ (\pm 1.2606)\ \text{Jhete} - 1.9822(\pm 0.4558)\ ^2\chi^V + 1.7115 \tag{5}$$

$n = 45$, SE $= 0.1410$, $R^2 = 0.5517$, $R^2_{adj} = 0.5188$, F-ratio$= 16.816$, $Q = 3.9127$

3-parametric model after deleting outliers:

$$\lg 1/IC_{50} = 1.8441 \ (\pm 0.2507) \ AlogP + 3.7738 \ (\pm 1.1028) \ Jhete \\ - 1.8773 \ (\pm 0.4157) \ ^2\chi^V + 0.8690 \tag{6}$$

$n = 41$, SE$= 0.1235$, $R^2 = 0.6412$, $R^2_{adj} = 0.6121$, F-ratio$=22.040$, $Q = 6.4838$

4-parametric model before deleting outliers:

$$\lg 1/IC_{50} = 2.0776 \ (\pm 0.3000) \ AlogP - 0.0119 \ (\pm 0.0030) \ W + 4.3821 \ (\pm 1.0794) \ ^1\chi \\ -2.3759 \ (\pm 0.5066) \ ^2\chi^V - 21.9821 \tag{7}$$

$n = 45$, SE$=0.1326$, $R^2 = 0.6133$, $R^2_{adj} = 0.5746$, F-ratio$= 15.858$, $Q = 5.9059$

4-parametric model after deleting outliers:

$$\lg 1/IC_{50} = 2.1117 \ (\pm 0.2583) \ AlogP - 0.0120 \ (\pm 0.0026) \ W + 4.3824 \ (\pm 0.9245) \ ^1\chi \\ - 2.2708 \ (\pm 0.4704) \ ^2\chi^V - 22.26291 \tag{8}$$

$n = 41$, SE$=0.1126$, $R^2 = 0.7093$, $R^2_{adj} = 0.6770$, F-ratio $= 21.964$, $Q = 7.4796$

5-parametric model before deleting outliers:

$$\lg 1/IC_{50} = 1.7458 \ (\pm 0.2088) \ AlogP - 0.1495 \ (\pm 0.0244) \ BAC + 20.6757 \\ (\pm 3.0360) \ Jhete - 0.1973 \ (\pm 0.0330) \ MR + 0.0095 \ (\pm 0.0015) \ W - 41.3870 \tag{9}$$

$n = 45$, SE$= 0.1114$, $R^2 = 0.7341$, $R^2_{adj} = 0.7000$, F-ratio$=21.529$, $Q = 7.6911$

5-parametric model after deleting outliers:

$$\lg 1/IC_{50} = 1.8253 \ (\pm 0.1669) \ AlogP - 0.1526 \ (\pm 0.0202) \ BAC + 20.9749 \\ (\pm 2.4959) \ Jhete - 0.1931 \ (\pm 0.0282) \ MR + 0.0095 \ (\pm 0.0013) \ W - 42.7405 \tag{10}$$

$n = 41$, SE$= 0.0875$, $R^2 = 0.8293$, $R^2_{adj} = 0.8050$, F-ratio$=34.018$, $Q = 10.4075$

6-parametric model before deleting outliers:

$$\lg 1/IC_{50} = 1.7279 \ (\pm 0.2041) \ AlogP - 0.1445 \ (\pm 0.0240) \ BAC + 19.8950 \\ (\pm 2.9994) \ Jhete - 0.8560 \ (\pm 0.3875) \ MR + 1.6690 \ (\pm 0.9784) \ Pol \\ + 0.0091 \ (\pm 0.0015) W - 39.2042 \tag{11}$$

$n = 45$, SE$= 0.1087$, $R^2 = 0.7530$, $R^2_{adj} = 0.7140$, F-ratio$=19.304$, $Q = 7.9830$

6-parametric model after deleting outliers:

$$\lg 1/IC_{50} = 1.8069 \ (\pm 0.1588) \ AlogP - 0.1463 \ (\pm 0.0194) \ BAC \\ + 20.0432 \ (\pm 2.4092) \ Jhete - 0.8400 \ (\pm 0.2971) \ MR + 1.6454 \ (\pm 0.7527) \ Pol \\ + 0.0090 \ (\pm 0.0013) \ W - 40.2915 \tag{12}$$

$n = 41$, SE$= 0.0832$, $R^2 = 0.8504$, $R^2_{adj} = 0.8240$, F-ratio$=32.205$, $Q = 11.0838$.

One can go up to 8-parametric models, the rule of thumb allows that, but in this case the quality of higher parametric models did not show further significant improvement in the statistics. Hence, higher parametric models have not been reported here.

The 6-parametric model reported above explains about 85% variance of the data. Very high Q (Refs 27 and 28) and small SE value also indicates that the quality

of the model is excellent. Hence, it may be concluded that the 6-parametric model mentioned above is the most appropriate model for modelling the lg $1/IC_{50}$ value of the compounds used under present study.

The sign of AlogP in the above model is positive suggesting that the lipophilicity favours the activity. Similarly, the Jhete and Wiener indices have positive signs indicating that the cyclisation and branching will favour the activity. The molar refractivity has a negative sign, therefore, it will have a retarding effect on the activity, but the polarisability certainly favours the activity. The parameter BAC has a negative coefficient in the model indicating its negative role towards the activity.

To check the predictive power of the model, the lg $1/IC_{50}$ values have been estimated by using the best 6-parametric model. Such values are reported in Table 6. A perusal of this table clearly indicates that the calculated values are in good agreement with the observed values. This confirms the finding that the 6-parametric model discussed above is the most appropriate model for modelling, estimating the lg $1/IC_{50}$ values of the compounds used in the present study.

Table 6. Observed and estimated lg $1/IC_{50}$ values using model No 6

Compd. No	Observed lg $1/IC_{50}$	Estimated lg $1/IC_{50}$	Residual
1	2	3	4
2	8.820	8.696	0.124
3	8.660	7.891	0.769
5	8.350	8.784	−0.434
6	8.290	7.983	0.307
7	8.220	7.568	0.652
8	8.190	8.012	0.178
9	8.120	7.788	0.332
10	7.800	8.071	−0.271
11	7.800	7.293	0.507
12	7.680	7.635	0.045
13	7.680	7.359	0.321
14	7.460	7.076	0.384
15	7.380	6.914	0.466
16	7.370	8.252	−0.882
17	7.330	7.491	−0.161
18	7.240	6.857	0.383
19	7.130	7.107	0.023
20	6.960	6.990	−0.030
21	6.960	7.141	−0.181
22	6.720	5.843	0.877
24	6.000	6.438	−0.438
25	5.700	4.989	0.711
26	5.220	4.973	0.247

to be continued

1	2	3	4
27	5.200	5.242	−0.042
28	4.400	5.567	−1.167
29	6.890	7.117	−0.227
30	5.400	6.694	−1.294
32	5.500	5.401	0.099
33	4.000	3.782	0.218
34	5.460	6.202	−0.742
35	5.090	5.096	−0.006
36	8.720	8.275	0.445
37	8.360	8.540	−0.180
38	8.120	8.636	−0.516
39	7.720	7.748	−0.028
40	7.520	6.992	0.528
41	7.030	7.180	−0.150
42	7.000	6.160	0.840
43	7.000	7.102	−0.102
44	6.400	7.260	−0.860
45	3.000	3.744	−0.744

The predictive power of the model was calculated by plotting a graph between the observed and estimated lg $1/IC_{50}$ values. Such plot is presented in Fig. 2. The predictive R^2 value comes out to be 0.8504.
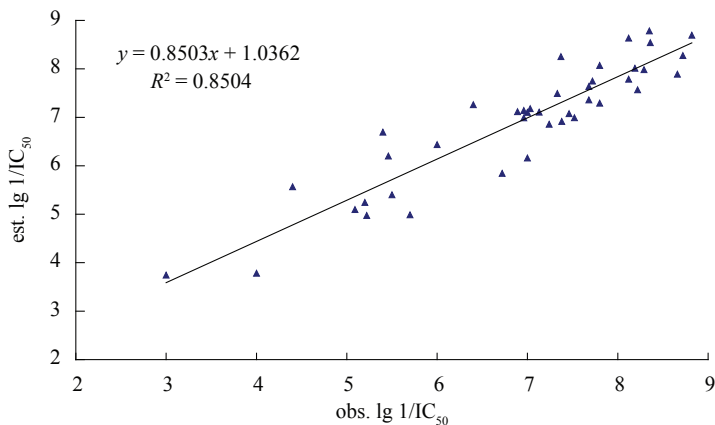

Fig. 2. Correlation between observed lg $1/IC_{50}$ versus estimated lg $1/IC_{50}$ using model No 6 (Table 4)

Final confirmation is obtained by calculating the cross-validated parameters which are recorded in Table 5. The predictive power for the best models was carried out by the leave-one-out cross-validation procedure. PRESS (predicted residual sum

of squares) appears to be the most important cross-validation parameter accounting for a good estimate of the real predictive error of the models. Its value less than SSY (sum of squares of response value) indicates that the model predicts better than the chance and can be considered statistically significant. In our case PRESS << SSY means that the value of PRESS is much lesser than SSY indicating that all the models obtained are statistically significant. The ratio PRESS/SSY can be used to calculate approximate confidence intervals of prediction of new compounds. To be a reasonable and significant QSAR model the ratio PRESS/SSY should be less than 0.4 (PRESS/SSY < 0.4) and the value of this ratio smaller than 0.1 indicates an excellent model. R^2_{cv} is the cross-validated squared correlation coefficient. The highest R^2_{cv} value for 6-parametric model (equation (12)) confirming our predictions. The 2 important cross-validation parameters Uncertainty in prediction (S_{PRESS}) and Predictive squared error (PSE) were also calculated. The lowest PSE of equation (12) supports its highest predictive potential. The highest R^2_{cv} and lowest PRESS/SSY, PSE and S_{PRESS} values for the 6-parametric model further confirm the above findings.

CONCLUSIONS

The following conclusions may be drawn.

1. No mono-parametric correlations are statistically allowed to model $1/lg\ IC_{50}$.

2. None of the 2-parametric correlations are found suitable for the modelling.

3. Even 3-parametric, 4-parametric correlations are not acceptable.

4. However, 5-parametric models were found to be statistically significant for modelling the biological activity. The best 5-parametric models contain AlogP, BAC, Jhete, MR, W as correlating parameters. For this model the R^2 value comes out to be 0.7341.

5. Only three 6-parametric correlations were obtained which have slightly better R^2 values as compare to 5-parametric correlation.

6. The best 6-parametric model contains AlogP, BAC, Jhete, MR, POL, and W as correlating parameters and the R^2 value comes out to be 0.7530.

On the basis of the Pogliani quality factor Q, the 6-parametric model is the best model for modelling $lg\ 1/IC_{50}$ values of the present set of compounds.

REFERENCES

1. B. B. ANA, M. A. ROSA, M. J. ROSA, W. WOLFGANG: Instability of Calcium Channel Antagonists during Sample Preparation for LC–MS–MS Analysis of Serum Samples. Forensic Sci Int, **156**, 23 (2006).
2. T. GODFRAIND, S. SALOMONE: New Advances in Hypertensive Treatment with Calcium Antagonists. J Cardiovasc Pharmacol, **30**, S1 (1997).
3. P. A. van ZWIETEN: Pharmacological Profile of Barnidipine: A Single Optical Isomer Dihydropyridine Calcium Antagonist. Blood Press Suppl, **7**, 5 (1998).

4. W. G. NAYLER: Calcium Antagonists: Past, Present and Future – A Personal View. J Clin Basic Cardia, **2**, 155 (1999).

5. V. K. AGRAWAL, K. C. MATHUR, P. V. KHADIKAR, M. MANDLOI, S. KARMARKAR: Estimation of Antihypertensive Activity of 2-aryl-imino-imidazolidines Using Szeged Index**.** Oxid Commun, **25**, 193 (2002).

6. V. K. AGRAWAL, P. V. KHADIKAR: QSAR Study on Antihypertensive Activity of a Series of Alkyl N-[biphenyl alkyl] aminoalkyl-4-aryl-1,4-dihydro-2,6-dimethyl Pyridine-3,5 Di-carboxylats. Oxid Commun, **26**, 1 (2003).

7. P. V. KHADIKAR, S. KARMARKAR, K. GAUR, S. SINGH, V. K. AGRAWAL: QSAR Study Using Distance-based Topological Indices. Oxid Commun, **27**, 1 (2004).

8. S. KARMARKAR, K. GAUR, S. SINGH, V. K. AGRAWAL, K. C. MATHUR, P. V. KHADIKAR: QSAR Studies on Anti-tuberculotic Activity. Oxid Commun, **27**, 12 (2004).

9. P. V. KHADIKAR, V. K. AGRAWAL: Thermal Characterization of Macrocyclic Cation Complexes: Gadolinium (III) Complex aith Dibenzo-18-Crown-6. Oxid Commun, **28**, 810 (2005).

10. V. K. AGRAWAL, J. SINGH, A. PANDEY, P. V. KHADIKAR: Modeling of Inhibitory Activities of Sulfanil-amide Schiff's Bases Using Physicochemical Properties. Oxid Commun, **29**, 803 (2006).

11. V. K. AGRAWAL, J. SINGH, A. PANDEY, P. V. KHADIKAR**:** QSAR Studies on Some Anti-HIV-1 Drugs: Deoxy Analogues of HEPT-1. Oxid Commun, **29**, 803 (2006).

12. J. SINGH, V. K. DUBEY, V. K. AGRAWAL, P. V. KHADIKAR: QSAR Study on Octanol–Water Partitioning: Dominating Role of Equalized Electronegativity. Oxid Commun, **31** (1), 27 (2008).

13. V. K. AGRAWAL, J. SINGH, S. SINGH, P. V. KHADIKAR: Use of Topological as Well as Quantum Chemical Parameters in Modeling Antimalarial Activity of 2,4-diamino-6-quinazoline Sulfonamides. Oxid Commun, **31**, 2 (2008).

14. J. SINGH, V. K. AGRAWAL, B. SHAIK, S. CHATURVEDI, P. V. KHADIKAR: Topological Modeling of Hydrophobicity of Compounds Exhibiting Narcosis. Oxid Commun, **31** (4), 264 (2008).

15. J. SHRIVASTAVA, J. SINGH, B. SHAIK, V. K. AGRAWAL: Prediction of Blood-brain Barrier Permeation Using Topological Descriptors. Oxid Commun, **31**, 776 (2008).

16. V. K. AGRAWAL, J. SINGH, K. C. MISHRA, K. SINGH, A. PANDEY, P. V. KHADIKAR: Topological Estimation of Binding Affinities (Δg_b) for Hept and Nevirapine Analogues with HIV-1 Reverse Transcriptase: Molecular Linearity Approach. Oxid Commun, **32**, 13 (2009).

17. P. V. KHADIKAR, J. SINGH, V. K. AGRAWAL**:** QSAR Study on Modeling of the Rate of Glycine Conjugation of Some Benzoic Acid Derivatives: A Topological Approach. Oxid Commun, **32**, 40 (2009).

18. J. SINGH, S. K. SHUKLA, B. SHAIK, V. K. AGRAWAL: Modeling Angiotensin II Antagonist Activity of 4H-1,2,4 -triazoles. J Eng Sci Mangt Edu, **1** (2), 57 (2010).

19. J. SINGH, B. SHAIK, V. K. AGRAWAL, P. V. KHADIKAR: SAR Studies on β-Cell K$_{ATP}$ Channel Openers. Inter Disciplinary Sci Comput Life Sci, **4**, 215 (2012).

20. B. SHAIK, J. SINGH, I. AHMAD, VENKATESHWAR, V. K. AGRAWAL: Modeling Toxicity of Some Aromatic Compounds towards *Tetrahymena pyriformis* Using Some Physicochemical Parameters. Oxid Commun, **36** (1), 205 (2013).

21. V. K. AGRAWAL, J. SINGH, M. GUPTA, P. V. KHADIKAR, C. T. SUPURAN: QSAR Studies on Benzopyrans as Potassium Ion Channel Activators. Eur J Med Chem, **41** (3), 360 (2006).

22. DRAGON: Software for Calculation of Topological Indices, www.disat.unimib.it.

23. CHEM SKETCH: www.acdlabs.com

24. M. C. A. COSTA, A. C. GAUDIO. Y. TAKAHATA: A Comparative Study of Principal Component and Linear Multiple Regression Analysis in SAR and QSAR Applied to 1,4-dihydropyridine Calcium Channel Antagonists (Nifedipine Analogues). Theochem, **394**, 291 (1997).

25. M. RANDIC: On Characterization of Chemical Structure. J Chem Inf Comput Sci, **37**, 672 (1997).

26. S. CHATERJEE, A. S. HADI, B. PRICE: Regression Analysis by Examples. 3rd ed. Wiley, New York, 2000, 51–80.

27. L. POGLIANI: Structure - Property Relationships of Amino Acids and Some Dipeptides. Amino Acids, **6**, 141 (1994).

28. L. POGLIANI: Modeling with Special Descriptors Derived from a Medium Size Set of Connectivity Indices. J Phys Chem, **100**, 18065 (1996).

NANO SILVER-DOPED MANGANESE OXIDE AS CATALYST FOR OXIDATION OF BENZYL ALCOHOL AND ITS DERIVATIVES: SYNTHESIS, CHARACTERISATION, THERMAL STUDY AND EVALUATION OF CATALYTIC PROPERTIES

S. F. ADIL, M. E. ASSAL, M. KHAN, A. AL-WARTHAN,
M. RAFIQ H. SIDDIQUI*

*Department of Chemistry, College of Science, King Saud University, P.O. 2455,
11 451 Riyadh, Kingdom of Saudi Arabia*
E-mail: *rafiqs@ksu.edu.sa*

ABSTRACT

Manganese oxide doped with silver nanoparticles was synthesised by co-precipitation method. The w/w percentage of silver was varied from 1 to 5 and was calcined at different temperatures. The oxidation catalytic properties of these materials were investigated for the conversion of benzyl alcohol to benzaldehyde using molecular oxygen as clean oxidant. It was observed that the calcination temperature and surface area of the catalyst play a significant role in the catalytic process. The w/w percentage of silver present in the catalyst affects the oxidation property. The catalyst 1% Ag–MnO$_2$ displayed > 99% conversion and > 99% selectivity towards benzaldehyde. The derivatives of benzyl alcohol such as 4-methylbenzyl alcohol, 4-methoxybenzyl alcohol, 4-chlorobenzyl alcohol, 4-nitrobenzyl alcohol, 4-*tert*-butylbenzyl alcohol, 4-(trifluoromethyl)benzyl alcohol and 3-nitrobenzyl alcohol were also converted into corresponding aldehydes using the synthesised catalyst with high conversion and selectivity. Selectivity towards aromatic alcohols was also observed.

Keywords: nano silver, manganese oxide, oxidation, benzyl alcohol, derivative of benzyl alcohol.

AIMS AND BACKGROUND

Oxidation of aromatic alcohols to corresponding aldehydes is an important area of research for scientists around the world as they play a significant role of building blocks for many organic compounds[1–3]. Several heterogeneous catalysts have been reported in literature[4–12] with regard to the conversion of alcohols to aldehydes us-

---

* For correspondence.

ing noble metals such as Pt, Ru, Au, Pd and their derivatives using oxygen as an oxidant. Pt-based catalysts can be easily poisoned which make them sensitive and hence can be used only in mild conditions, while gold catalysts have been reported for their high selectivity towards aldehydes[13]. Silica-supported catalysts have also been reported widely in literature[14,15] for gas-phase oxidations of ethylene and for methanol oxidations.

Nevertheless, the attention received by Ag-based catalyst[16–20] for the selective oxidation of alcohols in liquid phase is very little. Salker et al.[21] reported the use of nano Ag-doped manganese for the oxidation of CO, which illustrates that Ag can be explored as a potential for catalytic oxidation reactions in the liquid phase. Based on these earlier reports, recently our group has reported the use of Ag-based catalyst[22] for the oxidation of benzyl alcohol.

In continuation of our research work in the area of selective alcohol oxidation to aldehydes using mixed metal oxides, we herein report the synthesis of nano Ag-doped manganese oxide and its application as catalyst for the oxidation of benzyl alcohol as a model compound. We synthesised various catalysts by altering the w/w % of Ag doping on manganese dioxide, which were characterised by SEM, EDX, TEM, XRD, FT–IR, BET and TGA. The catalytic activity was evaluated and the conversion was monitored by gas chromatography.

EXPERIMENTAL

Catalyst preparation. Nanosized Ag-doped MnO_2 catalysts of the type %X Ag–MnO_2 (where X = 0, 1, 3 and 5) were prepared by co-precipitation method where %X denotes w/w %. Stoichiometric amount of manganese(II) nitrate-tetra-hydrate $(Mn(NO_3)_2 \cdot 4H_2O)$ and silver nitrate $(AgNO_3)$ were dissolved in distilled water. About 100 ml of the mixture of solutions were taken in a round bottomed flask. The solution was heated to 80°C, while stirring using a mechanical stirrer and 1 M solution of sodium hydrogen carbonate $(NaHCO_3)$ was added dropwise until the solution attained a pH 9. The solution was stirred at the same temperature for about 3 h and then left on stirring overnight at room temperature. The solution was filtered using a Buchner funnel under vacuum and the product obtained was dried at 70°C overnight and calcined at different temperatures.

Catalyst characterisation. Scanning electron microscopy (SEM) and elemental analysis (Energy Dispersive X-ray Analysis: EDX) were carried out using a Jeol SEM model JSM 6360A (Japan). This was used to determine the morphology of nanoparticles and its elemental composition. Transmission electron microscopy (TEM) was carried out using a Jeol TEM model JEM-1101 (Japan), which was used to determine the shape and size of nanoparticles. Powder X-ray diffraction studies were carried out using an Altima IV [Regaku] X-ray diffractometer. The infrared spectra obtained by the Fourier Transform Infrared Spectroscopy (FT–IR) were recorded as KBr pellets using a Perkin–Elmer 1000 FT–IR spectrophotometer. BET surface area was measured on a

NOVA 4200e surface area and pore size analyser. Thermogravimetric analysis was carried out using a Perkin–Elmer thermogravimetric analyser 7.

Catalyst testing. In a typical reaction run, 300 mg of catalyst were loaded in a glass flask pre-charged with 0.2 ml (2 mmol) benzyl alcohol with 10 ml toluene as solvent; the mixture was then heated to 100°C with vigorous stirring. Oxygen was bubbled at a flow rate of 20 ml min^{-1} into the mixture once the reaction temperature was attained. After reaction, the solid catalyst was separated by centrifugation and the liquid samples were analysed by gas chromatography to evaluate the conversion of the desired product by (GC, 7890A) Agilent Technologies Inc., equipped with a flame ionization detector (FID) and a 19019S-001 HP-PONA column.

RESULTS AND DISCUSSION

Microscopic and spectroscopic characterisation of the catalysts. The synthesised catalyst was characterised by electron microscopy to evaluate the morphology and particle size of the catalyst. The scanning electron microscopy analysis of the synthesised catalyst 1% Ag–MnO$_2$ calcined at different temperatures (300, 400 and 500°C) and MnO$_2$ at 400°C calcination temperature was carried out. The micrographs are shown in Figs 1 and 2. It suggests that the morphology of the synthesised catalysts is well defined and spherical in shape and it was observed that surface of the catalysts was very homogeneous without any obvious phase separation in the synthesised catalyst, the same observations were made for the undoped MnO$_2$.
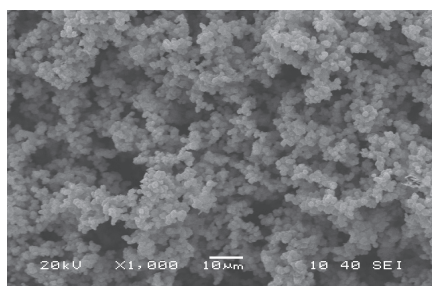

Fig. 1. SEM analysis of the synthesised catalyst 1% Ag–MnO$_2$ calcined at 400°C
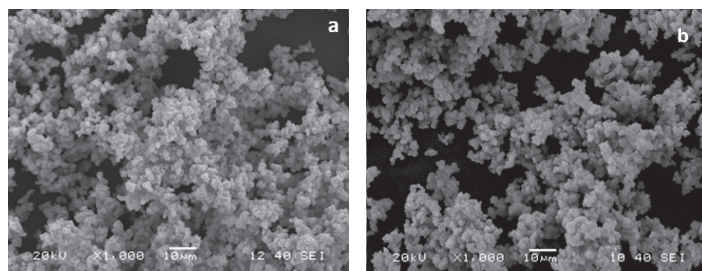

Fig. 2. SEM micrograph of the catalyst 1% Ag–MnO$_2$ calcined at 300°C (a) and 500°C (b)

The samples of undoped MnO_2 and the catalyst 1% Ag–MnO_2 were subjected to TEM. From Fig. 3, it can be noticed that the particle size of undoped MnO_2 which is calcined at 400°C is found to be larger, thus, when compared to the TEM image of synthesised catalyst 1% Ag–MnO_2 calcined at 400°C, it is clear that the Ag particles doped are present in nanosize, spherical in shape and are well dispersed on MnO_2. The particle size distributions graph, which was calculated by using the general-purpose image processing program Image J software, suggests that the catalyst calcined at 400°C contains particles ranging from 0.5 to 7 nm with a mean particle size of 3.68±0.02 nm and the results are illustrated in Fig. 4.
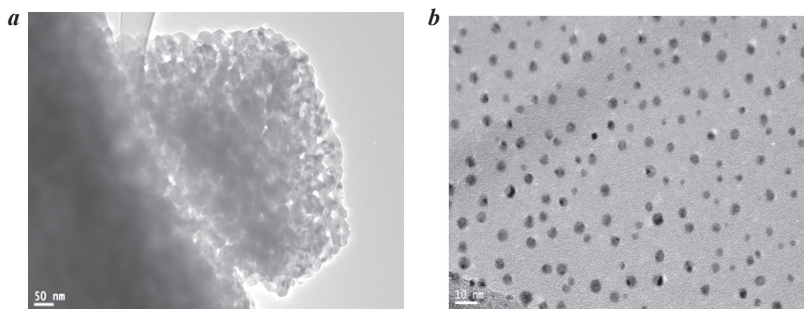

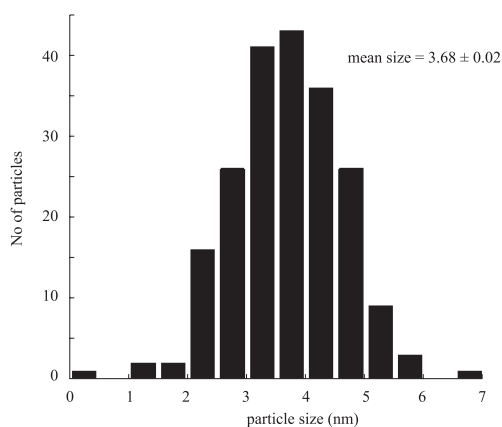**Fig. 3**. TEM micrograph of MnO_2 (*a*) and 1% Ag–MnO_2 calcined at 400°C (*b*)

Fig. 4. Particle distribution graph of the catalyst 1% Ag–MnO_2 calcined at 400°C

Figure 5 illustrates the X-ray diffraction pattern of 1% Ag–MnO_2 calcined at (300, 400 and 500°C), while Fig. 6 shows X-ray diffraction patterns of the mixed oxides of X% Ag–MnO_2 (where X= 1, 3 and 5) pre-calcined at 400°C. The symbols in Figs 5 and 6 indicate the peak of the corresponding phase. Observations made in the XRD spectrum (Fig. 5) indicate that the catalyst 1% Ag–MnO_2, calcined at 300°C contains a mixture of tetragonal α-manganese (1/2) oxide (ICSD # 73363) and trigonal rhombohedral manganese carbonate (ICSD # 100677). The catalyst calcined at 400°C was found to contain peaks corresponding to tetragonal β-manganese(IV) oxide (ICSD #

73716). The XRD pattern indicates that this phase is amorphous in nature, while the catalyst calcined at 500°C was found to contain peaks corresponding to cubic manganese (III) oxide (ICSD # 76087) and tetragonal α-manganese (1/2) oxide (ICSD # 73363). When similar study of the XRD spectrum of X% Ag–MnO$_2$ (Fig. 6) (where X = 1, 3 and 5) pre-calcined at 400°C was carried out it was found that the 1% Ag–MnO$_2$ contains peaks corresponding to tetragonal β-manganese dioxide (ICSD # 73716), while in the spectrum of 3% Ag–MnO$_2$ and 5% Ag–MnO$_2$ the phase corresponds to trigonal rhombohedral manganese carbonate (ICSD # 100677). When the XRD data were compared with the catalytic activity the best catalytic activity of the synthesised
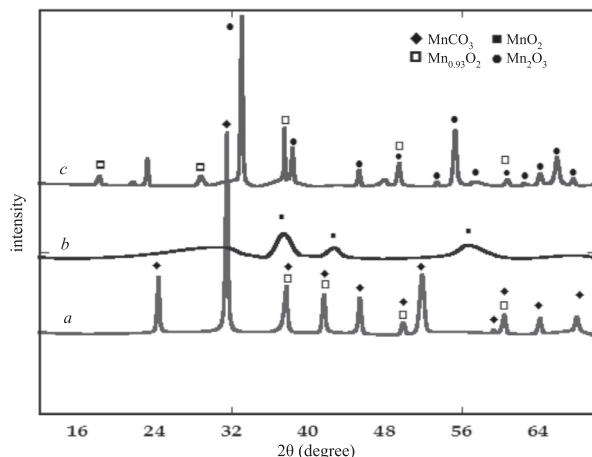

Fig. 5. XRD pattern of the catalyst 1% Ag–MnO$_2$ calcined at different temperatures: 300°C (*a*), 400°C (*b*), and 500°C (*c*)
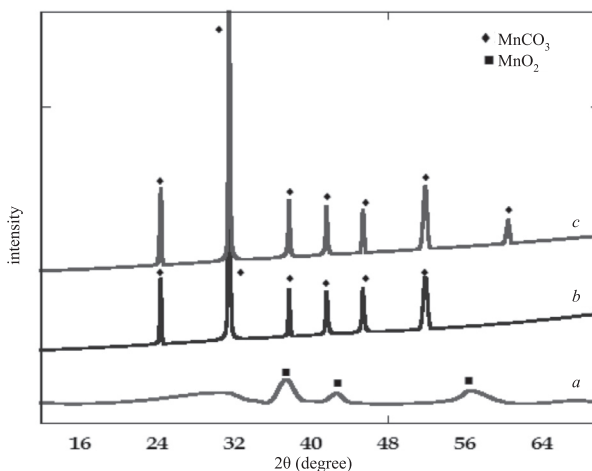

Fig. 6. XRD pattern of the catalyst Ag–MnO$_2$ with varying percentages of Ag: 1% Ag–MnO$_2$ (*a*); 3% Ag–MnO$_2$ (*b*), and 5% Ag–MnO$_2$ (*c*)

782

catalyst could be attributed to the presence of β-manganese(IV) oxide. When the XRD data were compared with the catalytic activity of the synthesised catalysts, it was found that the catalyst in which the presence of tetragonal β-manganese(IV) oxide was observed gave the best catalytic performance. The presence of other phases of manganese oxides, such as the mixture of tetragonal α-manganese (1/2) oxide and cubic manganese(III) oxide, found in the catalyst calcined at 500°C and tetragonal α-manganese (1/2) oxide along with trigonal rhombohedral manganese carbonate found in the catalyst calcined at 300°C may be responsible for the decrease in catalytic activity. The presence of different phases of oxides of manganese other than tetragonal β-manganese(IV) oxide may be attributed to the decrease in catalytic activity.

The broad nature of the peaks found in the XRD spectrum suggests that the particle size is small which was found in the XRD spectrum of 1% Ag–MnO$_2$ where the peaks were found to be broader when compared to the spectra of 3 and 5% Ag–MnO$_2$. The comparison among the catalyst of 1% Ag–MnO$_2$ calcined at different temperatures such as (300, 400 and 500°C), showed that the catalyst calcined at 400°C gave broader peaks than those of the catalysts calcined at 300 and 500°C as shown in Fig. 5. These assumptions were corroborated by the crystallite size calculation carried out by the Debye Scherer equation. The crystallite size of the catalyst 1% Ag–MnO$_2$ calcined at 400°C was found to be in the range 0.4–2.8 nm with an average crystallite size of 1.45 nm, while the catalysts calcined at 300 and 500°C have been found to have crystallite size in the range of 7.7–10.7 nm (average size 9.7 nm) and 7.9–13.3 nm (average size 10.5 nm), respectively. The crystallite size calculations done for the 3% Ag–MnO$_2$ and 5%Ag–MnO$_2$ were carried out according to the Debye Scherer equation and it was found that the crystallite size was in the range 13.7–16.1 nm (average size 13.22 nm) and 5.1–15.8 nm (average size 12.73 nm), respectively.

Figure 7 shows FT-IR spectra of the synthesised catalysts 1% Ag–MnO$_2$ at different calcination temperatures (300, 400 and 500°C). High wavenumber region reveals stretching vibrations of the hydroxyl groups. The characteristic bands of νOH located at approximately 3450 cm^{-1} were found to be present in the 400 and 500°C calcined catalyst, while in the catalyst calcined at 300°C there is no peak found in this area which suggests the absence of OH group on the catalyst surface. The decrease in the intensity of these bands with an increase of the calcination temperature depicts the decrease of the presence of hydroxyl group on the catalyst surface. Similar trends are visible for the bands located at around 1650 cm^{-1}, which identified as finger-print region for bending vibrations of the hydroxyl groups[23]. It can be said that the hydroxyl group does play an important role in the catalytic oxidation for the conversion of benzyl alcohol to benzaldehyde as the reaction when carried out by the catalyst 1% Ag–MnO$_2$ calcined at 400°C exhibits the highest catalytic activity when compared to the rest. The presence of peak at 1799.59 cm^{-1} suggests the presence of νC=O in the catalyst. The presence of a sharp peak at approximately 1380 cm^{-1} is a finger-print for surface nitrate (NO$_3^-$) and it could be stated that the 300°C calcination temperature

is not sufficient to decompose the nitrate. Significant peaks are observed in the range of 400–700 cm^{-1} typical for different oxides of manganese[24,25].
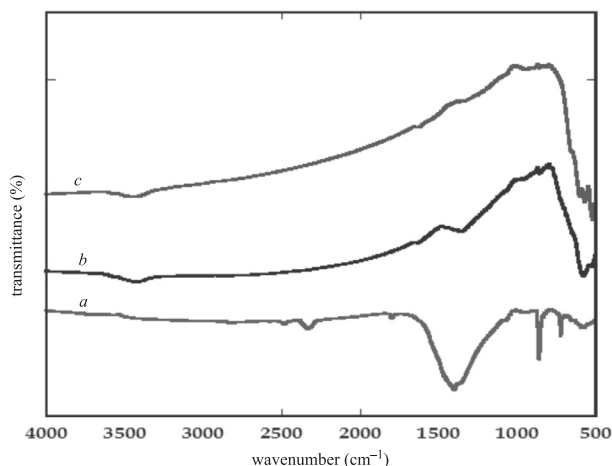

Fig. 7. FT–IR spectra of the catalyst 1% Ag–MnO$_2$ calcined at different temperatures: 300°C (*a*); 400°C (*b*), and 500°C (*c*)

Thermogravimetric and surface area analysis of catalyst. Thermal gravimetric analysis (TGA) was carried out to evaluate the thermal stability of the synthesised catalyst. The thermal gravimetric analysis was conducted to observe the change in the thermal behaviour of Ag nanoparticles doped on MnO$_2$ from the undoped MnO$_2$. It was observed that MnO$_2$ displays a gradual loss of weight from 30°C and trends down to a loss of weight of about 7% at 400°C, the weight is reduced to 86% by 480°C. When the same conditions were applied to the analysis of 1% Ag–MnO$_2$ catalyst the TGA exhibits first a slow degradation step, whose onset temperature is 50°C, attributed to decomposition of volatile impurities and moisture. The catalyst displays no weight loss till to temperature of 370°C. There is a sudden loss of weight observed in the temperature range 380–480°C. The loss of weight observed in this region was about 25%. Hence this can be concluded that the catalyst displays a thermal stability up to 400°C and a significant deterioration in thermal stability observed with increase in temperature thereon. The results are depicted in Fig. 8. A similar trend was observed in the thermogram for 3% Ag–MnO$_2$ and 5% Ag–MnO$_2$ catalysts.
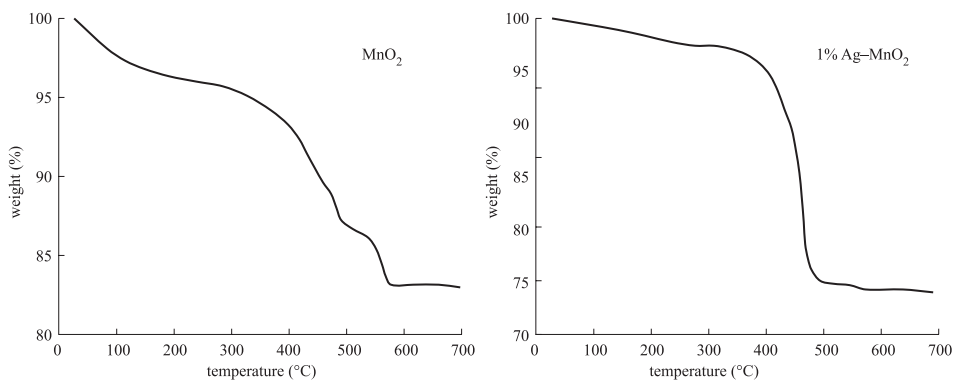
784

Fig. 8. Thermogravimetric analysis (TGA) curves of catalyst MnO_2 and 1% Ag–MnO_2

The results obtained from BET surface area analysis showed that the surface area of undoped MnO_2, calcined at 400°C was found to be 31.101 $m^2\,g^{-1}$, but after the incorporation of 1%Ag nanoparticles in MnO_2 which is calcined at 400°C there was a significant increase in the surface area, to 77.998 $m^2\,g^{-1}$. This considerable increase in surface areas can be assigned to the presence of Ag nanoparticles of the surface of MnO_2, which leads to a substantial increase in catalytic activity of the catalyst. The surface areas of the synthesised 1% Ag–MnO_2 catalyst at calcination temperatures 300 and 500°C were found to be less than that of the catalyst calcined at 400°C. The surface area analysis results of the synthesised 1% Ag–MnO_2 catalyst at different calcination temperatures (300, 400 and 500°C) and undoped MnO_2 at 400°C calcination temperature are summarised in Table 1.

Table 1. Effect of calcination temperature on the catalytic properties
Catalyst amount – 300 mg; temperature 100°C; oxygen flow rate 20 ml min^{-1}; benzyl alcohol – 2 mmol; toluene – 10 ml; reaction time 2 h

Entry	Catalyst	Temperature	SA (m^2g^{-1})	Conversion (%)	Selectivity (%)
1	MnO_2	400°C	31.101	52.56	99>
2	1% Ag–MnO_2	300°C	31.708	98.51	99>
3	1% Ag–MnO_2	400°C	77.998	100.00	99>
4	1% Ag–MnO_2	500°C	27.347	25.90	99>

Catalytic performance. In order to evaluate the catalytic performance of the synthesised catalyst, the conversion of benzyl alcohol to benzaldehyde was used as a model reaction.

Effect of % of Ag doped on the catalyst. In order to evaluate the optimum % of Ag doping on MnO_2 for best catalytic activity and its effect on the kinetics of the reaction, catalysts were prepared by varying the amount of Ag from 0 to 5% in the catalyst and these were used for the oxidation of benzyl alcohol to benzaldehyde. All the catalysts used were calcined at 400°C. When undoped manganese dioxide catalyst (0%

Ag–MnO$_2$) was employed for the similar reaction it yielded only 52.56%, while 1% Ag–MnO$_2$ gave about 100% conversion product, and 3% Ag–MnO$_2$, 5% Ag–MnO$_2$ give 77 and 53% conversion products, respectively (Table 2).

From the above finding it can be said that the Ag nanoparticles play an essential role in catalytic activity for the conversion of benzyl alcohol to benzaldehyde. It can be concluded from the above results that the catalyst with 1% Ag was the best among the series of the catalyst prepared, based on which 1% Ag–MnO$_2$ was used for all the further studies such as effect of calcination temperature and amount of catalyst. A graphical representation of the finding is given in Fig. 9. The results are summarised in Table 2.
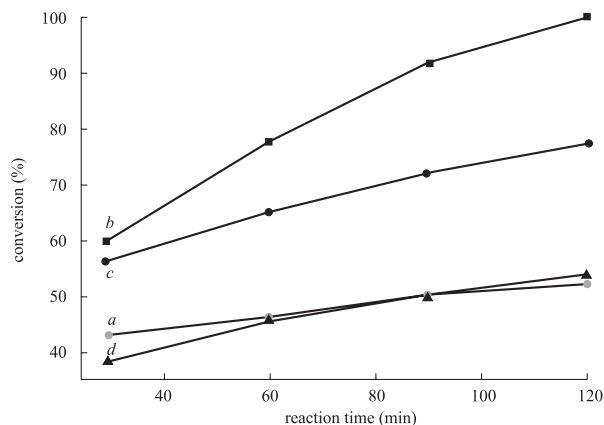

Fig. 9. Graphical representation of benzyl alcohol oxidation using catalyst: MnO$_2$ (*a*); 1% Ag–MnO$_2$ (*b*); 3% Ag–MnO$_2$ (*c*), and 5% Ag–MnO$_2$ (*d*)

Table 2. Effect on the catalytic properties by weight % of Ag in the catalyst
Catalyst amount – 300 mg; temperature 400°C; oxygen flow rate 20 ml min^{-1}; benzyl alcohol – 2 mmol; toluene – 10 ml; reaction time 2 h

Entry	% Ag	Conversion (%)
1	0	52.56
2	1	100.00
3	3	77.31
4	5	53.75

Effect of calcination temperature. Since calcination temperature also plays a vital role in the kinetics of the reaction the prepared catalyst was calcined at different temperatures such as 300, 400 and 500°C. These catalysts were employed for oxidation of benzyl alcohol and their effect on the kinetics of the reaction was studied. When the catalyst was calcined at 300°C it was observed that there is a less catalytic activity with 98.51% conversion of the product, while the catalyst calcined at 500°C gave just 25.90% conversion, which was the least catalytic activity observed among the catalysts prepared. This could be ascribed to the presence of different phases of man-

786

ganese oxide rather than to tetragonal/orthorhombic manganese(IV) oxide which was found in the catalyst calcined at 400°C and presence of impurities such as manganese carbonate found in the catalyst calcined at 300°C which was ascertained by the XRD spectrum. From the above findings it can be said that the catalyst calcined at 400°C displayed best catalytic activity and this calcinations temperature is most favourable for best catalytic performance of the synthesised catalyst 1% Ag–MnO_2. The results are summarised in Table 1 and graphical illustration is given in Fig. 10.
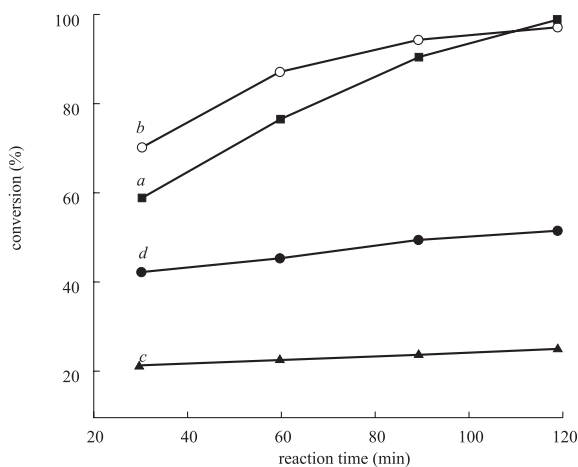

Fig. 10. Graphical representation of benzyl alcohol oxidation using catalyst calcined at different temperatures: 400°C (*a*); 300°C (*b*); 500°C (*c*), and MnO_2 (400°C) (*d*)

Effect of catalyst amount. In order to evaluate and standardise the amount of catalyst necessary for the reaction, a study was carried out by varying the amount of catalyst used in the reaction for oxidation of benzyl alcohol. The reaction was carried out using 100, 150, 200, 250 and 300 mg of catalyst calcined at 400°C. The reaction was carried out under identical conditions mentioned earlier and it was found that the reaction carried out using 300 mg catalyst displayed best activity by yielding a 100% conversion, while the rest gave less than 100%. It could be concluded that the necessary amount of catalyst for 100% conversion of product was 300 mg. The results are summarised in Table 3. It was observed that the conversion of benzyl alcohol to benzaldehyde increased by increasing the amount of catalyst. It suggests that the there is a linear relationship between the amount of catalyst and conversion of benzyl alcohol as shown in Fig. 11. In order to understand the effect of catalyst on the solvent used, which is toluene in the present study, a blank reaction was carried out without the substrate benzyl alcohol using 1% Ag–MnO_2 as catalyst and it was found that no product was formed. Hence it can be concluded that the conversion product benzaldehyde obtained is from the catalytic conversion of benzyl alcohol and not from toluene.
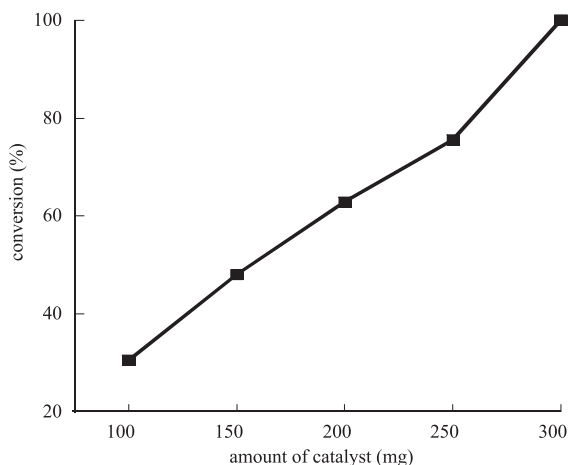
Fig. 11. Effect of catalyst amount (mg) on the conversion of benzyl alcohol

Table 3. Influence of catalyst amount on the reaction kinetics
Calcination temperature 400°C; reaction temperature 100°C; oxygen flow rate 20 ml min^{-1}; benzyl alcohol 2 mmol; toluene 10 ml; reaction time 2h

Entry	Amount of catalyst (mg)	Conversion (%)
1	100	30.59
2	150	48.11
3	200	62.94
4	250	75.61
5	300	100.00

Catalytic performance on different substituted benzyl alcohols. From the conversion of benzyl alcohol to benzaldehyde which was used as a model reaction it was ascertained that the best catalytic activity was displayed by 1% Ag–MnO$_2$, calcined at 400°C, which was also confirmed by spectral studies to contain tetragonal β-manganese(IV) oxide as confirmed by XRD spectral analysis and was found to possess the highest surface area among the catalyst synthesised according to the BET surface area analysis results. In order to determine the catalytic performance of the above-mentioned catalyst, the reaction was carried out under similar conditions using a series of substituted benzyl alcohols, containing 4-CH$_3$, 4-OCH$_3$, 4-Cl, 4-NO$_2$, 4-C(CH$_3$)$_3$, 4-CF$_3$ and 3-NO$_2$ groups as different substrates, and their conversion to corresponding aldehydes was studied. It was found that conversion product obtained was >70% and selectivity displayed by the catalyst was >99%. It was observed that the catalyst selectively oxidises aromatic alcohols, which was confirmed by the similar reaction carried out using citronellol as a substrate which yielded a conversion product of citronellal with 7.21% unlike the results obtained from aromatic substrates. The results are summarised in Table 4. A possible reaction pathway is represented in a schematic format in Fig. 12.

788
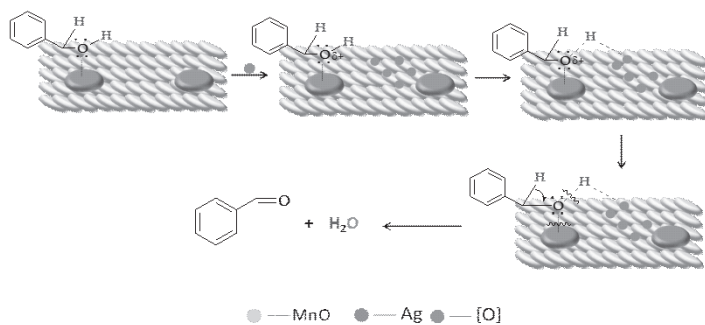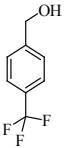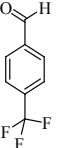
Fig. 12. Schematic representation of possible mechanistic approach of interaction between the catalyst and the substrate

Table 4. Selective oxidation of benzyl alcohol and its derivatives to the corresponding aldehydes in the presence of O_2 as clean oxidant

R. No	Reactants	Products	Conversion (%)	Selectivity (%)
1	2	3	4	5
1	OH (benzyl alcohol)	O (benzaldehyde)	100	>99
2	OH, CH₃	O, H, CH₃	100	>99
3	OH, OCH₃	O, H, OCH₃	80.91	>99
4	OH, Cl	O, H, Cl	95.32	>99
5	OH, NO₂	O, H, NO₂	72.07	>99
6	OH, C(CH₃)₃	O, H, C(CH₃)₃	77.94	>99

to be continued

789

1	2	3	4	5
7	4-(trifluoromethyl)benzyl alcohol (CH₂OH, CF₃)	4-(trifluoromethyl)benzaldehyde (CHO, CF₃)	83.12	>99

CONCLUSIONS

Among the synthesised catalysts, 1% nano Ag-doped manganese oxide showed high activity and stability for the oxidation of benzyl alcohol using molecular oxygen as a source of oxygen. A synergistic effect between calcination temperatures and the chemical kinetics of the reaction was observed, and it was ascertained that calcination temperature plays an important role towards catalytic performance of the catalyst. The presence of well-dispersed Ag nanoparticles has also shown to play a vital role in the catalytic activity. It was also observed that the catalyst displays selectivity towards aromatic alcohols yielding >70 % conversion product while the activity was found to be very low in the case of aliphatic alcohols. Further studies into the improvement of catalytic activity by diminution of reaction time and bringing down the amount of catalyst employed and their applications for the synthesis of other important aromatic and aliphatic aldehydes are being explored.

ACKNOWLEDGEMENTS

REFERENCES

1. W. F. HOELDERICH: Environmentally Benign Manufacturing of Fine and Intermediate Chemicals. Catal Today, **62**, 115 (2000).
2. R. A. SHELDON, I. ARENDS, G. J. TEN BRINK, A. DIJKSMAN: Green, Catalytic Oxidations of Alcohols. Acc Chem Res, **35**, 774 (2002).
3. T. MALLAT, A. A. BAIKER: Oxidation of Alcohols with Molecular Oxygen on Solid Catalysts. Chem Rev, **104**, 3037 (2004).
4. T. MALLAT, Z. BODNAR, A. BAIKER, O. GREIS, H. STRUBIG, A. RELLER: Preparation of Promoted Platinum Catalysts of Designed Geometry and the Role of Promoters in the Liquid-phase Oxidation of 1-methoxy-2-propanol. J Catal, **142**, 237 (1993).
5. Z. OPRE, J. D. GRUNWALDT, M. MACIEJEWSKI, D. FERRI, T. MALLAT, A. BAIKER: Promoted Ru-hydroxyapatite: Designed Structure for the Fast and Highly Selective Oxidation of Alcohols with Oxygen. J Catal, **230**, 406 (2005).
6. M. CARAVATI, J. D. GRUNWALDT, A. BAIKER: Selective Oxidation of Benzyl Alcohol to Benzaldehyde in 'Supercritical' Carbon Dioxide. Catal Today, **91**, 1 (2004).

7. D. I. ENACHE, J. K. EDWARDS, P. LANDON, B. SOLSONA-ESPRIU, A. F. CARLEY, A. A. HERZING, M. WATANABE, C. J. KIELY, D. W. KNIGHT, G. J. HUTCHINGS: Solvent-free Oxidation of Primary Alcohols to Aldehydes Using Au–Pd/TiO$_2$ Catalysts. Science, **311**, 362 (2006).

8. H. MIYAMURA, R. MATSUBARA, Y. MIYAZAKI, S. KOBAYASHI: Aerobic Oxidation of Alcohols at Room Temperature and Atmospheric Conditions Catalyzed by Reusable Gold Nanoclusters Stabilized by the Benzene Rings of Polystyrene Derivatives. Angew Chem Int Ed, **46**, 4151 (2007).

9. P. HAIDER, B. KIMMERLE, F. KRUMEICH, W. KLEIST, J. D. GRUNWALDT, A. BAIKER: Gold-catalyzed Aerobic Oxidation of Benzyl Alcohol: Effect of Gold Particle Size on Activity and Selectivity in Different Solvents. Catal Lett, **125**, 169 (2008).

10. A. ABAD, P. CONCEPCION, A. CORMA, H. GARCIA: A Collaborative Effect between Gold and a Support Induces the Selective Oxidation of Alcohols. Angew Chem Int Ed, **44**, 4066 (2005).

11. S. MARX, A. BAIKER: Beneficial Interaction of Gold and Palladium in Bimetallic Catalysts for the Selective Oxidation of Benzyl Alcohol. J Phys Chem C, **113**, 6191 (2009).

12. N. DIMITRATOS, J. A. LOPEZ-SANCHEZ, D. MORGAN, A. F. CARLEY, R. TIRUVALAM, C. J. KIELY, D. BETHELL, G. J. HUTCHINGS: Solvent-free Oxidation of Benzyl Alcohol Using Au-Pd Catalysts Prepared by Sol Immobilisation. Phys Chem Chem Phys, **11**, 5142 (2009).

13. C. DELLA PINA, E. FALLETTA, L. PRATI, M. ROSSI: Selective Oxidation Using Gold. Chem Soc Rev, **37**, 2077 (2008).

14. X. E. VERYKIOS, F. P. STEIN, R. W. COUGHLIN: Oxidation of Ethylene over Silver: Adsorption, Kinetics, Catalyst. Cat Rev Sci Eng, **22**, 197 (1980).

15. H. SPERBER: Herstellung von Formaldehyd aus Methanol in der BASF. Chemie Ingenieur Technik, **41**, 962 (1969).

16. L. F. LIOTTA, A. M. VENEZIA, G. DEGANELLO, A. LONGO, A. MARTORANA, Z. SCHAY, L. GUCZI: Liquid Phase Selective Oxidation of Benzyl Alcohol over Pd–Ag Catalysts Supported on Pumice. Catal Today, **66**, 271 (2001).

17. P. NAGARAJU, M. BALARAJU, K. M. REDDY, P. S. SAI PRASAD, N. LINGAIAH: Selective Oxidation of Allylic Alcohols Catalyzed by Silver Exchanged Molybdovanado Phosphoric Acid Catalyst in the Presence of Molecular Oxygen. Catal Commun, **9**, 1389 (2008).

18. S. RAKOVSKY, S. NIKOLOVA, L. DIMITROV, L. MINCHEV, J. ILKOVA: Selective Oxidation of 2,3-butanediol in the Aqueous Medium in the Presence of Ag and Cu Containing Catalyst. Oxid Commun, **18**, 407 (1995).

19. T. MITSUDOME, Y. MIKAMI, H. FUNAI, T. MIZUGAKI, K. JITSUKAWA, K. KANEDA: Oxidant-free Alcohol Dehydrogenation Using a Reusable Hydrotalcite-supported Silver Nanoparticle Catalyst. Angew Chem Int Ed, **47**, 138 (2008).

20. F. ADAM, A. E. AHMED, S. L. MIN: Silver Modified Porous Silica from Rice Husk and Its Catalytic Potential. J Porous Mater, **15**, 433 (2008).

21. R. K. KUNKALEKAR, A. V. SALKER: Low Temperature Carbon Monoxide Oxidation over Nanosized Silver Doped Manganese Dioxide Catalysts. Catal Commun, **12**, 193 (2010).

22. S. F. ADIL, M. E. ASSAL, A. ALWARTHAN, S. M. RAFIQ: Oxidant Free Alcohol Dehydrogenation Using Manganese Oxide Supported Silver and Gold Nanoparticles. Asian J Chem (in press).

23. G. WOJCIECH: The Influence of Silver on the Structural, Redox and Catalytic Properties of the Cryptomelane-type Manganese Oxides in the Low-temperature CO Oxidation Reaction. Appl Catal B Env, **75**, 107 (2007).

24. D. P. DUBAL, D. S. DHAWALE, R. R. SALUNKHE, S. M. PAWAR, C. D. LOKHANDE: A Novel Chemical Synthesis and Characterization of Mn$_3$O$_4$ Thin Films for Supercapacitor Application. Appl Surf Sci, **256**, 4411 (2010).

25. E. N. MASLEN, V. A. STRELTOV, N. R. STRELTSOVA, N. ISHIZAWA: Electron Density and Optical Anisotropy in Rhombohedral Carbonates. III. Synchrotron X-ray Studies of CaCO$_3$, MgCO$_3$ and MnCO$_3$. Acta Cryst B, **51**, 929 (1995).

SYNTHESIS OF 2,3-DI(METHOXYCARBONYL)-5-NORBORNENE OVER METAL TRIFLATES – N-BUTYL-4-METHYLPYRIDINIUM BISTRIFLIMIDE CATALYTIC SYSTEMS

B. BITTNER, E. JANUS*, E. MILCHERT

Institute of Organic Chemical Technology, West Pomeranian University of Technology, 10 Pulaskiego Street, 71 322 Szczecin, Poland
E-mail: *ejanus@zut.edu.pl*

ABSTRACT

The Diels-Alder reaction between cyclopentadiene and dimethyl maleate in the catalytic systems – metal triflates and ionic liquid was examined. The influence of catalyst amount on the yield and *endo*:*exo* stereoselectivity was determined. Two methods of product isolation from catalytic systems (extraction and vacuum distillation) were compared.

Keywords: ionic liquid, metal triflate, norbornene derivative, recycling.

AIMS AND BACKGROUND

With the potential of forming carbon–carbon, carbon–heteroatom or heteroatom–hetero atom bonds the Diels-Alder reaction is a versatile synthetic tool to obtain simple and complex molecules[1,2]. In view of continuous need to optimise the synthesis conditions according to economical and environmental aspects, ionic liquids were investigated as solvents[3]. They were considered as replacements of volatile organic solvents[4]. The first solvent from this group, applied in cycloaddition was ethylamonium nitrate[5]. Later cycloadditions in the presence of many ionic liquids such as sulphonium[6], imidazolium[7], pyridinium[8] and phosphonium[9] were studied. The advantage of using ionic liquids as solvents is a simple procedure for products isolation. If the product forms a different phase it is isolated by decantation. If the reaction mixture is homogeneous, product isolation may be performed by vacuum distillation or by extraction.

2,3-di(methoxycarbonyl)-5-norbornene was obtained earlier in solvent-free Diels-Alder reactions of *in situ* generated cyclopentadiene with dimethyl maleate[10]. Dienophile was placed in a round bottom flask equipped with a condenser. It was heated on stirring until it began to boil. Next dicyclopentadiene was added in a single

---

portion and the reaction was continued until the reflux stopped and the reaction mixture turned yellow. *Exo*, *exo* and *endo*, *endo* isomers (in short *exo* and *endo*, respectively) were separated by radial thin layer chromatography, eluting with mixture of ethyl acetate:hexane (1:4 by volume). After 25 min of reaction 75% isolated yield were obtained. In the mixture of products, *exo:endo* ratio was 1.62, so the reaction was more *exo*-stereoselective. Moreover, it was noticed that dimethyl maleate isomerised to dimethyl fumarate, because in the mixture of product 5% of dimethyl *trans*-5-norbornene-2,3-dicarboxylate was detected.

A preliminary investigation of the use of the biodegradable ionic liquid, 3-(butoxycarbonyl)-1-methylpyridinium bistriflimide as a reaction solvent was conducted[11]. As a result 2,3-di(methoxycarbonyl)-5-norbornene was obtained with 95% yield after 18 h. The reaction was *endo*-stereoselective (*endo:exo* ratio 19).
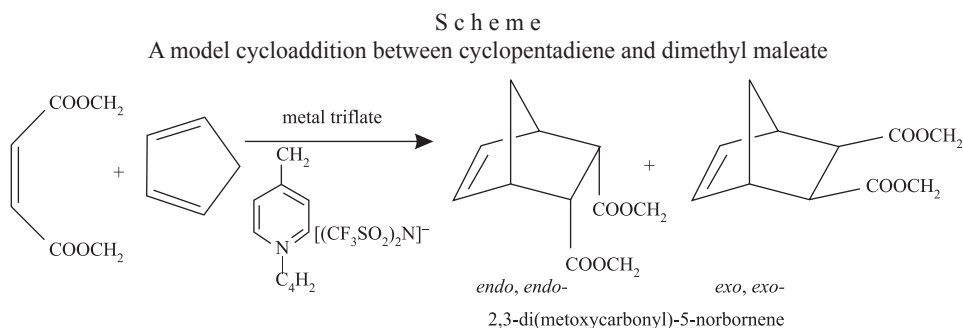
The interest of our group was to study the application and regeneration of catalytic systems consisting of Lewis acid catalysts (e.g. metal triflates or chlorides) and ionic liquids. The systems with 2 mol.% of $Mg(OTf)_2$ dissolved in N-hexylpyridinium bis(trifluoromethylsulphonyl)imide were active in the reaction of cyclopentadiene with dimethyl maleate in 5 subsequent cycles. Thus turnover frequency (TOF) synthesis of 2,3-di(methoxycarbonyl)-5-norbornene after 30 min decreased from 97 to 89 mol $mol^{-1} h^{-1}$. The *endo:exo* stereoselectivities obtained were around 7.0–6.4 (Ref. 12). Higher *endo:exo* ratios were determined in catalytic systems containing another ionic liquid, which was triethylsulphonium bis(trifluoromethylsulphonyl)imide[6]. In the first cycle the *endo*-stereoselectivity was 9.1 and it decreased to 7.7 in the 5th cycle. The decrease in *endo*-stereoselectivity value was accompanied by catalytic activity loss manifested by decreasing values of TOF, from 99 to 45 mol $mol^{-1} h^{-1}$ in the 5th reaction cycle. Much higher TOF values (more than 300 mol $mol^{-1} h^{-1}$) were determined in the reactions performed over catalytic systems with another catalyst – $Yb(OTf)_3 \cdot xH_2O$. The use of yttrium or ytterbium chlorides as catalyst with sulphonium ionic liquid allows obtaining the product with a similar TOF as $Mg(OTf)_2$ and much higher *endo:exo*-stereoselectivity (14.8 with YCl_3 and 13.6 with $YbCl_3$). However, the main disadvantage of their application in the synthesis of this norbornene derivative is the lack of stability under the product extraction procedure. The only possible method for product removal from the catalytic systems based on metal chlorides and ionic liquids was vacuum distillation.

Good results were obtained in the synthesis of 2-propanoyl-5-norbornene performed in catalytic system – pyridinium ionic liquid + Lewis acid[13]. The highest stereoselectivity and yield were obtained in reactions carried in ionic liquid with $[NTf_2]$ anion, which was the reason to study the Diels-Alder reaction between cyclopentadiene and dimethyl maleate, described in this article in N-butyl-4-methylpyridinium bis(trifluoromethylsulphonyl)imide $[C_4$-4-$C_1py][NTf_2]$. Previously metal chlorides were found to be the most active allowing several catalytic systems recirculation.

2,3-di(methoxycarbonyl)-5-norbornene and its derivatives have many possible applications, such as construction of poly(norbornene) block copolymer-based shell

cross-linked micelles with Co(III)-salen cores[14], noncovalent adhesion promoter in self-healing polymers[15], as a component of polymers obtained via ROMP with photoresistant properties[16], as matrix materials for platinum tetrakis(pentafluorophenyl) porphyrin-based optical oxygen sensors[17], as a starting material to form europium-containing polymers that act as humidity-sensing materials[18], drugs or ions transporters[19].

The objective of this study was to determine the yield of 2,3-di(methoxycarbonyl)-5-norbornene as a function of time and stereoselectivity, expressed as the ratio of *endo*, *endo* to *exo*, *exo* isomers (in short *endo*:*exo*) (Scheme). Reactions were carried out in catalytic systems composed of ionic liquid [C_4-4-C_1py][NTf_2] at different concentrations of metal (Y, Yb, Mg, Zn) triflates. A comparison of effectiveness of the catalytic systems (metal triflates and N-butyl-4-methylpyridinium bis(trifluoromethylsulphonyl) imide – M(OTf)$_x$/[C_4-4-C_1py][NTf_2], where M-metal, *x*-metal valency number) regeneration methods, extraction and vacuum distillation was performed.

S c h e m e
A model cycloaddition between cyclopentadiene and dimethyl maleate

endo, *endo*-   *exo*, *exo*-

2,3-di(metoxycarbonyl)-5-norbornene

EXPERIMENTAL

Materials. The ionic liquid [C_4-4-C_1py][NTf_2] was synthesised via a reaction between N-butyl-4-methylpyridinium chloride [C_4-4-C_1py][Cl] (Iolitec 98%) and lithium bis(trifluoromethylsulphonyl)imide [Li][NTf_2] (Iolitec 98%) in deionised water at room temperature. Prior to its use, the ionic liquid [C_4-4-C_1py][NTf_2] was washed with deionised water several times (until the test for chloride content performed with $AgNO_3$ titration was negative). Furthermore, it was dried in a vacuum drier at 323 K and 5 mbar for 24 h. Next the water content was measured by Karl Fisher titration (less than 100 ppm). Dimethyl maleate 96% was purchased from Aldrich.

The cyclopentadiene was obtained as a result of thermal cracking of dicyclopentadiene (≥95% pure) that was purchased from Fluka.

The metal trifluoromethanesulphonates (triflates) used as catalysts, were commercial products, purchased from Aldrich; ytterbium triflate (99%), yttrium triflate (98%), magnesium triflate (97%), zinc triflate (98%) and lithium triflate (98%).

Cyclohexanone 99%, used as internal standard in the GC analysis, was purchased from Merck.

Procedure for the Diels-Alder reaction. The reactions were carried out in 4-ml vials. Firstly the metal trifluoromethanesulphonate was dissolved in 0.25 ml of ionic liquid. Dimethyl maleate (1 mmol), cyclohexanone (20 µl) and freshly cracked cold cyclopentadiene (1.5 mmol) were added. The amount of the catalyst was always calculated according to the dienophile and expressed in mol% towards dimethyl maleate. The reaction was conducted at 25°C. The progress of the reaction was monitored by GC analysis over the time needed to obtain full conversion. As a result a mixture of *endo, endo* and *exo, exo* isomers: 2,3-di(methoxycarbonyl)-5-norbornene was obtained. The yield of products and *endo:exo* ratios were calculated on the basis of GC analysis.

Analysis. The GC analysis was carried out using a Carlo Erba GC 8000 TOP apparatus equipped with a FID detector and an Rxi™-17 column (Restek): 30 m × 0.53 mm × 1.5 µm. The column temperature was programmed as follows: at the moment of injection the temperature was increased from 80 to 120°C at a rate of 10°C/min, it was kept constant at 120°C for 2 min, then it was increased at a rate of 20°C/min and was kept constant at 240°C for 20 min, and finally it was decreased to 80°C. The detector temperature was 260°C. The quantitative analysis was performed according to the internal standard method. The product was identified by ^{1}H NMR and ^{13}C NMR.

RESULTS

The Diels-Alder reaction between cyclopentadiene and dimethyl maleate (Scheme) was chosen as a model reaction to investigate the catalytic activity of systems: metal triflate/N-butyl-4-methylpyridinium bis(triflouramethylsulphonyl)imide – M(OTf)$_x$/[C$_4$-4-C$_1$py][NIf$_2$].

For the purpose of the investigation the ionic liquid with bis(trifluoromethylsulphonyl) imide anion was chosen, because of its acid/base neutrality. This anion exhibits only weak electrostatic interactions with the cation and thus imparts advantageous low melting point (<25°C) and low viscosity (55 mPa s). The catalysts – metal triflates are commonly known from catalytic activity in cycloaddition[20,21].

The most active in cycloaddition process was Yb(OTf)$_3$ (Fig. 1*a*). In catalytic systems containing 0.75 and 1.0 mol% of this catalyst, the product was obtained after 15 min with 92 and 95% yield, respectively. The reaction time increased to 45 min or 60 min when the catalyst content was lower (0.5 and 0.25 mol%). The reaction stereoselectivity, expressed as *endo:exo* ratio was in all systems greater than 10.0. However, oligomerisation occurred as a side reaction. This was a serious drawback, which eliminates this catalytic system from further studies under recycling conditions. Longer time was needed to obtain the product with 94% yield when the catalytic system includes 1 mol% of Y(OTf)$_3$ (Fig. 1*b*), but also there oligomerisation was observed, that eliminates this system from recycling studies. For lower catalyst concentrations (0.75–0.25 mol%), the reaction time increased to 2 h. With increasing reaction time, the reaction became more *endo*-stereoselective. Applying 1.0 mol% of catalyst the *endo:exo* ratio was 9.5, while for 0.25 mol% of catalyst it increased to 14.6.
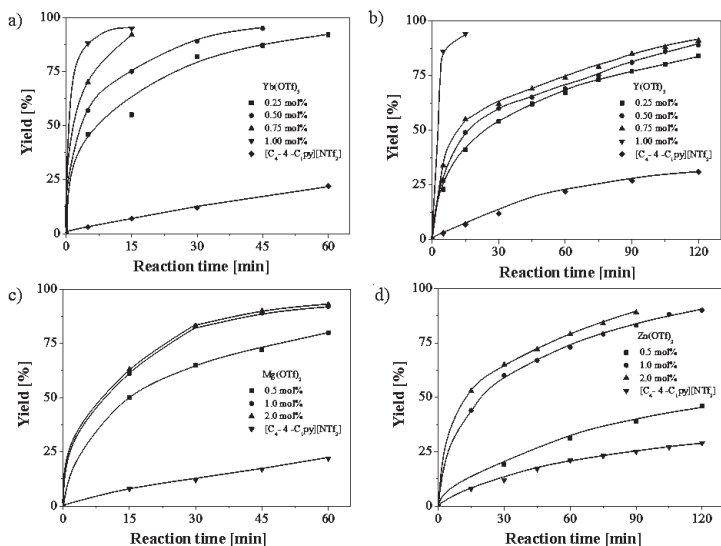
Fig. 1. Relation between reaction yield (*endo+exo*) and reaction time in cycloaddition performed in catalytic systems $[C_4-4-C_1py][NTf_2]$ and $Yb(OTf)_3$ (*a*); $Y(OTf)_3$ (*b*); $Mg(OTf)_2$ (*c*), and $Zn(OTf)_2$ (*d*) with different catalyst concentrations

Using a catalytic system containing 1 mol% of $Mg(OTf)_2$, 2,3-di(methoxycarbonyl)-5-norbornene was obtained with high yield after 1 h (Fig. 1*c*). No significant increase in the reaction rate was noted when the concentration of the catalyst was doubled. However, the system was less active with only 0.5 mol% of the catalyst (80% yield after 1 h). Stereoselectivity was similar in all studied systems.

The least active of all investigated catalysts was $Zn(OTf)_2$. When it was used a satisfactory yield of the product was obtained when the reaction was run for at least 2 h (Fig. 1*d*).

Because of a low price of magnesium triflate in comparison to that of yttrium and other transition metal triflates (ytterbium for example) and the lack of cyclopentadiene oligomerisation, that is making the recycling procedure impossible to perform, the studies on recycling of catalytic systems based on pyridinium ionic liquid and alkali metal triflates were undertaken.

The possibility of multiple use of catalytic systems was also examined. The first studied catalytic system under recycling conditions was formed from N-butyl-4-methylpyridinium bis(trifluoromethylsulphonyl)imide and magnesium triflate (Fig. 2). It contained 1 mol% of the catalyst towards dienophile. Product isolation was performed by extraction with organic solvent or vacuum distillation. Using the first method, catalytic system $Mg(OTf)_2/[C_4-4-C_1py][NTf_2]$ remained as the lower phase after decantation of solvents. When the second method was applied catalytic system remained in the distillation flask. The main criteria for extractant selection were good solubility of the norbornene derivatives and unconverted reagents, but the lack of

solubility of the components of the catalytic system. A mixture of solvents at a volume ratio 1:3, obtained by mixing 2 ml of cyclohexane with 6 ml of dibutyl ether, was used for product separation by extraction. Extraction of 8 mmols of the product from 2 ml of the catalytic system was completed after a 5-fold application of this solution. IR analysis of the catalytic systems after extraction of 2,3-di(methoxycarbonyl)-5-norbornene proved that the product was completely removed. In the catalytic systems recycled by vacuum distillation (0.1–1.0 mbar/65°C) the signals of the product carbonyl groups were still present, so a small amount of norbornene derivative remained in the system.
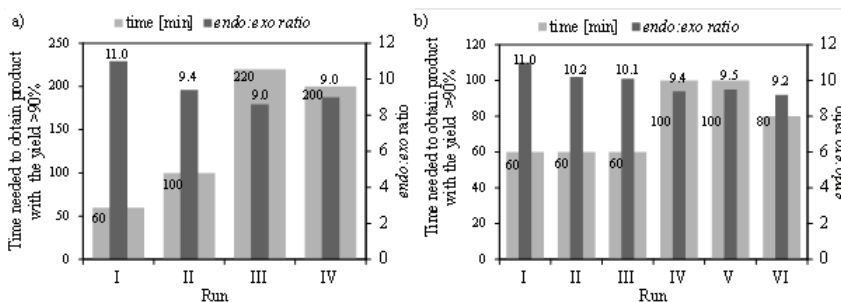

Fig. 2. Catalytic system – 1 mol.% $Mg(OTf)_2/[C_4\text{-}4\text{-}C_1py][NTf_2]$: (*a*) product isolation by extraction with organic solvents mixture (cyclohexane – dibutyl ether 1:3 in volume); (*b*) product isolation by vacuum distillation

In the method of separation by extraction, in the first run, the product was obtained with 94% yield after 1 h and with 11.0 *endo:exo* stereoselectivity (Fig. 2*a*). After the product isolation, the catalytic system was regenerated by removal of the residual extractant by vacuum evaporation and re-used to carry out the subsequent reaction. However, the time needed to obtain the product with a yield higher than 90% increased to 100 min in the 2nd run. In subsequent runs (III and IV) the time needed reached about 4 h, which indicates a significant loss of catalytic activity of the system investigated. In subsequent runs, the stereoselectivity also decreased from 11.0 in the 1st run to 9.0 in the 4th run.

The same catalytic system (1 mol.% $Mg(OTf)_2/[C_4\text{-}4\text{-}C_1py][NTf_2]$) was more stable under recycling conditions when vacuum distillation of the product was applied (Fig. 2*b*). Applying this method of the product isolation, the catalytic system had the same activity in the three subsequent runs. The reaction time needed to obtain higher than 90% yield of norbornene derivatives was 1 h. The same yield was obtained in the 4th and 5th runs, but reaction time had to be extended to 100 min. In each subsequent synthesis, after regeneration of the catalytic system, the *endo:exo* stereoselectivity decreased. Thus the catalytic system behaved similarly to the system (catalyst and ionic liquid) regenerated by extraction.
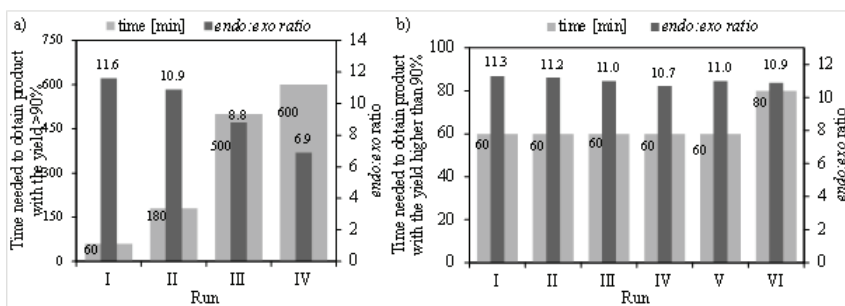
Fig. 3. Catalytic system – 3 mol.% LiOTf /[C$_4$-4-C$_1$py][NTf$_2$]: (*a*) product isolation by extraction with organic solvents mixture (cyclohexane – dibutyl ether 1:3 in volume); (*b*) product isolation by vacuum distillation

A comparison of the 2 methods for the product isolation was also made using the catalytic system of 3 mol.% LiOTf/[C$_4$-4-C$_1$py][NTf$_2$]. Because of the lower activity of the lithium catalyst, it was used in a higher concentration. The catalytic system containing lithium salt lost its activity when product was isolated by extraction with a mixture of organic solvents (cyclohexane – dibutyl ether 1:3 in volume). In each of the following reactions the yield at a level of 90% was obtained over a longer time (Fig. 3*a*). Most probably the catalyst was washed out together with product in sub-sequent extractions. The product – 2,3-di(methoxycarbonyl)-5-norbornene isolation by vacuum distillation made no damage to the catalytic system, because it remained active in 5 subsequent runs (Fig. 3*b*). In the 6th run, the time needed to obtain the product with a yield greater than 90% increased to 100 min. When the previously described catalytic system based on magnesium triflate was applied, it happened in the 4th cycle. Thus the reaction time may suggest that the catalytic system with lithium salt is much more active. Comparison of the turnover number (TON) obtained with the 2 catalytic systems shows that the catalytic system Mg(OTf)$_2$/[C$_4$-4-C$_1$py][NTf$_2$] is more active. For the catalytic system with Mg(OTf)$_2$ presented in Fig. 2*b* TON after 1 h is 90 mol mol^{-1}, while for the catalytic system presented in Fig. 3*b* (LiOTf) it is only 30 mol mol^{-1}.

Stability under recycling conditions of the systems investigated strongly depends on the method used to remove the product. Shorter reaction time in subsequent runs proved that the vacuum distillation is more recommended as the method for product removal from the catalytic system. Decomposition of [C$_4$-4-C$_1$py][NTf$_2$] starts at 450°C under normal pressure. However, it was noticed that in each reaction cycle after distillation the system was getting darker, it changed the colour from transparent to orange and finally brown. Darkening is caused by the presence of small amounts of the reaction by-products, such as cyclopentadiene oligomers. The catalytic systems absorbance in UV and visible light measured after the 5th cycle was 15 times higher than that measured before the 1st reaction. At the same time the absorbance of the systems from which the product was isolated by extraction with solvents was much

lower, because by-products that remained in the flask were systematically washed out during extraction.

CONCLUSIONS

Catalytic systems $[C_4\text{-}4\text{-}C_1py][NTf_2]$ and $Y(OTf)_3$ or $Yb(OTf)_3$ showed the highest and similar reactivity, however, cyclopentadiene oligomerisation eliminates them from recycling studies. The catalytic systems consisting of alkali and earth alkali metal triflates (Li, Mg) and N-butyl-4-methylpyridinium bis(trifluoromethylsulphonyl)imide were less active than those with transition (Y, Yb) metals triflates. However, they are more recommended for the synthesis of 2,3-di(methoxycarbonyl)-5-norbornene because of the possibility to recycle the system. Distillation under vacuum pressure is more suitable method for this norbornene diester derivative removal from the catalytic system based on N-butyl-4-methylpyridinium bis(trifluoromethylsulphonyl)imide and $Mg(OTf)_2$ or LiOTf than extraction with organic solvents. A number of possible runs with similar stereoselectivities is around 5 with slowly progressing catalytic systems deactivation.

REFERENCES

1. F. FRINGUELLI, A. TATICCHI: The Diels-Alder Reaction: Selected Practical Methods. Wiley and Sons, 2002; F. FRINGUELLI, A. TATICCHI: Dienes in the Diels-Alder Reaction. Wiley, New York, 1990.
2. K. C. NICOLAOU, S. A. SNYDER, T. MONTAGNON, G. VASSILIKOGIANNAKIS: The Diels-Alder Reaction in Total Synthesis. Angew Chem Int Ed, **41**, 1668 (2002).
3. T. FISCHER, A. SETHI, T. WELTON, J. WOOLF: Diels-Alder Reactions in Room-temperature Ionic Liquids. Tetrahedron Lett, **40**, 793 (1999).
4. R. D. ROGERS, K. R. SEDDON (Eds): Ionic Liquids, Industrial Applications for Green Chemistry. American Chemical Society, 2002.
5. D. A. JAEGER, C. E. TUCKER: Diels-Alder Reactions in Ethylammonium Nitrate, a Low-melting Fused Salt. Tetrahedron Lett, **30**, 1785 (1989).
6. E. JANUS, B. BITTNER: Triethylsulfonium Bistriflimide as the Reaction Medium in Catalyzed and Uncatalyzed Cycloaddition [4 + 2]. Catal Lett, **134**, 146 (2010).
7. I. HEMEON, C. DEAMICIS, H. JENKINS, P. SCAMMELLS, R. D. SINGER: *Endo* Selective Diels-Alder Reactions of Furan in Ionic Liquids. Synlett, **11**, 1815 (2002).
8. Y. XIAO, S.V. MALHOTRA: Diels-Alder Reactions in Pyridinium-based Ionic Liquids. Tetrahedron Lett, **45**, 8339 (2004).
9. P. LUDLEY, N. KARODIA: Phosphonium Tosylates as Solvents for the Diels-Alder Reaction. Tetrahedron Lett, **42**, 2011 (2001).
10. D. HUERTAS, M. FLORSCHER, V. DRAGOJLOVIC: Solvent-free Diels-Alder Reactions of *in situ* Generated Cyclopentadiene. Green Chem, **11**, 91 (2009).
11. J. R. HARJANI, R. D. SINGER, M. T. GARCIA, P. J. SCAMMELLS: Biodegradable Pyridinium Ionic Liquids: Design, Synthesis and Evaluation. Green Chem, **11**, 83 (2009).
12. B. BITTNER, E. MILCHERT, E. JANUS: $Mg(OTf)_2$ + Ionic Liquid – Recyclable Catalytic System in Diels-Alder Reaction. Pol J Chem Technol, **12**, 3 (2010).
13. B. BITTNER, R. PELECH, E. JANUS, E. MILCHERT: Synthesis of 2-propanoyl-5-norbornene in Pyridinium Ionic Liquids Catalyzed by Yttrium Salts. Catal Lett, **142** (3), 332 (2012).

14. Y. LIU, V. PINON, M. WECK: Poly(norbornene) Block Copolymer-based Shell Cross-linked Micelles with Co(III)–Salen Cores. Polym Chem, **2** (9), 1964 (2011).
15. G. O. WILSON, M. M. CARUSO, S. R. SCHELKOPF, N. R. SOTTOS, S. R. WHITE, J. S. MOORE: Adhesion–Promotion via Non-covalent Interactions in Self-healing Polymers. ACS Appl Mat Interf, **3** (8), 3072 (2011).
16. A. WOLFBERGER, B. RUPP, W. KERN, T. GRIESSER, C. SLUGOVC: Ring Opening Metathesis Polymerization Derived Polymers as Photoresists: Making Use of Thiol-ene Chemistry. Macromol Rapid Comm, **32** (6), 518 (2011).
17. K. STUBENRAUCH, M. SANDHOLZER, F. NIEDERMAIR, K. WAICH, T. MAYR, I. KLIMANT, G. TRIMMEL, C. SLUGOVC: Poly(norbornene)s as Matrix Materials for Platinum Tetrakis(pentafluorophenyl)porphyrin Based Optical Oxygen Sensors. Eur Polym J, **44** (8), 2558 (2008).
18. A. C. KNALL, C. SCHINAGL, A. PEIN, N. NOORMOFIDI, R.SAF, C. SLUGOVC: Polynorbornenes with Pendant Europium(III) Coordination Compounds. Macromol Chem Phys, **213**, 2618 (2012).
19. K. D. BELFIELD, L. ZHANG: Norbornene-functionalized Diblock Copolymers via Ring-opening Metathesis Polymerizarion for Magnetic Nanoparticle Stabilization. Chem Mater, **18**, 5929 (2006).
20. S. KOBAYASHI, I. HACHIYA, M. ARAKI, H. ISHITANI: Asymmetric Diels-Alder Reaction Catalyzed by a Chiral Ytterbium Trifluoromethanesulfonate. Tetrahedron Lett, **34**, 4535 (1993).
21. G. SILVERO, M. J. ALVARO, J. L. BRAVO, M. AVALOS, J. L. JIMENEZ, I. LOPEZ: An in-depth Look at the Effect of Lewis Acid Catalysts on Diels-Alder Cycloadditions in Ionic Liquids. Tetrahedron, **61**, 7105 (2005).

POLYMER-INORGANIC MATERIALS ON THE BASIS OF TETRAETHOXYSILANE

I. YU. YEVCHUK[a], O. I. DEMCHYNA[a]*, V. V. KOCHUBEY[b],
H. V. ROMANIUK[b], Z. M. KOVAL'[b], G. E. ZAIKOV[c],
YU. G. MEDVEDEVSKIKH[a]

[a]*Department of Physico-chemistry of Combustible Minerals, L. M. Lytvynenko Institute of Physico-organic Chemistry and Coal Chemistry, NAS of Ukraine, 3a Naukova Street, 79 059 Lviv, Ukraine*
E-mail: demchynaoksana@ukr.net
[b]*Lviv Polytechnic National University, 12 Bandera Street, 79 013 Lviv, Ukraine*
E-mail: groman@polynet.lviv.ua
[c]*N. M. Emanuel Institute of Biochemical Physics, Russian Academy of Sciences, 4 Kosygin Street, 119 334 Moscow, Russia*
E-mail: chembio@sky.chph.ras.ru

ABSTRACT

The paper is concerned with consideration of preparing of tetraethoxysilane-based organic-inorganic composites using sol–gel method. Two approaches are used: synthesis of organic-inorganic materials via sol–gel process in polymeric matrix of poly(vinylidene fluoride), and during photoinitiated polymerisation of diacrylate polymerising composition in the presence of sol–gel system. The kinetic parameters of the process of photoinitiated polymerisation of diacrylate composition were determined depending on gelation time, composition of polymerising system and concentration of sol–gel process catalyst as well. Complex thermogravimetric and differential-thermal analysis of polymer-inorganic material was carried out to define its thermal characteristics. Proton conductivity of obtained materials was evaluated by impedance spectrometry.

Keywords: polymer-inorganic nanocomposite, sol–gel processing, tetraethoxysilane, poly(vinylidene fluoride), photoinitiated polymerisation, impedance spectrometry.

AIMS AND BACKGROUND

Recently sol–gel synthesis of organic-inorganic hybrids has received an extensive attention. Sol–gel technique allows to obtain a lot of materials with a wide range of ap-

---

* For correspondence.

plication. Nowadays researchers attention is concentrated on the problem of obtaining of proton-conductive materials. Such materials can be used as polymeric electrolytes and proton-conductive membranes in fuel cells, gas sensors, solar cells[1,2].

Polymers containing sulphonic groups are the most widespread proton-conductive polymer materials. There are some methods of synthesis of such materials. At direct heterogeneous sulphonation of polymers by sulphonic groups the latter are disposed mainly on a surface, therefore, it is difficult to achieve a homogeneous structure of material. Destructive action of some sulphuring agents is the lack of sulphonation of solutions of polymers. Using another method – polymerisation of sulphonated monomers – results in obtaining of polymers with high water uptake that worsens the mechanical properties of material. The subsequent cross-linking of such polymers is a high-cost process.

Another method of synthesis of polymers containing sulphonic groups is condensation of polymers with sulphocompounds. In Ref. 3 the authors have shown possibility of obtaining of films on the basis of products of compatible condensation of aliphatic polyamides, *n*-phenolsulphonic acid and formaldehyde in the medium of organic solvent. The authors of Ref. 4 suggested preparing of film material by condensation of dissolved poly(vinylidene fluoride), *n*-phenolsulphonic acid and formaldehyde. In Ref. 5 a method of forming proton-conductive membranes by chemical cross-linking of poly(vinyl alcohol) by glutar aldehyde with addition of poly(styrene sulphonic acid) was offered. However, these materials do not possess the sufficient level of proton conductivity.

Membranes Nafion (Du Pont, USA) are the most commercially successful. Nafion is a perfluorosulphonic ionomer with high proton conductivity and chemical and mechanical stability[6]. However, limited operation temperature, low water uptake and high cost are disadvantages of this polymer.

Hence, alternative preparation methods for proton-conductive materials are required. The perspective approach seems to be the usage of composite materials. The combination of organic polymers and ceramics promises new hybrid materials with high performance. They may be prepared by incorporation of nanoscale filler particles into polymer matrix. In Ref. 7 nanoparticles of titanium(IV) oxide were added into triazol-containing proton-conductive membranes. The conductivity of sulphonated poly(arylene etherketone) was improved by incorporation of nanodisperse additives – acid zirconium phosphate[8]. It was suggested to introduce inorganic phosphosilicates into membrane material[9], and nanoparticles of silica functionalised by sulphogroups[10].

A simple method for obtaining of organic-inorganic composites is mixing of organic polymer with alkoxide (e.g. tetraethoxysilane) followed by a sol–gel process involving hydrolysis and polycondensation of precursor. Such a method provides new opportunities for preparing both inorganic and organic-inorganic two- and multicomponent composites at a relatively low temperature. In Ref. 11 silico-phosphate xerogels have been obtained on the basis of tetraethoxysilane and phosphoric acid

and under the pressure of 5000 kg/cm² electrolyte membranes with high proton conductivity (10^{-3}–10^{-2} S/cm) have been prepared. However, these membranes have low mechanical durability.

Therefore, it is reasonable to conduct sol–gel transformation in a matrix of soluble organic polymer or in monomer during simultaneous polymerisation. By these methods it is possible to obtain hybrid organic-inorganic materials possessing high proton-conducting and mechanical properties.

EXPERIMENTAL

The research reagents used were as follows: tetraethoxysilane $Si(OC_2H_5)_4$ (EKOS-1, Russia), ethanol (r.g.), orthophosphoric acid (r.g.), poly(vinylidene fluoride) (PVDF) M_w 175000 (Aldrich).

Polymerising mix 'Discophot-1' consists of: tetramethylene acrylate (TMDA) – 62; epoxyacrylate oligomer – 32; monofunctional vinyl monomer N-vinylpyrrolidone – 5, photoinitiator 2,2-dimethoxy-2-phenylacetophenone – 1 (% mass.). Such composition of polymerising mix provided insignificant shrinkage at hardening.

Organic-inorganic composites were synthesised as follows: first, 10 % wt. PVDF solution was prepared by dissolution polymer powder in dimethylformamidee at temperature of 40°C. Then, required quantities of sol–gel system $TEOS:C_2H_5OH:H_3PO_4:H_2O$ were added slowly into PVDF solution to obtain composites with different PVDF:TEOS ratios. Th obtained systems were mixed using a magnetic mixer for 2 h at 40°C and then were cast on glass substrate for films forming.

Alternatively, organic-inorganic films were prepared via photoinitiated polymerisation of diacrylate composition 'Discophot-1' in the presence of the above-mentioned sol–gel system. The kinetics of the process of photoinitiated polymerisation of the investigated systems was studied by laser interferometry. Photoinitiated curing of composition was conducted in a thin layer under cover glass at UV-irradiation (intensity of UV-irradiation was 14 W/m²). The changes of intensity of interference picture during contraction of polymerising composition were registered by a photodetector. The relative integral degree of monomer transformation or conversion P was calculated as follows:

$$P = H_t / H_0, \qquad (1)$$

where H_t is a layer contraction in the moment of time t; H_0 – a maximum achievable contraction, determined after the number of peaks on interferogram.

Measurements of proton conductivity of the samples were performed with the help of 'AUTOLAB' impedance spectrometer (Ecochem, Holland) with FRA program over the frequency range of 10 to 10^5 Hz. Samples were sandwiched between platinum electrodes by a diameter of 1 cm. The value of $1/R_F$ was considered as a value of proton

conductivity; R_F – a segment on an axis of real resistance in impedance hodograph[2]. Specific proton conductivity was determined after the following formula:

$$\sigma = l/RS, \tag{2}$$

where R is sample resistance, Ω; l – sample thickness, cm; S – electrodes area, cm².

Complex thermal analysis (thermogravimetric and differential-thermal) of composite samples was conducted by means of Derivatograph Q-1500D (Paulik–Paulik–Erdey) under dynamic conditions in a temperature range of 20–400°C. Heating of samples with mass of 200 mg was carried out in an air atmosphere at a heating rate of 5°C/min. Aluminium oxide was used as a reference.

RESULTS AND DISCUSSION

The operating temperature of fuel cells is required to be 120–130°C and more for providing an effective desorption of carbon oxide (CO), which is usually present in hydrogen fuel and 'poisons' the platinum catalyst. Therefore, heat-resistant polymers are used for making proton-conductive membranes.

For our investigations we have chosen poly(vinylidene fluoride) since it is known for its outstanding chemical and thermal stability as well as mechanical strength. Forming of inorganic structure took place *in situ* in polymeric matrix of PVDF using sol–gel technique. Sol–gel solution, consisting of TEOS, water, ethanol and orthophosphoric acid (TEOS:C_2H_5OH:H_3PO_4:H_2O = 2.2:7.24:0.2:0.36 p. v.), was added into PVDF solution in dimethylformamide. As a result of TEOS hydrolysis sol of polysiloxane particles appeared in polymeric matrix. Orthophosphoric acid served as a catalyst of TEOS hydrolysis. Sol structuring at temperature of 40°C in constant-temperature oven resulted in forming of organic-inorganic films.

Proton conductivity of nanocomposite films was determined by measuring the complex resistance – impedance. Real and imaginary constituents of a vector of impedance allow to evaluate the conducting property of the material. In Fig. 1 one can see the dependence of real and imaginary constituents of impedance on current frequency and the Nyquist plot of the cell Pt–sample–Pt for the sample PVDF:TEOS = 30:70 (wt. %) within a frequency range of $10–10^5$ Hz. Proton conductivity of investigated samples was about 10^{-4} S/cm.

Ion conductivity in these composites is provided by the inorganic component formed as a result of sol–gel process. In accordance with the Grotthus concept transmission of protons takes place in a water medium along channels due to the continuous exchange $H_2O + H^+ = H_3O^+$. Other mechanism assumes that protons pass by two ways: via diffusive transport of H_3O^+ ions, and via rotation of proton-containing groups[12]. Obviously, such groups are silanol and P–OH ones.
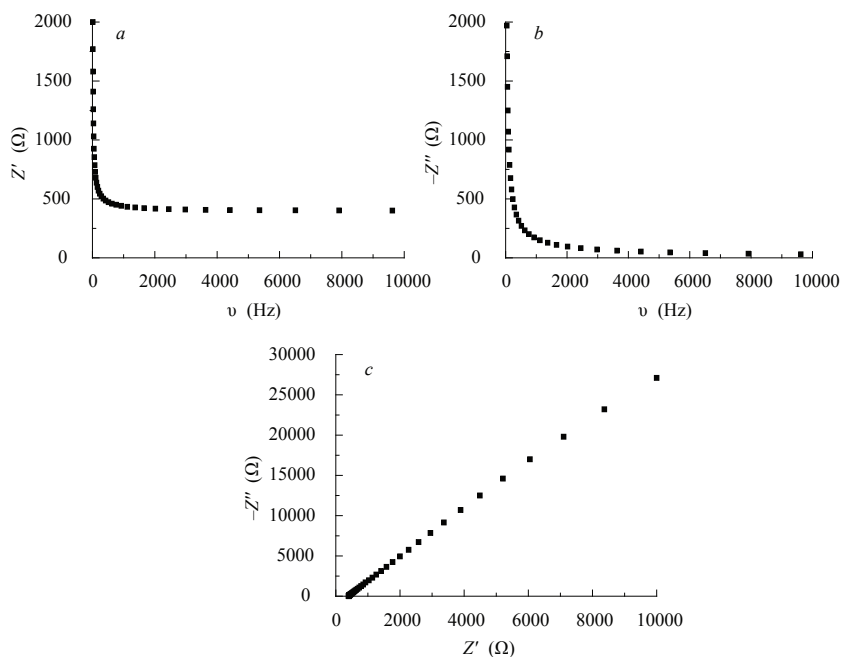
Fig. 1. Dependence of real (*a*) and imaginary (*b*) constituents of impedance on frequency and the Nyquist plot (*c*) for the sample PVDF:TEOS = 30:70 (wt. %)

The thermal stability of the prepared material was investigated by thermogravimetric and differential-thermal analyses, the results of which are shown in Fig. 2. Weight loss of the sample is observed at a temperature range of 20–150°C. It is accompanied by appearance of endothermal effect in the DTA curve. These effects may occur due to the presence of dimethylformamide remains. The second endothermal effect with maximum at 150°C in DTA curve can be observed at temperature range of 135–185°C. Probably, it is caused by the process of PVDF melting. Intensive weight loss of samples at temperatures higher than 385°C can be explained by the process of deep thermooxidising destruction of the polymer. Hence, this composite material is thermally stable up to approximately 135°C that is important for using it as proton-conductive membranes.

Photoinitiated polymerisation of diacrylate polymerising composition (PC) in the presence of sol–gel system (SGS) was the alternative way of synthesis of polymer-silica films. The kinetics of polymerisation was studied depending on gelation time, the catalyst concentration – orthophosphoric acid – in sol–gel system, as well as on mixture composition. The obtained results are presented in Figs 3–5 and in Tables 1–3.
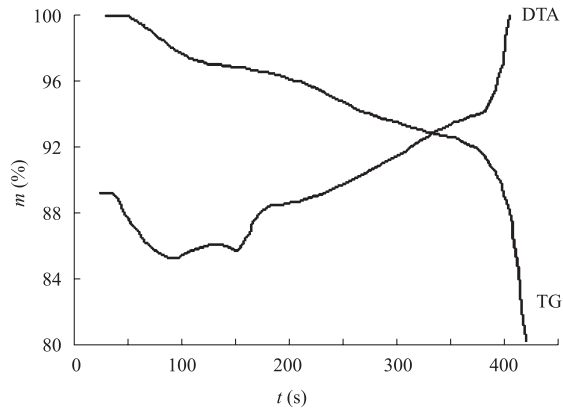
Fig. 2. Derivatograph curves of composite membrane (PVDF:TEOS = 30:70 % wt.)
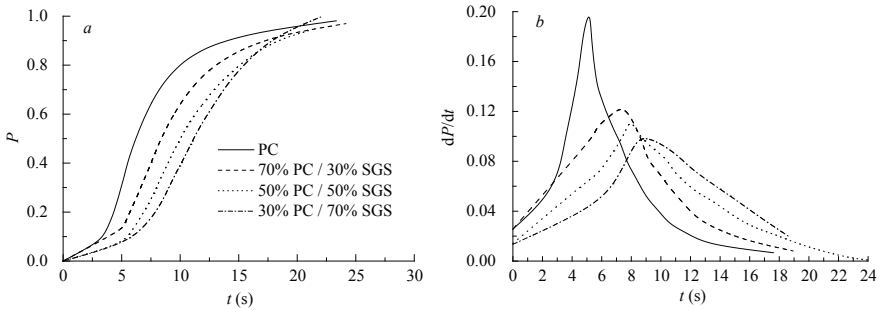
Fig. 3. Integral kinetic curves (*a*) and their differential anamorphoses (*b*) of photoinitiated polymerisation of PC–SGS depending on its composition

Table 1. Kinetic parameters of the process of photoinitiated polymerisation of PC–SGS depending on its composition

No	PC–SGS (% vol.)	Time of W_{max} achiev., t (s)	Conversion at W_{max}, P	Max. rate W_{max} (s^{-1})
1	100 : 0	5.2	0.34	0.203
2	70 : 30	7.3	0.38	0.124
3	50 : 50	9.1	0.41	0.108
4	30 : 70	10.4	0.43	0.102

806
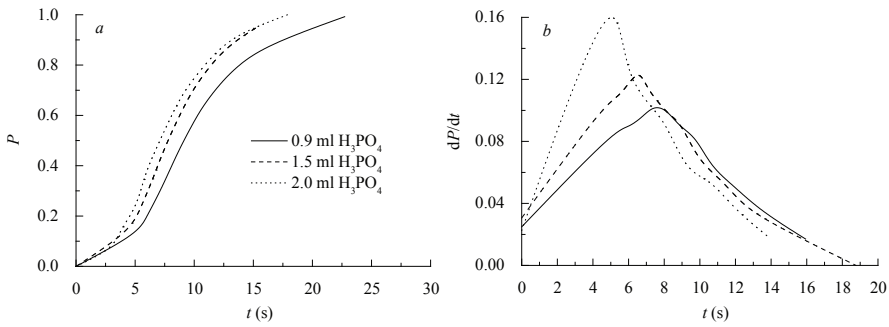
Fig. 4. Integral kinetic curves (*a*) and their differential anamorphoses (*b*) of photoinitiated polymerisation of PC:SGS = 50:50 (% vol.) depending on catalyst concentration

Table 2. Kinetic parameters of the process of photoinitiated polymerisation of PC:SGS depending on catalyst concentration

No	PC : SGS (% vol.)	H_3PO_4 in SGS (% vol.)	Time of W_{max} achiev., t (s)	Conversion at W_{max}, P	Max.rate W_{max} (s^{-1})
1	50:50	9	7.4	0.33	0.10
2	50:50	15	6.6	0.31	0.13
3	50:50	20	5.4	0.29	0.19
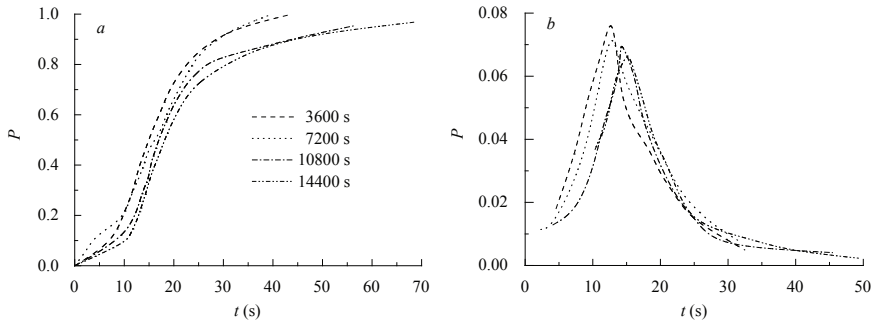
Fig. 5. Integral (*a*) and differential (*b*) kinetic curves of photoinitiated polymerisation of PC:SGS (9 % vol. H_3PO_4) = 50:50 (% vol.) depending on gelation time

Table 3. Kinetic parameters of the process of photoinitiated polymerisation of PC:SGS (9 % vol. H_3PO_4) depending on gelation time

No	PC:SGS (% vol.)	Time of gelation (s)	Time of W_{max} achiev., t (s)	Conversion at W_{max}, P	Max. rate, W_{max} (s^{-1})
1	50:50	3600	12.90	0.39	0.082
2	50:50	7200	13.10	0.35	0.075
3	50:50	10800	14.85	0.34	0.071
4	50:50	14400	15.08	0.33	0.067

807

As one can see in Figs 2–4, the kinetic curves of polymerisation in the presence of sol–gel system have typical S-like shape. However, the rate of photoinitiated polymerisation of diacrylate composition with increase of sol–gel system content decreases as compared with initial polymerising composition. The maximum rate of polymerisation W_{max} at SGS content of 70% vol. diminishes approximately by 2 times in comparison with W_{max} for initial composition, whereas time of achievement of maximum rate increases by 2 times. Possible explaination of this fact may be that the inorganic constituent forms steric limitations for the process of polymerisation of diacrylate monomer. An additional spatial network of nanoparticles of silica phase which appears as a result of sol–gel process leads to macroradicals decay and, accordingly, to deceleration of the polymerisation process.

At introducing into the polymerising composition sol–gel systems with larger gelation times we also observe decreasing of the maximum rate of the process for the same reasons.

At varying the orthophosphoric acid content in sol–gel system from 9 to 20% vol., the maximum rate of polymerisation increases almost by 2 times. We suggest a change of aggregation character of the inorganic phase: at large concentration of catalyst the process of TEOS hydrolysis passes with high rate, it is therefore possible to assume that nanoparticles of silica phase are incorporated into polymer network, and aggregates, which could be 'traps' for macroradicals.

Proton conductivity of composites, obtained by this method, was measured by impedance spectrometry over frequency range of $10–10^5$ Hz. In Fig. 6 one can see the dependence of real and imaginary impedance constituents on current frequency as well as the Nyquist plot for the sample PC:SGS = 50:50 (% vol.) at catalyst concentration of 20% vol. in SGS.

The proton conductivity of composites, obtained by photoinitiated polymerisation, was 10^{-6} S/cm. This value is by 2 orders smaller than the values of proton conductivity of nanocomposites on the basis of PVDF. It was also found to be dependent on catalyst concentration (Table 4).

Table 4. Proton conductivity of the samples PC:SGS

PC:SGS = 50:50 (% vol.)	
H_3PO_4 in SGS (% vol.)	σ (S/cm)
9	1.72×10^{-6}
20	4.13×10^{-6}
30	9.41×10^{-6}
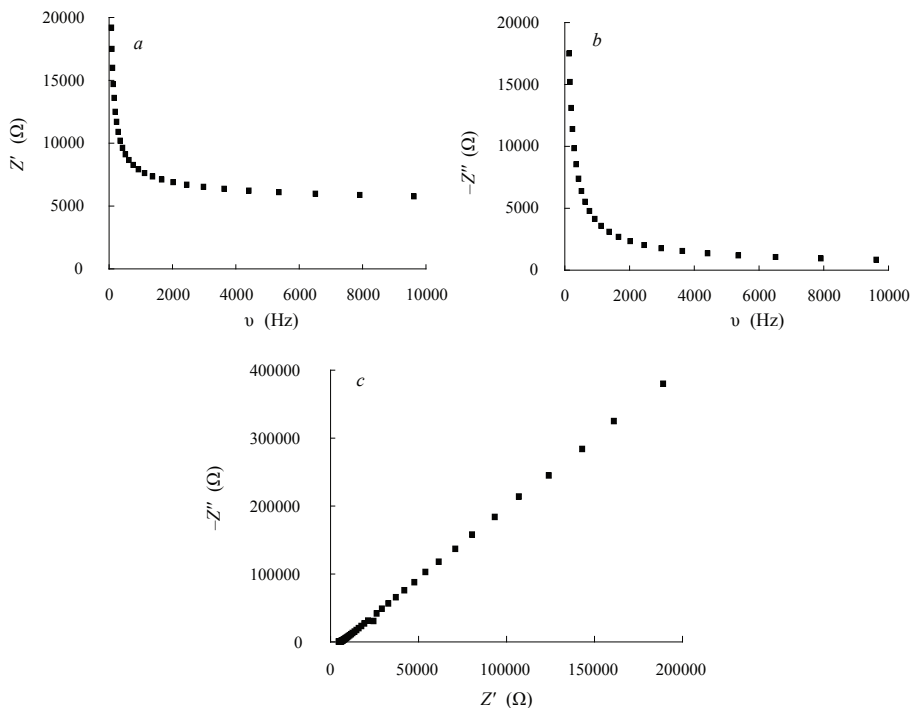
Fig. 6. Dependence of real (*a*) and imaginary (*b*) constituents of impedance on frequency and the Nyquist plot of impedance (*c*) for the sample PC:SGS = 50:50 (% vol.)

CONCLUSIONS

Polymer-silica nanocomposites were synthesised by 2 methods: by forming of silica phase as a result of sol–gel process *in situ* in polymeric matrix of PVDF and during photoinitiated polymerisation of composition on the basis of diacrylate monomer TMDA. Organic-inorganic materials, obtained by the first method, possess proton conductivity of 10^{-4} S/cm and can be used at temperatures up to 135°C.

REFERENCES

1. T. V. MALTSEVA: Inorganic Proton Conductive Nanomaterials: Outlook for Application in Membrane Fuel Cells. Nanosystems, Nanomaterials, Nanotechnologies, **2** (3), 875 (2004).
2. Yu. A. DOBROVOLSKY, A. V. PISAREVA, L. S. LEONOVA, A. I. KARELIN: New Proton Conductive Membranes for Fuel Cells and Gas Sensors. Alternative Energy and Ecology, **12** (20), 36 (2004).
3. Yu. M. KOBELCHUK, O. V. CHERVAKOV, K. O. GERASYMENKO: Synthesis of Sulfonated Derivative Polyamids and Film Materials on Their Basis. Voprosy khimiyi i chim. Tekhnologiyi, (1), 78 (2008) (in Russian).

4. P.-J. CHU, C.-S. WU, J.-Y. CHEN: PVDF-HFP/P-sulfonate-phenoline DMFC Membrane by *in situ* Synthesis. In: Proc. of 2003 Fuel Cell Seminar: Book Abstract, Miami Beach, Florida, No 3–7, 2003, 474–477.

5. I. A. STADNY, V. V. KONOVALOVA, V. O. YEVDOKYMENKO: Proton Conductive Membranes Based on Polyvinyl Alcohol and Polystyrenesulphonic Acid. Magisterium. Chem Sci, **33**, 3 (2008).

6. Z. SHI, S. HOLDCROFT: Synthesis of Block Copolymers Possessing Fluoropolymer and Non-fluoropolymer Segments by Radical Polymerisation. Macromolecules, **37** (6), 2084 (2004).

7. O. I. DANYLIV, V. V. KONOVALOVA, A. F. BURBAN: Developement of Method of Triazol-containing Proton Conductive Membranes Formation. In: Scientific Proc., Chemical Sciences and Technologies, NU 'Kyiv-Mohyla Academy', 'Pulsary', Kiev, Vol. 92, 2009, 12–18.

8. A. I. FOMENKOV, Yu. I. PINUS, A. S. PEREGUDOV, Ya. V. ZUBAVICHUS, A. B. YARO-SLAVTSEV, A. R. KHOKHLOV: Proton Conductivity of Poly(arylene ether ketones) with Different Sulphonation Degrees: Improvement via Incorporation of Nanodisperse Zirconium Acid Phosphate. Vysokomol Soedin, **49** (7), 1299 (2007) (in Russian).

9. JIN YONGGANG, C. JOAO, DINIZ da COSTA, G. Q. LU: Proton Conductive Composite Membrane of Phosphosilicate and Polyvinyl Alcohol. Solid State Ionics, **178**, 937 (2007).

10. A. MARTINELLI, A. MATIC, P. JACOBSSON, L. BORJESSON, M. A. NAVARRA, A. FERNI-COLA, S. PANERO, B. SCROSATI: Structural Analysis of PVA-based Proton Conducting Membranes. Solid State Ionics, **177**, 2431 (2006).

11. V. V. SHILOV, O. A. SHILOVA, L. N. YEFIMOVA, I. N. CVETKOVA, Yu. P. GOMZA, N. N. MINENKO, M. V. BURMISTR, K. M. SUKHOY: Sol–Gel Synthesis of Ion-conducting Composites and Their Use for Supercapacitors. Perspect Mater, (3), 24 (2003) (in Russian).

12. P. V. KOMAROV, I. N. VESELOV, P. G. KHALATUR: Nanoscale Morphology in Ionic Membranes on the Basis of Sulfonated Aromatic Poly(ether ketones): Mesoscopic Simulation. Vysokomol Soedin, **52A** (2), 279 (2010) (in Russian).

HOW FEED STOCK QUALITY AFFECTS THE FOULING PROCESSES IN HDS INSTALLATIONS

I. RANGELOV[a], N. PETKOVA[a], D. STRATIEV[b], IV. SHISHKOVA[b],
Z. TSONEV[a]*, P. PETKOV[a]

[a]*Department of Industrial Technologies and Management, Prof. Assen Zlatarov University, 1 Prof. Yakimov Street, 8010 Bourgas. Bulgaria*
E-mail: *zlatotsvet@abv.bg*
[b]*Lukoil Neftochim Bourgas JSC, 8104 Bourgas, Bulgaria*

ABSTRACT

Often, in practice accumulation of deposits on the surface of the main technological equipment can be observed, making it difficult to maintain the operational parameters of a unit or installation.

Classical fouling can be defined as accumulation of unwanted deposits associated with corrosive and other oxidation processes, resulting in accumulation of inorganic or organic material on the surface of the technological equipment. In many cases, this process make difficult the heat transfer, leading to increased fuel consumption, loss of production and increased maintenance costs. Deposits can stratify in equipment, located in different places of the installation – in furnaces, heaters, condensers, fractionating columns, reboilers, compressors, in separate sections of this equipment, and especially in stagnant areas.

Keywords: fouling, heat exchangers, hydrodesulphurisation unit.

AIMS AND BACKGROUND

The chemical analyses of this type deposits show that these deposits contain metal oxides, sulfides, organic material in the form of polymers and coke, salt, and various other particles. This makes the identification of the exact cause of fouling extremely difficult. Identifying the type of deposits in itself does not guarantee reveal of the essence of the problem. Often wrong assumptions are made that if the deposit contains mainly one compound (the others are in small quantities), then this compound is the cause of fouling. There are also side factors affecting the formation of the actual deposit. It is possible that the component that is in the lowest concentration in the

---

* For correspondence.

deposit to act as a binder, a catalyst or otherwise to make a stable connection between metal/deposit.

Inorganic deposit components are suspended fine particles in the process stream. They attach to the metal surface of the technological equipment due to gravity. The formation of this type of deposits does not require difference in temperature between the fluid flow and the metal surface, but with the fluid temperature increase its density decreases, which in turn increases the possibility of precipitation of inorganic components, carried by the stream. The organic components in the deposits such as coke and polymer products, however, are highly dependent on the metal surface temperature, especially in the presence of oxygen. Inorganic components act as germs on which coke and polymer products begin to deposit[1]. Fouling mainly precipitates on the metal surfaces of the heat exchange equipment where all the conditions for the formation of deposits are present. In Fig. 1 is presented a classical formation of the fouling[1–3].
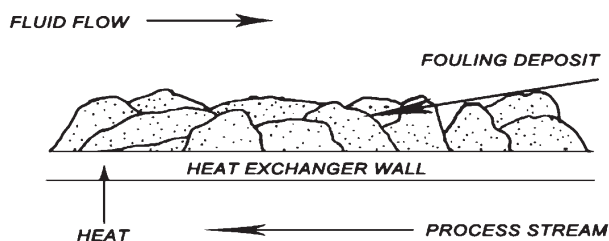
Fig. 1. Fouling processes

Many authors[4–6] define fouling formation as a result of processes described below. Fouling from inorganic formations is formed from crystallised from the solution inorganic substances and then precipitated on the metal surface, while fouling of solid particles is a result of accumulation of solid particles, carried by the process stream, on the metal surfaces. Fouling may be formed also as a result of chemical reactions on the metal surface. It is possible that the formation of deposits is due to corrosive processes on the very metal surface of the problematic process equipment[3] and also due to processes, occurred before it, in the process along the flow diagram and carried to it by the flow. Usually during the storage of the feed some biological processes occur, as a result of which are formed deposits and fouling with microorganisms on the metal surfaces. These types of deposits are transported by the flow to the areas, where there are favourable conditions for their precipitation on the metal surfaces of the process equipment. Biological processes mainly occur in low temperature areas.

The combinations of inorganic, organic and biological products make it very difficult to determine the primary fouling.

Factors concerning the mechanism of fouling formation are various and too many. They are related to operation variable parameters of the process stream. The behaviour of one and the same stream may vary, depending on the specific conditions existing in a particular situation.

Mainly, the conditions conducive to the formation of fouling are: flow temperature – higher temperature favours the formation of fouling, the temperature of the metal surface affects all possible mechanisms for fouling formation. Hot spots, result of a poor distribution of fluid flow, in great extent accelerate the formation of a local fouling. Of great significance is also the flow velocity, as low velocity implies better conditions for the formation of deposits. Improper design of the process units will provide the so-called 'dead zones' where the formed fouling products will easily precipitate[4]. Influence on this type of processes brings also the alloys from which the equipment is made – for the specific environment and conditions they corrode in different degrees. Significant contribution to the easy deposition of the fouling has the preliminary preparation of the metal surface. The rough surface, on the one hand, creates high turbulence and thus the possibility of fouling precipitation is reduced, except in the deep cracks, which, after being filled, the cracks become smooth, thus eliminating the conditions for the further fouling deposition.

The basic processes for fouling formation are the following:

• Polymerisation processes – run faster in the presence of oxygen to the formation of high molecular weight products due to binding of similar molecules to one another;

• Condensation processes – high molecular compounds are formed from condensed ring-shape compounds;

• Chemical reactions such as oxidation of organic molecules, salts formation, etc.;

• At high ratio carbon/hydrogen, presence of hydrocarbons with high molecular weight and very high temperature of the metal surface, as well as at high operation temperatures, a vey hard coke deposit is formed;

• The deposition processes also favour the formation of fouling – the presence of mechanical impurities of clay, sand, solid particles, etc. deposit on the heat exchange surface, especially in areas with low flow rates. Thus they appear as germs for the faster fouling formation;

• Ongoing corrosion processes are also one of the main processes for the formation of fouling. The already formed corrosion products detach and the stream carries them to the favourable areas where they attached to the metal surface. This results in reduced heat transfer due to their low heat conductivity and thus provide a rough surface for deposition of another type of fouling, formed by other mechanisms[7].

EXPERIMENTAL

In the HDS plant of Insa oil refinery arose a serious problem with the formation of deposits in the exchange equipment before the reactor, and the speed of fouling deposition is disastrously high. The heat transfer is disturbed, leading to disruption of the overall operation of the plant; the contamination of the catalyst in the reactor is possible. For this reason it is often necessary to shut down the plant for heat exchangers

cleaning from the hard sintered deposits. This process is connected with production loss, accumulation of deposition during shut down and start up of the plant up to its normal mode of operation, with energy losses, with additional cost for labour and many other inconveniences. The refinery processes gasoil purchased from the market.

Referring to those theoretically possible reasons for fouling formation, the research has been focused primarily on establishing the nature and stability of the feed and its impact on the observed fouling processes. In our other publication[8] samples of deposits taken from the problematic heat exchange equipment have been analysed as well as analysed in details the process conditions and heat exchangers design.

Analysis method that have been used. The main methods of analysing in details the nature of the feed for processing in both of the installations are:

Densities of investigated samples were determined by digital density-meter according to standard test method ASTM D4052. The distillation was performed according to procedure described in ASTM D-86. Standard practice ASTM D4737 was applied to calculate the cetane indices of diesel samples on the base of density and ASTM D86 data.

Atomic absorption spectrometry: The sample is coked, after that the ash formed is dissolved in aqua regia. Content of metals (Al, Si, Ni, V, Co, Mo, Fe and Na) was determined by applying of Atomic absorption spectrometry.

K-factor and the molecular weight are calculated based on the dependencies, represented in Refs 9 and 10, respectively.

The methods used for analysis of the sample of deposits are described below.

The deposit as received at 105ºC overnight. It is then subjected to XRF and XRD to determine metals content in the deposit. Part of the dried sample is used to determine the C, H, and N content. Remaining portion is used to measure dichloromethane extractable and for infrared analysis.

X-ray fluorescence (XRF): XRF is a non-destructive analytical technique used to identify and determine the concentration of elements present in solids. XRF is capable of measuring metals and sulphur. Because every element has a different electron shell configuration, each element emitted a unique X-ray.

X-ray diffraction (XRD): XRD is a non-destructive technique for identification and quantitative determination of various crystalline compounds (know as phases) present in a solid material. Identification is achieved by comparing the X-ray diffraction pattern obtained from an unknown sample with an internationally recognised database containing reference patterns of more than 70 000 crystal phases.

C, H, and N Analysis (CNM): CHN is a destructive technique for quantification of carbon, hydrogen, and nitrogen. A small amount of sample is oxidised at high temperature converting carbon and hydrogen to CO_2 and H_2O respectively. The nitrogen in the sample is converted to NO_x and then reduced to N_2. The resulting mixture is analysed by gas chromatography to calculate % C, H and N present in the sample.

Loss on ignition (LOI): LOI is a destructive technique for quantification of ash (% ash = 100–%LOI). %LOI is obtained from the weight lost after ignition at 800ºC. This process results in loss of all organics (C, H, N and organic sulphur). The sulphur tied to inorganics is lost and replaced with oxygen. Certain inorganic halides, such as $FeCl_2$ and amine salts (e.g. NH_4Cl) are also lost under these conditions.

Dichloromethane extractable: A Soxhlet extraction yields the portion of the deposit soluble in dichloromethane. Soluble materials may include small molecules, low molecular weight polymers, asphaltenes, and residual stream components. Insoluble materials may include large molecules, high molecular weight, cross-linked and oxidised polymers, oxidised and dehydrogenated asphaltenes, as well as coke.

Infrared (IR) analysis: The dichloromethane soluble and insoluble portions of the deposits are further characterised by IR to determine the nature of the organic material in the deposit.

The main objective of the study is to determine the extent to which the feed, purchased from INSA OIL for hydrotreatment, affects the formation of fouling in heat exchange unit of the plant before the reactor. It is known that the reasons are complex, so it is necessary each one to be surveyed in details. For this purpose we conducted a comparative analysis of feed samples from 2 hydrotreating plants – one with fouling problems, and in the second the hydrotreating processes run normally.

RESULTS AND DISCUSSION

The results of the analytical study of both feeds are represented in Table 1.

The data in Table 1 show that both feeds are almost identical except for the analyses for metals content. From the chemical analysis of the feed sample of INSA Oil has been found presence of Na = 2.1 mg/kg and Fe = 0.14 mg/kg., which favours the deposits formation processes. While in the feed sample from Lukoil Neftochim Burgas AD no metal content has been found. This is the first difference found between the 2 types of feedstock. To obtain a more complete picture of the nature of the two feeds, they were analysed for content and size of the solid particles. Laser method with LPA has been used – an analyser of NALCO company, and the results are presented graphically in Fig. 2.

Table 1. Analysis of INSA OIL HDS feed and LNB HDS feed

Properties	INSA Oil Feed	LNB. HDS feed
Density at 20°C (g/cm³)	0.8349	0.8495
Density at 15°C (g/cm³)	0.8385	0.8531
Sulphur (wt. %)	0.152	
Distillation, ASTM D-86		
IBP (°C)	172	183
5%	193	209
10%	207	226
20%	227	249
30%	242	264
50%	270	289
70%	300	312
80%	317	326
90%	340	343
FBP (°C)	372	370
Bromine number, ASTM D 1159 (g Br/100 g)	<1	3.5
Cetane index, ASTM D 4737	51.3	50.0
MW	201.0	214
Kw factor	11.8	11.77
Contents of metals (mg/kg)		
Al	< 0.3	–
Si	< 3.0	–
V	< 1.0	–
Ni	< 0.1	–
Co	< 0.05	–
Mo	< 0.2	–
Fe	0.14	–
Na	2.1	–
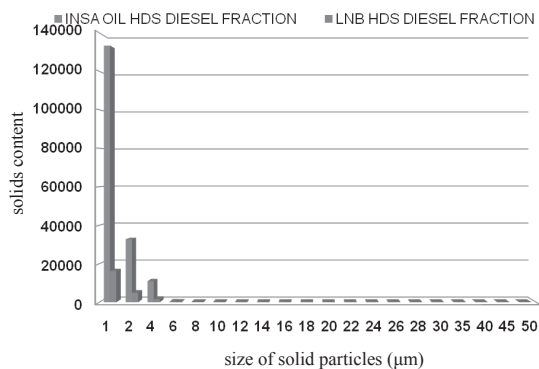
Fig 2. Average cumulative particle data in diesel fraction

From the analysis data of both feedstocks from INSA Oil and Lukoil Neftochim Burgas AD for the hydrotreating units by the laser method (see Fig. 2) of LPA – analyser of Nalco company it has been found out that the solids content in INSA Oil feed is 7–8 times more than in the feed of Lukoil Neftochim Burgas AD. They are very small in size, but the number is too big. It is known that the presence of solids in feedstock accelerates the fouling processes. They act as germs for rapid agglomeration of the deposits. These particles may be a result of corrosion processes in the production and transportation of feed; it is possible to be result of presence of fine particles of catalyst powder and from other accompanying side processes. It is fact that their content in INSA Oil feed is bigger than the content in Lukoil Neftochim Burgas feed. This is the second serious difference.

An attempt has been made to establish the connection between the feed and the nature of the deposits. For this purpose, a sample of fouling taken from the problematic heat exchange equipment has been analysed in the laboratories of Nalco. The results are presented in Table 2.

Obviously, the ratio of carbon to hydrogen is 74:6.8 (INSA Oil feed), which is almost equal to 10.9. Figure 3 gives us information that for ratio 10.9 the deposits are mainly from asphaltenes. Therefore, given the right operation conditions in the plant, inevitably there will be processes of coke formation and polymer products. In our previous researches related to the design of the heat exchanger unit and temperature conditions in it, it has been proved the existence of favourable conditions for fouling formation.
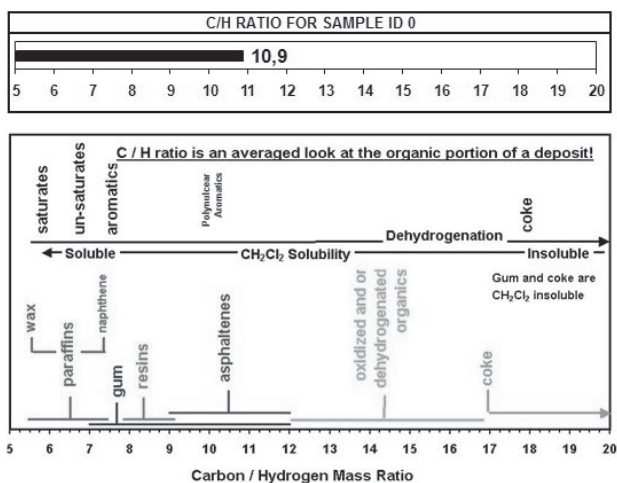

Fig. 3. Deposit characterisation

Table 2. Results of laboratory feed analysis

Laboratory results (%)		Calculated inorganics (%)	
Aluminum	0.0	Iron sulphide (as FeS)	0.8
Antimony	0.0	Iron salts, other (as Fe_2O_3)	0.0
Arsenic	0.0	Aluminum (as oxide)	0.0
Barium	0.0	Antimony (as oxide)	0.0
Boron	0.0	Arsenic (as oxide)	0.0
Bromine	0.0	Barium (as oxide)	0.0
Calcium	0.0	Boron (as oxide)	0.0
Chlorine	0.0	Calcium (as oxide)	0.0
Chromium	0.0	Chromium (as oxide)	0.0
Cobalt	0.0	Cobalt (as oxide)	0.0
Copper	0.0	Copper (as oxide)	0.0
Iron	0.5	Lanthanum (as oxide)	0.0
Lanthanum	0.0	Lead (as oxide)	0.0
Lead	0.0	Magnesium (as oxide)	0.0
Magnesium	0.0	Manganese (as oxide)	0.0
Manganese	0.0	Molybdenum (as oxide)	0.0
Molybdenum	0.0	Nickel (as oxide)	0.0
Nickel	0.0	Phosphorus (as oxide)	0.0
Phosphorus	0.0	Potassium (as oxide)	0.0
Potassium	0.0	Silicon (as oxide)	0.0
Silicon	0.0	Sodium (as chloride)	0.0
Sodium	0.0	Sodium (as oxide)	0.0
Sulfur	1.7	Tin (as oxide)	0.0
Tin	0.0	Titanium (as oxide)	0.0
Titanium	0.0	Vanadium (as oxide)	0.0
Vanadium	0.0	Zinc (as oxide)	0.0
Zinc	0.0	Subtotal for inorganics	0.8
XRF- S	0.5	Ammonium chloride	0.0
Carbon	74	Inorg. + NH_4 Cl (if any)	0.8
Hydrogen	6.8		
Nitrogen	3.2	Infrared analysis	
		CH_2Cl_2 solubles	
Elements content CHNS	85.7	Test not performed	
Oxygen	13.8		
Losses at 800°C	99	CH_2Cl_2 insolubles	
CH_2Cl_2 extractables	18	Test not performed	

CONCLUSIONS

It has been found from the study that two are the main reasons, related to the feedstock of INSA Oil, favourable fouling formation processes:

1. The presence of solid particles in it, although small, acts as germs in the process of agglomeration.

2. The presence of heavy metals in it leads to catalysing of the packing processes, i.e. the deposition of fouling on the metal surface of the heat exchange equipment is speeded up.

In support of these findings is the reported ratio of carbon/hydrogen in the analysed sample of deposits, taken from the heat exchange equipment which shows that mainly they contain asphaltenes.

REFERENCES

 1. T. R. BOTT: Fouling of Heat Exchangers. Elsevier Science & Technology Books, 1995.
 2. T. KUPPAN: Heat Exchanger Design Handbook. Marcel Dekker, Inc., New York, 2000.
 3. R. K. SHAH, D. P. SEKUL: Fundamentals of Heat Exchanger Design. John Wiley & Sons, Inc., 2003.
 4. R. LIRA, S. SENGUPTA: Effects of Wall Shear on Biofilm Growth, Heat Transfer and Fluid Resistance in Shell and Tube Heat Exchangers. In: Proc. of the 1989 National Heat Transfer Conference, HTD, Vol. 129, 1989, 101–109.
 5. I. WIEHE, R. J. KENNEDY: The Oil Compatibility Model and Crude Oil Incompatibility. Energy & Fuels, **14**, 56 (2000).
 6. I. WIEHE, R. J. KENNEDY: Application of the Oil Compatibility Model to Refinery Streams. Energy & Fuels, **14**, 56 (2000).
 7. G. ALI MANSOORI: Physicochemical Basis of Fouling Prediction and Prevention in the Process Industry. J Chin Inst Chem Engrs, **33** (1), 25 (2002).
 8. N. RANGELOV, N. PETKOVA, Z. TSONEV, P. PETKOV: Opportunities to Reduce the Fouling Processes in HDS Installation. Petroleum & Coal, **55** (1), 57 (2013).
 9. R. SADEGHBEIGI: Fluid Catalytic Cracking Handbook. 2nd ed. Butterworth-Heinemann Publications, 2000.
10. A. G. GOOSSEN: Prediction of Molecular Weight of Petroleum Fractions. Ind Eng Chem Res, **35** (3), 985 (1996).

OCCURRENCE OF ARSENIC IN WATER IN SEMBERIJA: CONNECTION WITH FACTORS AFFECTING ARSENIC MOBILITY

T. J. LAKETIC[a], A. N. PAVLOVIC[b]*, M. J. SAVIC[a], S. S. MITIC[b], S. B. TOSIC[b], M. S. DJORDJEVIC[b], M. N. MITIC[c]

[a]*Institute for Water of Bijeljina, 51 Milosa Obilica Street, 76 300 Bijeljina, Bosnia and Herzegovina*
[b]*Department of Chemistry, Faculty of Sciences and Mathematics, University of Nis, 33 Visegradska Street, P. O. Box 224, 18 000 Nis, Serbia*
E-mail: *aleksandra.pavlovic@pmf.edu.rs*
[c]*Department of Mathematics, Faculty of Sciences and Mathematics, University of Nis, 33 Visegradska Street, P. O. Box 224, 18 000 Nis, Serbia*

ABSTRACT

Water from artesian wells in Semberija region was tested. In water from 6 localities arsenic has been found above the limit recommended by the WHO of 10 µg l^{-1}. Arsenic concentration in water from other 4 localities is below WHO guideline, but still is greater than the US EPA and Agency for Toxic Substances and Disease Registry (ATSDR) of 2 µg l^{-1}. Our results also suggested that arsenic adsorption and desorption reactions are influenced by changes in pH, occurrence of redox reaction and presence of competing anions such are iron and *ortho*-phosphate. The study also tested the water for alkalinity and conductivity. The average results for alkalinity (200–400 µg ml^{-1}) and conductivity (474–928 µS cm^{-1}) appear to be higher than the safe drinking water standard. The results obtained suggested that the water from artesian wells in Semberija is unsafe for human consumption.

Keywords: arsenic, artesian well water, seasonal changes, atomic absorption spectrometry (AAS), inductively coupled plasma optical emission spectrometry (ICP–OES), Semberija.

AIMS AND BACKGROUND

Water is a precious resource and it needs to be aware of groundwater quality and how much is available for consummation. Until recently, As was not traditionally on the

---

* For correspondence.

list of elements routinely tested by water-quality testing laboratories and so many high As water sources may have been missed. Pollution from domestic sewage connected to rapid urbanisation and the lack of accompanying wastewater works also remains a major environmental challenge, especially in developing countries or in the countries in which monitoring system was destroyed during the war. Results obtained of arsenic in water from artesian wells in Semberija are in correlation with other reports available in literature related to controlling factors of arsenic mobility.

Arsenic occurs naturally in rocks and soil, water, air, and plants and animals. There are many arsenic compounds, both organic and inorganic, in the environment. A WHO (2001) (Ref. 1) working group on arsenic conducted a quantitative risk assessment for arsenic, assuming a linear relationship between the cumulative arsenic dose and the relative risk of developing lung cancer. Also, in severe cases of arsenical poisoning, agranulocytosis or thrombopenia may develop[2]. According to WHO (2009) (Ref. 3) and Commission of the European Communities, Directorate-General Health and Consumer Protection (2004) (Ref. 4), the daily human intake of total arsenic is between 20 to 300 μg day^{-1}.

Long-term human exposure, through drinking of contaminated water, is an important public health problem in some regions and countries. Immediate symptoms on an acute poisoning typically include vomiting, esophageal and abdominal pain and bloody 'rice-water' diarrhea[1]. Also, gene-specific hypermethylation has been detected in arsenic exposed persons[5].

Major arsenic incidents have occurred in Taiwan, Mexico, Chile, and Bangladesh. Other incidents involving smaller population groups have been reported in USA, Canada, Japan, Alaska and Poland[6,7].

Artesian well water is utilised abundantly as an alternative to surface water, especially in the northern Bosnia and Herzegovina (B&H) (Semberija), where some residents of this area, especially those living in villages, have been using water from artesian wells (100 to 300 m deep) since the 1970's. Semberija is very rich in underground water with a number of artesian wells, stored in an alluvial aquifer spreading across of some 400 km[2]. Systematic water quality testing and analysis in B&H were undertaken since 1965 at 58 locations, but the complete monitoring system was destroyed during the war. Establishment of new monitoring station relies on appropriate human and financial resources[8]. However, most of these wells are not controlled by authorised institutions, which would confirm its chemical and microbiological quality. Also, some patients from this region have been identified with As-related health problems, including skin pigmentation changes and endemic nephropathy[9].

As far as we know, there are no data about exposure to arsenic in artesian water in Semberija. The purpose of this study is to monitoring As concentration in water from artesian wells in Semberija region. These results can also be applied to evaluate As contamination potential and safety concerning the domestic use of well water in the future.

EXPERIMENTAL

Study area. Morphologically, Semberija represents a part of the Pannonian basin located between the present Dinarides, Alps and Carpathians. After regression of the Pannonian sea, many lakes and swamps were left, in which diverse shallow-water sedimentation was carried out throughout Cenozoic. This area, composed of Cenozoic deposits, gradually descending to the flat land with alluvial tablelands and fluvial terraces, is the most fertile area in the northern B&H. Geological units consist of alluvial sand and gravel deposits of the rivers Drina and Sava and Paludin sand and sandy gravel with layers of clay. This layer of clay protected alluvial gravel deposits, but in some zones it becoming very thin. Thus, there are some vulnerable areas where the groundwater resources are not protected naturally[10]. The main underground water reserves are found in alluvial sediments of uneven texture along the Sava river and its tributaries. Ten sampling stations (Table 1, Fig. 1) were selected along the river Sava in the north Semberija, near the mouth of the river Drina.

Table 1. Sample site information

Sampling station	Code	Coordinate x	Coordinate y	Height (m)
Velino selo	AW1	4971402.95	6603088.40	91.91
Donji Brodac	AW2	4969694.65	6601470.07	91.63
Gornji Brodac	AW3	4969628.35	6600407.21	95.46
Begov put	AW4	4974180.85	6599992.08	82.93
Ostojicevo	AW5	4968954.74	6597855.93	88.51
Gornje Crnjelovo	AW6	4967205.14	6589324.61	88.82
Subotiste	AW7	4970564.44	6586400.59	75.81
Burum	AW8	4968162.64	6584848.72	75.55
Vrsani	AW9	4965523.75	6581705.50	91.40
Cadavica	AW10	4960569.74	6586649.81	96.59

Fig. 1. Map of study area and location of artesian wells

Water sampling and analysis. A series of investigations was conducted from February 2011 to January 2012. Artesian well waters were analysed at depths from 100 to 200 m. Sampling periods occurred once a month, every 18th in a month. Water samples (3×2 l) were collected in clean PVC sample bottles filtered with a Whatman 0.45-μm membrane filter and acidified by the addition of 3 ml of conc. HNO_3 per l of water. All samples were stored at 4ºC until analysis.

The concentration of As as well as other analysis included measuring temperature, pH, electrical conductivity, alkalinity, ortho-phosphate and iron concentrations were made according to the methods described in Table 2.

Table 2. Analytical methods and instrumentation for measuring artesian well waters quality parameters

Parameter	Analytical instrument	Analytical method	Procedure
pH	WTW profiline 197 pH-meter	electrometric	150.1[a]
alkalinity	titration glassware	titrimetric	310.1[a]
conductivity	WTW 197/LF 197-S conductance-meter	electrometric	120.1[a]
As	Shimadzu 6300 AAS; Thermo Scientific iCAP 6000 ICP-OES	direct aspiration	7061A; 6010C[a]
Fe	Shimadzu 6300 AAS; Thermo Scientific iCAP 6000 ICP-OES	direct aspiration	200.5[a]
Ortho-phosphate	Cecil Aquarius CE 7200 double beam spectrophotometer	ammonium molybdate spectrometric	ISO6878:2004[b]

[a]US EPA (Refs 11 and 12); [b]International Organisation for Standardisation (ISO) (Ref. 13).

Reagent and standards. Ultra-scientific (USA) ICP standard solution of about 20.00 ± 0.10 mg l^{-1} and Perkin Elmer AAS standard solution of $100\pm0.5\%$ mg l^{-1} of As and Fe, were used as stock solutions for calibration. A solution of 50 mg l^{-1} of phosphors was prepared from KH_2PO_4 (Merck®, KGaA, Darmstadt, Germany). Sample bottles were treated with 5% nitric acid and washed with ultra-pure water 0.05 μS cm^{-1} (MicroMed high purity water system, TKA Wasseraufbereitungs system GmbH). Buffer standards 4, 7 and 10 (WTW, PL4, PL7 and PL10) were used for calibration pH-meter. Standard electrical conductivity of 1413 μS cm^{-1} was used for calibration of conductance-meter.

Statistical analysis. Data were reported as mean ± standard deviation (SD) for triplicate determinations. The Tamhan and Friedman test was performed using a statistical package running on a computer (Statistica 8.0, StatSoft, Inc, Tulsa, OK, USA). The aim of performed tests was to determine are there statistically significant differences of level of As concentration in observed location and is there a statistically significant change of level of As concentration during the year. A probability of $p < 0.05$ was considered to be statistically significant[14].

RESULTS AND DISCUSSION

The water samples from artisien wells collected from February 2011 to January 2012 were analysed for the parameters, such as pH, conductivity and alaklinity. Although pH usually has no direct impact on water consumers, it is one of the most important operational water-quality parameters. The pH ranges from 7.45 to 8.21 in the present study. According to WHO (1996) (Ref. 15) and US EPA (2002) (Ref. 16), optimum pH is often in the range 6.5–9.5 and 5.0–9.0, respectively. The pH values are well within the safe drinking standards.

Electrical conductivity is a measurement of water capacity and is directly related to the concentration of ionized substance in the water. Water with electrical conductivity up to 200 µS cm^{-1} is considered suitable for human consumption (WHO, 1996) (Ref. 15). The overall conductivity values range from 474–928 µS cm^{-1}. As can be seen, the conductivity higher than the limits that have been set by the WHO. Conductivity can be indicative of mineralisation or salinity problems, which in turn can affect physical properties such as colour, taste and odour[15].

Carbonates and bicarbonates are the most common cause of alkalinity in water. Water from artesian wells investigated contains between 200 and 400 µg ml^{-1} CaCO$_3$. The US EPA Secondary Drinking Water Regulations (2001) (Ref. 17) limit alkalinity only in terms of total dissolved solids (TDS) (500 µg ml^{-1}) and to some extent by the limitation on pH. According to WHO (2011) (Ref. 18), water with a TDS level of less than about 600 mg l^{-1} is generally considered to be good.

Arsenic concentrations measured monthly over a period of 1 year at 10 locations are given in Table 3 and shown in Fig. 2.

Table 3. Total arsenic concentration (µg l^{-1}) in water samples from artesian wells

Code	February		March		April	
	AAS	ICP–OES	AAS	ICP–OES	AAS	ICP–OES
AW1	44.55 ± 1.13	42.43 ± 1.09	32.10 ± 0.69	30.55 ± 0.65	53.52 ± 0.82	51.30 ± 0.79
AW2	60.20 ± 1.32	57.87 ± 1.29	74.30 ± 0.05	71.24 ± 0.06	81.45 ± 0.85	78.02 ± 0.82
AW3	28.56 ± 2.13	27.07 ± 2.04	40.78 ± 0.07	39.16 ± 0.09	33.92 ± 0.76	31.28 ± 0.74
AW4	130.2 ± 0.86	124.9 ± 0.8	130.0 ± 2.30	126.67 ± 2.25	167.40 ± 3.34	162.19 ± 3.23
AW5	43.05 ± 2.75	41.17 ± 2.68	11.86 ± 0.75	11.25 ± 0.78	35.15 ± 0.02	33.68 ± 0.03
AW6	6.35 ± 0.32	6.01 ± 0.29	6.46 ± 0.06	6.11 ± 0.07	5.00 ± 0.09	4.76 ± 0.11
AW7	1.13 ± 0.27	1.06 ± 0.25	0.56 ± 0.25	0.53 ± 0.23	1.46 ± 0.55	1.38 ± 0.53
AW8	1.77 ± 0.27	1.68 ± 0.26	1.40 ± 0.31	1.32 ± 0.29	1.91 ± 0.03	1.82 ± 0.04
AW9	15.45 ± 0.13	14.79 ± 0.12	13.42 ± 0.22	12.73 ± 0.21	12.82 ± 0.32	12.17 ± 0.30
AW10	1.56 ± 0.36	1.47 ± 0.34	0.75 ± 0.10	0.71 ± 0.12	1.01 ± 0.06	0.95 ± 0.07

May		June		July	
AAS	ICP–OES	AAS	ICP–OES	AAS	ICP–OES
42.75 ± 0.04	41.13 ± 0.04	49.95 ± 0.65	47.89 ± 0.63	41.05 ± 0.71	39.38 ± 0.69
74.40 ± 0.24	71.62 ± 0.23	81.00 ± 0.04	77.81 ± 0.04	61.75 ± 1.63	59.29 ± 1.56
30.74 ± 0.73	29.53 ± 0.70	32.08 ± 0.11	30.62 ± 0.10	19.09 ± 0.20	18.23 ± 0.19
131.5 ± 3.16	127.76 ± 3.08	143.8 ± 0.40	139.31 ± 0.38	125.4 ± 1.28	121.36 ± 1.23
46.55 ± 0.54	44.61 ± 0.52	49.15 ± 0.60	46.92 ± 0.58	38.40 ± 1.93	36.75 ± 1.86
6.20 ± 0.69	5.87 ± 0.70	6.71 ± 0.18	6.34 ± 0.19	4.23 ± 0.02	3.98 ± 0.02
1.07 ± 0.26	1.01 ± 0.25	1.76 ± 0.01	1.66 ± 0.01	1.15 ± 0.16	1.09 ± 0.17
2.23 ± 0.18	2.12 ± 0.17	2.76 ± 0.06	2.59 ± 0.06	1.47 ± 0.06	1.39 ± 0.06
15.63 ± 0.11	14.90 ± 0.12	15.50 ± 0.37	14.71 ± 0.35	10.61 ± 0.04	10.08 ± 0.04
1.97 ± 0.19	1.86 ± 0.18	1.48 ± 0.14	1.39 ± 0.15	1.16 ± 0.00	1.07 ± 0.01

to be continued

Continuation of Table 3

August		September		October	
AAS	ICP–OES	AAS	ICP–OES	AAS	ICP–OES
44.25 ± 0.73	42.37 ± 2.63	47.60 ± 2.74	45.57 ± 2.63	50.75 ± 1.05	48.66 ± 1.02
73.52 ± 1.12	70.67 ± 1.09	82.35 ± 6.35	79.25 ± 6.11	91.30 ± 1.03	87.82 ±1.00
29.06 ± 0.71	27.58 ± 0.68	35.88 ± 0.16	34.39 ± 0.15	37.02 ± 0.89	35.49 ± 0.86
133.27 ± 1.07	128.62 ± 1.04	156.0 ± 1.91	151.23 ± 1.87	157.4 ± 0.95	152.54 ± 0.93
48.56 ± 1.65	46.39 ± 1.61	46.15 ± 0.65	44.17 ± 0.63	57.05 ± 3.66	54.32 ± 3.61
6.75 ± 0.76	6.42 ± 0.50	7.55 ± 0.53	7.19 ± 0.55	8.60 ± 0.12	8.17 ± 0.13
1.09 ± 0.15	1.03 ± 0.15	2.02 ± 0.39	1.98 ± 0.37	1.91 ± 0.41	1.84 ± 0.38
2.55 ± 0.08	2.46 ± 0.08	2.15 ± 0.10	2.04 ± 0.10	3.07 ± 0.22	2.92 ± 0.20
14.25 ± 0.42	13.54 ± 0.40	15.56 ± 0.15	14.82 ± 0.14	17.89 ± 0.10	17.03 ± 0.11
1.34 ± 0.07	1.27 ± 0.07	1.56 ± 0.30	1.47 ± 0.28	1.64 ± 0.29	1.55 ± 0.27

| November		December		January	
AAS	ICP–OES	AAS	ICP–OES	AAS	ICP–OES
56.80 ± 0.54	54.39 ± 0.51	40.85 ± 3.67	38.83 ± 3.58	34.15 ± 3.80	32.49 ± 3.56
81.95 ± 0.99	78.03 ± 0.95	79.95 ± 2.74	76.87 ± 2.69	63.05 ± 0.37	60.41 ± 0.32
31.66 ± 0.08	30.09 ± 0.09	33.38 ± 0.25	31.99 ± 0.24	32.72 ± 1.40	31.15 ± 1.34
171.8 ± 4.53	166.32 ± 4.48	132.5 ± 7.67	128.27 ± 7.54	164.2 ± 6.99	158.96 ± 6.70
51.00 ± 0.56	48.67 ± 0.54	49.65 ± 0.62	47.58 ± 0.59	62.70 ± 4.98	60.28± 4.77
6.25 ± 0.16	5.98 ± 0.15	7.07 ± 0.07	6.68 ± 0.07	6.07 ± 0.45	5.75 ± 0.43
1.54 ± 0.17	1.47 ± 0.17	2.57 ± 0.05	2.42 ±0.05	1.75 ± 0.49	1.66 ± 0.46
2.06 ± 0.03	1.95 ± 0.03	2.65 ± 0.06	2.49 ± 0.06	2.40 ± 0.06	2.25 ± 0.05
15.05 ± 0.57	14.21 ± 0.54	16.97 ± 0.09	16.12 ±0.10	15.83 ± 0.14	14.98 ± 0.15
0.62 ± 0.04	0.58 ± 0.04	1.98 ± 0.03	1.86 ± 0.03	1.53 ± 0.27	1.44 ± 0.29
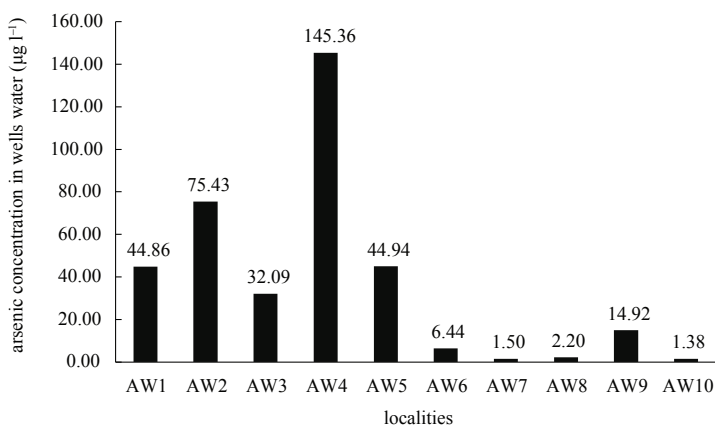
Fig. 2. Values of as As concentration measured in different localities

The accuracy and confidence of the experimental results were assured by using reference ICP-OES method according to US EPA (2009, 2000) (Refs 11 and 12). As

can be seen from Table 3, As concentrations for artesian water samples are ranged over 2 orders of magnitude. US EPA has set the arsenic standard for drinking water at 10 µg l⁻¹. The WHO (1993) (Ref. 19) guideline value for As in drinking water was provisionally reduced in 1993 from 50 to 10 µg l⁻¹. The new recommended value was based on the increasing awareness of the toxicity of As, particularly its carcinogenicity, and on the ability to measure it quantitatively. Artesian well 10 (AW10) showed consistently lower As concentration ranging from 0.75 to 1.98 µg l⁻¹ (average concentration 1.38 µg l⁻¹) followed by AW7 (0.56–2.57 µg l⁻¹, average concentration 1.50 µg l⁻¹), AW8 (1.40–3.07 µg l⁻¹, average concentration 2.20 µg l⁻¹) and AW6 (4.23–8.60 µg l⁻¹, average concentration 6.44 µg l⁻¹). Arsenic concentration in water from these localities is below WHO (1993) (Ref. 19) provisional guideline, but still is greater than the value of 2 µg l⁻¹ recommended by the Agency for Toxic Substances and Disease Registry (ATSDR) (2007) (Ref. 20). The As concentrations in water from other 6 artesian wells AW1 (31.15–56.80 µg l⁻¹, average concentration 44.86 µg l⁻¹), AW2 (60.20–91.30 µg l⁻¹, average concentration 75.43 µg l⁻¹), AW3 (19.09–40.78 µg l⁻¹, average concentration 32.07 µg l⁻¹), AW4 (125.40–171.80 µg l⁻¹, average concentration 145.29 µg l⁻¹), AW5 (11.86–62.70 µg l⁻¹, average concentration 44.94 µg l⁻¹), and AW9 (10.61–17.89 µg l⁻¹, average concentration 14.92 µg l⁻¹) are above the safe drinking standards. The descriptive statistics show that locality AW4 has the highest level of As concentration. The locality with the lowest level of As is AW10 (Fig. 2).

In order to reveal detailed differences between localities the Tamhan test was performed. Based on significances (0.000<0.05) it can be concluded that there are not a significant differences of mean level of concentration of As between localities AW1 and AW5, between AW3 and AW5, between AW7 and AW8 and between AW7 and AW10. Between the other localities there are significant differences of mean level of concentration of As.

Concentration of As in water from artesian wells varies seasonally, but not much (Fig. 3). Low average levels of As concentration were observed during the summer (dry) and winter seasons. During rainfall periods concentration of As was increased. Rainfall can cause washing varying As amounts from farmland into nearby waterways.

Differences of mean levels of As concentration measured in different months were checked by the Friedman test. The significance of the Friedman test is 0.000 < 0.05 which means that there are significant changes of mean level of As concentration during the year. The results of the Friedman tests show that there are no significant changes of mean level of As concentration in localities AW3 (0.053), AW6 (0.056) and AW10 (0.059). In all the others localities significant changes of mean level of As concentrations has been noted. Seasonal variation in As concentration has been also noted[21–23]. According to literature reports[24], arsenic is mainly transported in the environment by water. The concentrations in groundwater depend on the arsenic content of the bed-rock. Other threats come from inadequate maintenance of sewage system, intense exploitation of forests, uncontrolled use of pesticides, etc. [25] There is no valid

information on the degree of pollution of ground water in B&H by pesticides. Some reports[26,27] deal with the facts that high concentrations of phosphorus and ammonium are found in Northern B&H (Posavina). This area contains very fertile agricultural land along the river Sava. According to WHO (2001) (Ref. 1), several authors suggested that the widespread withdrawal of groundwater may have mobilised phosphate derived from fertilisers and from the decay of natural organic materials in shallow aquifers. Also, arsenic may be present in a variety of redox states. Arsenate and arsenite are two forms of arsenic commonly found in ground water[28]. These different arsenic species adsorb to surfaces a variety of aquifer materials, including iron oxides, aluminium oxides and clay minerals. In acidic and near-neutral pH water arsenate adsorbs strongly to iron-oxide surfaces. Where pH values are above 8, the negative net surface charge of iron oxide can repel negatively charged ions such as arsenate[29,30]. However, desorption at high pH (>7.5) is the most likely mechanism for the development of groundwater-As problems under the oxidising conditions and would account for the observed positive correlation of As concentration with increasing pH.
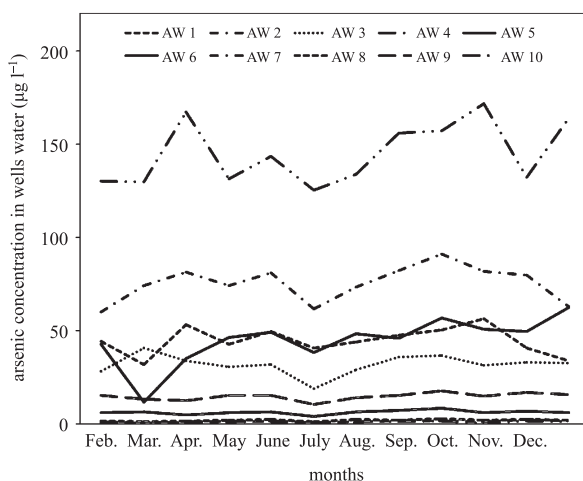

Fig. 3. Values of As concentration measured during the year in observed localities

Two additional analyses for total iron and phosphate were done. Water from artesian wells AW1 (up to 0.1 mg l^{-1}), AW2 (up to 0.1 mg l^{-1}), AW3 (up to 0.1 mg l^{-1}), AW4 (up to 0.17 mg l^{-1}), AW5 (up to 0.11 mg l^{-1}), AW9 (up to 0.13 mg l^{-1}) not only had high total iron concentrations, but also had high concentrations of phosphate (0.116–0.368 mg l^{-1}). Nearly all fertilisers contain phosphates. Since are tightly fixed in soil, elevated concentrations of phosphate (>0.1 mg l^{-1}) in agricultural areas may indicate rapid passage between the soil surface and the groundwater.

pH in all samples was ranged from 7.45 to 8.21. Results obtained from pH and presence of competing anions in water from artesian wells in Semberija are in correla-

tion with other reports available in literature related to controlling factors of arsenic mobility[24,29–31].

CONCLUSIONS

Our findings indicate that the water from artesian wells in Semberija is unhealthy to drink, due to occurrence of As above the safe standards. The water is also unhealthy due to high conductivity. Because of these high levels in water from artesian well samples we recommend that all sites in our study area should be analysed further before a true assessment of drinking water quality. Also, the data obtained suggest that for water from artesian wells in Semberija, presence of competing ions such as iron oxides and phosphate may be important controlling factors in arsenic adsorption and desorption reactions. These processes commonly results from high pH (>7.5). Our results also suggest that, at least in our study area, a measurements of As concentration can be used to predict the As exposure in a particular well over a period of many years. And finally, this investigation of As concentrations in wells water in Semberija region will be useful to water resource managers, the medical community, and those using water from wells for drinking and cooking.

ACKNOWLEDGEMENTS

REFERENCES

1. World Health Organization: Arsenic and Arsenic Compounds. Environment Health Criteria No 224, World Health Organization, Geneva, Switzerland, 2001.
2. M. M. KARIM: Arsenic in Ground Water and Health Problems in Bangladesh. Water Res, **34** (1), 304 (2000).
3. World Health Organization: Arsenic in Drinking Water. Fact Sheet, No 210 Retrieved June 6; World Health Organization, Geneva, Switzerland, 2009. http://www.who.int/mediacentre/factsheet/fs210/en/.
4. Commission of the European Communities: Assessment of the Dietary Exposure to Arsenic, Cadmium, Lead and Mercury of the Population of the EU Member States. Directorate-General of Health and Consumer Protection, Brussels, Belgium http://ec.europa.eu/food/food/chemicalsafety/contaminants/scoop_3-2-11_heavy_metals_report _en.pdf, accessed 13 February 2010, 2004.
5. S. MAJUMDAR, S. CHANDA, B. GANGULI, D. N. GUHA MAZUMDER, S. LAHIRI, U. B. DASGUPTA: Arsenic Exposure Induces Genomic Hypermethylation. Environ Toxicol, **25** (3), 315 (2010).
6. D. K. NORDSTROM: Public Health – Worldwide Occurrences of Arsenic in Ground Water. Science, **296**, 2143 (2002).
7. A. H. WELCH, D. B. WESTLOHN, D. R. HELSEL, R. B. WANTY: Arsenic Occurrence in Ground Water of the United State: Occurrence and Geochemistry. Ground Water, **38** (4), 589 (2000).
8. Economic Commission for Europe, Committee on Environmental Policy: Environmental Performance Reviews of Bosnia and Herzegovina (EPR). United Nations, New York-Geneva, 2004.
9. M. ALECKOVIC, E. MESIC, S. TRNACEVIC, Z. STIPANCIC, D. HAMIDOVIC, E. HASANOVIC: Glomerular Filtration Rate in Examined Population of Bosnia Posavina Region of Balkan Endemic Nephropathy. Bosn J Basic Med Sci, **1**(suppl. 1), S68 (2010).

10. D. POKRAJAC: Interrelation of Wastewater and Groundwater Management in the City of Bijeljina in Bosnia. Urban Water, **1** (3), 243 (1999).
11. US Environmental Protection Agency: Test Methods for Evaluating Solid Waste, Physical/Chemical Methods, SW-846. United States Environmental Protection Agency, Washington, D.C, 2009.
12. US Environmental Protection Agency: Method 6010C. Revision 3. Trace Elements in Solution by ICP AES. United States Environmental Protection Agency, Washington, D.C., 2000. http://www.epa.gov/epawaste/hazard/testmethods/sw846/online/index.htm#table.
13. International Organization for Standardization (ISO): Water quality. Determination of phosphorus. Ammonium molybdate spectrometric method, ISO 6878:2004, Geneva, Switzerland, 2004.
14. J. N. MILLER, J. C. MILLER: Statistics and Chemometrics for Analytical Chemistry. Pearson Education Limited, London, 2005, p. 165
15. World Health Organization: Guidelines for drinking-water quality. Health criteria and other supporting information, World Health Organization, Geneva, Switzerland, 1996.
16. US Environmental Protection Agency: National Recommended Water Quality Criteria, EPA-822-R-02-012; United States Environmental Protection Agency, Washington, D.C., 2002.
17. US Environmental Protection Agency: Secondary Drinking Water Regulations: Guidance for Nuisance Chemicals, 816-F-10-079. United States Environmental Protection Agency, Washington, D.C., 2001. http://water.epa.gov/drink/contaminants/secondarystandards.cfm
18. World Health Organization: Guidelines for Drinking-water Quality. World Health Organization, Geneva, Switzerland, 2011.
19. World Health Organization: Guidelines for Drinking-water Quality. Vol. I., Recommendations, World Health Organization, Geneva, Switzerland, 1993.
20. Agency for Toxic Substances and Disease Registry (ATSDR): Toxicological Profile for Arsenic. U.S. Department of Health and Human Services, Public Health Services, Atlanta, GA, 2007.
21. G. F. RIEDEL: The Annual Cycle of Arsenic in a Temperate Estuary. Estuaries, **16** (3), 533 (1993).
22. F. FROST, D. FRANKE, K. PIERSON, L. WOODRUFF, B. RAASINA, R. DAVIS, J. DAVIES: A Seasonal Study of Arsenic in Groundwater, Snohomish County, Washington, USA. Environ Geochem Health, **15** (4), 209 (1993).
23. S. J. McLAREN, N. D. KIM: Evidence for a Seasonal Fluctuation of Arsenic in New Zealand's Longest River and the Effect of Treatment on Concentrations in Drinking Water. Environ Pollut, **90** (1), 67 (1995).
24. P. L. SMEDLEY, D. G. KINNIBURGH: A Review of the Source, Behavior and Distribution of Arsenic in Natural Waters. Appl Geochem, **17** (5), 517 (2002).
25. E. MERIAN: Introduction on Environmental Chemistry and Global Cycles of Chromium, Nickel, Cobalt, Beryllium, Arsenic, Cadmium and Selenium and Their Derivatives. Toxicol Environ Chem, **8** (1), 9 (1984).
26. J. GANOULIS, I. L. MURPHY, M. BRILLY: Transboundary Water Resources in the Balkans: Initiating a Sustainable Co-operative Network. Kluwer Academic Publishers, Dordrecht, 2000, p. 21
27. International Sava River Basin Commission (ISRBC): Sava River Basin Analysis Report. Zagreb, Croatia, 2009.
28. P. H. MASSCHELEYN, R. D. DELAUNE, W. H. PATRIC, Jr.: Effect of Redox Potential and pH on Arsenic Speciation and Solubility in a Contaminated Soil. Environ Sci Technol, **25** (8), 1414 (1991).
29. D. A. DZOMBAK, F. M. M. MOREL: Surface Complexation Modeling – Hydrous Ferric Oxide. John Wiley & Sons, New York, 1990, p.319
30. G. A. WAYCHUNAS, B. A. REA, C. C. FULLER, J. A. DAVIS: Surface Chemistry of Ferrihydrite: Part 1. EXAFS Studies of the Geometry of Coprecipitated and Adsorbed Arsenate. Geochim Cosmochim Ac, **57** (10), 2251 (1993).
31. Yu. A. MIKHEEV, L. N. GUSEVA, E. Ya. DAVYDOV, G. E. ZAIKOV: Heterogeneous-heterophase Mechanism of the Hydrophobic Compound Dissolution Water. Oxid Commun, **31** (1), 52 (2008).

REVIEW OF THE PROTECTION FROM NON-IONIZING RADIATION AND THE IMPORTANCE OF ESTABLISHING THE LEGAL FRAMEWORK

Z. BJELAJAC[a], Z. SPALEVIC[b], M. DUKIC-MIJATOVIC[a]*, M. JOVANOVIC[a]

[a]*Law Faculty of Economics and Justice, University of Business Academy, Novi Sad, Serbia*
E-mail: *marijana.dukic.mijatovic@gmail.com*; *zdjbjelajac@gmail.com*;
miki80miki@gmail.com
[b]*Faculty of Law, Sinegija University, Bijeljina, Bosnia and Herzegovina*
E-mail: *zspalevic@sinergija.edu.ba*

ABSTRACT

Recently, we have witnessed a kind of expansion in the development and use of radiation sources of non-ionizing radiation on a global level. In short, the whole planet is electrified and equipped with the mobile telephony. It has been undoubtedly concluded that non-ionizing radiation has a negative impact on biological and physiological balance of every living organism, in sense that it gradually destroys the cells of water which is necessary for living. However, it is impossible to avoid the exposure of the population to non-ionizing radiation, because it is hard to imagine the modern lifestyle without the devices that, on the one hand, make life easier and on the other emit non-ionizing radiation. Therefore, the international community agrees on a number of recommendations and regulations in order to regulate the conditions and measures to protect human health and the environment from the harmful effects of non-ionizing radiation while utilising the sources of non-ionizing radiation.

Keywords: non-ionizing radiation, non-ionizing radiation protection, referent border levels, the European standards.

AIMS AND BACKGROUND

It is obvious that knowledge about the radiation reaches far into the past. Back then the people have, as a matter of fact, only taken care about the impact of natural radiation. Over time, man has increasingly turning to the study of natural phenomena, natural laws, etc. However, with the beginning of industrialisation at the same time

---

* For correspondence.

technical radiation sources occurred, which have continuously multiplied along with the advancement of technology, i.e. consumer electronics. This area has been neglected for a long time, and especially by large companies, which, above all, were the main source of radiation, ignoring the harmful effects of electric and magnetic fields, for the sake of commercialisation of their products. Non-ionizing radiation is electromagnetic radiation with photon energy less than 12.4 eV. These include: ultraviolet radiation (wavelength 100 nm), visible radiation (400–780 nm wavelength), the infrared optical radiation (wavelength 780–1 nm), radio-frequency radiation (frequency 10 kHz–300 GHz) , the electromagnetic fields of low frequency (0–10 kHz frequency) and laser radiation. In this area very important method is radiolysis as a purification method at least four additional ways to utilize non ionizing radiation for pollutant destructions in combinations with TiO$_2$ as fotocatalytic[1]. Also, non-ionizing radiation includes ultrasound or sound with a frequency greater than 20 KHz, although it is not an EM radiation[2].

Non-ionizing radiation is actually the electromagnetic radiation that does not have sufficient energy to cause the ionization in living organisms. When it comes to natural sources of non-ionizing radiation, these are rare and extremely weak. The only sources are: the Sun, distant pulsars, other cosmic sources, including terrestrial sources, such as lightning or the Earth magnetic and electric field. It is instructive to note that all other sources of non-ionizing radiation are the product of human activity[3].

By definition, non-ionizing radiation source is a device, the installation or facility that emits or may be transmitted by non-ionizing radiation. Such sources can be found in everyday life, from working and living surroundings to the modern means of communication. The living area has a variety of sources that usually emit non-ionizing radiation. Let us mention a few of them: computers, television, cordless phones, microwave ovens, irons, freezers, refrigerators, electric cookers and other electrical devices. When it comes to the environment, in it we also encounter many sources of non-ionizing radiation: substations, transmission lines, cable and satellite communication, electric trains, trams and trolleybuses, TV and radio transmitters, and more recently, the base stations for mobile telephony.

Experts have for a long time warned that the first symptoms of diseases caused by this harmful radiation are nervousness, insomnia, increased irritability, anxiety, headaches, chronic fatigue and weakness, tendency to depression, reduced mental and physical activities, problems with concentration and memory, and other. A number of studies and researches confirm that the joint operation geopathic fields with harmful effects and electromagnetic radiation can lead to the specific exposures and the weakening of the organism.

Therefore, protection against non-ionizing radiation on the supranational and national level coincides with the development of awareness of the adverse impacts, risks and dangers to human health caused by this radiation, and in accordance with the existing necessities, i.e. setting the absolute standards in the domain of normative development of the latter. The adoption of appropriate regulations in this, in many

ways specific and complex field, caused a large and diverse number of sources of non-ionizing radiation in our environment. The available data suggest that the regulations in protection against non-ionizing radiation in the EU countries are rather fragmented. For the purposes of the European Commission, a study of European Committee for Standardisation in Electrical Engineering (CENELEC), which states that there are over 130 laws, regulations, standards and recommendations in the area of the radio-frequency radiation, was made by the member states. In addition to this, several EU directives in the field of non-ionizing radiation protection are issued. In its resolution from 5 May 1994, and in the fight against the harmful effects of non-ionizing radiation, The European Parliament invited the Commission to propose legislative measures in order to limit the exposure of workers and citizens of non-ionizing electromagnetic radiation, urging the measures for improving the safety and health, pregnant and women with babies in particular, and among other matters to obligate the employers to estimate the activities that involve the specific risks of exposure to non-ionizing radiation.

Table 1. Basic restrictions for electric, magnetic and electromagnetic fields (0 to 300 GHz)

Frequency range	Magnetic flux density (mT)	Current density (mA/m^2) (rms)	Whole body average SAR (W/kg)	Localised SAR (head and trunk) (W/kg)	Localised SAR (limbs) (W/kg)	Power density S (W/m^2)
0 Hz	40					
> 0–1 Hz		8				
1–4 Hz		8/f				
4–1 000 Hz		2				
1000 Hz –100 kHz		f/500				
100 kHz–10 MHz		f/500	0.8	2	4	
10 MHz–10 GHz			0.8	2	4	
10–300 GHz						10

The recommendation of the Council of Europe from 12 July 1999 is of particular importance[4]. On the one hand, the Member States presented the responsibility to protect the people from potential health risks, on the other it has established a set of basic restrictions and referent values for Member states, at the same time setting the limits that must be met by other countries which are applying for the EU membership (see for example, Table 1). Within the context of meeting the international standards in this area it is appropriate to mention the recommendations of the World Health Organisation (WHO) regarding the use of non-ionizing radiation sources, where a cautious approach is advised as a preventive measure that would include: strict implementation of national and international standards, application of protective measures of non-ionizing radiation, the active participation of local authorities and population and public information[5].

Realising the importance of this phenomenon the Republic of Serbia, with the intention to round up the legislation for the first time, and order conditions and measures to protect human health and the environment from harmful effects of non-ionizing radiation sources in the use of non-ionizing radiation, adopted the Law on Non-ionizing Radiation Protection[6], which entered into force in May 2009. This Act sublimated the present knowledge in the field of non-ionizing radiation protection, relying on the regulation in this area of the EU countries, especially taking into account the above-mentioned recommendations of the Council of Europe, as well as the recommendations of the World Health Organisation (WHO). Also when using non-ionizing radiation sources is taken into account and applying the principles of ALARA principle, 'as low as reasonably achievable' ('So little as possible/reasonable/to reach')[7].

On the basis of the non-ionizing radiation protection, other supporting regulations have been adopted:

● Regulation on non-ionizing radiation sources of particular interest, types of sources, methods and their testing period (Official Gazette of the RS, No 104/09);

● Regulation on non-ionizing radiation exposure limits (Official Gazette of the RS, No 104/09);

● Regulation on the contents of the records of non-ionizing radiation sources of special interest (Official Gazette of the RS, No 104/09);

● Regulation on the content and form of reports on systematic testing of non-ionizing radiation levels in the environment (Official Gazette of the RS, No 104/09);

● Regulation on conditions that must be met by legislative persons performing duties of systematic testing of non-ionizing radiation levels, and the manner and methods of systematic testing of the Environment (Official Gazette of the RS, No 104/09);

● Regulation on conditions which have to be met by legal persons engaged in testing the level of radiation sources of non-ionizing radiation of particular interest in the environment (Official Gazette of the RS, No 104/09).

In addition to these sub-legislative acts, which are important for the implementation of the Act, it is necessary to point out that this law establishes the necessary link with other 'similar' laws, primarily the Law on Environmental Protection (Official Gazette of RS, No 135/04 and 36/09), the Law on Environmental Impact Assessment (Official Gazette of the RS, No 135/04 and 36/09), Law on Strategic Environmental Impact Assessment (Official Gazette of the RS, No 135/04), Law on Planning and Construction (Official Gazette of the RS, No 72/09) and the Telecommunications Act (Official Gazette of the RS, No 44/03 and 36/06). These extensive activities were carried out in compliance with the relevant international regulations and directives. By analysing the Law on Non-ionizing Radiation Protection some of its important characteristics may be emphasised:

● Managing the non-ionizing radiation protection is based on internationally affirmed principles: the principle of prohibition or exposure above the prescribed limit, i.e. any unnecessary exposure to non-ionizing radiation is prohibited; the principle of

proportionality – conditions and permissibility of using non-ionizing radiation sources of particular interest are determined and valued according to the benefits which their use provides to the society with regard to potential risks of adverse effects occurrence due to their use...; general-public, non-ionizing radiation on the data available to the public.

● In the goal of the implementation of protection against non-ionized radiation, comprehensive and concrete measures are provided, starting from the prescription of non-ionizing radiation exposure limits, to detect the presence and determining the level of exposure to non-ionizing radiation, determining the conditions for the usage of non-ionizing radiation sources of special interest, providing organisational, technical, financial and other conditions for the implementation of non-ionizing radiation protection and other. And finally the education and training of personnel in the field of protection from non-ionizing radiation in the environment, and ultimately raising the awareness among the people about the health effects of exposure to the non-ionizing radiation, and protection measures and information on the level of non-ionizing radiation exposure in the environment.

● The provisions of this Act and regulations, amongst other matters, the non-ionizing radiation sources of particular interest are defined, for which a permit for use by the competent authority with the prescribed conditions, to a company, enterprise or other legal entity or entrepreneur can use non-ionizing radiation sources of special interest if they meet the following requirements: for the mentioned non-ionizing radiation sources there is an environmental impact assessment, in accordance with the law, so that the level of exposure of the population does not exceed prescribed limits. By definition, non-ionizing radiation sources of special interest are considered to be sources of electromagnetic radiation that can be hazardous to human health, and are defined as stationary and mobile sources whose electromagnetic field in the zone of increased sensitivity reaches at least 10% of the reference, the limit values for the proper frequency.

● The law determined the zones of increased sensitivity: the residential areas where people may stay for 24 h a day, such as schools, homes, preschools, hospitals, maternity hospitals, tourist facilities, playgrounds, but also the undeveloped land areas intended, according to the master plan for the presented purpose, which is in accordance with the assessments and recommendations of the World Health Organisation.

● Special legislative attention is paid the expansion and development of mobile telephony, and to setting up and usage of radio base stations of mobile telephony, emphasising the risk of radiation-generating non-ionizing base stations for mobile telephony and mobile phones. Related to this, the conditions for setting up base stations and determining the location are developed, the procedures of obtaining the permits from the competent authorities. However, as recommended by the Ministry of Environment and Spatial Planning, the following facilities are exempted regarding the avoidance of locations for placing base stations of mobile telephony: schools, kindergartens, medical facilities and nursering homes.

● The Act absolutely accepted the proper conditions and standards which defined the non-ionizing radiation sources, with the parameters given in the introduction to this work.

● This Act provides the establishment of decentralisation measures, conditions and supervision by competent authorities at all levels, when using non-ionizing radiation sources by different operators.

● Monitoring of the implementation of the Law on Non-ionizing Radiation Protection and the regulations made under this Law perform the ministry, through the inspector for environmental protection within the scope stipulated in this Act.

● Thus, the Act on Non-ionizing Radiation Protection of the Republic of Serbia, made the harmonisation with the European standards in this area, as a motivation to achieving the levels that can respond to increased security requirements which arose as a result of a complex major developments and changes on a global scale over the last decade.

EXPERIMENTAL

Measuring the level of non-ionizing radiation in local area mobile telephony base stations consisted of 2 phases. In the first phase, the level of non-ionizing radiation was analysed in the frequency range from 30 MHz to 3 GHz by a Rohde & Schwarz FSH6 spectrum analyser. Based on this analysis, all the components of the electric field that significantly affected the overall volume level of the electric field were determined. In the second phase, was carried out a detailed measuring of the electromagnetic emissions in a number of positions within the measurement locations, in order to determine the spatial distribution of levels of electromagnetic radiation. These measurements were made in 2 ways using:
  – the principle of superposition of components,
  – wide band measurement receiver.
According to the existing measurement standards is required the measurement of the mean intensity of the electric field. Regardless of whether the electric field is measured component by component, or it is measured by present value of the total electric field intensity, in order to increase safety, it is necessary to record the maximum value in the interval of 60 s for each component and for each measurement position. In this way, the maximum value is obtained from the total electric field strength, so it is certainly larger than the average values.

In order to eliminate the influence of a person body that conducts the measurement, the level of the electric field was measured at a height of approximately 2.2 m. In this way, the values are obtained from higher levels of the electric field than those levels where could possibly be a person.

Measurement of the electric field of GSM base stations was performed only on the active control channel, as traffic channels operate in broadcast mode on and off. Therefore, when calculating the total intensity of the electric field of the base station

operating at full capacity, it is assumed that the value of the intensity of the electric field originating from the traffic channel is equal to the value of the intensity of the electric field originating from the control channel. This assumption corresponds to the worst case scenario that the traffic channel is active, as is often the case in practice.

Measuring the level of electromagnetic emissions on the principle of superposition components was carried out using measuring devices for accurate measurement of the electric field Anritsu ML521B (25–300 MHz) and ML522B (300–1000 MHz), and the spectrum analyser RF Field Analyzer Protek 3201 (0.1–2060 MHz). When measured, this measurement system is utilising specially calibrated measuring antenna in the form of dipoles: Anritsu MP663a (200–500 MHz), MP524A (25–250 MHz), MP524B (200–500 MHz) and MP524C (520–1000 MHz).

By measuring levels of broadband electromagnetic emission measurement receiver Narda EMR300 gets the overall level of electromagnetic emissions in the whole frequency range. When measuring, a specially calibrated probe E-field probe type 18c (intended to measure the overall level of the electric field in the frequency range of 100 kHz to 3 GHz) and the E-field probe type 9c (intended to measure the overall level of the electric field in the frequency range from 3 MHz to 18 GHz) were used.

Depending on the installation of the antenna system, the locations of base stations are classified into 3 main categories: outdoor, antenna mast and locations with installations of objects.

Indoor locations are those locations where the base station antenna system is placed inside a closed area. Such installations are common in case you need to provide coverage in buildings intended for a wide audience, such as shopping centers or large office buildings. These base stations typically emit less signal strength than the base stations covering the macro cell. In this case, if someone can be close to the antenna system, it is necessary to analyse the radiation of base stations in indoor locations.

Antenna mast include those locations where the base station antenna system located on the pole, whether it is purpose-built for the GSM/UMTS network or not. In public mobile systems is typically used antenna masts with a height of 18 to 50 m. Chimneys heating or water towers are classified into this category, although this is not the main purpose.

In locations with installations of objects, base station antenna system is installed on the outside of the house, whether it is a side wall or roof of a building. To analyse these sites is essential to determine the use of the facility, in order to know how much time people spend in it, bearing in mind that all objects can be viewed as residential, industrial, office and medical facilities.

RESULTS AND DISCUSSION

The measurements were performed on sample of mobile telephony base stations, where 47% are the antennas on antenna towers, 11% are indoor antennas and 42% are the antenna installations located on the buildings. Serbia has received the Regulation on

the limits of exposure of humans to non-ionizing radiation[7] and the Regulations on Non-ionizing Radiation sources[8], in December 2009. The importance of the adoption of these regulations is supported not only by experts, but also by the general public, where an increasing awareness about the harmful effects of the growing number of electrical devices in their environment is exposed. Regulation descibed in Ref. 6 defines a referent exposure limit levels of the population to the electric, magnetic and electromagnetic fields as well as levels that are used for practical exposure assessment, in order to determine the possibility of exceeding of the basic restrictions. Regulation[9] has a lower limit reference levels of electric and magnetic fields than those given in the Recommendation of the Council of Europe[4], although the basic limitations are the same.

From Table 2 it can be seen that compared to the Recommendation of the Council of Europe, our national Regulations allow only 40% of the limit reference levels either for the electric field strength or for magnetic induction in the whole frequency range. The comparison of reference limits with the volume level for the electric field strength and magnetic induction[10] is shown in Fig. 1. Figure 2 shows that the frequency ranges of interest for the mobile National Regulation[7], with respect to international recommendations[4,11,12] allows 40% of the electric field strength, 16% of the power density. This fact indicates the good intentions of our legislators to better protect the population[10,13].

In the Regulations on the types of non-ionizing radiation sources and testing methods[9], the important characteristics of sources of electromagnetic fields are defined. However, it should be noted that modern sources often have their own internal control, the possibility of adaptation, and technological solutions which largely complicate the definition of important parameters in an unambiguous way[2,14]. In Art. 3 of this Regulation, it is said that 'non-ionizing radiation sources of special interest are considered to be the sources of electromagnetic radiation that can be harmful to human health, and designated as stationary and mobile sources whose electromagnetic field in the zone of increased sensitivity reaches 10% of the reference, the limit value prescribed for that frequency.'

Table 2. Reference limit levels for the electric field strength (E_L) and reference threshold levels of magnetic induction (B_L) (f-frequency, corresponding to values in the column for the frequency range)

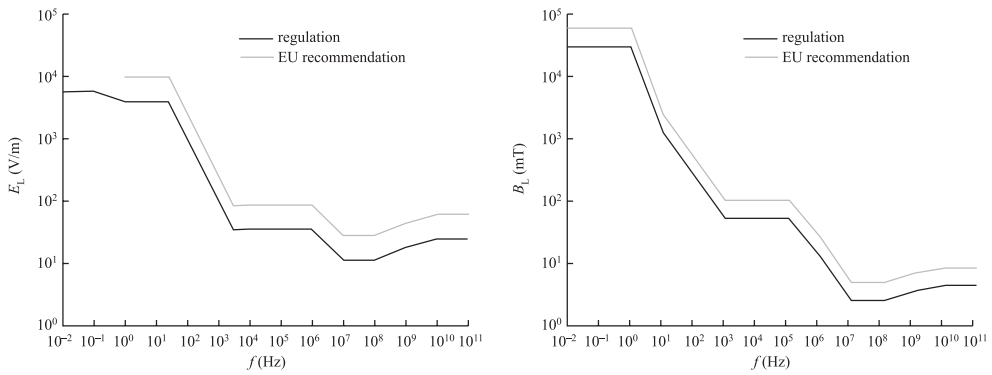| Frequency range	E_L (V/m)		B_L (μT)	
	regulation[2]	regulation[2]	regulation[2]	EU sugg.[5]
< 1Hz	5600	16000	16000	40000
1–25 Hz	4000	$16000/f^2$	$16000/f^2$	$40000/f^2$
0.025–3 kHz	$100/f$	$2000/f$	$2000/f$	$5000/f$
0.003–1 MHz	34.8	2.5	2.5	6.25
1–10 MHz	$34.8/f^{1/2}$	$0.368/f$	$0.368/f$	$0.92/f$
10–400 MHz	11.2	0.0368	0.0368	0.092
400–2000 MHz	$0.55\,f^{1/2}$	$0.00184\,f^{1/2}$	$0.00184\,f^{1/2}$	$0.0046\,f^{1/2}$
2–300 GHz	24.4	0.08	0.08	0.2

Fig. 1. Reference threshold levels for the electric field strength and magnetic induction
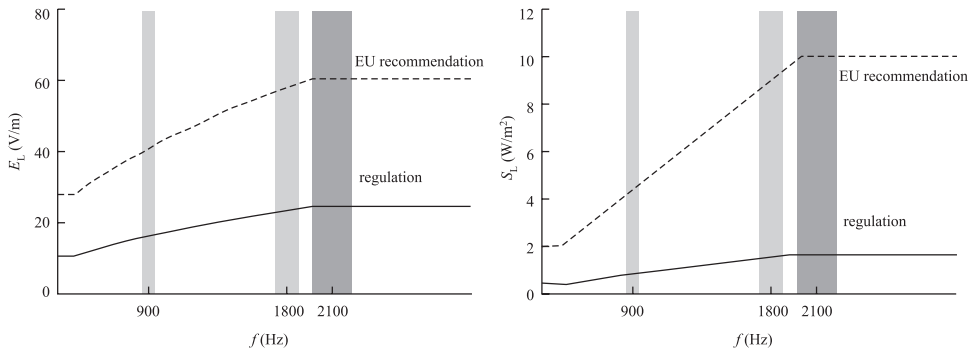

Fig. 2. Reference threshold levels for the electric field strength and power density in the frequency bands of interest for mobile telephony

Many countries and professional organisations over the years of work in numerous laboratory and experimental studies established standards for protection from the exposure to low-frequency electromagnetic fields. Due to very hard maintenance of the basic sizes, the regulations provide the reference sizes which enable easier assess to meeting the basic restrictions. Physical quantities that can be used as reference sizes are: electric field strength (E), magnetic field intensity (H), magnetic flux density (B) the contact electricity (I) (Refs 11 and 12).

Table 3. Recommendations of limit values of the strength of electric and magnetic fields

Index		Public area		Occupational area	
		E (kV/m)	B (µT)	E (kV/m)	B (µT)
1	ICNIRP	5	100	10	500
2	IEEE	5	904		
3	CENELEC, 1995	10	640	30	1600
4	European Union	5	100	10	500

Table 4. Limit values of the strengths of electric and magnetic fields in some countries

No	Country	Public area E (kV/m)	Public area B (μT)	Occupational area E (kV/m)	Occupational area B (μT)	No	Country	Public area E (kV/m)	Public area B (μT)	Occupational area E (kV/m)	Occupational area B (μT)
1	Argentina	3	25			18	Latvia	10	640	30	1600
2	Australia	5	100	10	500	19	Luxemburg	5	100	10	500
3	Austria	5	100	10	500	20	Malta	5	100	10	500
4	Belgium	5	100			21	Nederland	8	120	62.5	600
5	Costa Rica	2	15			22	Poland	1	75		
6	Croatia	2	40	5	100	23	Portugal	5	100	10	251
7	Czech Rep.	5	100	10	500	24	Russia	0.5	10	5	100
8	Denmark	5	100	10	500	25	Singapore	5	100	10	500
9	Estonia	0.5	10	5	100	26	Slovakia	20	300		
10	Finland	5	100			27	Slovenia	0.5	10	10	100
11	France	5	100	10	500	28	South Africa	5	100	10	500
12	Germany	5	100	6.66	424.4	29	South Korea	5	100	10	500
13	Greece	4	8			30	Spain	5	100	10	500
14	Hungary	5	100	10	500	31	Switzerland	5	100		
15	Ireland	5	100	10	500	32	Taiwan	5	100	10	500
16	Italy	5	100	10	500	33	United Kingdom	5	100	10	500
17	Japan	3		10							

The determined strength of electric and magnetic fields in areas of increased sensitivity (general population) and exposure to the professional (professional staff) based on the recommendations, directives and guidelines are given in Table 3. It is evident that a large number of countries have adopted a 5 kV/m for electric and 100 µT for magnetic fields (Table 4). These values are recommended by the ICNIRP (International Commission on Non-ionizing Radiation Protection) and the relevant bodies of the European Union.

CONCLUSIONS

'I have no doubts that an increase in electromagnetic fields in this moment is an element that largely pollute the environment on the Earth. I think that at the global level is more important than warming ... and the increasing amounts of chemical elements in the environment' (Robert Becker, MD). In support of this bold conclusion, there is a number of scientific studies which confirm that at the present time, the greatest threat and danger to our health and other goods that we enjoy, is an invisible, insidious, and also the ubiquitous form, which we call a word 'electro-pollution'.

Every citizen and every worker worldwide is exposed to sources of non-ionizing radiation, such as high-voltage transmission lines and substations, electric household appliances and other. With the development of environmental awareness over the years initiatives of the European Commission (EC) have matured, which has followed the expansion of the negative consequences of this phenomenon for a long time, contributing to establishing a legal framework to protect citizens and workers. Regarding this, given the guidelines and recommendations, i.e. demands that the EU member states have to adopt, in order to ensure a high level of protection of public health as well as the frame reference which limits the exposure of the population, to affirm the principles of safety, quality of life and human health, must be subordinated to all activities and interests of human society. Serbia has adopted recommendations as part of civilised value agreed in the international scale, through the harmonisation of its national legislation with the European standards in this field of scientific research.

REFERENCES

1. M. TSVETKOV, M. MILANOVA, R. KRALCHEVSKA, D. TODOROVSKY: On the Influence of Gamma-irradiation on the Photocatalytic Activity of TiO. Oxid Commun, **35** (2), 303 (2012).
2. International Commission on Non-ionizing Radiation Protection: Guidelines for Limiting Exposure to Time-varying Electric, Magnetic and Electromagnetic Fields (up to 300 GHz). Health Phys, **74** (4), 494 (1998).
3. I. GENOV, R. GANEV, I. GLAVCHEV: Dependence between Electronic Oxide Polarisability of Several Ores and Their Production of Singlet Oxygen after Irradiation. Oxid Commun, **34** (3), 501 (2011).
4. Council Recommendation of 12 July 1999 or the Limitation of Exposure of the General Public to Electromagnetic Fields (0 Hz to 300 GHz) 1999/519/EC: Official J L 199, 30/07/1999, 0059-0070.
5. World Health Organization: www.who.int, 12th November 2012.

6. Law on Non-ionizing Radiation Protection: Official Gazette of the RS, No 36/09.
7. www.iem-inc.com/pralar.html/4/09/2011, 12th November 2012.
8. Regulation on Limits of Exposure to Non-ionizing Radiation: Official Gazette of the RS, No 104/09.
9. Regulation on Non-ionizing Radiation Sources of Special Interest, Source Types, Methods and Period of Their Examination: Official Gazette of the RS, No 104/09.
10. A. JUHAS, M. MILUTINOV, N. PEKARIC-NADJ: Experience in the Implementation of National Regulations on Non-ionizing Radiation. J Telecommun, 7 (2011).
11. A. KRAWCZYK, E. LADA-TONDYRA: The Evolution of Electromagnetic Field Standards – Case Study of ICNIRP Standards. Electrical Review, **87** (12b), 89 (2011).
12. E. MULASALIHOVIC, H. PFUTZNER, P. ZANOLIN: 3D Stray Field Analysis of Transformer Cores Considering DC-bias. Electrical Review, **87** (9b), 57 (2011).
13. M. PENHAKER, R. HAJOVSKY, D. KORPAS: Measurement and Analysis of EMC Parameters of Implantable Pacemaker. Electrical Review, **87** (5), 265 (2011).
14. P. NOSOVIC, M. BAKALOVIĆ: Electromagnetic Fields and Safety Distances from Overhead Lines. Infoteh-Jahorina, East Sarajevo, Bosnia and Herzegovina, 2011, 1043–1047.

INSTRUCTION FOR AUTHORS

Starting from 2011, the authors can publish their manuscripts as rapid publication (6 months after the receipt of positive referees comments and the revised version) after they pay a fee of 100 Euro. The articles intended to be published as rapid publication should follow the requirements for contribution length as pointed below. Authors from Universities and Organisations, which have a subscription or sponsorship to the Journal publish their papers free of charge. The authors receive a hard copy of the Journal issue containing their published article free of charge. Some figures, according to authors decision, can be published coloured in order to make them more understandable to the reader. The additional payment is 75 Euro per printed page.

The authors are kindly requested to send a declaration on copyright transfer simultaneously with the manuscript submission to the editorial board of *Oxidation Communications*.

All authors must agree to be so listed and must have seen and approved the manuscript, its content, and its submission to *Oxidation Communications*. Submission of a paper that has not been approved by all authors will not be forwarded for evaluation and publication. Any changes in authorship must be approved in writing by all the original authors.

Manuscripts should present original results not previously published and not considered for publication elsewhere.Authors declare this in the notification letter. Only relevant experimental data that are discussed in the manuscript should be described. Authors are encouraged to present the experimental data in the form of tables. The duplication of experimental data in tables and figures should be avoided.

MANUSCRIPTS TYPE

Short communications – up to 4 printed pages (about 14 000 characters) including text, all illustrative materials (tables, figures, etc.) and references.

Research articles – up to 8 printed pages (without figures – about 28 100 characters) and 10 printed pages with figures (up to 35 260 characters) including main text, tables, figures, schemes and references.

Reviews – up to 15 printed pages (52 890 characters) including main text, tables, figures, schemes and references.

The Editorial Board will strictly follow the requirement for contribution length in view of the over-accumulation of scientific papers, submitted for publication in the Journal and the restricted volume of each book. Contributions within the stated lengths will be published free of page charges. Depending on the exceeding length are introduced page charges (up to 100 Euro).

Receipt of a contribution for consideration will be acknowledged immediately by the Editorial Office. The acknowledgement will indicate the paper reference number assigned to the contribution. Authors are particularly asked to quote this number on all subsequent correspondence.

ORGANISATION

The title page should include the title, authors and their affiliations, complete address of the author to whom correspondence should be sent and an Abstract.

Abstract – should not exceed 200 words and should give the subjects and conclusions of the article and all results of general interest. References, compound numbers and abbreviations should be avoided. A maximum of five keywords should follow the Abstract.

Aims and Background – should include brief and clear remarks outlining the specific purpose of the work and a short summary of the background material including numbered references.

Experimental – should be sufficiently detailed (but concise) to guarantee reproducibility.

Results and Discussion – should indicate the logic used for the interpretation of data without lengthy speculations. Authors submitting material on purely theoretical problems or on a new experimental technique might unite the sections Experimental, Results and Discussion into one section under the heading Discussion. Authors should avoid doubling of results in the form of Tables and Figures.

Conclusions – short summary of the main achievements of the research.

References – should be typed at the end of the manuscript and numbered in the order as first cited in the text as superscript Arabic numerals. In the list of references the original papers should be given with their titles. Abbreviations of journal titles should follow the style used in ISI Journal Title Abbreviations. Sequence and punctuation of references should be:

1. E. SZABÓ, G. L. ZÜGNER, M. FARKAS, I. SZILÁGYI, S. DÓBÉ: Direct Kinetic Study of the OH-radical Initiated Oxidation of Pivalaldehyde, $(CH_3)_3CC(O)H$, in the Gas Phase. Oxid Commun, **35** (3), 538 (2012).
2. M. B. NEIMAN, D. GAL: The Kinetic Isotope Method. Akademiai Kiado, Budapest, 1971.
3. J. A. HOWARD: In: Advances in Free Radical Chemistry. Vol. 4 (Ed. G. H. Williams). Lagos Press, London, 1972, 49–69.
4. C. HANSCH (Ed.): Comprehensive Drug Design. Pergamon Press, New York, 1990, p. 19.

In preparing the list of References attention must be drawn to the following points:

(a) Names of all authors of cited publications should be given. Use of 'et al.' in the list of references is not acceptable;

(b) Only the initials of first and middle names should be given.

Tables – each bearing a brief title and numbered in Arabic numerals. The tables should be placed in the text as first cited.

Figures and captions – should be numbered consecutively with captions and must be placed at their first mentioning in the text.

Particular attention is drawn to the use of SI Units, IUPAC nomenclature for compounds and standard methods of literature citation.

ELECTRONIC SUBMISSION OF MANUSCRIPTS

Manuscripts should be submitted in electronic form. Submission not in electronic form may face a delay in publication. All text (including the title page, abstract, keywords, all sections of the manuscript, figure captions, and references) and tabular material should be in one file. The manuscript must be prepared using MS Word 6.0 and above. Manuscripts in PDF format are not accepted.

Chemical equations must be supplied using equation editor. Tables must be created using table format feature.

Graphics, i.e. figures, schemes, etc. should be in a separate file. The file name should be descriptive for the graphic. Structures and schemes may be supplied in ChemWindow format and other graphics in Microsoft Excel or Microsoft PowerPoint format.

SUBMISSION OF MANUSCRIPTS

Manuscripts should be sent to the following address:
Prof. Dr. **Slavi K. Ivanov**
SciBulCom Ltd., P. O. Box 249, 7 Nezabravka Str., 1113 Sofia, Bulgaria
Phone/Fax: +359 2 872 42 65, +359 2 978 72 12
E-mail: scibulcom2@abv.bg

All manuscripts are subject to critical review and the names of referees will not be disclosed to the authors. The manuscript sent back to the author for revision should be returned within 2 months by e-mail. Otherwise it will be considered withdrawn. Revised manuscripts are generally sent back to the original referees for comments, unless (in case of minor revisions) the editors accept them without seeking further opinions. Proofs should be corrected and returned as soon as possible. The authors receive CD-ROM containing copy of the book.